



National Library
of Canada

Acquisitions and
Bibliographic Services Branch

395 Wellington Street
Ottawa, Ontario
K1A 0N4

Bibliothèque nationale
du Canada

Direction des acquisitions et
des services bibliographiques

395, rue Wellington
Ottawa (Ontario)
K1A 0N4

Your file Votre référence

Our file Notre référence

NOTICE

The quality of this microform is heavily dependent upon the quality of the original thesis submitted for microfilming. Every effort has been made to ensure the highest quality of reproduction possible.

If pages are missing, contact the university which granted the degree.

Some pages may have indistinct print especially if the original pages were typed with a poor typewriter ribbon or if the university sent us an inferior photocopy.

Reproduction in full or in part of this microform is governed by the Canadian Copyright Act, R.S.C. 1970, c. C-30, and subsequent amendments.

AVIS

La qualité de cette microforme dépend grandement de la qualité de la thèse soumise au microfilmage. Nous avons tout fait pour assurer une qualité supérieure de reproduction.

S'il manque des pages, veuillez communiquer avec l'université qui a conféré le grade.

La qualité d'impression de certaines pages peut laisser à désirer, surtout si les pages originales ont été dactylographiées à l'aide d'un ruban usé ou si l'université nous a fait parvenir une photocopie de qualité inférieure.

La reproduction, même partielle, de cette microforme est soumise à la Loi canadienne sur le droit d'auteur, SRC 1970, c. C-30, et ses amendements subséquents.

UNIVERSITY OF ALBERTA

**LABORATORY STUDY OF HYPERCONCENTRATED
OPEN CHANNEL FLOWS**

by

ARBIND PRASAD MAINALI



A THESIS

SUBMITTED TO THE FACULTY OF GRADUATE STUDIES AND RESEARCH IN
PARTIAL FULFILMENT OF THE REQUIREMENTS FOR THE DEGREE OF
DOCTOR OF PHILOSOPHY

in

WATER RESOURCES

DEPARTMENT OF CIVIL ENGINEERING

EDMONTON, ALBERTA



National Library
of Canada

Acquisitions and
Bibliographic Services Branch

395 Wellington Street
Ottawa, Ontario
K1A 0N4

Bibliothèque nationale
du Canada

Direction des acquisitions et
des services bibliographiques

395, rue Wellington
Ottawa (Ontario)
K1A 0N4

Your file Votre référence

Our file Notre référence

The author has granted an irrevocable non-exclusive licence allowing the National Library of Canada to reproduce, loan, distribute or sell copies of his/her thesis by any means and in any form or format, making this thesis available to interested persons.

L'auteur a accordé une licence irrévocable et non exclusive permettant à la Bibliothèque nationale du Canada de reproduire, prêter, distribuer ou vendre des copies de sa thèse de quelque manière et sous quelque forme que ce soit pour mettre des exemplaires de cette thèse à la disposition des personnes intéressées.

The author retains ownership of the copyright in his/her thesis. Neither the thesis nor substantial extracts from it may be printed or otherwise reproduced without his/her permission.

L'auteur conserve la propriété du droit d'auteur qui protège sa thèse. Ni la thèse ni des extraits substantiels de celle-ci ne doivent être imprimés ou autrement reproduits sans son autorisation.

ISBN 0-315-82070-5

Canada

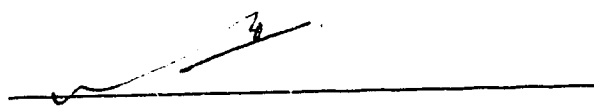
UNIVERSITY OF ALBERTA

RELEASE FORM

NAME OF AUTHOR: ARBIND PRASAD MAINALI
TITLE OF THESIS: LABORATORY STUDY OF
HYPERCONCENTRATED OPEN CHANNEL
FLOWS
DEGREE: DOCTOR OF PHILOSOPHY
YEAR THIS DEGREE GRANTED: SPRING 1993

Permission is hereby granted to THE UNIVERSITY OF ALBERTA LIBRARY to reproduce single copies of this thesis and to lend or sell such copies for private, scholarly or scientific research purposes only.

The author reserves other publication rights, and neither the thesis or extensive extracts from it may be printed nor otherwise reproduced without the author's written permission.



Permanent Address:

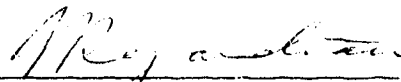
The University of Alberta
T. Blench Hydraulics Lab
Edmonton, Alberta
Canada, T6G 2N4

Date: March 23, 1993

THE UNIVERSITY OF ALBERTA

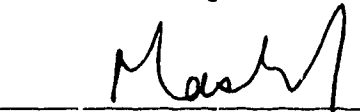
FACULTY OF GRADUATE STUDIES AND RESEARCH

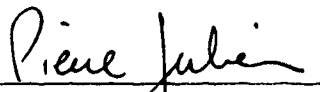
The undersigned certify that they have read, and recommended to the faculty of Graduate Studies and Research for acceptance, a thesis entitled LABORATORY STUDY OF HYPERCONCENTRATED OPEN CHANNEL FLOWS submitted by ARBIND PRASAD MAINALI in partial fulfilment of the requirements for the degree of DOCTOR OF PHILOSOPHY


Dr. N. Rajaratnam


Dr. P. M. Steffler


Dr. N. Morgenstern


Dr. J. H. Masliyah


Dr. P. Y. Julien

Date: 23rd Mar 1993

ABSTRACT

Since Bagnold proposed his dilatant fluid model in 1954, several other constitutive laws have been put forward for the flow of granular material under continuous shear. One of the serious limitations of these laws is that they have not been fully verified using reliable field or experimental data. Most experiments have been either general or performed under limited conditions. The field studies, on the other hand, have been more qualitative only providing information on some mean flow parameters.

This study examines some of the fundamental ideas on the mechanics of high concentration flows with a special focus on debris flows from a large volume of available literature. The various constitutive laws and steady flow solutions are examined. In addition to this, the present study examines three areas of hyperconcentrated flow research in the laboratory. The first stage presents a new approach to generating a steady, uniform flow of hyperconcentrated slurry in a channel for a considerable duration. The second stage discusses the development of a measuring device for a narrow flume so that the velocity and the concentration profiles along the depth can be measured. Finally, velocity and concentration distributions have been measured for three near uniform particle sizes with mean diameters of, 0.430, 0.335, 0.215mm and a mixture of these particles with a mean diameter

of 0.330mm. These measurements have been made at various mean volumetric concentrations ranging from 2.5% to 40%. The general behavioral trend of these mixtures are discussed and comparisons are made with well known steady flow solutions using dilatant flow models and Bingham plastic models.

The measured velocity profiles appear to range from parabolic at lower mean concentrations to approach almost linear profiles at higher concentrations. The laboratory flows considered in this study indicate that dispersive stresses are less than 5% of the total stress. Turbulence plays a major role in the dispersion of the particles even at volumetric concentrations approaching 40%. The particle size plays a dominant role in the dispersion mechanism with the velocity profiles approaching semi-logarithmic for low mean concentrations. The slopes of the velocity profiles deviate from that observed in clear water flows displaying a decreasing trend with concentration of the von Karman's constant.

ACKNOWLEDGEMENTS

First and foremost I would like to express my gratitude to Dr. N. Rajaratnam for his continuous support and encouragement throughout this study. His enthusiasm and concern for his students' efforts is second to none.

I am thankful to Dr. Peter Steffler for his patience, time and plenty of valuable advice. I am thankful to Dr. Terry M. Hrudehy for his help in deciphering some of the literature in rheology.

I am indebted to Sheldon Lovell for building the experimental set-up and making the whole system work. He has always impressed me with his ingenuity in the laboratory.

My total educational experience is hardly complete without the hours of discussion with other graduate students in the Laboratory and my friends Doug Weir, Sheldon Lovell and Stephen Stanley.

My work at the university would not have been possible without the sacrifice of my parents and my sisters. I am grateful to them.

Finally I would like to acknowledge the support given by the *Natural Sciences and Engineering Research Council, Canada* for this research through grants received by Dr N. Rajaratnam and to the *Central Research Fund, The University of Alberta* for providing a seed grant.

TABLE OF CONTENTS

CHAPTER	page
1 INTRODUCTION	1
1.1 Nature of the Problem	1
1.1.1 Documented debris flows	2
1.1.2 Extent of destruction	5
1.1.3 Objectives of the study	6
2 MECHANICS OF DEBRIS FLOWS	8
2.1 Introduction	8
2.2 Initiation of Flow	9
2.3 Debris Flow Modeling	9
2.3.1 Frictional Nature of Granular Material	12
2.3.2 Dilatant fluid model	13
2.3.3 Dilatancy	17
2.3.4 Bagnold's shear vs turbulent shear	18
2.3.5 Quadratic Model of O'Brien and Julien	19
2.3.6 Bingham plastic and pseudo-plastic fluid models	21
2.3.7 Coulomb viscous model	22
2.3.8 Generalized viscoplastic fluid model	24
2.3.9 Ackermann and Shen's Model	29
2.4 Choice of a model	30
2.5 Viscosity studies in suspensions	32
3 MECHANICS OF STEADY DEBRIS FLOWS	34
3.1 Empirical approach	34
3.2 Uniform flow using rheological models	37

3.2.1 Bingham Plastic and power law models.....	37
3.2.1.1 Chen's analysis.....	38
3.2.2 Dilatant fluid model.....	40
3.2.3 Generalized viscoplastic model.....	43
3.2.4 Arai and Takahashi's Equation.....	45
3.2.5 Turbulent diffusion of sediment.....	46
4 LABORATORY MEASUREMENTS OF HYPERCONCENTRATED FLOWS	49
4.1 Introduction	49
4.1.1 Past Experiments	50
4.1.1.1 Velocity and Concentration.....	50
4.2 Present study	52
4.2.1 Preliminary Works	52
4.2.1.1 Dry Granular Flows.....	53
4.2.1.2 Sand Water Mixtures.....	55
4.3 Steady Debris Flows	57
4.3.1 Experimental Arrangement	59
4.3.2 Sampler Development and Calibration.....	62
4.4 Velocity and Concentration Measurements	70
4.5 Limitations and Discussions	121
4.6 Error Analysis	123
5 DISCUSSION OF EXPERIMENTAL RESULTS	126
5.1 Introduction	126
5.2 General Trends	126
5.2.1 Concentration distribution.....	126
5.2.2 Velocity distribution.....	151
5.2.3 Shear distribution.....	154

5.3 Analysis of Experimental Data	159
5.3.1 Total shear versus grain shear	159
5.3.2 Velocity distribution	164
5.3.3 Concentration distribution	177
5.3.4 Manning's equation	194
6 DISCUSSIONS AND CONCLUSIONS	197
6.1 Theoretical	198
6.2 Experimental	199
6.3 Field studies	199
6.4 CONCLUSIONS	200
CITED REFERENCES	203
APPENDIX A	216
A.1 Favorable conditions for debris flows	216
A.2 Definitions	217
A.2.1 Introduction	217
A.2.2 Debris slides and debris avalanches	218
A.2.3 Debris flows and debris torrents	219
A.2.4 Mudflows	219
APPENDIX B	220
B Classifications	220
B.1 Classification of Sediment-Water Flows	220
B.1.1 Streamflow	221
B.1.2 Hyperconcentrated flows	222
B.1.3 Granular flows	222
APPENDIX C	225
C Characteristics Of Debris Flows	225
C.1 Debris Sources	225

C.2 Composition of Debris Flows	226
C.3 Nature of Flows	227
C.3.1 Physical Behavior	227
C.3.2 Velocity	228
C.3.3 Slopes	231
C.4 Important Concepts in Particle Support Mechanism	233
C.4.1 Dispersive stress	234
C.4.2 Matrix Strength in Debris Flows	235
C.4.3 Buoyancy in Debris Flow	237
C.4.4 Inverse Grading	239
APPENDIX D	241
D.1 Rheological properties of debris flows	241
D.1.1 Fluid viscosity and shear strength under field conditions	242
D.2 Viscosity and yield measurements in debris flows	244
APPENDIX E	248
E.1 Curve fit	248
E.2 Viscosity	263

List of Plates

Plates	page
4-1 Inverse grading in dry granular flow (flow left to right)	54
4-2 Segregation on the surface of dry granular flow deposit (flow from top to bottom)	54
4-3 Shear layer near the wall in dry granular flow	56
4-4 Shear layer near the wall in a flow of saturated sand water mixture	56
4-5 Segregation in the surge front of a saturated granular flow. Surge frozen at high shutter speed (flow top to bottom)	58
4-6 Run-out after flume exit (flow left to right)	58
4-7 Continuous pumping system for steady uniform debris flow	60
4-8 Downstream hopper for adding sediment and mixing	60
4-9 Centre and side samplers with tapered duct and surface floats	64
4-10 Sampling of flow	64
4-11 View of sampler looking downstream	65
4-12 Typical sampler being weighed	65
4-13 Surface velocity using a float (flow right to left)	72

List of Figures

Figures		page
2-1	Definition sketch for Bagnold's(1954) analysis of sheared granular material	14
3-1	Dimensionless velocity profiles for sediment water mixtures using turbulent dispersive model with $D=0.215\text{mm}$	46
4-1(a-c)	Experimental set-up and sketch of samplers	61
4-2a	Depth vs velocity for steady uniform water flow using pitot tube and sampler #2 $Q=6.48\text{L/s}$, slope= 28.6%	66
4-2b	Depth vs velocity for steady uniform water flow using pitot tube and corrected sampler #3 at channel centre	67
4-2c	Depth vs velocity for steady uniform water flow using pitot tube and corrected sampler #5 at channel centre	68
4-3	Grain size analysis for particles D1-D4	74
4-4a	Normalised depth-velocity for steady uniform sand water mixture, particle D1, group C1, slope 28.6% , channel side	77
4-4b	Normalized Depth-Concentration for steady uniform sand water mixture, particle D1, group C1, slope 28.6% , channel side	78
4-5a	Normalized Depth-velocity for steady uniform sand water mixture, particle D1, group C2, slope 28.6% , channel side	80
4-5b	Normalized Depth-Concentration for steady uniform sand water mixture, particle D1, group C2, slope 28.6% , channel side	81
4-6a	Normalized Depth-velocity for steady uniform sand water mixture, particle D1, group C3-C6, slope 28.6% , channel side	83

4-6b	Normalized Depth-Concentration for steady uniform sand water mixture, particle D1, group C3-C6, slope 28.6%, channel side	84
4-7a	Normalized Depth-velocity for steady uniform sand water mixture, particle D1, group 6.45, slope 28.6%, channel centre	86
4-7b	Normalized Depth-Concentration for steady uniform sand water mixture, particle D1, group 6.45, slope 28.6%, channel centre	87
4-8a	Normalized Depth-velocity for steady uniform sand water mixture, particle D1, group 7.90, slope 28.6%, channel centre	90
4-8b	Normalized Depth-Concentration for steady uniform sand water mixture, particle D1, group 7.90, slope 28.6%, channel centre	91
4-9a	Normalized Depth-velocity for steady uniform sand water mixture, particle D2, group 6.45, slope 28.6%, channel centre	96
4-9b	Normalized Depth-Concentration for steady uniform sand water mixture, particle D2, group 6.45, slope 28.6%, channel centre	97
4-10a	Normalized Depth-velocity for steady uniform sand water mixture, particle D2, group 7.90, slope 28.6%, channel centre	99
4-10b	Normalized Depth-Concentration for steady uniform sand water mixture, particle D2, group 7.90, slope 28.6%, channel centre	100
4-11a	Normalized Depth-velocity for steady uniform sand water mixture, particle D3, group 6.45, slope 28.6%, channel centre	103
4-11b	Normalized Depth-Concentration for steady uniform sand water mixture, particle D3, group 6.45, slope 28.6%, channel centre	104
4-12a	Normalized Depth-velocity for steady uniform sand water mixture, particle D3, group 7.90, slope 28.6%, channel centre	108

4-12b	Normalized Depth-Concentration for steady uniform sand water mixture, particle D3, group 7.90, slope 28.6%, channel centre.....	109
4-13a	Normalized Depth-velocity for steady uniform sand water mixture, particle D4, group 6.45, slope 28.6%, channel centre.....	113
4-13b	Normalized Depth-Concentration for steady uniform sand water mixture, particle D4, group 6.45, slope 28.6%, channel centre.....	114
4-14a	Normalized Depth-velocity for steady uniform sand water mixture, particle D4, group 7.90, slope 28.6%, channel centre.....	117
4-14b	Normalized Depth-Concentration for steady uniform sand water mixture, particle D4, group 7.90, slope 28.6%, channel centre.....	118
4-15	Depth vs velocity for steady uniform water flow using pitot tube at channel centre and close to the channel centre.....	122
5-1a	Depth-velocity for steady uniform sand water mixture, particle D1, group C1, slope 28.6%, channel side.....	128
5-1b	Depth-Concentration for steady uniform sand water mixture, particle D1, group C1, slope 28.6%, channel side.....	129
5-2a	Depth-velocity for steady uniform sand water mixture, particle D1, group C2, slope 28.6%, channel side.....	130
5-2b	Depth-Concentration for steady uniform sand water mixture, particle D1, group C2, slope 28.6%, channel side.....	131
5-3a	Depth-velocity for steady uniform sand water mixture, particle D1, group C3-C6, slope 28.6%, channel side.....	132

5-3b	Depth-Concentration for steady uniform sand water mixture, particle D1, group C3-C6, slope 28.6%, channel side	133
5-4a	Depth-velocity for steady uniform sand water mixture, particle D1, group 6.45, slope 28.6%, channel centre	134
5-4b	Depth-Concentration for steady uniform sand water mixture, particle D1, group 6.45, slope 28.6%, channel centre	135
5-5a	Depth-velocity for steady uniform sand water mixture, particle D1, group 7.90, slope 28.6%, channel centre	136
5-5b	Depth-Concentration for steady uniform sand water mixture, particle D1, group 7.90, slope 28.6%, channel centre	137
5-6a	Depth-velocity for steady uniform sand water mixture, particle D2, group 6.45, slope 28.6%, channel centre	138
5-6b	Depth-Concentration for steady uniform sand water mixture, particle D2, group 6.45, slope 28.6%, channel centre	139
5-7a	Depth-velocity for steady uniform sand water mixture, particle D2, group 7.90, slope 28.6%, channel centre	140
5-7b	Depth-Concentration for steady uniform sand water mixture, particle D2, group 7.90, slope 28.6%, channel centre	141
5-8a	Depth-velocity for steady uniform sand water mixture, particle D3, group 6.45, slope 28.6%, channel centre	143
5-8b	Depth-Concentration for steady uniform sand water mixture, particle D3, group 6.45, slope 28.6%, channel centre	144
5-9a	Depth-velocity for steady uniform sand water mixture, particle D3, group 7.90, slope 28.6%, channel centre	145

5-9b	Depth-Concentration for steady uniform sand water mixture, particle D3, group 7.90, slope 28.6%, channel centre	146
5-10a	Depth-velocity for steady uniform sand water mixture, particle D4, group 6.45, slope 28.6%, channel centre	147
5-10b	Depth-Concentration for steady uniform sand water mixture, particle D4, group 6.45, slope 28.6%, channel centre	148
5-11a	Depth-velocity for steady uniform sand water mixture, particle D4, group 7.90, slope 28.6%, channel centre	149
5-11b	Depth-Concentration for steady uniform sand water mixture, particle D4, group 7.90, slope 28.6%, channel centre	150
5-12	Cv vs μ , particle D1 to D4	153
5-13	Dimensionless shear stress profiles for particle D1	155
5-14	Dimensionless shear stress profiles for particle D2	156
5-15	Dimensionless shear stress profiles for particle D3	157
5-16	Dimensionless shear stress profiles for particle D4	158
5-17	Ratio of Bagnold's shear to the measured driving shear particle D1	160
5-18	Ratio of Bagnold's shear to the measured driving shear particle D2	161
5-19	Ratio of Bagnold's shear to the measured driving shear particle D3	162
5-20	Ratio of Bagnold's shear to the measured driving shear particle D4	163
5-21	Comparison of dimensionless velocity profiles for particle D1	165
5-22	Comparison of dimensionless velocity profiles for particle D2	166

5-23	Comparison of dimensionless velocity profiles for particle D3.....	167
5-24	Comparison of dimensionless velocity profiles for particle D4.....	168
5-25	Semi-log velocity distribution for particle D1	172
5-26	Semi-log velocity distribution for particle D2	173
5-27	Semi-log velocity distribution for particle D3	174
5-28	Semi-log velocity distribution for particle D4	175
5-29	Cm vs von Karman's constant for high concentration flows.....	176
5-30a	Concentration distribution using Rouse's equation, particle D1, group 6.45, channel centre.....	178
5-30b	Concentration distribution using modified Rouse equation particle D1, group 6.45, channel centre.....	179
5-31a	Concentration distribution using Rouse's equation, particle D1, group 7.9, channel centre.....	180
5-31b	Concentration distribution using modified Rouse equation particle D1, group 7.9, channel centre.....	181
5-32a	Concentration distribution using Rouse's equation, particle D2, group 6.45, channel centre.....	182
5-32b	Concentration distribution using modified Rouse equation particle D2, group 6.45, channel centre.....	183
5-33a	Concentration distribution using Rouse's equation, particle D2, group 7.9, channel centre.....	184
5-33b	Concentration distribution using modified Rouse equation particle D2, group 7.9, channel centre.....	185

5-34a	Concentration distribution using Rouse's equation, particle D3, group 6.45, channel centre.....	186
5-34b	Concentration distribution using modified Rouse equation particle D3, group 6.45, channel centre.....	187
5-35a	Concentration distribution using Rouse's equation, particle D3, group 7.9, channel centre.....	188
5-35b	Concentration distribution using modified Rouse equation particle D3, group 7.9, channel centre.....	189
5-36a	Concentration distribution using Rouse's equation, particle D4, group 6.45, channel centre.....	190
5-36b	Concentration distribution using modified Rouse equation particle D4, group 6.45, channel centre.....	191
5-37a	Concentration distribution using Rouse's equation, particle D4, group 7.9, channel centre.....	192
5-37b	Concentration distribution using modified Rouse equation particle D4, group 7.9, channel centre.....	193
5-38	Mean Concentration Cv vs Manning's roughness coefficient n^* for sand water mixture, Slope 28.6*	195
5-39	Specific discharge vs Manning's roughness coefficient n^* for sand water mixture, Slope 28.6*	196
C-1	Definition sketch of mass of debris flowing down a slope.....	232
E-1	Polynomial velocity and velocity gradient for particle D1, group 6.45, channel centre.....	249
E-2	Polynomial velocity and velocity gradient for particle D1, group 7.90, channel centre.....	250

E-3	Polynomial velocity and velocity gradient for particle D2, group 6.45, channel centre	251
E-4	Polynomial velocity and velocity gradient for particle D2, group 7.90 channel centre	252
E-5	Polynomial velocity and velocity gradient for particle D3, group 6.45, channel centre	253
E-6	Polynomial velocity and velocity gradient for particle D3, group 7.90 channel centre	254
E-7	Polynomial velocity and velocity gradient for particle D4, group 6.45, channel centre	255
E-8	Polynomial velocity and velocity gradient for particle D4, group 7.90 channel centre	256
E-9a	Concentration vs velocity coefficients for particle D1, slope 28.6%, channel centre	259
E-9b	Concentration vs velocity coefficients for particle D2, slope 28.6%, channel centre	260
E-9c	Concentration vs velocity coefficients for particle D3, slope 28.6%, channel centre	261
E-9d	Concentration vs velocity coefficients for particle D4, slope 28.6%, channel centre	262
E-10	C_v vs μ_r , particle D1	264
E-11	C_v vs μ_r , particle D2	265
E-12	C_v vs μ_r , particle D3	266
E-13	C_v vs μ_r , particle D4	267

List of Tables

Tables	page
4-1 Summary of velocity and concentration profiles for group C1, Channel side.....	79
4-2 Summary of velocity and concentration profiles for group C2, Channel side.....	82
4-3 Summary of velocity and concentration profiles for group C3-C6, Channel side.....	85
4-4 Summary of velocity and concentration profiles for concentration set C1 to C4, sediment D1, group 6.45, Channel centre.....	88
4-5 Summary of velocity and concentration profiles for concentration set C1 to C6, sediment D1, group 7.90, Channel centre.....	92
4-6 Summary of velocity and concentration profiles for group 6.45, set C1 to C4, sediment D2, Channel centre.....	98
4-7 Summary of velocity and concentration profiles for group 7.90, set C1 to C4, sediment D2, Channel centre.....	101
4-8 Summary of velocity and concentration profiles for group 6.45, set C1 to C5, sediment D3, Channel centre.....	105
4-9 Summary of velocity and concentration profiles for group 7.90, set C1 to C5, sediment D3, Channel centre.....	110
4-10 Summary of velocity and concentration profiles for group 6.45, set C1 to C4, sediment D4, Channel centre.....	115
4-11 Summary of velocity and concentration profiles for group 7.90, set C1 to C3, sediment D4, Channel centre.....	119
4-12 Measurement variables and their variances	125
5-1 Details of the measurements	169

C-1	Physical properties of observed debris flows (after Costa, 1987)	229
E1	Polynomial velocity and velocity gradients for particle D1, channel centre	257
E2	Polynomial velocity and velocity gradients for particle D2, channel centre	257
E3	Polynomial velocity and velocity gradients for particle D3, channel centre	258
E4	Polynomial velocity and velocity gradients for particle D4, channel centre	258

NOTATIONS

$A_{1,2}$	=	numerical constants given by Equations 2-3.24 and 2-3.25
a	=	sampler area
a'	=	constant
a_i	=	Bagnold's empirical constant for inertial flow
a_v	=	Bagnold's empirical constant for viscous flow
a_η	=	generalized Bagnold's numerical constant representing various flow regimes indicated by various η values
B	=	Intrinsic viscosity (similar to Einstein's 2.5)
b'	=	constant
$b_{3,4}$	=	constants
$b_{1,2}$	=	constants
C	=	Concentration at a point
C_1	=	turbulent dispersive parameter
C_b	=	concentration at the bed
C_{ch}	=	dimensionless Chezy's coefficient
C_d	=	drag coefficient
C_o	=	concentration at reference point o above the bed
C_m	=	mean concentration of the solid fluid mixture
C'_m	=	mean concentration in the truncated profile
C_s	=	the concentration at the free surface
C_v	=	volumetric sediment concentration at
C_∞	=	maximum volumetric sediment packing
c	=	cohesion
D	=	particle diameter

D_{ij}	=	the rate of deformation tensor
D_{ij}'	=	deviatoric rate-of-deformation tensor
D_L	=	the height of the largest deposited boulder
d_p	=	the depth of the plug
d'	=	width of sampler
g	=	acceleration due to gravity
h	=	depth of flow
h_o	=	height above the bed where plug flow starts
K	=	ratio of the volume of the sediment particle plus the bound water to that of sediment particle
k_s	=	equivalent sand grain roughness of the bed
l_m	=	the mixing length of mixture
m	=	mass of sample collected
m'	=	exponent
m_p	=	parameter
n	=	volume fraction of the clast submerged in debris
n^*	=	Manning's roughness coefficient
N	=	inertial to viscous regime viscosity ratios
P	=	normal stress
p	=	dynamic pressure
q	=	integrated unit discharge at a section
Q	=	discharge
R	=	Reynolds number
Re^*	=	roughness Reynolds number
S_o	=	channel slope
s	=	yield
s_p	=	separation distance between two particles

τ	=	shear stress
T_{ij}	=	total stress tensor
t	=	time
t_d	=	thickness of the equilibrium debris deposit
u	=	mean velocity at a point in the flow
u'	=	fluctuating velocity in the direction of flow
u_*	=	Shear velocity
u_p	=	pore pressure in the saturated material
U	=	mean velocity in the channel
U_m	=	average velocity at a section
U'_m	=	Depth averaged velocity of the truncated profile at a section
U_{max}	=	velocity at the top of the channel
Δu	=	difference in velocity between the centre and the side of the sampler
V	=	volume of sample
v'	=	fluctuating velocity in the direction perpendicular to the flow
W	=	weight of the control section/unit width
w_c	=	the width of the channel
w_p	=	the width of the plug
y	=	distance away from the bed-vertical coordinate
y'	=	height above the bed of the truncated velocity profile
y_{cm}	=	height above bed where C_v is equal to C_m
y_{um}	=	height above bed where u is equal to U_m

Y_{10}	=	height above the bed where the concentration is 10% of bed concentration
α	=	exponent for hindered settling
α'	=	constant
δ_{ij}	=	the Kronecker delta
ϵ	=	coefficient of restitution
ϕ	=	static angle of friction
ϕ_d	=	dynamic angle of friction
η	=	flow behavior index
γ_m	=	unit weight of the mixture
γ_s	=	unit weight of solids
γ_{sat}	=	saturated unit weight of the material
γ_w	=	unit weight of water
λ	=	linear concentration
K	=	the compressibility of the mixture
κ_v	=	Karman constant
μ	=	dynamic viscosity
μ_1	=	the consistency index
μ_2	=	the cross-consistency index
μ_a	=	apparent viscosity
μ_f	=	coefficient of kinetic friction
μ_r	=	mixture-water viscosity ratio (μ/μ_w)
μ_w	=	viscosity of water
ν_w	=	kinematic viscosity of water
θ	=	bed inclination
ρ_f	=	fluid density
ρ_m	=	the density of the mixture

ρ_s	=	the density of sediment
ρ_w	=	density of water
ρ'	=	effective density i.e. $\rho - \rho_w$
σ	=	standard deviation
σ_n	=	stress normal to the bed
$\bar{\sigma}$	=	effective normal stress
τ	=	shear stress
τ_b	=	bed shear stress
τ_L	=	limiting shear strength for the soil mass
τ_g	=	Bagnold's grain shear
τ_t	=	turbulent shear
τ_v	=	the viscous stress
τ_y	=	the yield stress
ω	=	the fall velocity of a single particle
ω_m	=	the velocity oduring hindered settling
II_D	=	the second invariant of the deviatoric rate of deformation tensor

1 INTRODUCTION

1.1 Nature of the Problem

The cycle of erosion and subsequent deposition is a natural process that shapes the surface of the earth. The varying geologic features are a reflection of these ongoing denudation and construction processes of nature. One of these natural processes is debris flow.

The steep slopes of mountains generally have numerous channels carved on their faces that meet the gradual valley slopes at their feet that enter the gentler slopes of the alluvial fans. These alluvial fans have continuously been the most attractive areas for human habitation. The fertile soils as well as the gentle topography make these alluvial fans very attractive for agriculture as well as for residential development. In many heavily populated areas this may be the only space available for settlement. Since these developments in the alluvial fans lie in nature's dumping grounds, they have to reckon with possible floods and torrents which may be heavily freighted with mud and debris rushing out from the mountains.

In almost all the disastrous events of this nature the wisest choice would be to abandon the hazardous areas and move to a safer location. This is a discreet alternative not only based on common sense but also based on the lessons learned from all the past experiences of this nature. Though reasonable in most cases, these choices fail to be practical

when it comes to moving and relocating the developed homes and people. The catastrophic event is eventually forgotten and a new sequence of developments start only to be struck by devastation one more time. This has been the story of many areas in North Central Utah, especially around the area of Farmington (Jeppson, 1985).

1.1.1 Documented debris flows

Debris flows and other associated phenomena of mass wasting and material transport are part of many ongoing geological processes associated with mountainous regions. In other words, these events have been reshaping landscapes for a long time and will continue to do so for a long time to come. In most cases the majority of these episodic events occur in the mountains and remote areas and normally may never get noticed until they directly or indirectly affect lives.

One of the earliest references to mudflow was made by McGee (1897) where it was called *sheet flood*. Blackwelder (1928) gave an interesting account of mudflows in Utah. Some of the accounts related by people who witnessed the flow paint a very graphic picture.

" The typical mudspate consists of mire charged with a great number of rock-splinters and blocks, but sometimes it may be composed

almost entirely of clean stones ranging in size from a peppercorn to large boulders...

"enormous boulder will float in this thick porridge like cork on water or iron on quicksilver..."

"Operating with a minimum water, the mudspate liquefies itself automatically when, during its descent, it becomes too thick. Sloping for a while, it dams the water runlet in the gully and this proceeds several times..."

"When left on an even slope, the middle of the mud runs faster, because there is less friction, while the slides, retarded by friction, deposition takes place, giving rise to an embankment..."

In May, 1941 the resort town of Wrightwood in the Southern California mountains was partly covered by mudflows which occurred for a week(Sharpe & Nobles, 1953). The debris was carried down 15 miles on a very gentle slope of 75 ft per mile with occasional surges whose fronts moved nearly at speeds of 15ft/sec.

Curry (1966) gave an account of the alpine mudflows of August, 1961 at the head of Mayflower Gulch in the Tenmile Range of Central Colorado. An extended rainfall of 24.5 cm over 24 hours initiated the mudflow that advanced in pulses at 16m/sec. Study showed that such events occurred in this area every 150-400 years. Older deposits were observed as concentric low ridges and mounds which were the remains of the lobate toes

Many of these events have also been reported in Canada. To June 1984, 41 such events had been reported with the first one being reported in 1963 (VanDine, 1985). On July 1967, alpine mudflows were observed (Broscoe & Thompson, 1969) on the ridges above Steele Creek, St Elias Range, Yukon. Four areas, namely, the Squamish Highway, Lower Fraser Valley, Coquihalla Freeway and Kicking Horse Pass have been identified as the locations of major debris flow activity in Southern B. C. (Hungry et al., 1987). Some of these events in these areas have resulted in loss of life and property damage. The creeks around Howe Sound, Southwest B.C. were responsible for the debris flow events of 1981 and 1983 (Russell, 1988) where 12 lives were lost. The debris flow event of Dec. 1980 around Hope (Miles & Kellerhals, 1981, Church & Miles, 1987) were responsible for damage to major highways and railway lines. Another study of alluvial fans of the Canadian Rockies (Jackson et al., 1987) showed evidence of the effects of past debris flow events.

Besides North America, debris flows are equally widespread in the European Alps, the Himalayas (Nash et al., 1987) and the Andes. These problems have been reported in Czechoslovakia (Midriak, 1985), China (Zhang et al, 1985), Indonesia (Legowo, 1985) and many other mountainous areas of the world. Several debris flow studies in Japan are probably some of the most detailed work done in this area. Every summer, the valleys in Mt. Yakedake in the Northern Japan Alps experience many mud and debris flow events. Suwa and Okuda (1980) have given extensive report of the nature of these events. One survey indicated that close to 63000 creeks in Japan were potential sources of debris flows (VanDine, 1985). In many of these cases there has been significant damage to property and life.

1.1.2 Extent of destruction

Some of the largest damages due to debris and mud flows have been documented in South America. The avalanche in Nevados Huascaron in the Peruvian Andes in 1970 involved $70 \times 10^9 \text{ m}^3$ of rock and debris that flowed down, traveling 16 Km of horizontal distance in 3 minutes. The damage was catastrophic (Plafker & Eriksen, 1978).

The damage from the 1983 debris flow in Utah was estimated as in excess of 250 million U.S. dollars with 2 million people sustaining direct damages. 22 out of 28 counties in the state were declared national disaster areas

(Jeppson, 1985). In the Canadian context up to 1984, 17 lives were lost and damage to bridges, roads and property was estimated at above 100 million dollars (VanDine, 1985). The risk is even more in Japan where close to 90 lives are lost each year (Takahashi, 1981). This significant loss to life and property necessitates the establishment of effective mitigative measures. These measures can be realized only when the flow of highly concentrated fluid is sufficiently understood. Appendices A-C discuss some general concepts in debris flows.

1.1.3 Objectives of the study

As a true debris flow is only possible under field conditions, laboratory studies represent only idealized situations covering a small band of a large spectrum of high concentrated fluid flows. However, laboratory studies present the possibility of controlled investigations. This study was approached with two objective. The first objective was to investigate the state-of-the-art in debris flows and establish a framework of the present understanding of high concentrated flows. The second objective was to generate and study debris flows in the laboratory. There is a practical difficulty in achieving, in a laboratory setting, the concentration range and particle gradation observed in a typical field debris flow. As one of the major component of the second objective included the measurement of velocity and

concentration distributions in open channel flows, hyperconcentrated flows were studied. Although hyperconcentrated flows carry smaller sediment load than debris flows, these flows represented the closest approximations to real debris flows that could be measured in the laboratory.

2 MECHANICS OF DEBRIS FLOWS

2.1 Introduction

The study of the behavior of a fluid requires that a suitable constitutive law be defined before a prediction can be made of any specific flow field. Because of the non-Newtonian nature of debris flows, the synthesis of a suitable constitutive law has proved to be a rather complex task. Debris flow presents itself as having a wide variation in its constituents and, therefore, its fluid properties. Thus, any comprehensive constitutive law will have to accommodate this variant nature of the fluid.

The flow of debris surge in a channel has three distinct regions of inhomogeneity. The gravely head, the viscous trunk and the turbulent tail comprise a flow situation that is far from any idealized slurry flow. It is probably more accurate to describe the flow by three different constitutive relations. But practically speaking, in the absence of a more comprehensive method of determining the properties of the fluid, this additional regard to details would probably not be a prolific effort. As a start, a simple approach will most likely lead to a better understanding of the mechanics of debris flows.

2.2 Initiation of Flow

The initiation of debris flows have been related to the following three reasons (Takahashi, 1981):

1. Landslide turning into debris flows
2. Breaking of naturally built dam turning into debris flows
3. Appearance of surface water stream during heavy rainfall mobilizing accumulated debris

The third reason can be looked at from a simple stability point of view and some general initiation criteria can be determined. Bagnold's (1954) limiting slope criteria is exactly the same as Eq.(3-3.6) except that he writes ϕ as ϕ_d where ϕ is the static internal friction angle and ϕ_d is the dynamic angle of internal friction.

Takahashi (1978) gives the initiation criteria for a non-cohesive debris flow which has been reviewed by Chen (1987).

2.3 Debris Flow Modeling

The flow of sediment water mixture is essentially a multiphase flow, and the behavior of the fluid phase and the solid phase and their interactions will have to be understood and then modeled. At the microscopic level, the non-uniformly distributed grains are going through inelastic collisions,

losing energy at each contact. As they travel at a mean longitudinal velocity, they carry fluctuating components with them. During all this time, they constantly interact with the fluid matrix exchanging momentum. The degree of this interaction will vary with the particle concentration of the mixture.

As one grain approaches another, one would expect a local increase in fluid pressure and a squeezing out of fluid into adjacent pores. As the fluid escapes, it dissipates energy. At the same time, it cushions the particle collisions resulting in further energy loss as well as the transfer of momentum from one particle to the other. In a two particle collision, Davis et al.(1986) found that as two spheres approach each other, the interparticle fluid is expelled and there is a severe increase in the pressure which results in an elastic repulsion of the spheres. The result showed that these particles finally approached an equilibrium spacing dictated by the effect of viscosity and the negative fluid pressure generated as the particles move away. It has yet to be found what extensions of this microscopic behavior can be made to multi-particle collisions, similar to that experienced in debris flows.

The above multi-particle dynamics combined with statistical approximations have been one of the approaches to modeling granular flows. Several attempts have been made in the case of dry granular flows(Lun et. al, 1984; Ogawa, 1978). These microstructure theories analyze, in detail, the dynamics

of individual particle collision and, with the use of statistical averaging, determine the continuum properties.

Bagnold's(1954) theory was the first approximate attempt to analyze this flow. One of the problems in directly applying most of these theories to debris flows is that they consider dry flow situations and thus avoid the inclusion of fluid and particle interactions. Bagnold's theory considers the case of neutrally buoyant spheres. Since Bagnold considers only the geometric and the kinematic conditions, the interactions of the fluid and the particles do not appear in his theory. Ackermann and Shen(1982), Shen and Ackermann(1982) proposed a theory where they not only account for the inelastic collisions and the surface friction of the particles, but also the viscous dissipation in the interstitial fluid in the form of drag as the grains move through the fluid containing them.

In addition to the above approaches, there are other rheological approaches (Goodman-Cowin, 1972; McTigue, 1978; Sayed & Savage, 1983) that are based on the mechanics of continuous media. These approaches involve the analysis of a mixture of the grain and fluid as a whole without considering the individual microstructure involved in the continuum. The drawback is that the parameters involved in these models have to be determined experimentally.

From the above discussions it is clear that a good constitutive model for debris flow should account for its

frictional nature, its viscous nature and the sediment fluid interaction.

2.3.1 Frictional Nature of Granular Material

The problems of mobility in avalanches and slope movements have been studied in great detail at the University of Alberta (Hung, 1981; De Matos, 1987). Hung and Morgenstern (1984a & b) conducted two sets of experiments to investigate the hypothesis of mechanical fluidization. Mechanical fluidization which attempts to explain the high mobility of stürzstroms is based on the premise that at high strain rates Coulomb's friction law breaks down because of a change in the type of particle contact. This results in a reduction of the apparent friction coefficient of the shearing mass which allows rock avalanches to move at steady velocities over flat slopes.

The first experiment involved sand and polystyrene beads flowing down a flume at velocities up to 6m/s with a typical depth of 10cm. Measurements of surface velocity, surface acceleration, depth of flow, mean density, bed shear, normal shear and mean velocity were made using a high speed camera and three load cells. Hung and Morgenstern (1984a) discovered from these experiments that the internal friction angle of the granular material studies showed no systematic dependence on the strain rate. In order to extend this finding to conditions with higher levels of normal and shear stresses, ring shear tests were also carried out on two types

of sand, wet and dry, sand-rock flour mixtures and polystyrene beads. These tests were carried out at circumferential velocities of 2m/s at normal stresses of up to 200 kPa. The results from this experiment indicated that the friction angle was again independent of strain rate and normal stress.

2.3.2 Dilatant fluid model

Bagnold's earlier interests were on the mechanics of the bed load transport of sediment. This interest motivated Bagnold to perform the classical experiment with neutrally buoyant, uniform 0.13 cm spherical wax beads suspended in water and glycerine-water-alcohol mixture (Newtonian fluid) and sheared in a coaxial rotating cylinder (Bagnold, 1954). A flexible rubber was used to form the inner wall of the cylinder. In this way Bagnold was able to measure the normal pressure in the radial direction as well as the torque. This experiment involved the shearing of various concentrations of grains in the rotating cylinder. Bagnold defined the following three regimes of flow behavior based on the degree of shear rate:

- i macroviscous
- ii transitional
- iii grain inertia

The ratio between the stress in the inertial regime and the viscous stress was defined as the dimensionless shear group N where

$$N = \frac{\lambda^{1/2} \rho_p D^2}{\mu} \frac{\partial u}{\partial y} \quad (2-3.1)$$

ρ_p is the mass density of the particle

μ is the viscosity of the interstitial fluid

D is the particle diameter

λ is the linear concentration of the particles

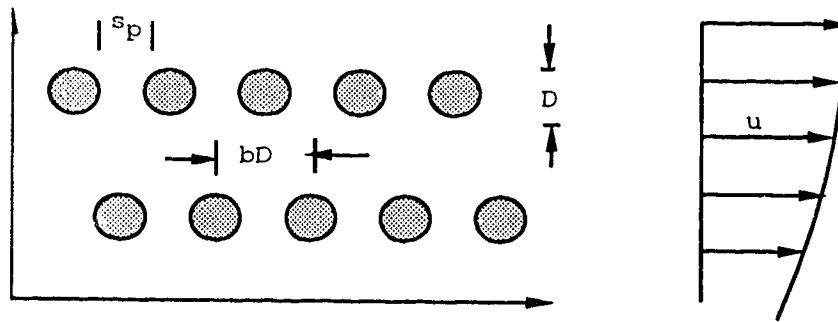


Figure 2-1 Definition sketch for Bagnold's (1954)
analysis of sheared granular material

If the mean center to center spacing of two particles is defined as bD and the distance of separation between two particles is s_p (Figure 2-2) then

$$bD = D + s_p \quad (2-3.2)$$

or

$$b = 1 + \frac{s_p}{D} \quad (2-3.3a)$$

or

$$b = 1 + \frac{1}{\lambda} \quad (2-3.3b)$$

where λ is $\frac{D}{s_p}$. The volume concentration is expressed as

$$C_v = \frac{C_\infty}{b^3} = \frac{C_\infty}{(1 + \frac{1}{\lambda})^3} \quad (2-3.4)$$

where C_∞ is the maximum possible concentration i.e. large λ . For uniform spheres with cannonball packing this is found to be $\pi/3\sqrt{2} = 0.74$.

Bagnold developed expressions for the two limiting regimes namely *macroviscous* and *grain inertia* regimes. These are defined based on the relative degree of shear rate in the flow. This can directly be translated in terms of N i.e. larger the N value, the bigger the importance of inertia hence the grain inertia regime. When N is low, there is more viscous effects than inertial effects and hence macroviscous regime.

In the macroviscous regime ($N < 40$) the viscosity is dominant and the normal and shear stresses are linear functions of the velocity gradient $\partial u / \partial y$.

$$P = a_v \lambda^{3/2} \mu \left(\frac{\partial u}{\partial y} \right) \cos \phi_d \quad (2-3.5a)$$

where P is the normal stress and a_v is a constant for the flow in the macroviscous regime. In the grain inertia regime ($N > 450$) the interstitial fluid has less influence in momentum transfer and the main effects are due to the grain-to-grain interaction. Bagnold attributed the primary mechanism for momentum transfer to the collision of one layer of particles

moving over a slower layer of particles. By using the analogy similar to the kinetic theory of gases, Bagnold gave the following expression for the normal dispersive pressure:

$$P = a_i \rho_s \lambda f(\lambda) D^2 \left(\frac{\partial u}{\partial y} \right)^2 \cos \phi_d \quad (2-3.5b)$$

From experiments, Bagnold found that the normal dispersive stress was related to the grain shear stress by

$$\tau_g = P \tan \phi_d \quad (2-3.6a)$$

or

$$\tau_g = a_i \rho_s \lambda^2 D^2 \left(\frac{\partial u}{\partial y} \right)^2 \sin \phi_d \quad (2-3.6b)$$

where

a_i is a constant to be determined from experiment for the grain inertia regime (Bagnold gave $a_i=0.042$)

ρ_s density of the particles

$f(\lambda)$ is an unknown function of λ

This grain shear stress is in addition to other fluid stresses such as turbulent stress. However, at high concentration, Bagnold argued that turbulence was damped. Equations (2-3.6) is also called **Bagnold's dilatant fluid model**. The presence of dispersive pressure was attributed to a "statistically preferred anisotropy in the spatial particle distribution" (Savage, 1984). The region in between the macroviscous and the quasistatic region has been defined by Bagnold as the transition region. In terms of N it lies in the range $40 < N < 450$.

For debris flow in the inertial regime, Takahashi(1978) uses the Equations (2-3.5b) and (2-3.6a) with a modification in the value of the constant a_i . The value of a_i , according to Takahashi, ranges between 0.35 to 0.5 determined from his flume experiments. This is different from 0.042 given by Bagnold. Julien and Lan(1991) find from the analysis of Bagnold's and other data that the value of a_i is 0.0087, assuming turbulent stress is negligible to dispersive stress. This discrepancy probably illustrates the limitation of Bagnold's dilatant fluid model to adequately describe debris flow. The important assumption in Bagnold's theory is that the particles are uniformly dispersed. This means that in a steady open channel flow the gravitational shear given by $\tau = \rho_{sat} g y \sin \theta$ is a straight line. However, the dynamic shear given by Equation(2-3.6b) is parabolic in nature. Therefore, it appears that a uniformly distributed model results in an inconsistent shear prediction.

2.3.3 Dilatancy

One concept that is important in granular flow is the concept of dilatancy. Dilatancy was first proposed by Reynolds (1885) who defined it as the nature of granular material to change the volume due to a change in grain arrangement. When a closely packed grain mass is sheared, the particles overriding each other cause the increase in volume of the mass. From experiment Bagnold (1954) found the *dispersive stress* to be proportional to the square of the

velocity gradient (shear rate). Therefore, during shearing of these kinds of material, the normal stress (dispersive stress) has a tendency to increase the thickness of the shear layer. Thus the sheared granular material gets its name "dilatant " material (Savage, 1987)

2.3.4 Bagnold's shear vs turbulent shear

Bagnold's model and the turbulent shear models are based on the ideas similar to the kinetic theory of gases. Both use this analogy to describe the shear between two layers of fluid in motion. Therefore a close examination reveals that both the equations have similar forms. Bagnold's dilatant fluid model which can be written as

$$\tau_g = a_i \rho_s \lambda^2 D^2 \left(\frac{\partial u}{\partial y} \right)^2 \sin \phi_d \quad (2-3.6b)$$

is a non-Newtonian fluid model. One of the turbulent shear models can be written as (Schlichting, 1968)

$$\tau_t = \rho_f \kappa_v^2 y^2 \left(\frac{\partial u}{\partial y} \right)^2 \quad (2-3.7a)$$

where

- τ_t is the turbulent shear
- ρ_f is the density of the fluid
- κ_v is the von Karman constant
- y is the distance from the wall

gives a clear indication of the non-Newtonian nature of turbulent flows. In the case of dilute sediment mixtures κ_v may be a function of sediment concentration C_v (Vanoni,

1975). In high concentration flows λ is also a function of C_v . In sediment transport turbulence is responsible for suspending the sediment particles. Similarly, in debris flows the dispersive pressure is responsible for dispersing the sediment particles. In many cases of granular flows both of these mechanisms are responsible for dispersion. O'Brien and Julien (1985) have used this idea in their model for debris flows. For the case of a highly sediment laden flow with particle size sufficiently small to be suspended by turbulence in water, Arai and Takahashi (1986) included a turbulent shear τ_t (analogous to the pure water turbulent stress) to the grain shear τ_g to give the total shear stress.

$$\tau = \tau_t + \tau_g \quad (2-3.8)$$

where

$$\tau_t = -\rho_m \overline{u'v'} = \rho_m l_m^2 \left| \frac{\partial u}{\partial y} \right| \frac{\partial u}{\partial y} \quad (2-3.7b)$$

$\rho_m = \rho_f + C_v (\rho_s - \rho_f)$, the mixture density, ρ_f is the fluid density and l_m is the mixing length. u' and v' are the fluctuating velocity in the direction of flow and perpendicular to it.

2.3.5 Quadratic Model of O'Brien and Julien

A general quadratic rheological model (Equation 2-3.9) was proposed by O'Brien and Julien (1985).

$$\tau = \tau_y + \mu \frac{\partial u}{\partial y} + C_1 \left(\frac{\partial u}{\partial y} \right)^2 \quad (2-3.9a)$$

μ is the dynamic viscosity

C_1 is the turbulent-dispersive parameter

The first term τ_y considered the yield strength of the fluid which was independent of the velocity gradient. The second term accounts for the viscous interaction of the fluid and the particles. The third term is a combination of Equation 2-3.6b and Equation 2-3.7b and accounts for the turbulent and the dispersive stresses. At sufficiently high concentration, the presence of particles would dampen turbulence but would increase dispersive stress. At low concentration the effect of turbulence would be pronounced. The constant C_1 was given as

$$C_1 = \rho_m l_m^2 + a_i \rho_s \lambda^2 D^2 \quad (2-3.9b)$$

where ρ_m is the density of the mixture

l_m is the mixing length

Julien and Lan(1991) rearranged the Equation (2-3.9a) in the following non-dimensional form

$$\tau^* = 1 + (1-T_d^*) a_i D_v^* \quad (2-3.9c)$$

where $\tau^* = \frac{\tau - \tau_y}{\mu \frac{\partial u}{\partial y}} \quad \tau_d^* = \frac{\rho_m l_m^2}{a_i \rho_s \lambda^2 D^2} \quad D_v^* = \frac{\rho_s \lambda^2 D^2}{\mu} \frac{\partial u}{\partial y}$

They used the data of Bagnold(1954), Savage and McKeown(1983) and Govier et. al. (1957) and fit their Equation(2-3.9a) to get τ_y , μ , C_1 . They used this to plot D_v^* vs τ^* and get a good fit with the above three sets of data. This model definitely is more physically based than some of the other available models. However, it needs to be verified by further measurements.

2.3.6 Bingham plastic and pseudo-plastic fluid models

The Bingham plastic fluid model has been observed to describe the flow of mud and fine grained debris under low shear rates (O'Brien and Julien, 1985, Major and Pierson, 1990, 1992). The Bingham plastic fluid model is characterized by a linear relation between the shear stress and the rate of strain. The yield stress τ_y and the viscosity μ are the two parameters.

$$\tau = \tau_y + \mu \frac{\partial u}{\partial y} \quad (2-3.10)$$

Yano & Daido (1965) used Bingham fluid model to describe the flow of mud. Johnson (1970) used this model to describe the flow of a steady debris flow in a circular channel. While studying the failure of tailings dams, Jeyapalan et al.(1983a & b) considered the case of flow in the laminar flow regime and used the Bingham model. Other unsteady debris flow models

also have employed the Bingham plastic constitutive equation (Schamber & MacArthur, 1985; MacArthur & Schamber, 1986).

The two parameters in the Bingham model are determined from experiments. These have been shown to depend on the sediment concentration and particle size. This will be discussed later.

The model that did not generate as much enthusiasm was the pseudoplastic or the power law fluid model

$$\tau = \mu \left(\frac{\partial u}{\partial y} \right)^\eta \quad (2-3.11)$$

where μ is the apparent viscosity and η is the flow behavior index which, in this case, is less than one. Yano and Daido (1965) have studied this in the case of mudflows. Other studies (Thomas 1963) failed to find any improvement over the Bingham model.

2.3.7 Coulomb viscous model

Generally speaking a highly concentrated mixture of solid and fluid tends to follow the *Mohr-Coulomb* criteria defined by

$$\tau = c + \sigma_n \tan \phi \quad (2-3.12)$$

where c is the cohesion
 σ_n is the normal stress
 ϕ is the angle of internal friction

The first term c is the cohesion and the second term describes the frictional resistance. In this equation the normal stress component σ_n can be dependent on the strain rate. This model is generally believed to be good for flow with small velocity. Johnson(1970) proposed that the total dynamic resistance is a combination of yield, frictional resistance and viscous resistance and called it the *coulomb viscous model*

$$\tau = c + \sigma_n \tan \phi + \mu \frac{\partial u}{\partial y} \quad (2-3.13)$$

where

μ is the viscous resistance
 $\frac{\partial u}{\partial y}$ is the shear rate

For continuous deformation σ_n is dependent on the shear rate, therefore, Johnson's addition of the last term would appear redundant. It is one of the earliest models for debris flows. It, however, provides a plausible insight into the problem.

In the viscoplastic models, the central assumption is that the continuous matrix is responsible for the yield strength and the viscous behavior of the debris and mud flows. Therefore, the properties of the matrix determine the dynamic resistance to shear as indicated by each form of the equation. One of the important drawbacks of these models is that these models fail to explicitly include the interparticle and particle-fluid dynamics. The effects of the interstitial

fluid is expressed through the rheological parameters. These effects are, however, dealt with in more explicit terms in the microstructural approach (Shen and Ackermann (1982), described later on, where the details of the collision and the partition of energy is considered.

2.3.8 Generalized viscoplastic fluid model

In an attempt to describe a more general form of a constitutive equation for debris flows Chen (1983) started first with a generalized Bingham plastic fluid model to be discussed in section 2.4.3. Three limiting regimes of flow were defined:

quasi static
macroviscous
grain inertia

Quasistatic state is an incipient state where the behavior is predominantly plastic. In the **macroviscous** state the mixture flows at low shear rates and the interstitial fluids are dominated by viscosity. The **grain inertia** regime is characterized by rapidly flowing granular materials where grain to grain interaction dominates the flow with the interstitial fluid playing a minor role. These regimes have been defined along similar lines as defined by Bagnold (section 2.3.2). Later Chen (1985a) presented a general model for debris flow which he called the generalized viscoplastic model. Chen (1988a) indicated that "a generally applicable

model which can realistically describe the rheological properties of debris flows should possess":

- i the ability to describe the dilatancy of the mixture
- ii soil yield criteria such as those developed by Mohr-Coulomb
- iii the ability to describe the role of the intergranular fluid

In order to satisfy the first two requirements, Chen proposed a model with both rate dependent (i.e. which has a shear rate term) and rate independent (i.e. which has a yield term) parts. This logic stems from the fact that a general solution should be able to describe all the regimes of flow i.e. quasistatic to grain inertia. If the flow was in a quasistatic flow (i.e. incipient flow) regime, then the rate dependent part would be less important and the rate independent part would dominate. At the other limit, if the flow was in a dynamic state, (i.e. the state of high shear rate) the rate dependent part would be more important. The third requirement is met by extending McTigue's (1982) equation where the rheological parameters are related to the interstitial fluid and its unknown particle concentrations.

The generalized viscoplastic flow (GVF) equation in 3D expressed in cartesian tensorial notation is given as (Chen, 1988c):

$$T_{ij} = -p \delta_{ij} + s D_{ij} / \sqrt{II_D} + 2 \mu_1 |4 II_D|^{(\eta-1)/2} D_{ij}$$

$$+ 4 \mu_2 |4 II_{D'}|^{(\eta-2)/2} D_{ik} D_{kj} \quad (2-3.14)$$

and

$$s = c \cos \phi + p \sin \phi \quad (2-3.15)$$

where

- T_{ij} is the total stress tensor
- p is the dynamic pressure
- δ_{ij} is the Kronecker delta
- s describes the yield
- c is cohesion
- ϕ is the static angle of internal friction
- D_{ij} is the rate of deformation tensor given by

$$D_{ij} = \frac{\partial u_i}{\partial x_j} + \frac{\partial u_j}{\partial x_i} \quad (2-3.16)$$

- u_i are the velocity components and
- x_i describe the coordinate axes

$$II_{D'} = \frac{1}{2} D_{ij}' D_{ij}' \quad (2-3.17)$$

which is the second invariant of the deviatoric rate-of-deformation tensor where

$$D_{ij}' = D_{ij} - \frac{1}{3} D_{ii} \quad (2-3.18)$$

i.e. stress less the isotropic component $\frac{1}{3} D_{ii}$.

- μ_1 is the consistency index

- μ_2 is the cross consistency index
- η is the flow behavior index
- $D_{ik}D_{kj}$ is the tensor product of the rate of deformation tensors in indicial notation

In the above GVF Equation(2-3.14) the second, third and the fourth terms respectively represent the plasticity, viscosity and the dilatancy of the mixtures.

In the case of one-dimensional simple shear flow situation the only non-zero velocity gradient is $\partial u/\partial y$ with u being the longitudinal velocity component, y is the vertical coordinate normal to the bed and positive upwards, the plasticity term reduces to s . The final equations for shear stress T and normal stress P are:

$$T = s + \mu_1 \left(\frac{\partial u}{\partial y} \right) \eta \quad (2-3.19)$$

$$P = -p + \mu_2 \left(\frac{\partial u}{\partial y} \right) \eta \quad (2-3.20)$$

$$s = c \cos \phi + p \sin \phi \quad (2-3.21)$$

The expression for s was given by Kanatani (1982) for isotropic, incompressible granular material.

In the above equations η may vary from 1 to 2 as the flow changes from a macroviscous state to a grain inertia state. The consistency and the cross-consistency terms given below

were determined using the form similar to the derivation of Kreiger & Dougherty(1959).

$$\mu_1 = A_1 (1 - KC_v)^{-B/K} \quad (2-3.22)$$

$$\mu_2 = A_2 (1 - KC_v)^{-B/K} \quad (2-3.23)$$

where K , often written as $1/C_\infty$, is the ratio of the volume of the sediment particle plus the bound water to that of sediment particle. B is the intrinsic viscosity similar to the theoretical value given by Einstein(i.e. 2.5). A_1 and A_2 are numerical constants expressed by Chen(1988c) as:

$$A_1 = a_\eta \rho_s^{\eta-1} D^{2(\eta-1)} \mu_w^{2-\eta} C_\infty^{-B/K} \quad (2-3.24)$$

$$A_2 = - a_\eta \rho_s^{\eta-1} D^{2(\eta-1)} \mu_w^{2-\eta} C_\infty^{-B/K} \quad (2-3.25)$$

where

a_η is Bagnold's a_i and a_v for debris flow in the grain inertia($\eta=2$) and macroviscous($\eta=1$) regimes, respectively (explained in Chen, 1986).

ϕ_d is the dynamic angle of internal friction.

The pressure p is modeled by Chen (1987) in a differential form developed from an equation of state under isothermal condition as:

$$dp = \frac{1}{K} \frac{dp}{\rho^{m'}} \quad (2-3.26)$$

K is the compressibility of the mixture, ρ is the bulk density of the flow, $d\rho = (\rho_s - \rho_w) dC_v$ and m' is an exponent. Since ρ is dependent on C_v , a variety of relations between ρ and C_v can be had from Equation (2-3.26) by varying K and m' . McTigue (1982) has used the following form of p :

$$p = \alpha' (C_v^2 - C_s^2) \quad (2-3.27)$$

where α' is a constant ≥ 0 and C_s is the concentration at the free surface. The form of p in Equation (2-3.27) can be obtained from Equation (2-3.26) by assuming $m' = -1$. Thus Equation (2-3.26) appears to be a somewhat general form for expressing p . Chen has attempted to define the various parameters of this model. Despite Chen's effort to generalize the rheology of debris flow, the model ends up having many parameters which are difficult to determine.

2.3.9 Ackermann and Shen's Model

The interaction between grain and fluid has often been ignored in granular flows until Shen and Ackermann (1982) included the viscous dissipation by drag as well as dissipation due to inelasticity and surface friction. Their constitutive relation for inertial granular flow is given as

$$\tau = \mu_a \frac{\partial u}{\partial y} \quad (2-3.28)$$

$$\mu_a = \frac{C_\infty}{2} \rho_s D^2 \lambda \left\{ \frac{(1+\epsilon)^3 (0.05 + 0.08\mu_f)^3}{\Gamma} \left(\frac{\lambda}{1+\lambda} \right)^3 \right\}^{1/2} \left(\frac{\partial u}{\partial y} \right) \quad (2-3.29)$$

$$\Gamma = \frac{3C_d\rho_f}{2\lambda\rho_s} + \frac{(1-\epsilon)^2}{8} + \frac{\mu_f(1+\epsilon)}{2\pi} - \frac{\mu_f^2(1+\epsilon)^2}{8} \quad (2-3.30)$$

where ϵ is the coefficient of restitution, μ_f is the coefficient of kinetic friction and C_d is the drag coefficient of the particle as it moves through the interstitial fluid.

2.4 Choice of a model

The next big question in debris flow modeling is which model do I choose. The models that have been developed so far range from a simple viscoplastic model (Bingham plastic) to highly theoretical models like the ones used in the study of rapid granular flows (Savage, 1979; McTigue, 1978). The simple models tend to operate satisfactorily within a narrow range while the theoretical model becomes too clumsy to be practical. Most of the work so far has been done using simple models (Chen, 1986). Some Japanese researchers have been using the dilatant fluid model in the form used by Takahashi(1978) in the modeling of debris flows in Japan. In dealing with the simple models, it is often more difficult to decide which one of the models gives a true description of the flow. In many cases the decision can be made solely by trial

and error procedure. Rickenmann(1991) suggests that if appropriate apparent viscosity is evaluated, even a Newtonian model is adequate for debris flows in steep channels.

Yamaoka et al.(discussed in Chen, 1986) have attempted to define a boundary between a material behaving as a dilatant fluid or a Bingham fluid. Their method does not have any theoretical basis but relies on experimental data. They define a roughness Reynolds number $R_s = u_* k_s / \nu_w$

where

$$u_* = \sqrt{gh \sin \theta} \quad (2-4.1)$$

h is flow depth

θ is the channel slope

k_s is the roughness size

g is the acceleration due to gravity

$\nu_w = \mu_w / \rho_w$ which is the kinematic viscosity of water

The second parameter represents the importance of the particle size D and concentration C_v and is defined as

$$D'_* = \sqrt{(\rho_s / \rho_w - 1) g D^3 \lambda / \nu_w} \quad (2-4.2)$$

such that D'_* decreases as D and C_v decrease. Their finding was:-

$R_s > 70$ and $D'_* > 1500$ dilatant fluid

$350 < D'_* < 800$ Bingham Fluid

$800 < D'_* < 1500$ transition

$D'_* < 250$ Newtonian fluid

There appears to be no definite guidelines as to what is a good choice.

2.5 Viscosity studies in suspensions

For infinitely dilute suspensions ($C \approx 0.05$), Einstein(1906) gave

$$\mu_a = \mu_w (1 + 2.5C_v) \quad (2-5.1)$$

where μ_w is the viscosity of water. For higher concentrations, several extensions have been made to account for the size and shape variations. Roscoe(1952) proposed two equations, one for non uniform particles and the other for uniform particles.

$$\text{non uniform} \quad \mu_a = \mu_w (1 - C_v)^{-2.5} \quad (2-5.2)$$

$$\text{uniform} \quad \mu_a = \mu_w (1 - 1.35C_v)^{-2.5} \quad (2-5.3)$$

Using the data of Ward and Whitmore(1950) with 50% particles of sizes 150micron to 190 micron and Eilers' (1941) study of sizes 3.4micron and 6.0micron, Roscoe showed that Equation (2-5.1) and (2-5.2) agreed well with the measurements.

An empirical approach has been used further by Thomas (in Bradley & McCutcheon, 1985) for particles sizes of 0.1 to 20 microns and concentrations up to 30% to give the apparent viscosity as

$$\frac{\mu_a}{\mu_w} = 1 + 2.5 C_v + 10.05 C_v^2 + 0.062 \exp \left(\frac{1.875 C_v}{1 - 1.595 C_v} \right) \quad (2-5.4)$$

Similarly, Do Ik Lee(1969) gave the following expression

$$\mu_a = \mu_w (1 - C_v)^{-(2.5 + 1.9C_v + 7.7 C_v^2)} \quad (2-5.5)$$

Chen (1986) used the expression for relative viscosity proposed by Kreiger & Dougherty (1959) in his GVF model

$$\frac{\mu}{\mu_w} = (1 - KC_v)^{-B/K} \quad (2-5.6)$$

where K, often written as $1/C_\infty$, is the ratio of the volume of the sediment particle plus the bound water to that of sediment particle. B is the intrinsic viscosity similar to the theoretical value given by Einstein(i.e. 2.5). Both the parameters B and K can be functions of shear rates.

3 MECHANICS OF STEADY DEBRIS FLOWS

The solutions of steady debris flows in the past have been presented under three different conditions. The normal practice has been to empirically correlate the velocity or the flow rate with physical parameters like the catchment area, particle size, depth of flow, slope and the intensity of rainfall.

The second form of debris flow analysis involves the use of one of the constitutive equations to get an integral solution of a steady, uniform debris flow with specific boundary conditions.

The third approach uses the steady Saint Venant's equation. In this approach one of the constitutive equations is used for modeling the flow resistance and the Saint Venant's equation is solved for a spatially varied flow situation (DeLeon and Jeppson, 1982).

3.1 Empirical approach

The earliest methods of predicting mudflows attempted to use Chezy's equation which worked satisfactorily with streamflows but not so well with mudflows. Some experiments were conducted with artificial mudflows in a natural environment in Kazakhstan (Gol'din & Lyubashevskiy, 1966) and the importance of the term $\frac{\gamma_s - \gamma_m}{\gamma_m}$ was recognized to give the channel mean velocity as

$$U = 3.15 h^{1/6} D^{1/3} \sqrt{\frac{\gamma_s - \gamma_m}{\gamma_m}} \quad (3-1.1)$$

where h is the average depth of flow (m)
 D is the diameter of a rock in the flow (m)
 γ_s is the specific wt. of rocks
 γ_m is the specific weight of mud and rock mass

Equation(3-1.1) does not use slope as one of its variables. Sribney's modified Chezy's formula which includes the effect of slope of the channel is given as (Takahashi 1981):

$$U = \Pi \left[\frac{\rho_s}{\rho_w} \frac{(\rho_s - \rho_w) C_v}{(\rho_s + \rho_w) (1 - C_v)} + 1 \right]^{-1/2} \quad (3-1.2)$$

where

$$\Pi = 6.5 h^{2/3} (\sin \theta)^{1/4} \quad (3-1.3)$$

and other symbols have their usual meaning. This formula has been found to yield satisfactory results in the debris flows in the Kamikamihori valley in the study done by Okuda et. al.(1980).

Takahashi(1981) has pointed out the study of Tsubaki and others done in 1972 in a flume of slope $\sin \theta = 0.383$ and 0.285 . The d_{50} of debris was 8mm and 0.32mm with a mixing ratio of 1:1.

The velocity of the front of the flow is given by

$$U = 2.5 (gh \sin \theta)^{0.5} \quad (3-1.4)$$

Recent studies of debris flows in Hunshui Gully in the Yuannan Province, China (Zhang et al., 1985) show a correlation between velocity and the depth of flow h and slope S_o .

$$U = 21 h^{0.48} S_o^{0.5} \quad (3-1.5)$$

This is very similar to the Chezy's equation for steady uniform flow in a wide channel:

$$U = C_{ch} \sqrt{g h S_o} \quad (3-1.6)$$

where C_{ch} is the dimensionless Chezy's coefficient. The Manning's equation

$$U = \frac{1}{n^*} h^{2/3} S_o^{0.5} \quad (3-1.7)$$

where n^* is the Manning's roughness, has also been used to estimate a mean velocity in a channelized debris flow (Chen, 1983). Equation (3-1.7) and the integrated form of the semi-logarithmic equation for turbulent flow in a channel discussed later in the text Equation (3-2.29) can be combined to give the following expression for n^* in terms of the equivalent sandgrain roughness k_s (Ranga Raju, 1981) in SI units

$$n^* = \frac{k_s^{1/6}}{25.6} \quad (3-1.8)$$

3.2 Uniform flow using rheological models

In this section the solutions for debris flows using the following more prominent rheological models will be reviewed.

- i Bingham plastic and pseudoplastic
- ii Dilatant fluid model
- iii Generalized viscoplastic model

3.2.1 Bingham Plastic and power law models

The rheological relation for Bingham plastic fluid may be written as

$$\tau = \tau_y + \mu \frac{du}{dy} \quad (2-3.10)$$

For uniform flow in open channels with linear shear distribution we have

$$\tau = \gamma h \sin \theta \left(1 - \frac{y}{h}\right) \quad (3-2.1)$$

where h is the depth of flow, y is the distance from the bed and $\sin \theta$ is the slope of the bed.

In the simplest form, Equation(2-3.10) is used with Equation(3-2.1) and integrated with the boundary condition $u=0$ at $y=h$ to give

$$u = \frac{1}{\mu} \gamma_m y \sin \theta \left[\left(h - \frac{y}{2}\right) - \frac{\tau_y}{\gamma} \right] \quad (3-2.2)$$

In order to locate the point where the plug starts (h_0) with $u=U_{\max}$ and $\frac{du}{dy} = 0$

$$\frac{du}{dy} = 0 = \frac{1}{\mu} [\gamma_m \sin \theta (h - h_0) - \tau_y] \quad (3-2.3)$$

or

$$h_0 = h - \frac{\tau_y}{\gamma_m \sin \theta} \quad (3-2.4)$$

3.2.1.1 Chen's analysis

Chen(1983) gave a solution for a generalized Bingham plastic model. It is one form of the generalized viscoplastic model which Chen later proposed. The model is given as:

$$\tau = \tau_y + \mu_1 \left(\frac{du}{dy} \right)^\eta \quad (3-2.5)$$

$$\text{for } |\tau| \geq \tau_y ; \text{ and } \frac{du}{dy} = 0 \text{ for } |\tau| \leq \tau_y$$

where μ_1 and η are referred to as the consistency index and flow behavior index, respectively. For a general case, when $\tau_y \neq 0$ and $\eta=1$ Equation (3-2.5) can be solved. Equation (3-2.1) is used to model the shear in the mud debris flow, where ρ is the bulk density of the mixture, g is the gravitational acceleration, $\sin \theta \approx S_0$ is the slope of the bed, h is the depth of flow perpendicular to the bed. If h_0 is the depth at which $\tau = \tau_y$ then

$$\tau_y = \gamma S_0 (h - h_0) \quad (3-2.6)$$

Incorporating this in Equation(3-2.5) yields,

$$\frac{du}{dy} = \left[\frac{\rho g \sin \theta (h_o - y)}{\mu_1} \right]^{1/\eta} \quad (3-2.7)$$

for $0 \leq y \leq h_o$; and $\frac{du}{dy} = 0$ for $h_o \leq y \leq h$

Assuming that ρ and μ_1 do not change over the depth in the flow, which is an idealization, the Equation(3-2.7) can be integrated with boundary condition $u=0$ at $y=0$ to give

$$u = \frac{1}{\eta_*} \left(\frac{\rho g S_o}{\mu_1} \right)^{1/\eta} h_o^{\eta_*} \left[1 - \left(1 - \frac{y}{h_o} \right)^{\eta_*} \right] \quad (3-2.8)$$

for $0 \leq y \leq h_o$

$$\text{where} \quad \eta_* = \frac{\eta+1}{\eta}$$

$$\text{and} \quad u = \frac{1}{\eta_*} \left(\frac{\rho g S_o}{\mu_1} \right)^{1/\eta} h_o^{\eta_*} \quad (3-2.9)$$

for $h_o \leq y \leq h$

The mean velocity for the section is obtained by integrating Equation (3-2.8) over y and dividing the result by h gives

$$U_m = \frac{1}{\eta_*} \left(\frac{\rho g S_o}{\mu_1} \right)^{1/\eta} \left(\frac{h_o}{h} \right)^{\eta_*} \left[1 - \frac{\eta}{2\eta+1} \left(\frac{h_o}{h} \right) \right] h^{\eta_*} \quad (3-2.10)$$

The normalized form of Equations(3-2.8) is

$$\frac{u}{U_m} = \frac{1 - \left[1 - \left(\frac{y}{h} \right) \left(\frac{h}{h_o} \right) \right]^{\eta_*}}{1 - \frac{\eta}{2\eta+1} \left(\frac{h_o}{h} \right)} \quad \text{for } 0 \leq \frac{y}{h} \leq \frac{h_o}{h} \quad (3-2.11a)$$

When the yield is negligible (i.e. $h/h_o = 1$) and $\eta=1$, Equation (3-2.11a) can be written as

$$\frac{u}{U_m} = \frac{3y}{h} \left(1 - \frac{y}{2h} \right) \quad (3-2.11b)$$

The normalized form of Equations(3-2.9) is

$$\frac{u}{U_m} = \frac{1}{1 - \frac{\eta}{2\eta+1} \left(\frac{h_o}{h} \right)} \quad \text{for } \frac{h_o}{h} \leq \frac{y}{h} \leq 1 \quad (3-2.12)$$

The parameter h_o/h indicates the relative strength of the yield τ_y against the bed shear τ_b . Chen(1983) refers to h_o/h as the **yield stress index**.

3.2.2 Dilatant fluid model

The concept of dispersive stress was first introduced by Bagnold(1954). This model described by Equations(2-3.5b) and (2-3.6) have been used by Takahashi(1978) in the analysis of steady uniform debris flow.

In a channel of depth h , say, a layer above a distance y from the bed starts moving. The effective normal stress at impending motion is given as:

$$\sigma_n = \gamma_{sat} (h-y) \cos \theta - \gamma_w(h-y) \cos \theta \quad (3-2.13)$$

The first term is the normal component of the stress due to the body force. The second term is the hydrostatic stress in a flow inclined to the bed of slope $\sin \theta$.

Replacing γ_{sat} by $[\gamma_w + (\gamma_s - \gamma_w)C_v]$ the above expressions yield

$$\sigma_n = C_v(\gamma_s - \gamma_w) (h-y) \cos \theta \quad (3-2.14)$$

Similarly, the gravitational shear component τ for uniformly distributed particle solid mixture is given as

$$\tau = \gamma_{sat}(h-y) \sin \theta \quad (3-2.15)$$

replacing γ_{sat} by $[\gamma_w + (\gamma_s - \gamma_w)C_v]$ the above expression can be written as

$$\tau = [\gamma_w + (\gamma_s - \gamma_w)C_v] (h-y) \sin \theta \quad (3-2.16)$$

By combining Equation(3-2.16) with Bagnold's model for fully inertial flow in open channels yields

$$a_i \rho_s \lambda^2 D^2 \left(\frac{\partial u}{\partial y} \right)^2 \cos \phi_d = C_v(\gamma_s - \gamma_w) (h-y) \cos \theta \quad (3-2.17)$$

$$a_i \rho_s \lambda^2 D^2 \left(\frac{\partial u}{\partial y} \right)^2 \sin \phi_d = [\gamma_w + (\gamma_s - \gamma_w)C_v] (h-y) \sin \theta \quad (3-2.18)$$

where

- a_i is a constant
 ρ_s is the grain density
 γ_w is the unit weight of the fluid
 λ is the linear concentration defined by

$$\lambda = \left[\left(\frac{C_\infty}{C_v} \right)^{1/3} - 1 \right]^{-1} \quad (3-2.19)$$

- C_∞ is the volumetric grain concentration in static debris bed
 C_v is the volume concentration of solids in debris flow
 θ is the slope angle of the flow surface
 ϕ_d is the dynamic angle of friction
 D is the particle diameter

On solving Equation(3-2.17) with the boundary condition $u=0$ at $y=0$ yields

$$u = \frac{2}{3D} \left\{ \frac{g \sin \theta}{a_i \sin \phi_d} \left[C_v + (1 - C_v) \frac{\rho_w}{\rho_s} \right] \right\}^{1/2} \frac{1}{\lambda} [h^{3/2} - (h-y)^{3/2}] \quad (3-2.20)$$

where h is the depth of flow. The mean velocity is given by

$$U_m = \frac{2}{5D} \left\{ \frac{g \sin \theta}{a_i \sin \phi_d} \left[C_v + (1 - C_v) \frac{\rho_w}{\rho_s} \right] \right\}^{1/2} \frac{1}{\lambda} h^{3/2} \quad (3-2.21)$$

Making use of Bagnold's experiments Takahashi(1978) deduced

$$C_v < 0.81 C_\infty ; \quad a_i = 0.022$$

$$\text{for } C_v \geq 0.81 C_\infty ; \quad a_i = 0.066 (\lambda - 12) + 0.022$$

The normalized velocity profile can be written as

$$\frac{u}{U_m} = \frac{5}{3} \left\{ 1 - \left(1 - \frac{y}{h} \right)^{3/2} \right\} \quad (3-2.22)$$

The above expression is typical of a dilatant fluid model.

This expression can also be arrived at by writing the momentum equation for non-accelerating flow in a channel and integrating it to obtain the τ_{12} component of the stress.

This component after equating with Ackermann and Shen's equations (Eqs.2-3.28 to 2-3.30) can be integrated to give the same normalized expression as (3-2.22).

3.2.3 Generalized viscoplastic model

Chen used the GVF model and gave an effective stress version of the equations of motion as

$$\rho_m g (h-y) \sin \theta = c \cos \theta + \bar{p} \sin \phi + \mu_1 \left(\frac{\partial u}{\partial y} \right)^\eta \quad (3-2.23)$$

and

$$- \rho' g (h-y) \cos \theta = \mu_2 \left(\frac{\partial u}{\partial y} \right)^\eta \quad (3-2.24)$$

where \bar{p} is the effective dynamic pressure and $\rho' = \rho_m - \rho_w$.

Solving Equations (3-2.23) and (3-2.24) simultaneously for u gives

$$u = \frac{1}{\eta_*} \left(\frac{\rho^* g \sin \theta}{\mu_1} \right)^{1/\eta} h_o^{\eta_*} \left[1 - \left(1 - \frac{y}{h_o} \right)^{\eta_*} \right] \quad (3-2.25)$$

$$\text{for } 0 \leq y \leq h_o$$

where $\eta_* = \frac{\eta+1}{\eta}$

$$\rho^* = \left[\frac{1 - (\rho'/\rho_m) \cot \theta \sin \phi}{1 + (\mu_1/\mu_2) \sin \phi} \right] \rho$$

and
$$u = \frac{1}{\eta_*} \left(\frac{\rho^* g \sin \theta}{\mu_1} \right)^{1/\eta} h_o^{\eta_*} \quad (3-2.26)$$

$$\text{for } h_o \leq y \leq h$$

These equations are almost exactly the same as the solutions presented earlier for generalized Bingham plastic fluid (Equations 3-2.8 and 3-2.9). The equation for the mean velocity is also same as Equation (3-2.24). An alternative form of the equations of motion for flow with concentrations varying in the vertical direction has been given by Chen (1987, 1988a & b) using the differential form of the GVF model. The details of the generalized solutions for the viscoplastic debris flow can be found in the paper by Chen (1988a & b).

3.2.4 Arai and Takahashi's Equation

Assuming a linear shearing stress and $l_m = \kappa_v Y$ where κ_v is the Karman constant, Equations 2-3.6, 2-3.7, 2-3.8 are used to give the velocity distribution in the channel as

$$\frac{u}{u_*} = \frac{1}{\kappa_v} \ln \frac{Y + \sqrt{Y^2 + \phi^2}}{Y_o + \sqrt{Y_o^2 + \phi^2}} \quad (3-2.27)$$

where for rough bed

$$Y = \frac{Y}{h} ; \quad Y_o = \frac{k_s}{30 h} ; \quad u_* = \sqrt{g h \sin \theta}$$

$$\phi^2 = \lambda^2 \left(\frac{a_i \sin \phi_d}{\kappa_v^2} \right) \left(\frac{\rho_s}{\rho_m} \right) \left(\frac{D}{h} \right)^2 \quad (3-2.28)$$

k_s is the equivalent sand grain roughness of the bed, θ is the bed slope and ϕ_d is the dynamic angle of friction. For vanishing concentrations, ϕ tends to zero and Equation (3-2.27) reduces to the velocity profile for rough turbulent clear water flow in a rectangular channel

$$\frac{u}{u_*} = \frac{1}{\kappa_v} \ln \frac{Y}{k_s} + 8.5 \quad (3-2.29)$$

It can be observed from Fig.3-1 that the presence of particles in the fluid has the effect of increasing the friction in the fluid and hence reducing the velocity. It is interesting to note that the nature of the profile remains unaltered.

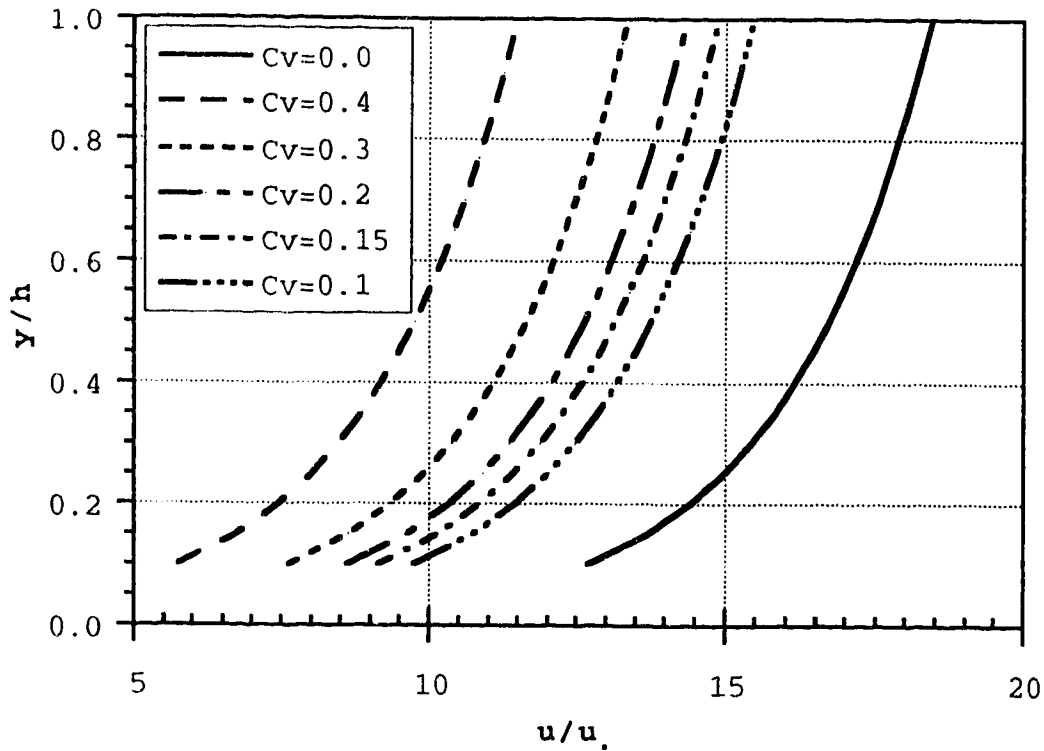


Figure 3-1 Dimensionless velocity profiles for sediment water mixtures using turbulent dispersive model with $D=0.215\text{mm}$

3.2.5 Turbulent diffusion of sediment

After writing continuity equations for both fluid and sediment, Hunt(1954) gave the following sediment diffusion equation.

$$\frac{dC}{dy} + C(1-C)w = 0 \quad (3-2.30)$$

where C is the concentration at a depth y and w is the fall velocity. When the concentration of sediment is small and the motions of particles and the fluid are identical, i.e momentum diffusion rate and particle diffusion rate are equal, Rouse(1937) solved Equation (3-2.30) to give the

following equation for the vertical distribution of sediment particles

$$\frac{C}{C_o} = \left[\left(\frac{d - y}{y} \right) \left(\frac{a}{d - a} \right) \right]^Z \quad (3-2.31)$$

where $Z = \frac{w}{\beta \kappa u_*}$

This equation shows that the sediment concentration C at any point y depends on the depth of flow d , the reference concentration C_o at a distance a from the bed. Z represents the ratio between the fall velocity w to the product of von Karman constant κ , the shear velocity u_* , and the ratio of sediment diffusivity to the momentum diffusivity κ . Einstein and Chien (1955) found that Equation (3-2.31) was not able to reproduce the concentration distributions at mean concentrations beyond 3% by volume. Woo and Julien (1988) numerically solve Equation (3-2.30) in the concentration range 4 to 20% by volume. The following expression for the fall velocity for hindered settling w_m given by Richardson and Zaki (1954) was used.

$$w_m = w(1-C)^\alpha \quad (3-2.32)$$

α , which depends on the particle Reynolds number and particle shape, decreases from 4.65 to 2.35 as the particle size increases from silt to gravel. Winterwerp et al. (1991) have examined Equation (3-2.31) with modified Z using w_m instead of w . By using the measured concentration C_o , w_m and C_o were

solved iteratively using Equations (3-2.31) and (3-2.32).
The use of w_m in Equation (3-2.31) resulted in concentration
distributions that were closer to their measurements.

4 LABORATORY MEASUREMENTS OF HYPERCONCENTRATED FLOWS

4.1 Introduction

A major limiting factor in our understanding of debris flows has been the lack of measurement of its hydraulic properties. There is a general dearth of field observations because the incidental occurrences usually find the observer unprepared. Furthermore, conventional measuring techniques are primitive and new techniques have yet to be tried and implemented (Pierson 1985). Unlike studying streamflow, the very dense nature of debris flow poses most of the difficulties in the field for making reliable measurements of velocity and concentration profiles. In larger scale events the safety of those in the field is a serious concern.

In debris and mud flows, the general practice has been to borrow ideas from granular flow theories and adapt them to the individual flow regimes. This has called for a serious experimental approach to define the mechanics of these flows. The high concentration fluid behaves very differently from the ordinary Newtonian fluid. Several constitutive laws have been proposed for these fluids but the lack of reliable velocity measurements has made it difficult to confirm the validity of these constitutive laws. The concentration distribution of the particles is also of equal importance because it gives us the shear distribution in the flow. Because of the complex nature of the flows, it is essential

to conduct experiments in the laboratory under controlled conditions with as few constraints as possible.

4.1.1 Past Experiments

4.1.1.1 Velocity and Concentration

Most of the earlier experiments on debris flows focussed on understanding the rheology of the fluid (Sayed 1981, Kang and Zhang 1980, O' Brien & Julien 1988, Ghahramani-Wright 1987) using either viscometers and shear cells or using flow in open channels (Johnson 1970, Savage 1979, Takahashi 1980, Tsubaki and Hashimoto 1983, Ghahramani-Wright 1987, Winterwerp et. al. 1990). In some of these cases actual debris flow deposits have been used while others have used ordinary sand and clay in their respective works.

Debris flows in the field have been observed to be predominantly unsteady. However, steady flows are also possible. One of the many difficulties of studying debris flows in the laboratory is the generation of the flow under controlled conditions. The unsteady flow, in principle, may be easier to generate but very difficult to record. The measurements are difficult because of the very short duration of the flow and the need to work with long channels. One trial conducted in a preliminary study with 15L of saturated sand water mixture, released suddenly on a slope of 25 degrees, travelled as a surge, a distance 4.25m in 4 sec. These problems have been dealt with, with some degree of success, in a few studies (Hirano & Iwamoto 1981, Davies

1988, Chi-Hai et. al. 1990) by arresting the flow in a belt driven flume.

Velocity and concentration distributions have been more difficult to measure than the rheological properties. Because of the highly abrasive nature of the flow, it is not possible to use standard probes used in the study of Newtonian fluid flow. The few measurements that have been made are sketchy and of short duration. Yano and Daido (1965) measured the velocity distribution in a clay slurry ($C_v < 13\%$), using a *modified pitot tube*. The dynamic and static pressure needed to inject water into the flow to prevent clogging of the tube, gave the required velocity. Wang (1990) used a similar method combined with tracer particles to measure velocity profiles and radioisotope concentration meter to measure concentration profiles. Takahashi (1978) made velocity and concentration measurements in a channel inclined at 10° to 20° with C_w 33% to 44%. Debris flow was generated by passing a constant discharge over a saturated mass which failed and flowed down in a quasi-steady manner. Velocity was measured using *close-up photographs* of particle movement in contact with the wall. Arai and Takahashi (1983) injected salt into a flow and measured the conductivity change at points downstream using two or three serial probes. The velocity was given by the time lag between two points. Hirano and Iwamoto (1981) measured velocity and concentration profiles in a bore using cine-camera. The concentration was determined by counting

particles in contact with the wall. The velocity distribution appeared to be almost uniform and the concentration was found to be smaller near the bed. It is yet to be confirmed how representative these measurements are because they were obtained by tracking particles next to the wall. An **optical sensor method** has been tried in the case of dry granular flows (Savage 1979). In this technique, two optical sensors were arranged side by side next to a transparent wall. A cross correlation of the output of the two sensors gave the velocity of the particle. This, however, has the same limitations as the photographic technique. Recently Winterwerp et al. (1990) used an electromagnetic flow meter for their measurement. They report turbulent flow in 30 cm deep, 30 cm wide and 9m long flume with specific flow rates of 10-150 m²/s and laminar flow in 4.5 cm deep, 11.8 cm wide and 1.5 m long flume with specific flow rates of 1-5 m²/s. It is interesting to see that even at high mean concentration, the equilibrium slope in a large flume is almost an order of magnitude smaller than in the case of the small flume.

4.2 Present study

4.2.1 Preliminary Works

Several trials were made in the earlier stages of the study to understand the physical behavior of granular materials. Since the primary interests were to generate a flow and improve the slurry handling capabilities in the

laboratory, various trials were made to define the appropriate conditions suited to debris flow generation. One of the aims of the trial was to find an appropriate flume and the method of producing a flow. In order to improve an overall preliminary understanding of granular flows, both dry and wet granular flows were examined in the lab.

4.2.1.1 Dry Granular Flows

Poorly sorted sand 0.5 mm median diameter was used in this experiment. Sand was released suddenly by opening a swivel gate at the upstream end of a flume in the form of a dam break. Two sizes of plexiglass flumes were used. The small flume was 1.35m long, 16cm wide and 21cm high. The large flume was 4.25m long, 15cm wide and 0.54m high. Sandpaper with roughness 0.5mm was glued to the bed of the flumes. The volumes of the material released in the large flume was around 20L and 2L in the small flume. The flumes were inclined at 20-30° and the surges were studied using a video camera and an ordinary camera with 35mm lens and varying shutter speeds.

The main aim of this exercise was to observe the general behavior of dry granular material. The first observations were of the nature of the surges, the inverse grading in the flow (Plate 4-1) as well as segregation on the deposits (Plate 4-2). Note the fine sand on the bed in Plate 4-1. It was observed that the surge front was a cloud of fines with

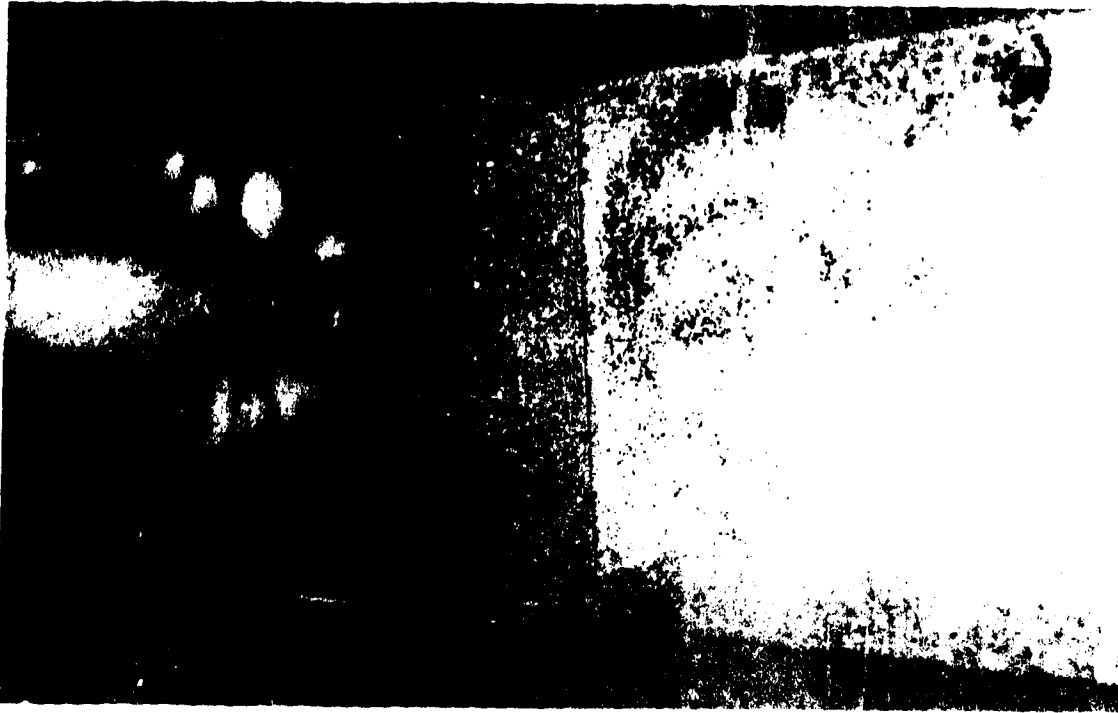


Plate 4-1 Inverse grading in dry granular flow (flow l to r)

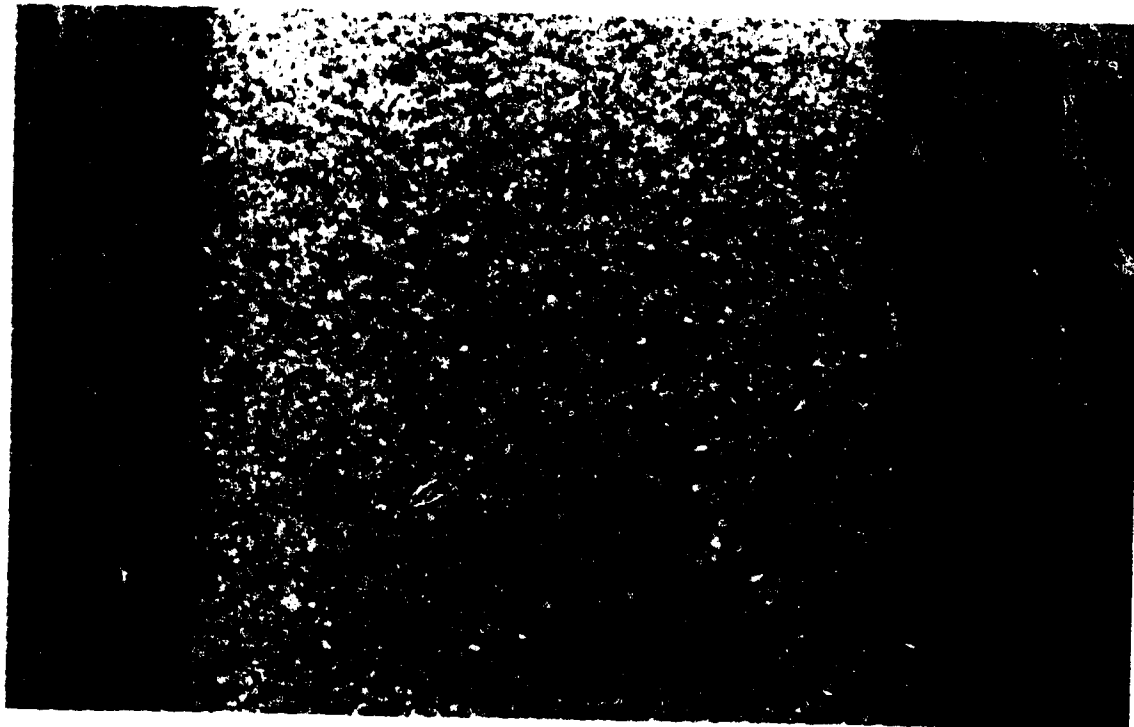


Plate 4-2 Segregation on the surface of dry granular flow deposit (flow from top to bottom)

the main flow trailing behind. It was interesting to note from the streak lines on the flow surface that the dry granular flow had distinct shear layers next to the wall (Plate 4-3) compared to saturated flow for which shear layer was virtually missing (Plate 4-4). If it was present, it was confined to approximately 5mm from the wall (which were the closest streak lines observed in the photograph)

4.2.1.2 Sand Water Mixtures

Studies similar to dry granular flows were done with saturated sand water mixtures. The same two flumes were used with the same roughness. It was observed in the large flume that a volume of 20L of saturated mass produced a flow depth of around 2cm as it flowed down. This gave some indication regarding the flow depths achievable in the laboratory with small volumes.

The surges were well formed if the mass was kept agitated before the gate was released. Otherwise progressive rotational failures, very similar to slope failures, were observed once the gate was opened. Several attempts were made to deflect away from the bed that part of the main flow next to the wall and study the streak lines at the centre of the channel through the plexiglass walls of the flume. Photographic problems were encountered as a result of poor lighting in the area of flow deflection. The large flume,

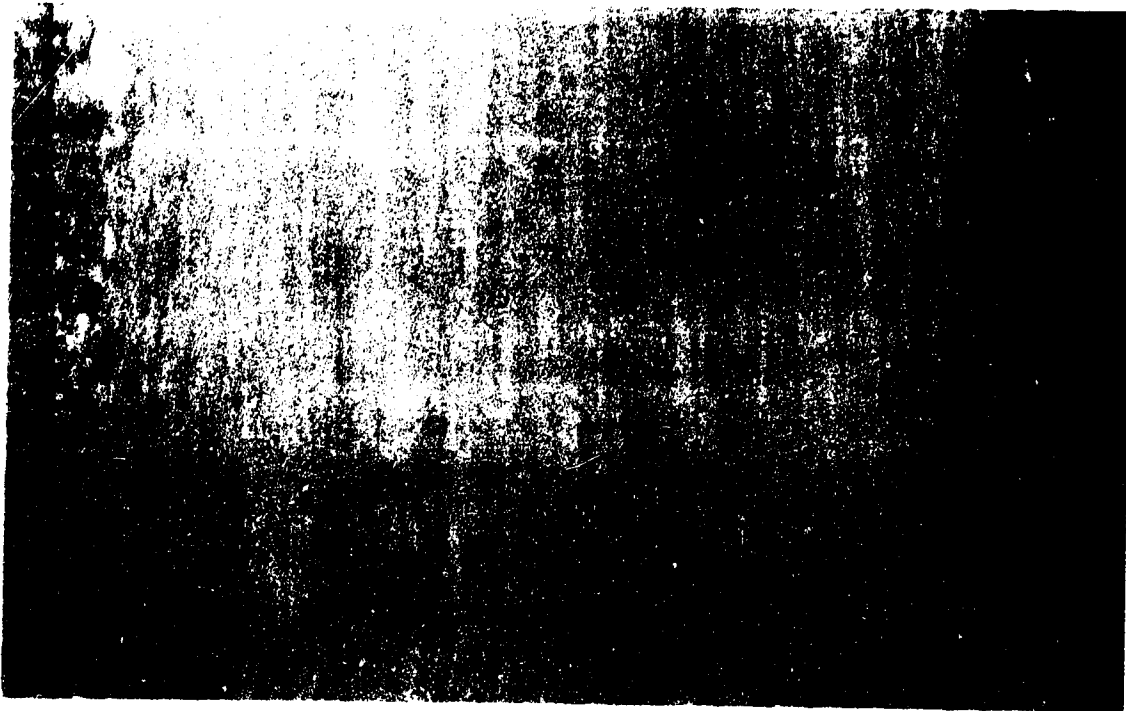


Plate 4-3 Shear layer near the wall in dry granular flow

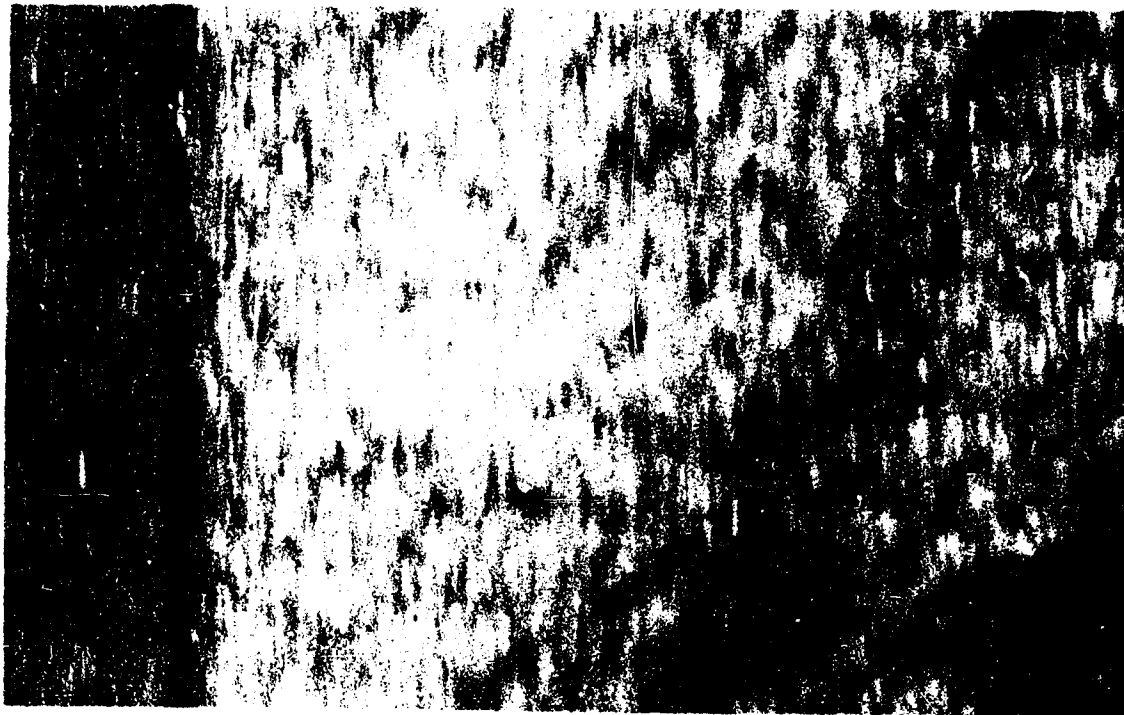


Plate 4-4 Shear layer near the wall in a flow of saturated
sand water mixture

therefore, gave some qualitative information on the shear layer next to the wall as described earlier and inverse grading in the flow deposit and the surge front (Plate 4-5). It also opened up possible avenues for future investigation such as the run-out distances for debris flows (Plate 4-6).

In the last stage of the preliminary study, a conveyor belt driven flume 3m long and 25 cm wide, very similar to that used by Hirano and Iwamoto(1981), was tried. Since the flume leaked and the particles produced unwanted abrasion in between the belt and the flume bed, this technique was not pursued seriously. However, this technique holds significant promise for future studies of unsteady surges.

4.3 Steady Debris Flows

For both steady and unsteady debris flows, the main difficulty in the laboratory lies in generating representative flows. Unsteady flows are of shorter duration and may require significant channel length. Steady debris flow, on the other hand, requires a long duration before any direct measurements can be made. Without recirculating, this would require large volumes of material to be fed continuously.

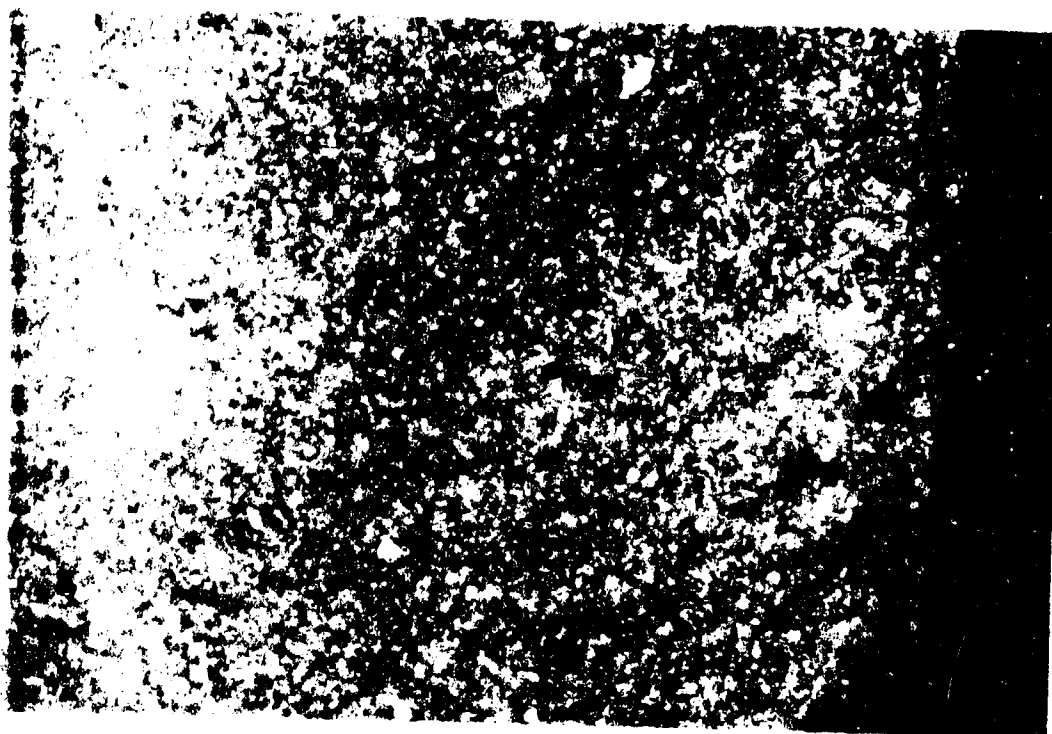


Plate 4-5 Segregation in the surge front of a saturated granular flow. Surge frozen at high shutter speed (flow top to bottom)

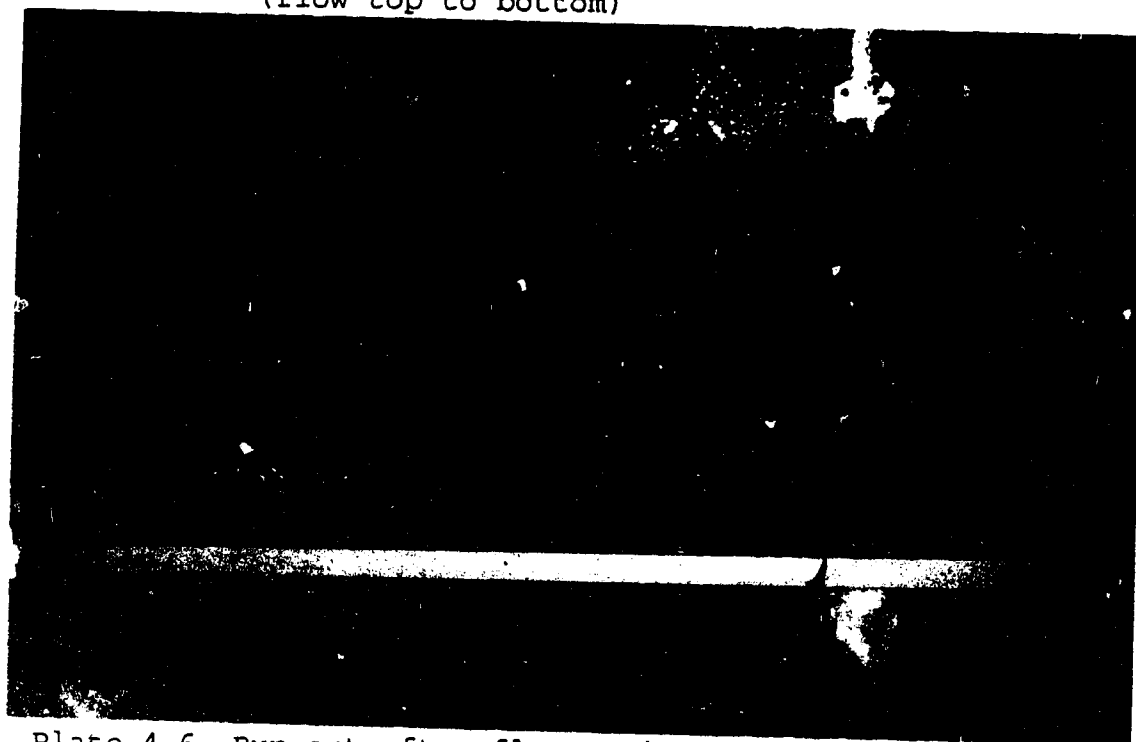


Plate 4-6 Run-out after flume exit (flow left to right)

4.3.1 Experimental Arrangement

The objective of the study was to generate a steady, uniform flow of a highly concentrated sand-water slurry, initially, without mixing any clay or silt size particles. In order to avoid using large volumes of the material, but at the same time generate the flow for a long duration (typically two hours), a continuous pumping system (Plate 4-7, Fig. 4-1c) was designed (Mainali & Rajaratnam 1991). The channel was on a slope of 28.6% which was slightly above a slope at which sediment started to deposit on the bed. Bed roughness was provided by gluing sand paper cloth having an equivalent roughness of 0.56mm. A mixture of sand and water in a hopper was pumped using a Seepex eccentric screw pump 35-6L BN/110-1531-203-111 which, when pumping water, operated at 86 to 375 RPM producing discharges of 3L/s to 12L/s respectively. The maximum discharge was reduced by approximately 15% when the concentration of the mixture was around 20%. The stator was made of soft natural rubber and the rotor was a hardened tool steel 0.64 m long. Mixing took place at the upstream end of the flume when the fluid poured from the hose into the flume and when the fluid entered the rectangular hopper at the downstream end of the flume. The system was first started with some water and then sediment was gradually added into the hopper. At steady state, there was some deposit of sediment that remained in the upstream corners of the hopper. As this deposit did not grow and as

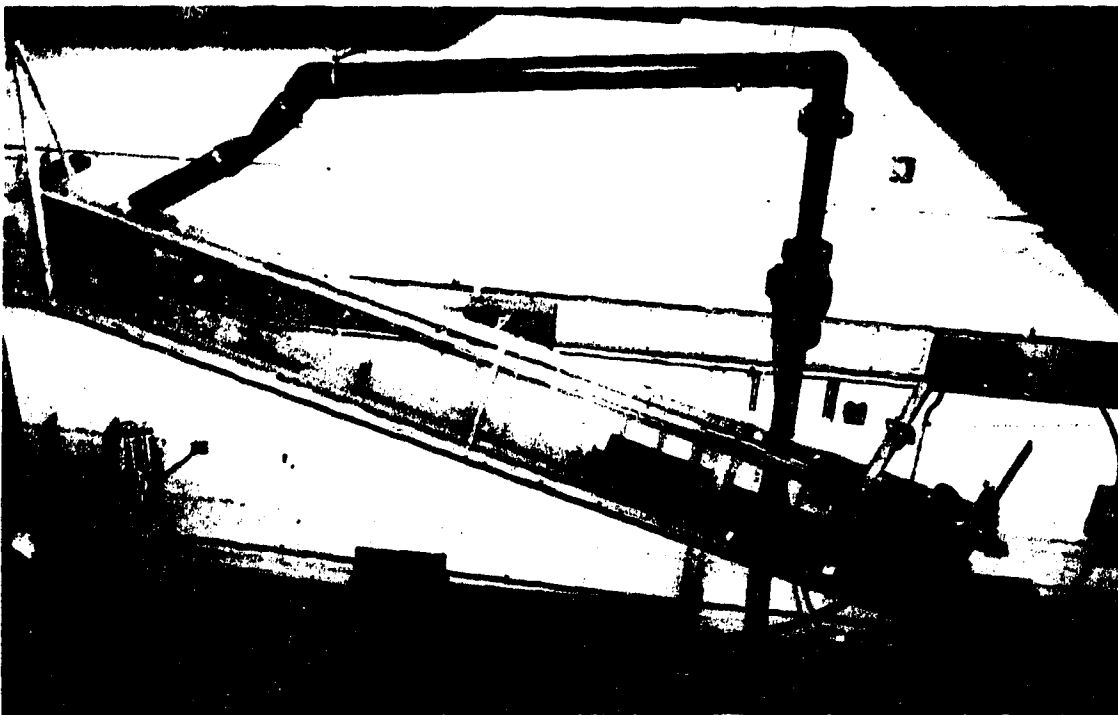


Plate 4-7 Continuous pumping system for steady uniform debris flow

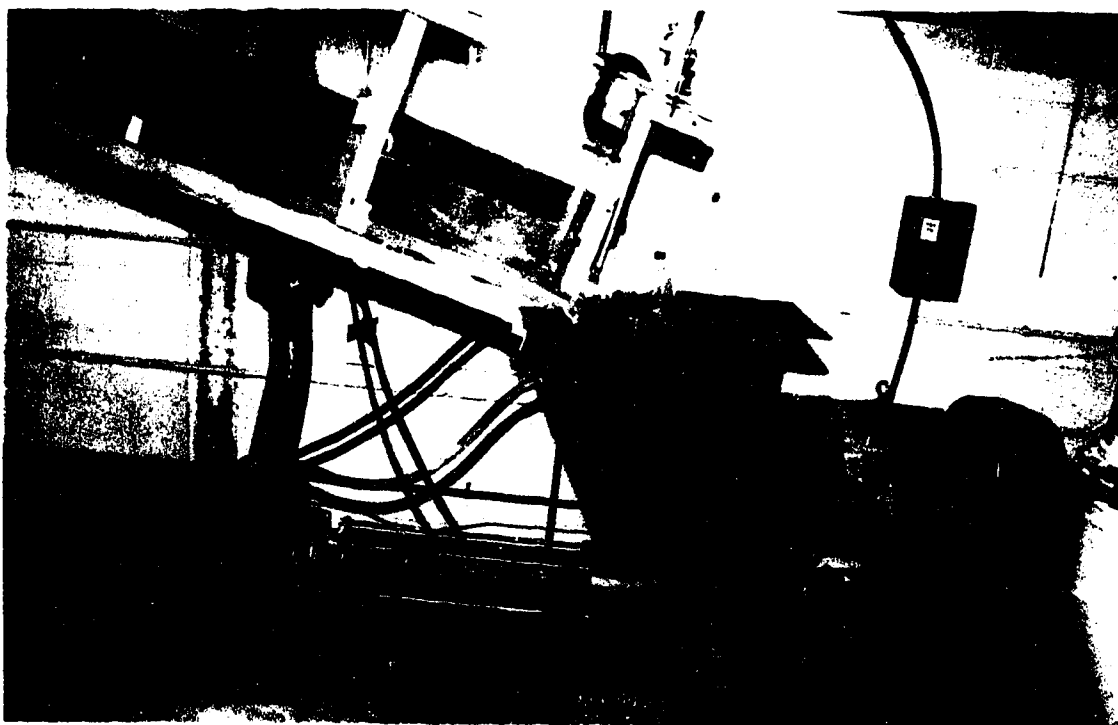
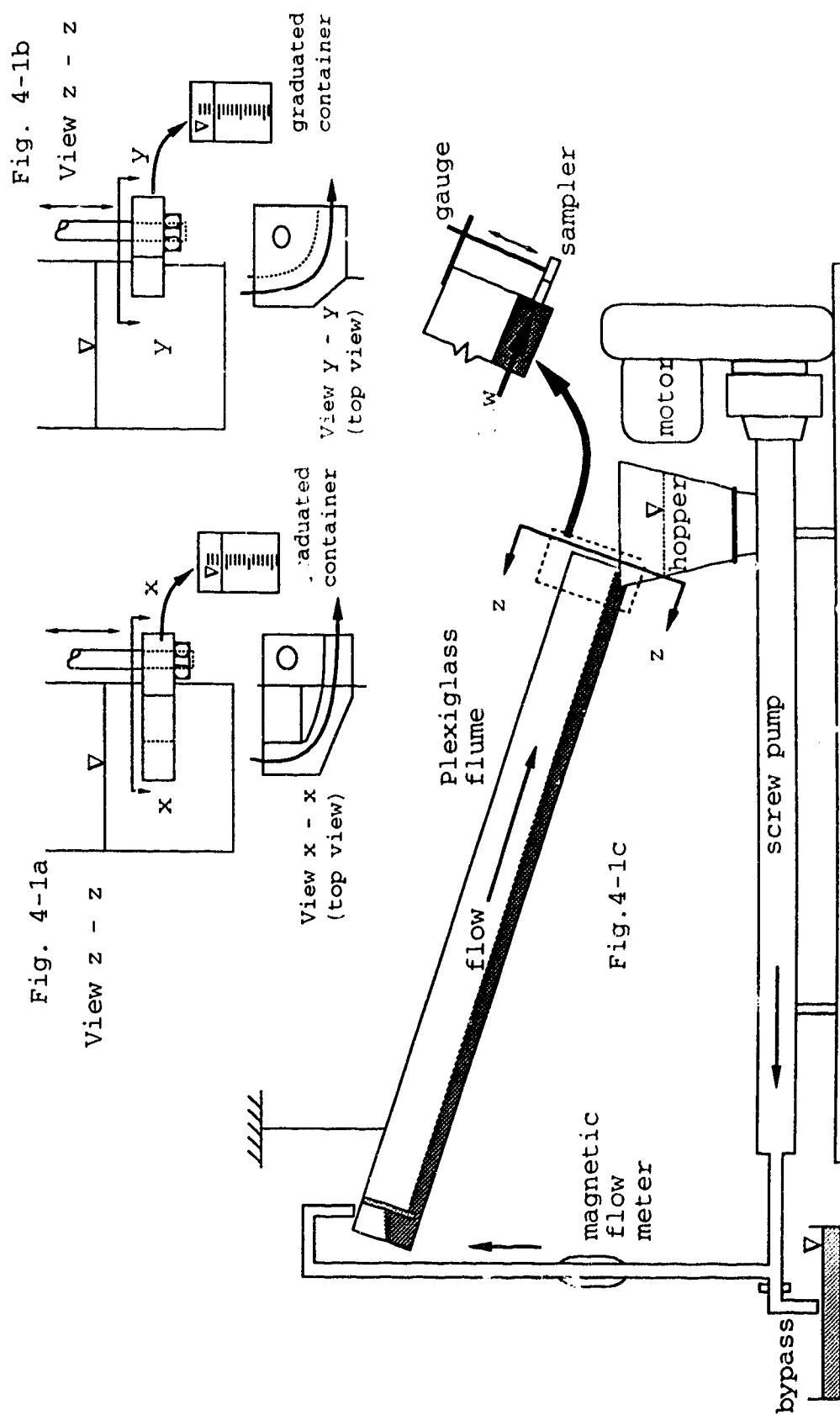


Plate 4-8 Downstream hopper for adding sediment and mixing

Figure 4-1(a-c) Experimental Set up and Sketch of Samplers



there was nowhere in the system for deposition to take place, the slurry was assumed fully mixed. The system could be gradually emptied by opening the bypass valve. Since the discharge was limited by the pump capacity, a narrow plexiglass flume 4.25m long, 51mm wide and 0.54m high was used to achieve a depth of flow up to 4.9 cm. This limitation of channel width, however, made it possible to mount a sampler at the end of the flume (Fig. 4-1c) and make measurements at the channel center and side.

4.3.2 Sampler Development and Calibration

In the early stage of the study several photographic techniques were tried. The goal was to obtain streak lines using a 35mm camera and light colored sand, which could then be calibrated for velocity measurement. The drawback of this technique was that the velocity measured was of particles moving next to the wall and the concentration profile had to be measured independently. Freezing the motion with a high speed camera and counting particles yielded concentration values of little confidence. Another attempt to obtain data was to use video motion pictures photographed at 2000 frames per second. This method although promising initially, resulted in images of poor resolution. Owing to these difficulties, the direct sampling technique was tried. Several tube designs having a variety of lips were tried. It was discovered that the tube had to be short in order to prevent choking and it had to have sharp edged lips to

increase the capture efficiency. The sampler finally used had a square opening of area (a) of approximately 1cm^2 and was 5cm long. It was slightly tapered away from the direction of flow and diverted the sample into a graduated container (Plate 4-9). Plate 4-9 also shows the inner construction of the side sampler. Fig. 4-1a & 4-1b show the view from the end of the channel looking upstream. The centre sampler had a knife edge flow deflector to pass the flow down the channel from areas other than the opening. This size of sampler was finally adopted because any opening smaller than this choked the sampler. The above sampler worked well for flows with a volumetric concentration approaching up to 50%. This sample was collected in a graduated container (plate 4-10) and weighed. The sampling time was noted using a stop watch. Despite being tapered, the sampler flowed full without trapping air.

Since the flow velocity at the flume exit was 3-3.5m/s, it came out of the flume almost as a jet. As the flow was inertia dominated, the jet travelled in a straight line for about one half the channel width, away from the edge of the flume, before it assumed its standard trajectory. The sampler was mounted on a graduated rod which could be moved vertically allowing samples to be taken at any point in the flow (plate 4-10). At any point in the flow three samples were taken and the mean of these three readings was used. Plate 4-11 is a view of the sampler looking downstream and Plate 4-12 gives a view of a typical sample that is collected

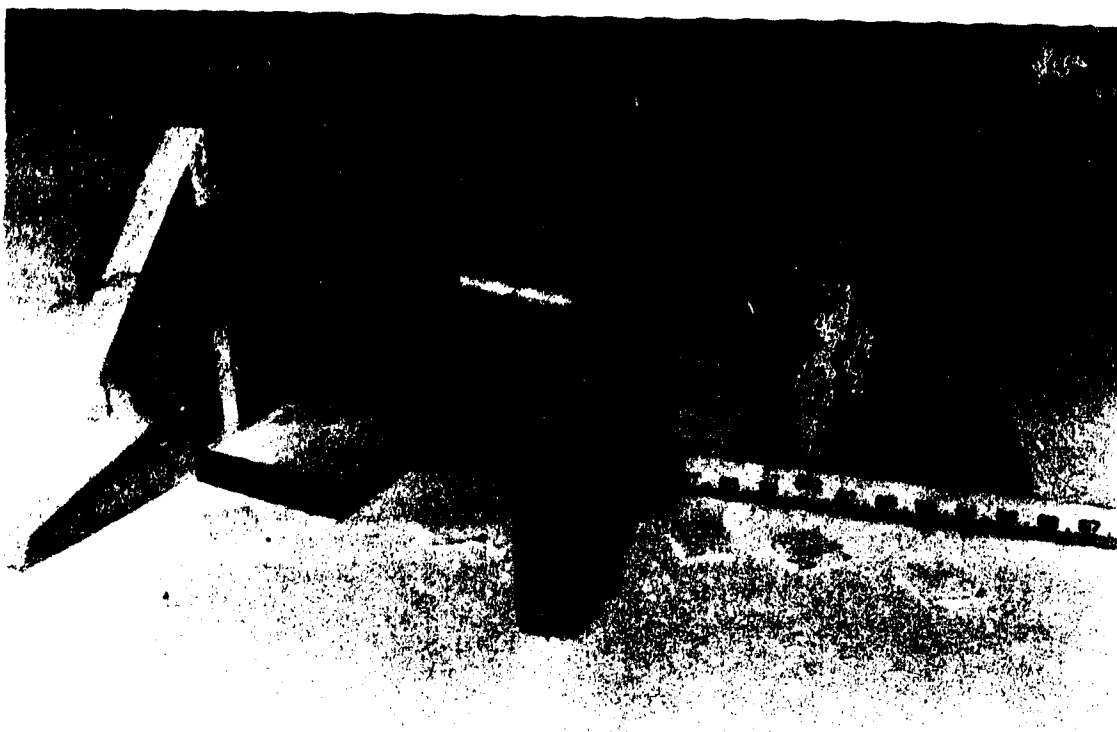


Plate 4-9 Centre and side samplers with tapered duct and surface floats



Plate 4-10 Sampling of flow



Plate 4.11 View of sampler looking downstream

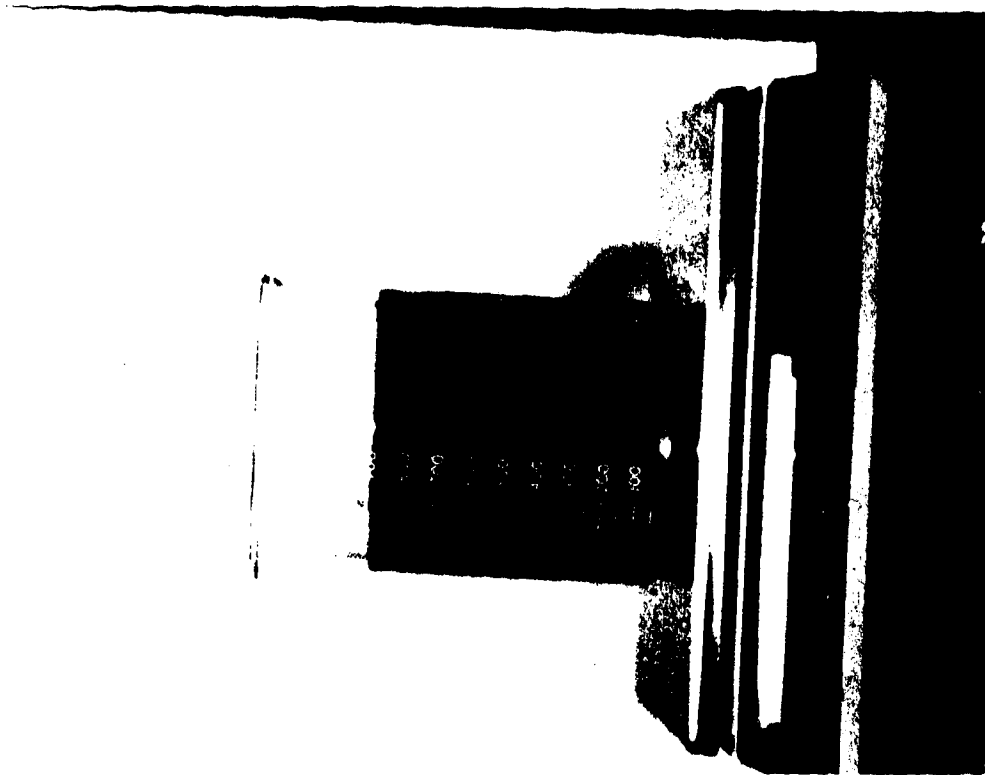


Plate 4.12 Typical sample being weighed

Figure 4-2a Depth vs velocity for steady uniform water flow
using pitot tube & sampler#2 $Q=6.48\text{L/s}$, slope=28.6%

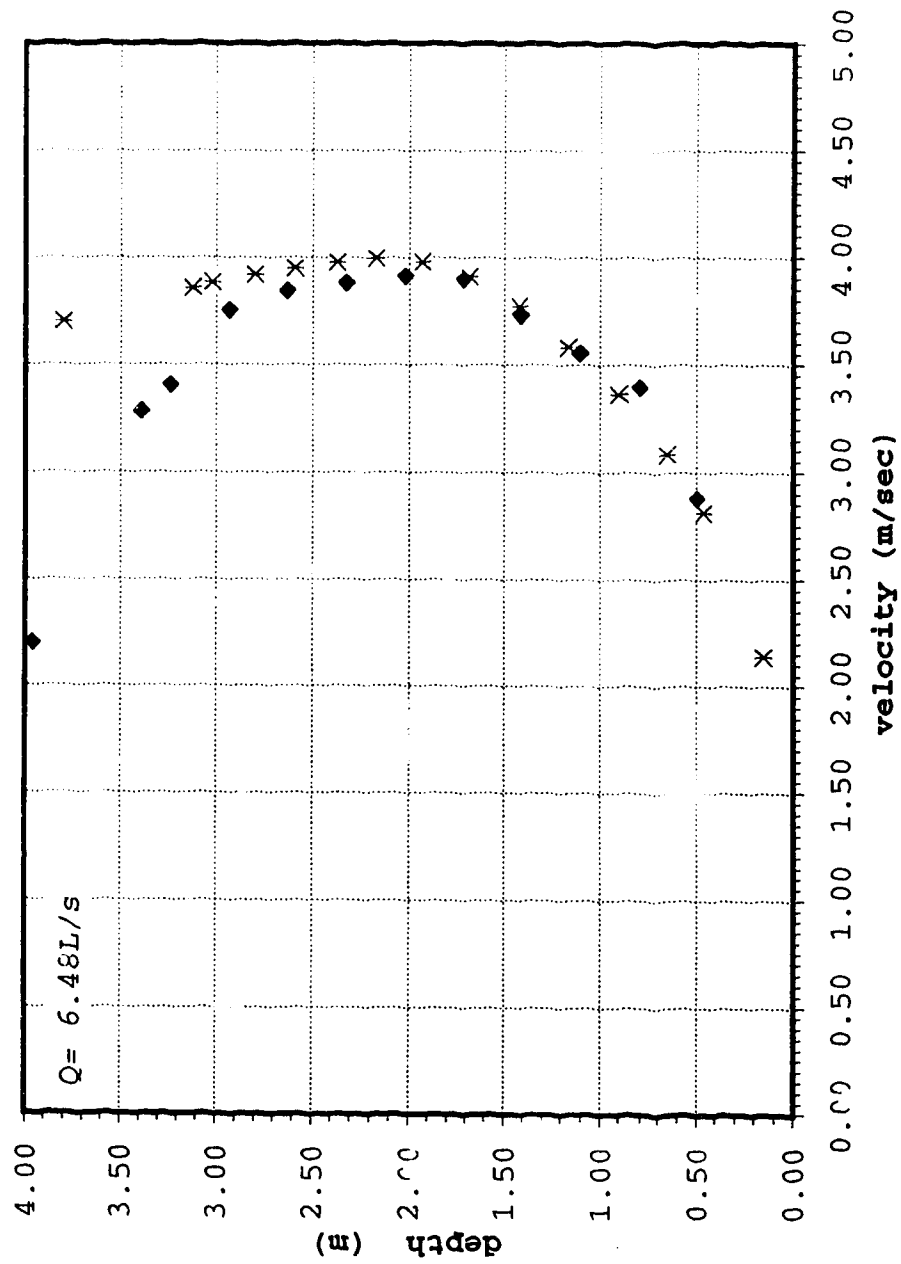


Figure 4-2b Depth vs Velocity for steady uniform water flow using pitot tube and corrected sampler #3 at channel centre

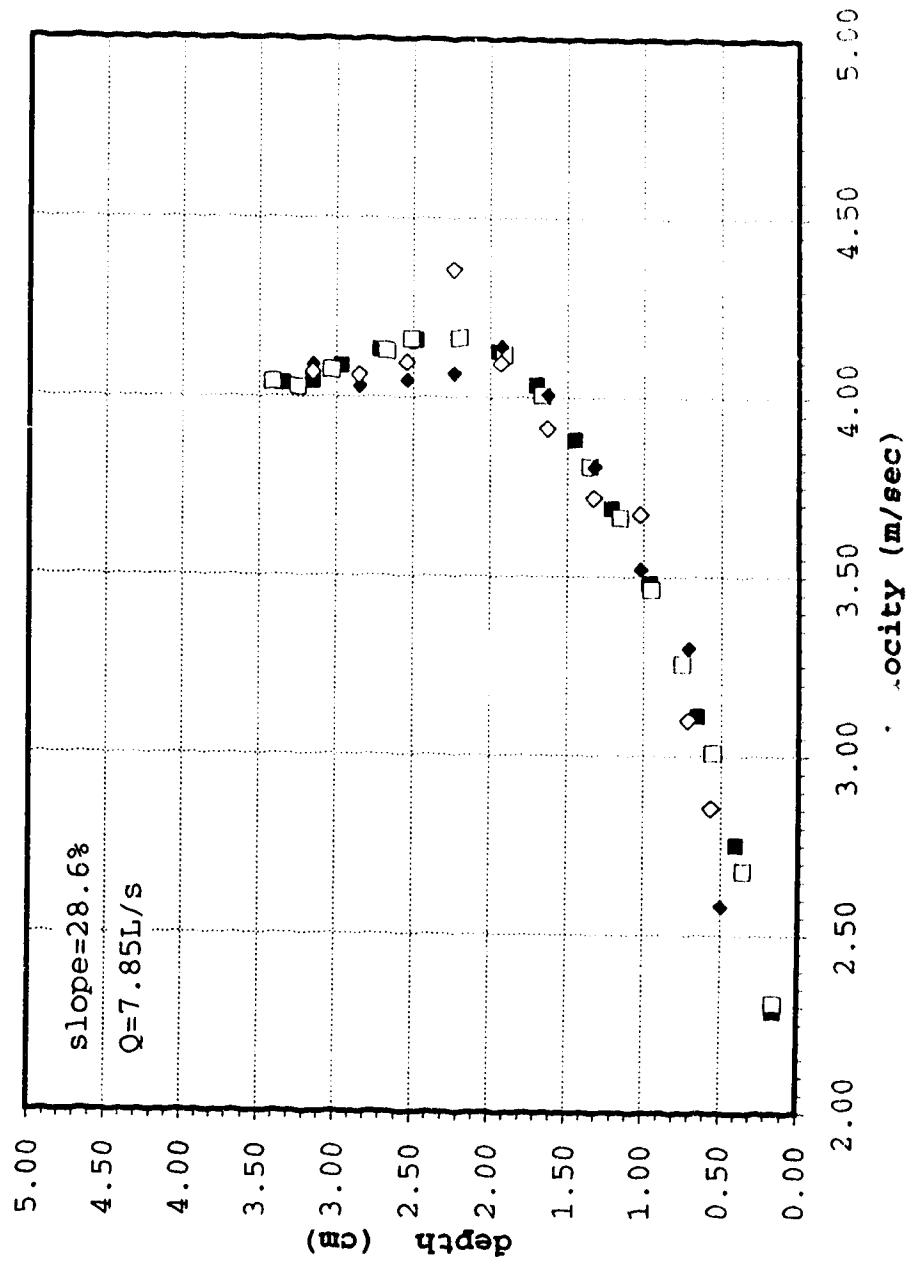
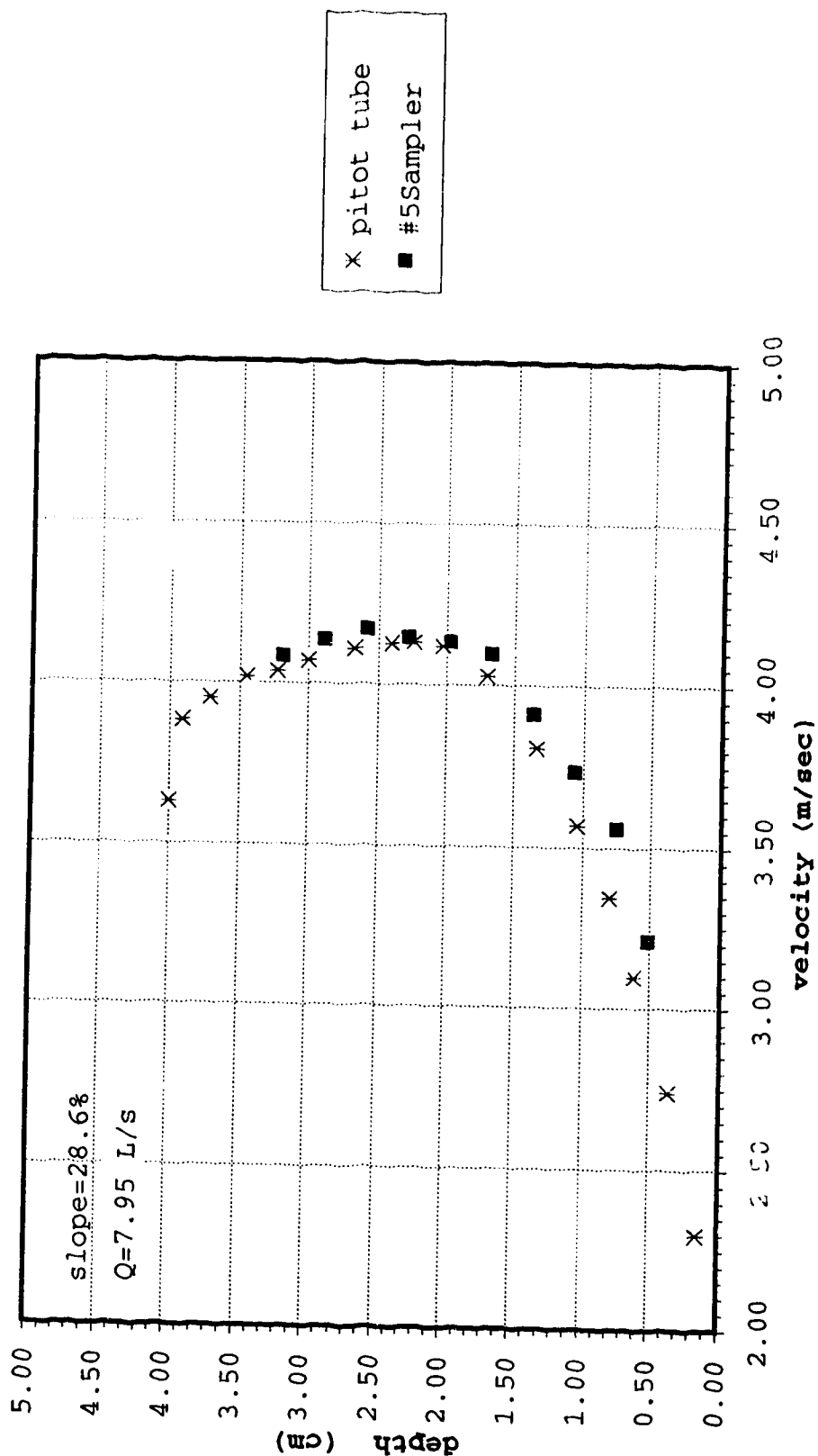


Figure 4-2c Depth vs Velocity for Steady Uniform water Flow
using pitot tube and sampler #5 at channel centre



and weighed. Note the distinct segregation of particles in the mixture following settling. The sampler was calibrated with pitot tube measurements with water flowing in the channel. Of the three samplers used, #5 produced less than 5% error and therefore was not calibrated (Fig. 4-2c). For sampler #2 and #3 the profile had to be shifted slightly to match the pitot tube readings (Fig. 4-2b).

It was found that for sampler #3 if 0.2s was added to each of the measured time of collection, the new velocity profile matched the pitot tube reading very well as shown in Fig. 4-2b. For sampler #2 approximately 0.2 sec had to be deducted to match the profile. If the sampler malfunctioned either due to trapped air pocket or if the sampler was choked by rubber strippings from the rotor, distinct outliers were observed in the velocity profiles as indicated by the point in Fig 4-2b at a depth of 2.25cm. The above figures show two sets of readings of water flow using the sampler and pitot tube which indicate good repeatability for both these measuring techniques. The small difference in the velocity measurement using pitot tube and the sampler demonstrated that the disturbance of introducing a 1 cm² cross section sampler was smaller than anticipated. There were also concerns regarding the accuracy of the measurements when averaging was performed by such large sampling space moving through the depth in such small increments i.e. when 8 to 10 readings were taken in a depth of 2 to 3 cm using a 1 cm² sampler. The author believes that the excellent matching

throughout the depth of these two sets of profiles described earlier show that the change in velocity gradients recorded by pitot tube measurements are preserved by this new sampling technique. This alleviates some of the concerns regarding the accuracy of measurements. The ideal procedure would be to make measurements using a non-intrusive technique. This, however, is yet to be developed. Fig. 4-2c also shows that the velocity profile measurements using a pitot tube 0.5 cm away from the channel center is almost the same as that at the center of the channel. This shows that there is almost no influence of the side wall at the channel center. This was also confirmed by comparing the streak lines of white sand particles at the centerline and next to the wall. These streak lines were observed on a surface photograph of the slurry flowing in the channel. The streak lines were clearly equal in length throughout the channel width and were shorter only within 5mm from the wall. The secondary circulation in the narrow channel caused the reduction of velocity near the free surface. Similar effect can be observed in the case of a sand water mixture although this effect is suppressed when the concentration is high.

4.4 Velocity and Concentration Measurements

Once the sample was collected and weighed, the information at hand included the volume of the sample (V), the mass of the sample (m), the sampling time (t) and the

sampler area (a). The velocity and concentration at a location in the flow was then evaluated using the following equations:

$$u = \frac{V}{a \cdot t} \quad (4-4.1)$$

$$C_v = \frac{1}{1.65} \left[\frac{m}{V} - 1 \right] \quad (4-4.2)$$

where m is in grams and V is in ml. This location was taken as the centre point of the sampler. In order to use the Equation(4-4.1), the sampler had to be flowing full for velocity measurement. Therefore, the velocity at the surface of the flow had to be evaluated independently. As the concentration measurement, Equation(4-4.2) derived from Equation (C-3.4) from Appendix C, required only the volume and mass of the sampler, the sampler didn't have to flow full as long as a representative sample was taken. Therefore, a sample could be skimmed from the surface of the flow and the concentration determined. The velocity at the surface was determined using a camera with a 35mm lens, a Minolta 5200i flash which had multiple strobing capability of up to 10 flashes at 50 Hz and a square polyethylene surface float 12.5mm on each side and approximately 2mm thick of specific gravity 0.92 (Plate 4-9). Several images of the float were captured in a single frame as it moved down using the multiple flash with the camera wide open Plate(4-13). The flow is from right to left. This process proved to be

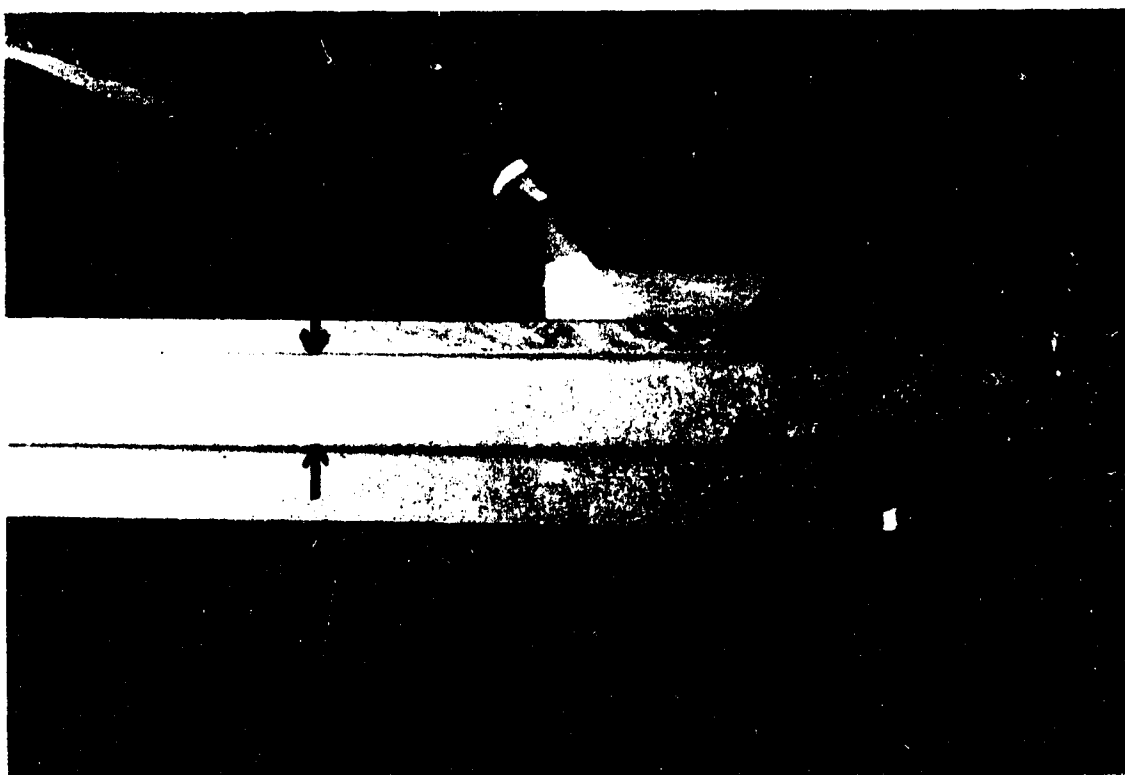


Plate 4-13 Surface velocity using a float (flow right to left)

reasonably difficult. The difficulty lied mainly in synchronizing the release of the float and triggering the flash. The success rate was low therefore only two measurements were made, one for low concentration and one for high concentration. The surface velocities for the rest of the measurements were eventually extrapolated based on these two measurements. The surface velocity measurements $q_{1401}C_{m15.4}$ and $q_{1594}C_{m15.4}$ for particle D2 (Fig.4-10a) were done using the above described technique. Here q_{1401} stands for specific discharge $1401 \text{ cm}^2/\text{s}$ and $C_{m15.4}$ stands for the profile mean concentration by volume of 15.4%.

The present set of experiments were performed using four sizes (D1 to D4), three of which (D1-D3), were uniformly graded silica sand particles. Size D4 was mixed in the laboratory taking equal portions of sizes D1 to D3. Figure 4-3 gives the sieve analysis results for the four particle sizes. Velocity and concentration profiles were measured for each particle size at several mean concentrations. One of the limitations of the set-up was that the mean concentration for any run could not be predetermined. This would have been possible if the mass of sand and the volume of water in the system could have been predetermined. The mass of sand in the system could not be fixed. This would require a lot more effort and time before each run to completely dry the sand. If the effort had been made to dry the sand, then the volume of water in the system would not have been

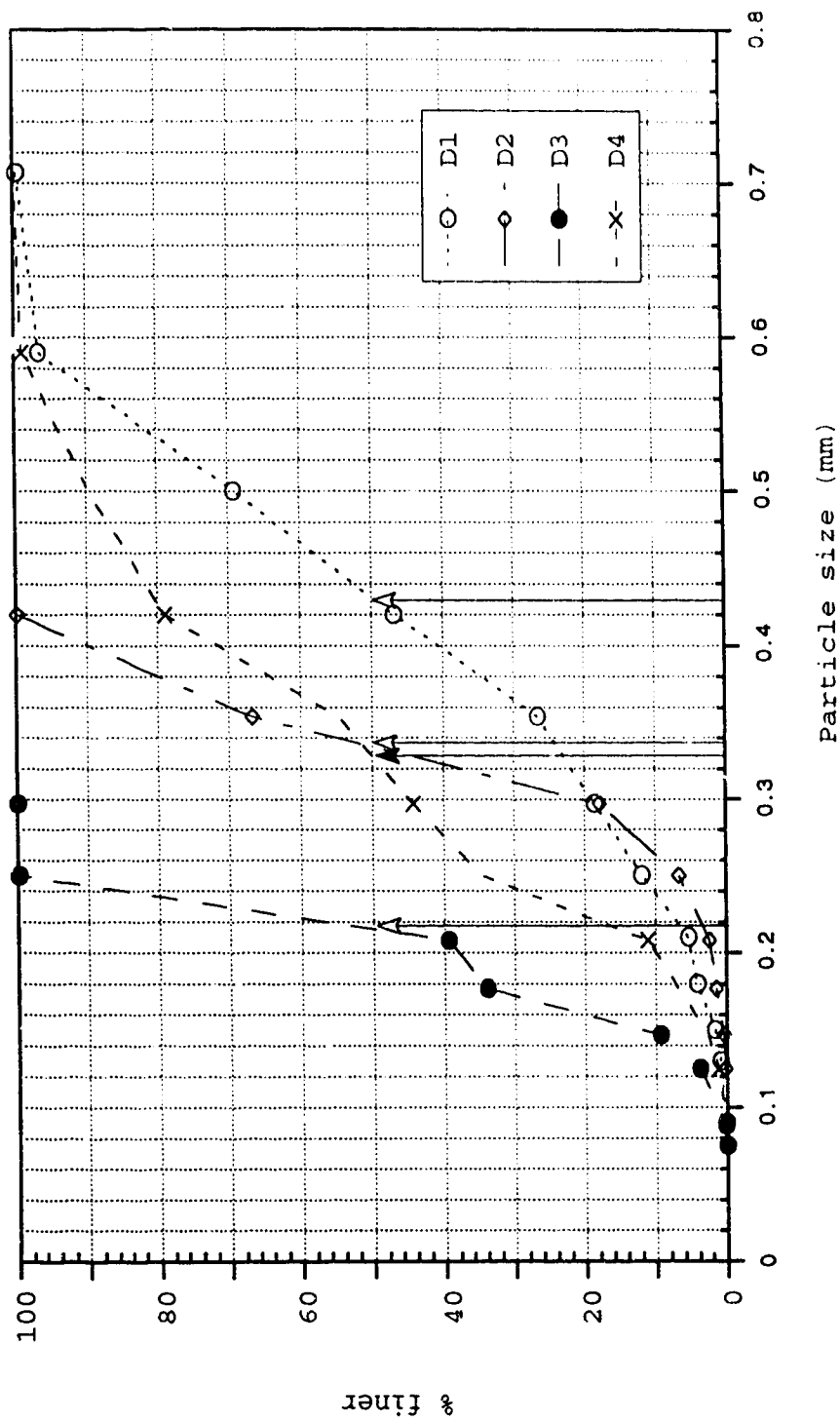


Figure 4-3 Grain Size Analysis for Particles D1-D4

difficult to fix. On the other hand, even if both the masses of sand and water had been fixed, there were still two difficulties in bulk sampling of the flow in order to get a mean concentration and velocity for the whole system.

- a. The flow was coming out of the channel at a velocity of about 3 m/s which made it impossible to collect it in a small container without splashing the sample
- b. As the total volume in the system was small (around 80-100 Liters), fluctuation in discharge could be noticed if more than 4 or 5 liter of slurry was extracted from the system. This limited the general sampling volume.

The mean concentrations and the unit discharges were therefore evaluated by integrating the measured profiles. This procedure has been adopted because it was discovered that the magnetic flow meter which is normally calibrated for water flow did not produce accurate discharge measurements when a slurry was flowing through it. The performance was obviously better when the magflow meter was placed in the vertical line (Fig. 4-1c). The possible explanation for this could be that in the horizontal line the particle concentration is more close to the bottom boundary. This results in a non symmetrical velocity profile which appears to invalidate the factory calibration factors. When the magnetic flow meter was put in the vertical line, the mixture flowing through the pipe was better mixed which possibly gave

a more symmetrical velocity distribution that resulted in a flow similar to that achieved during the factory calibration.

The velocity and concentration profiles were measured at the centre of the channel and at 0.5 cm from the wall. The measurements next to the wall were made only for particle size D1. Figures 4-4 to 4-6 give the normalized velocity and concentration profiles. y is the vertical location above the bed, u is the velocity at this location, h is the depth of flow, U is the integrated mean velocity at the section, C is the integrated mean concentration for the section. The details for these runs are presented in Tables 4-1 to 4-3. The group names C1 to C6 do not indicate any particular significance.

Similar sets of data have also been presented for measurements at the centre of the channel. Figures 4-7 to 4-8 represent normalized velocity and concentration profiles for particle size D1 (≈ 0.430 mm). Tables 4-4 to 4-5 present all the data for the profiles given in Figures 4-7 to 4-8. The specific discharge is given as q , y_{um} represents the height above the bed where the velocity is equal to the section mean velocity U_m , y_{10} represents the height above the bed where the concentration is 10% of the concentration at the bed, C_b . The group designation such as **group 6.45** represent the approximate magnetic flow meter reading in L/s maintained through the runs.

Figure 4-4a Normalized Depth-Velocity for steady uniform sand water mixture, particle D1, group C1, slope=28.6%, channel side

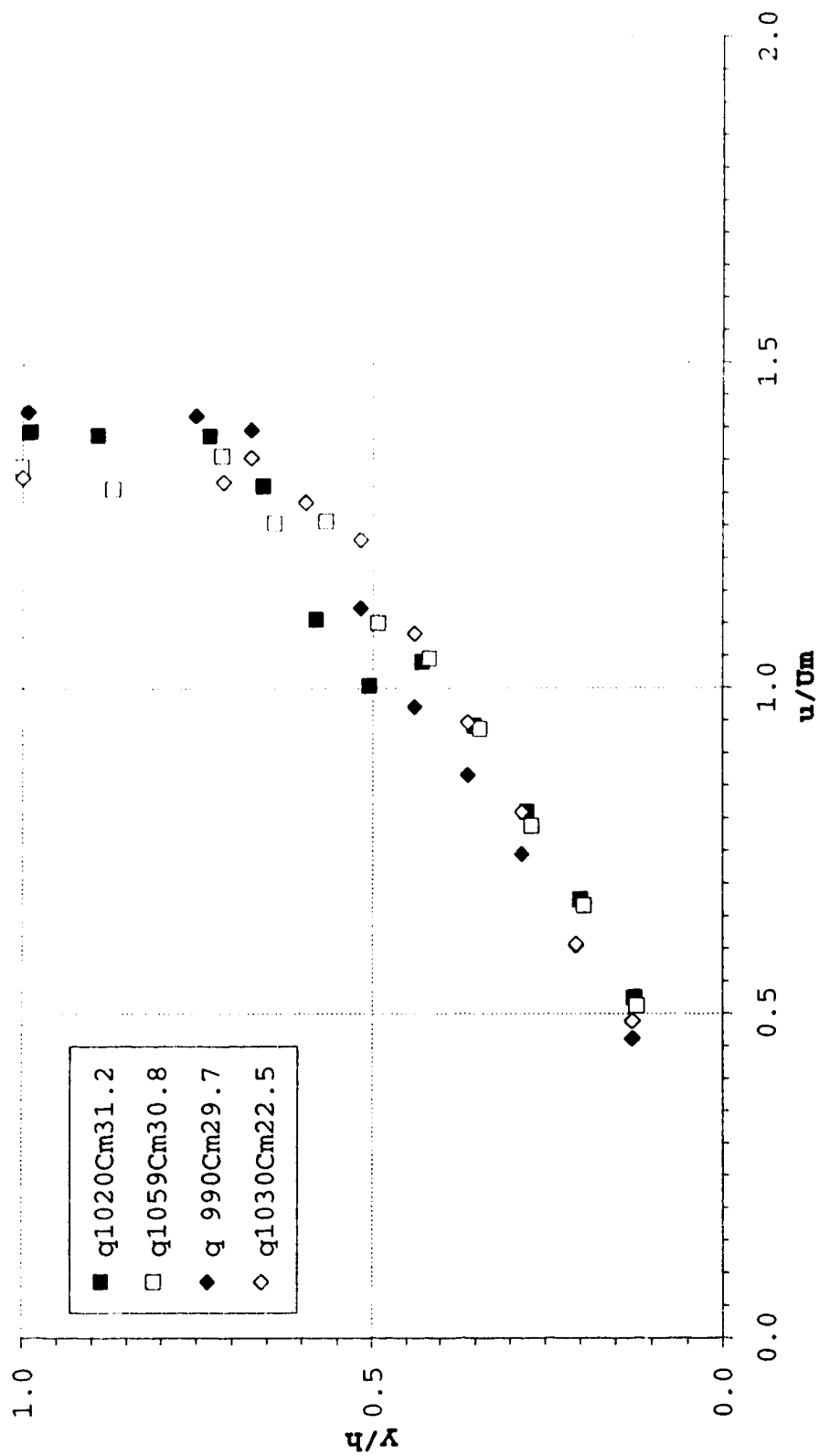


Figure 4-4b Normalized Depth-Concentration for steady Uniform sand water mixture, particle D₁, group C1, slope=28.6%, channel side

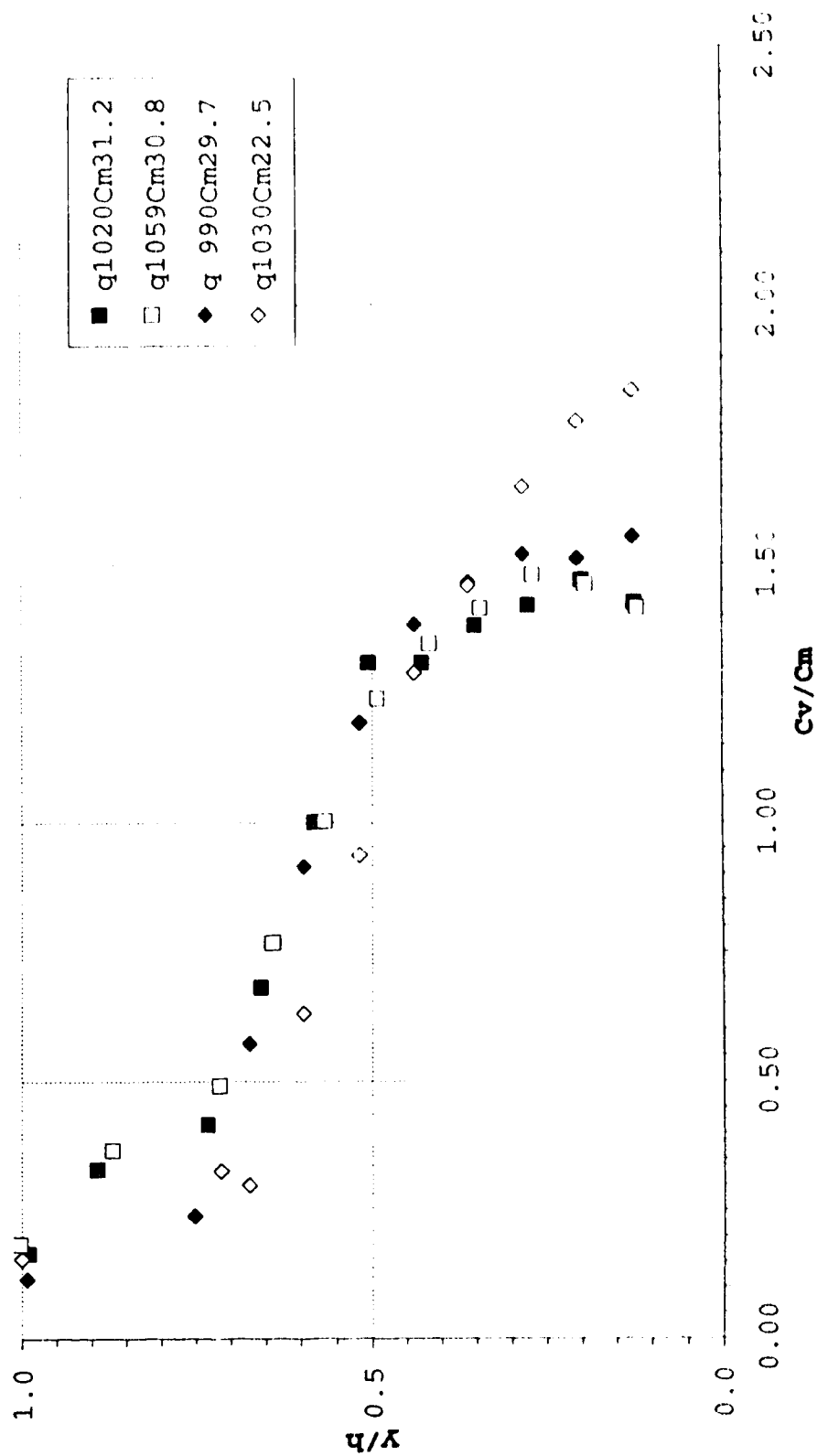


Table 4-1 Summary of velocity and concentration profiles for group C1, Channel Side

q=1030sq cm/s Cm=22.5 h = 3.9						q=990sq cm/s Cm=29.7 h = 3.9					
Um= 2.64						Um= 2.56					
y/h	u/Um	u	Cv/Cm	Cv	Cw	y/h	u/Um	u	Cv/Cm	Cv	Cw
2.64						2.56					
(m/s) (%) (%)						(m/s) (%) (%)					
q1030Cm22.5						wall (q 990Cm29.7					
0.1	0.5	1.29	1.84	41.3	65.1	0.1	0.5	1.18	1.55	46.8	69.9
0.2	0.6	1.60	1.78	40.0	63.8	0.2	0.6	1.55	1.51	45.5	68.9
0.3	0.8	2.14	1.65	37.1	61.0	0.3	0.7	1.91	1.52	45.7	69.1
0.4	0.9	2.50	1.46	32.8	56.4	0.4	0.9	2.22	1.47	44.1	67.7
0.4	1.1	2.87	1.29	29.0	52.0	0.4	1.0	2.49	1.38	41.7	65.4
0.5	1.2	3.25	0.94	21.1	41.4	0.5	1.1	2.88	1.19	35.9	59.8
0.6	1.3	3.40	0.63	14.2	30.5	0.6	1.3	3.30	0.92	27.5	50.2
0.7	1.4	3.58	0.30	6.7	16.1	0.7	1.4	3.58	0.57	17.2	35.5
0.7	1.3	3.48	0.33	7.4	17.4	0.8	1.4	3.63	0.24	7.2	17.1
1.0	1.3	3.50	0.16	3.5	8.8	1.0	1.4	3.65	0.12	3.5	8.8

q=1020sq cm/s Cm=31.2 h = 4.0						q=1059sq cm/s Cm=30.8 h = 4.1					
Um= 2.58						Um= 2.57					
y/h	u/Um	u	Cv/Cm	Cv	Cw	y/h	u/Um	u	Cv/Cm	Cv	Cw
2.58						2.57					
(m/s) (%) (%)						(m/s) (%) (%)					
wall (q1020Cm31.2						wall (q1059Cm30.8					
0.1	0.5	1.35	1.43	44.9	68.3	0.1	0.5	1.31	1.42	44.0	67.6
0.2	0.7	1.74	1.47	46.3	69.5	0.2	0.7	1.71	1.46	45.5	68.8
0.3	0.8	2.09	1.42	44.8	68.2	0.3	0.8	2.03	1.48	46.0	69.3
0.4	0.9	2.43	1.38	43.5	67.1	0.3	0.9	2.41	1.42	44.0	67.6
0.4	1.0	2.69	1.31	41.2	65.0	0.4	1.0	2.69	1.35	41.9	65.6
0.5	1.0	2.59	1.31	41.2	65.0	0.5	1.1	2.83	1.24	38.6	62.4
0.6	1.1	2.85	1.00	31.5	55.0	0.6	1.3	3.23	1.00	31.2	54.5
0.7	1.3	3.38	0.68	21.4	42.0	0.6	1.3	3.22	0.77	23.8	45.3
0.7	1.4	3.58	0.42	13.1	28.6	0.7	1.4	3.49	0.49	15.3	32.4
0.9	1.4	3.58	0.33	10.4	23.5	0.9	1.3	3.36	0.37	11.4	25.5
1.0	1.4	3.60	0.17	5.2	12.7	1.0	1.3	3.45	0.18	5.7	13.8

Figure 4-5a Normalized Depth-Velocity for steady uniform sand water mixture, particle D1, group C2, slope=28.6%, channel side

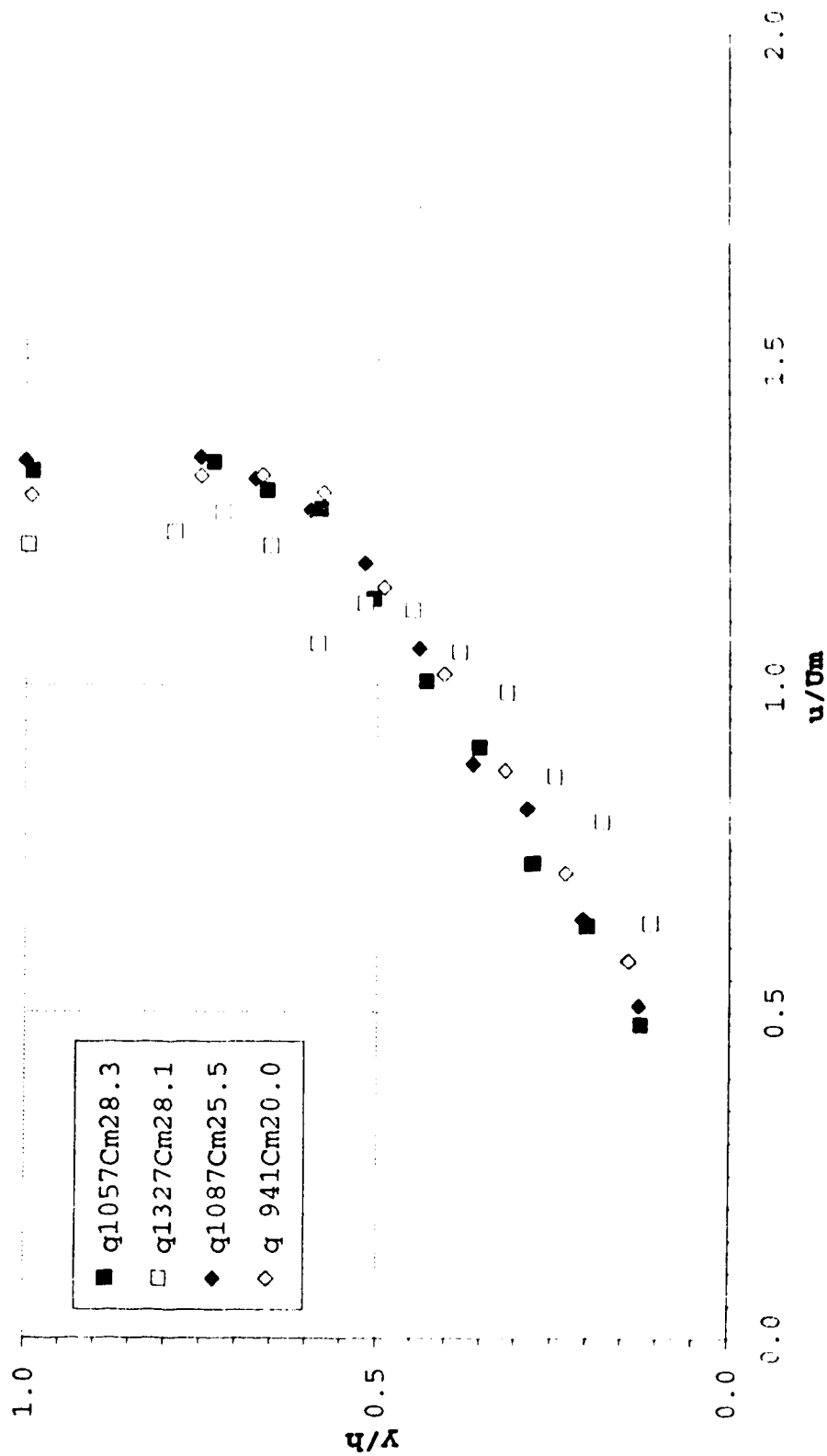


Figure 4-5b Normalized Depth-Concentration for steady uniform sand water mixture, particle D1, group C2, slope=28.6%, channel side

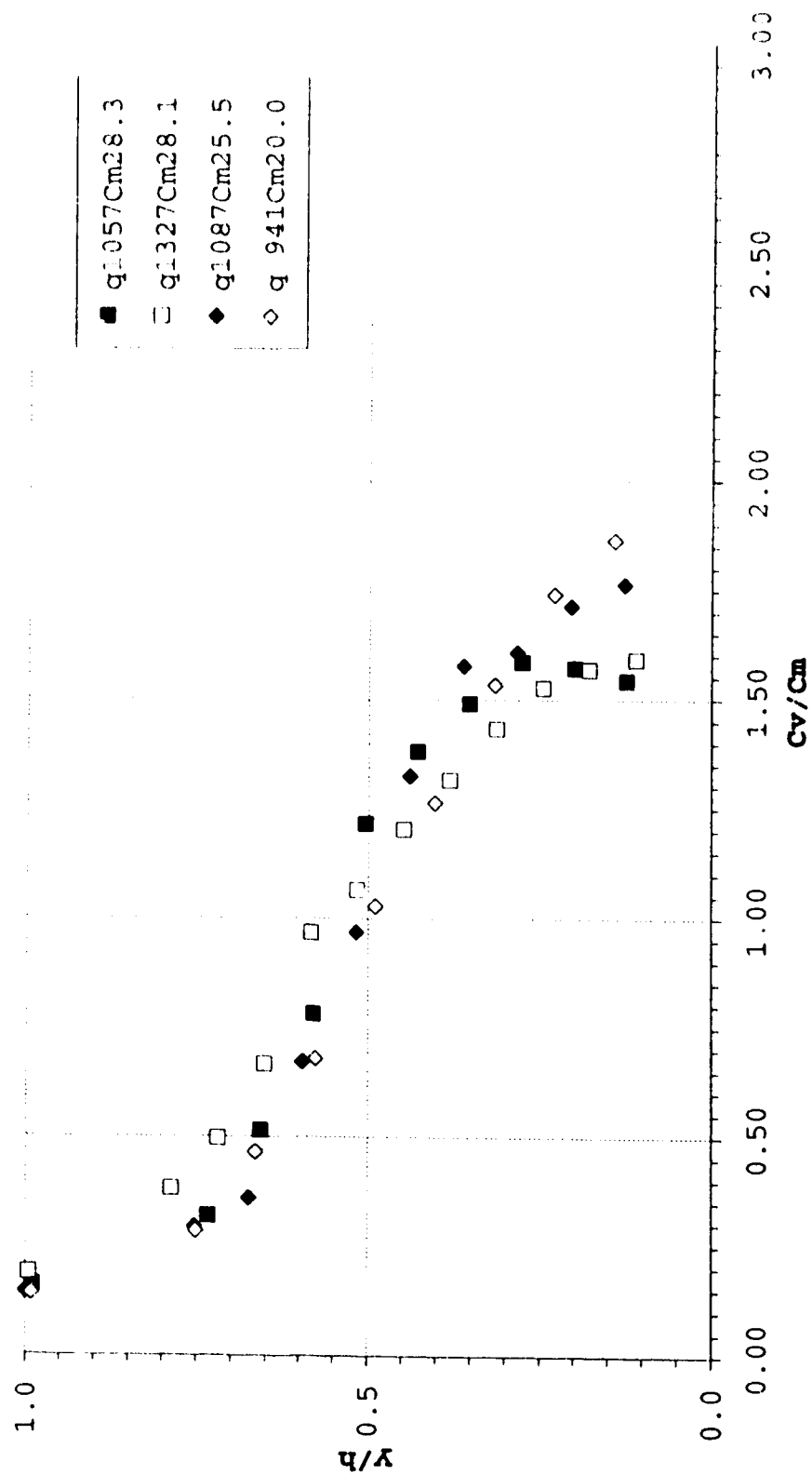


Table 4-2 Summary of velocity and concentration profiles for group C2, channel side

q=184sq cm/s Cm=20.0 h= 3.50						q=1087sq cm/s Cm=25.5 h= 3.90					
Um= 2.71						Um= 2.79					
y/h	u/Um	u	Cv/Cm	Cv	Cw	y/h	u/Um	u	Cv/Cm	Cv	Cw
2.71						2.79					
(m/s) (%) (%)						(m/s) (%) (%)					
q 941Cm20.0						q1087Cm25.5					
0.1	0.6	1.57	1.87	37.3	61.2	0.1	0.5	1.42	1.76	45.0	68.4
0.2	0.7	1.94	1.74	34.8	58.6	0.2	0.6	1.79	1.71	43.7	67.3
0.3	0.9	2.36	1.53	30.7	54.0	0.3	0.8	2.27	1.61	41.0	64.8
0.4	1.0	2.76	1.26	25.3	47.3	0.4	0.9	2.46	1.58	40.2	64.1
0.5	1.2	3.12	1.03	20.6	40.7	0.4	1.1	2.95	1.32	33.8	57.5
0.6	1.3	3.51	0.68	13.6	29.4	0.5	1.2	3.32	0.97	24.7	46.5
0.7	1.3	3.58	0.47	9.3	21.4	0.6	1.3	3.54	0.67	17.1	35.4
0.8	1.3	3.58	0.28	5.7	13.8	0.7	1.3	3.67	0.36	9.2	21.1
1.0	1.3	3.50	0.14	2.8	7.1	0.8	1.3	3.76	0.29	7.5	17.6
						1.0	1.3	3.75	0.15	3.7	9.2

q=1057sq cm/s Cm=28.3 h= 4.00						q=1327sq cm/s Cm=28.1 h= 4.50					
Um= 2.71						Um= 2.96					
y/h	u/Um	u	Cv/Cm	Cv	Cw	y/h	u/Um		Cv/Cm	Cv	Cw
2.71						2.96					
(m/s) (%) (%)						(m/s) (%) (%)					
q1057Cm28.3						q1327Cm28.1					
0.1	0.5	1.30	1.54	43.7	67.3	0.1	0.6	1.89	1.59	44.7	68.2
0.2	0.6	1.71	1.57	44.5	68.0	0.2	0.8	2.35	1.57	44.1	67.6
0.3	0.7	1.97	1.58	44.9	68.3	0.2	0.9	2.55	1.53	42.9	66.6
0.4	0.9	2.46	1.49	42.2	65.9	0.3	1.0	2.93	1.43	40.3	64.1
0.4	1.0	2.73	1.38	39.1	63.0	0.4	1.1	3.11	1.32	37.0	60.8
0.5	1.1	3.07	1.21	34.4	58.1	0.4	1.1	3.31	1.20	33.8	57.5
0.6	1.3	3.44	0.78	22.1	42.9	0.5	1.1	3.33	1.06	29.9	53.1
0.7	1.3	3.52	0.51	14.5	31.0	0.6	1.1	3.15	0.97	27.2	49.7
0.7	1.3	3.64	0.32	9.0	20.7	0.7	1.2	3.60	0.67	18.7	37.9
1.0	1.3	3.60	0.16	4.5	11.1	0.7	1.3	3.75	0.50	13.9	30.0
						0.8	1.2	3.66	0.38	10.7	24.1
						1.0	1.2	3.60	0.19	5.3	12.9

Figure 4-6a Normalized Depth-Velocity for steady uniform sand water mixture, particle D₁, group C3-C6, slope=28.6%, channel side

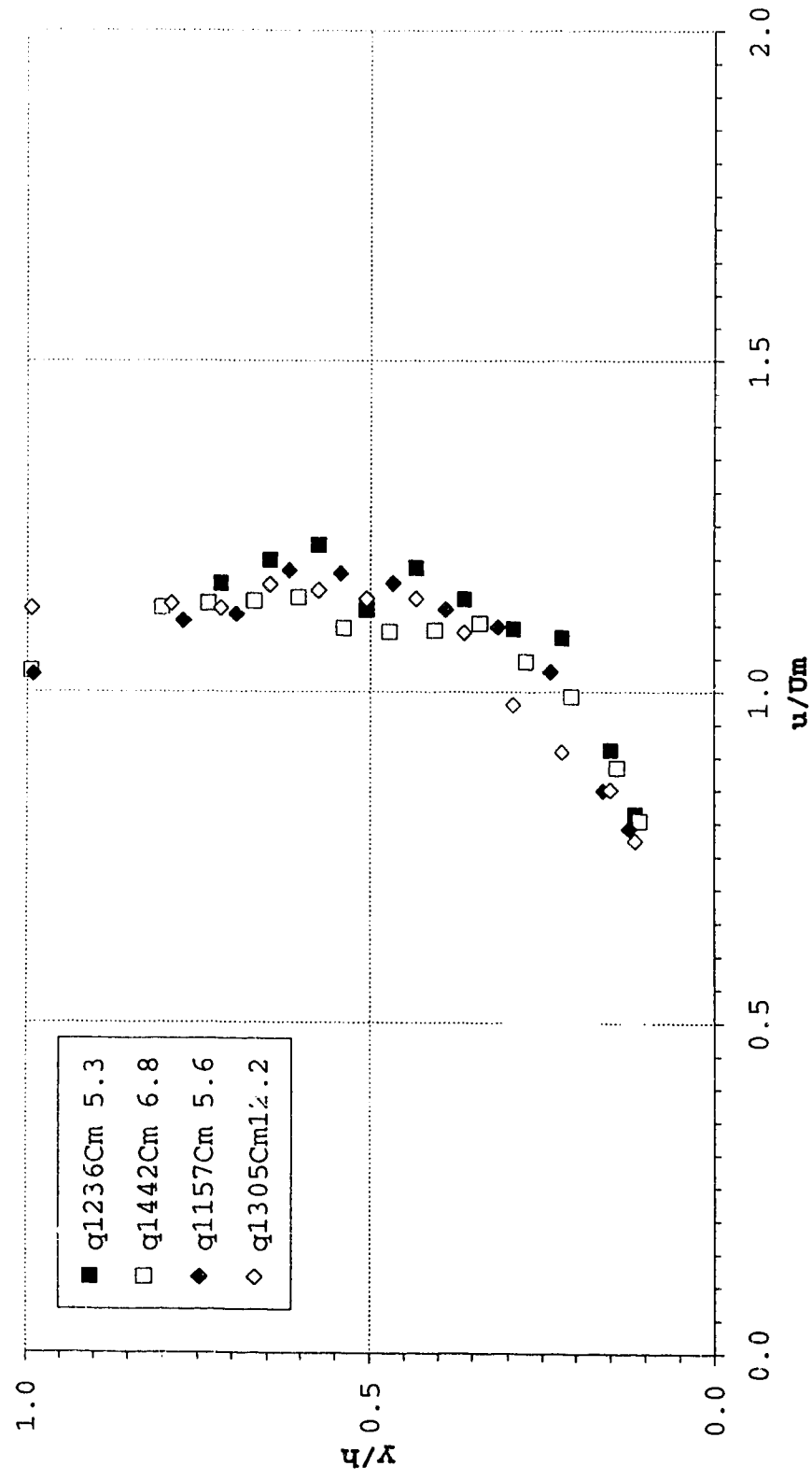


Figure 4-6b Normalized Depth-Concentration for steady uniform sand water mixture, particle D1, group C3-C6, slope=28.6%, channel side

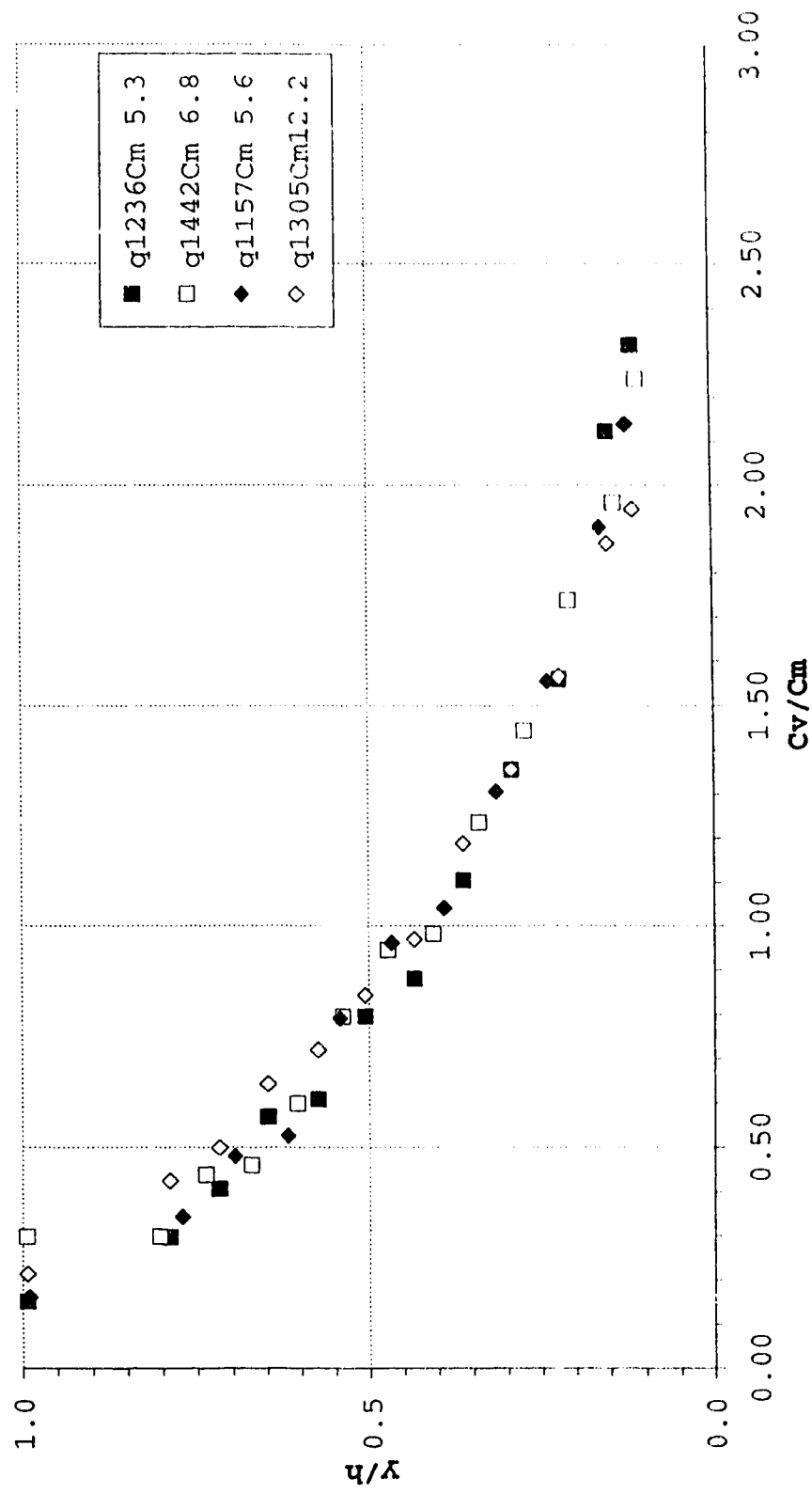


Table 4-3 Summary of velocity and concentration profiles for group C3-4, Channel Side

q=1236sq cm/s Cm=5.3 h= 4.30						q=1442sq cm/s Cm=6.8 h= 4.60					
Um= 2.90						Um= 3.15					
y/h	u/Um	u	Cv/Cm	Cv	Cw	y/h	u/Um	u	Cv/Cm	Cv	Cw
2.90						3.15					
(m/s) (%) (%)						(m/s) (%) (%)					
q1236Cm 5.3						q1442Cm 6.8					
0.1	0.8	2.36	2.32	12.3	27.1	0.1	0.8	2.53	2.24	15.2	32.3
0.2	0.9	2.64	2.12	11.3	25.2	0.1	0.9	2.79	1.96	13.3	28.9
0.2	1.1	3.14	1.56	8.3	19.3	0.2	1.0	3.13	1.74	11.8	26.2
0.3	1.1	3.18	1.35	7.2	17.0	0.3	1.0	3.29	1.44	9.8	22.4
0.4	1.1	3.31	1.10	5.9	14.2	0.3	1.1	3.48	1.24	8.4	19.6
0.4	1.2	3.44	0.88	4.7	11.5	0.4	1.1	3.44	0.98	6.7	15.9
0.5	1.1	3.26	0.79	4.2	10.5	0.5	1.1	3.44	0.95	6.4	15.4
0.6	1.2	3.54	0.61	3.2	8.1	0.5	1.1	3.45	0.79	5.4	13.1
0.6	1.2	3.48	0.57	3.0	7.6	0.6	1.1	3.60	0.60	4.1	10.1
0.7	1.2	3.37	0.41	2.2	5.5	0.7	1.1	3.58	0.46	3.1	7.9
0.8	1.0	2.82	0.30	1.6	4.1	0.7	1.1	3.57	0.44	3.0	7.5
1.0	0.9	2.50	0.15	0.8	2.5	0.8	1.1	3.55	0.30	2.0	5.2
						1.0	1.0	3.25	0.30	2.0	5.2

group C5-6, Channel Side

q=1157sq cm/s Cm=5.6 h= 4.00						q=1305sq cm/s Cm=12.2 h= 4.30					
Um= 2.92						Um= 3.06					
y/h	u/Um	u	Cv/Cm	Cv	Cw	y/h	u/Um	u	Cv/Cm	Cv	Cw
2.92						3.06					
(m/s) (%) (%)						(m/s) (%) (%)					
q1157Cm 5.6						q1305Cm12.2					
0.1	0.8	2.31	2.14	12.0	26.5	0.1	0.8	2.37	1.95	23.7	45.2
0.2	0.8	2.48	1.90	10.7	24.1	0.2	0.9	2.60	1.87	22.8	43.9
0.2	1.0	3.01	1.56	8.7	20.2	0.2	0.9	2.78	1.57	19.1	38.5
0.3	1.1	3.21	1.31	7.3	17.3	0.3	1.0	3.00	1.36	16.5	34.4
0.4	1.1	3.29	1.04	5.8	14.1	0.4	1.1	3.34	1.19	14.5	31.0
0.5	1.2	3.40	0.96	5.4	13.1	0.4	1.1	3.49	0.97	11.8	26.2
0.5	1.2	3.44	0.79	4.4	11.0	0.5	1.1	3.49	0.84	10.3	23.3
0.6	1.2	3.46	0.53	2.9	7.5	0.6	1.2	3.53	0.72	8.8	20.3
0.7	1.1	3.27	0.48	2.7	6.8	0.6	1.2	3.56	0.64	7.8	18.4
0.8	1.1	3.24	0.34	1.9	4.9	0.7	1.1	3.45	0.50	6.1	14.7
1.0	1.0	3.00	0.16	0.9	2.4	0.8	1.1	3.47	0.42	5.2	12.6
						1.0	1.1	3.45	0.21	2.6	6.6

Figure 4-7a Normalized Depth-Velocity for steady uniform sand water mixture, particle D1, group 6.45, slope=28.6% channel centre

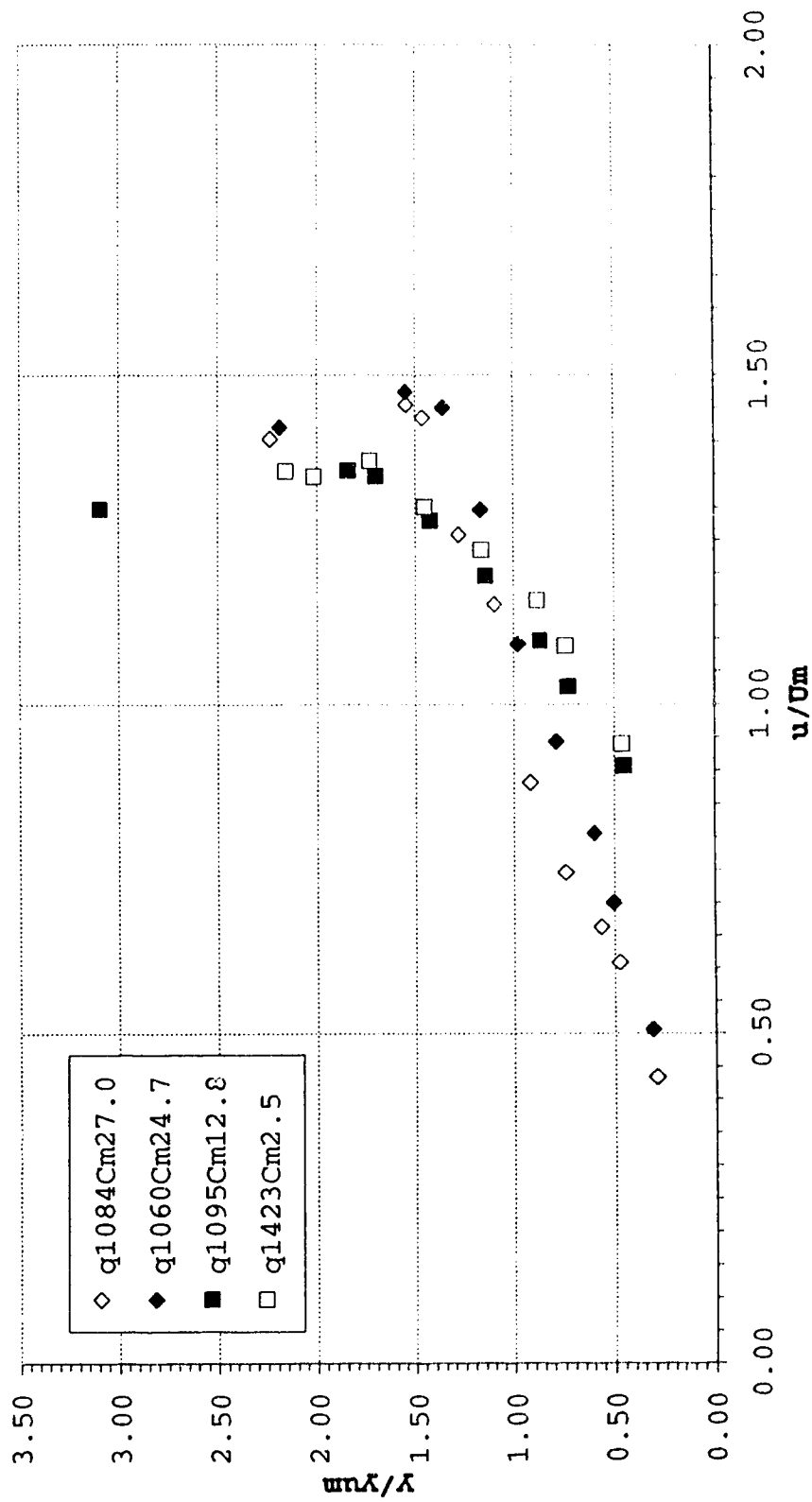


Figure 4-7b Normalized Depth-Concentration for steady uniform sand water mixture, particle D1, group 6.45, slope=28.6%, channel centre

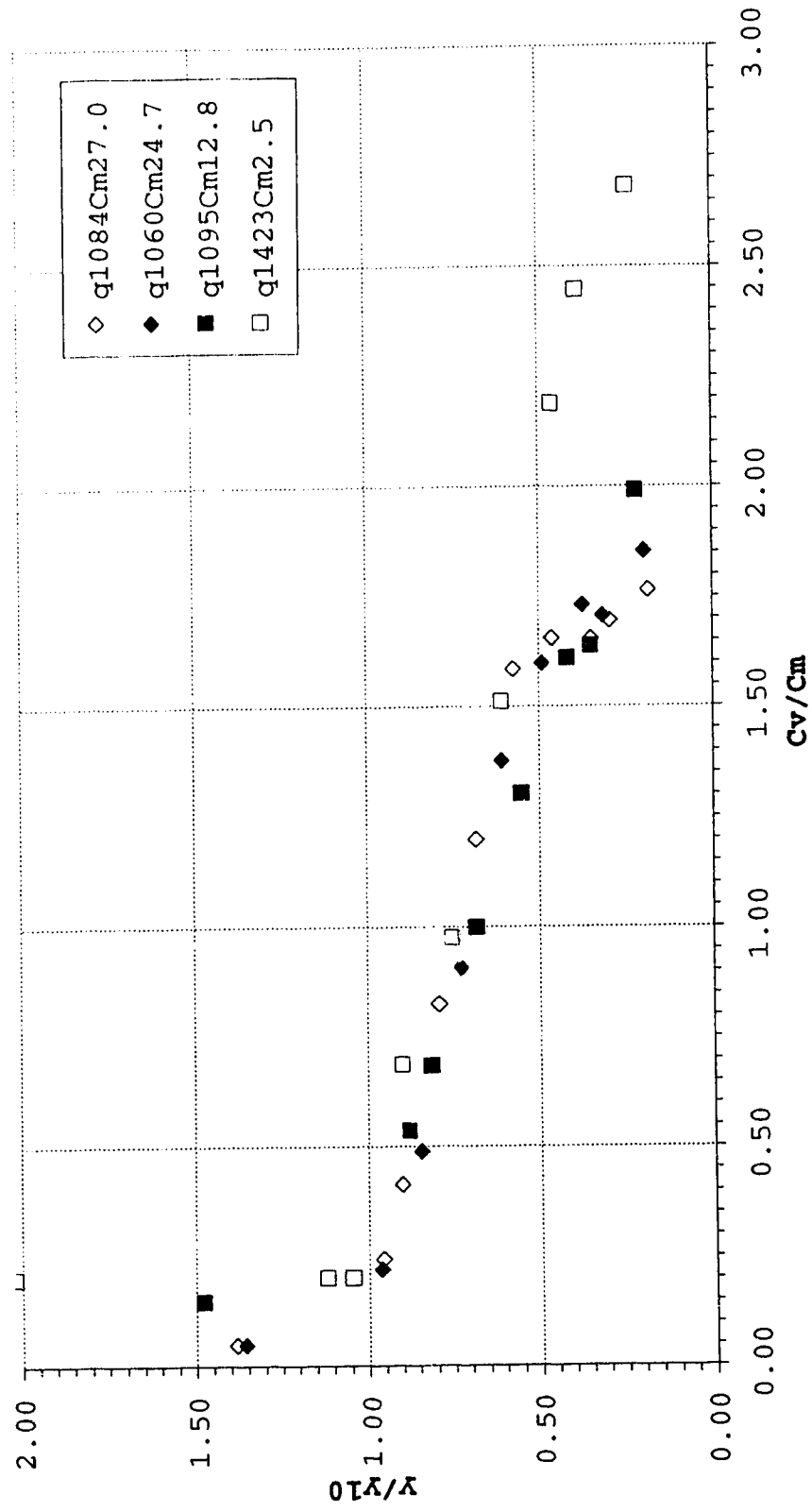


Table 4-4 Summary of Velocity and Concentration
profiles for Concentration set C1 to C4 Sediment D1
Group 6.45, Channel centre

q=1084sq cm/s Cm=27.0				h = 3.8				q=1060sq cm/s Cm=24.7				h = 3.5					
Um=		2.85 yum=		1.70 y10=		2.75		Um=		3.03 yum=		1.60 y10=		2.58			
Y	Y/yum	Y/y10	u/U _m	Cv/C _m	Cv	u		Y	Y/yum	Y/y10	u/U _m	Cv/C _m	Cv	u			
(cm)							(%)	(m/s)	(cm)							(%)	(m/s)
q1084Cm27.0																	
0.5	0.29	0.18	0.43	1.77	47.7	1.24		0.5	0.31	0.19	0.51	1.85	45.8	1.54			
0.8	0.47	0.29	0.61	1.69	45.8	1.73		0.8	0.50	0.31	0.70	1.71	42.1	2.00			
1.0	0.56	0.35	0.66	1.65	44.7	1.89		1.0	0.60	0.37	0.81	1.73	42.8	2.30			
1.3	0.74	0.46	0.75	1.66	44.7	2.13		1.3	0.79	0.49	0.94	1.60	39.5	2.69			
1.6	0.92	0.57	0.88	1.59	42.8	2.51		1.6	0.98	0.61	1.09	1.38	34.0	3.11			
1.9	1.10	0.68	1.15	1.20	32.4	3.28		1.9	1.17	0.73	1.30	0.91	22.4	3.69			
2.2	1.28	0.79	1.26	0.82	22.3	3.59		2.2	1.36	0.84	1.45	0.49	12.1	4.13			
2.5	1.46	0.90	1.44	0.41	11.2	4.09		2.5	1.55	0.96	1.47	0.22	5.4	4.20			
2.6	1.55	0.96	1.45	0.24	6.5	4.14		3.5	2.19	1.36	1.42	0.05	1.2	4.05			
3.8	2.24	1.38	1.40	0.05	1.3	4.00											
q1060Cm24.7																	
0.5	0.29	0.18	0.43	1.77	47.7	1.24		0.5	0.31	0.19	0.51	1.85	45.8	1.54			
0.8	0.47	0.29	0.61	1.69	45.8	1.73		0.8	0.50	0.31	0.70	1.71	42.1	2.00			
1.0	0.56	0.35	0.66	1.65	44.7	1.89		1.0	0.60	0.37	0.81	1.73	42.8	2.30			
1.3	0.74	0.46	0.75	1.66	44.7	2.13		1.3	0.79	0.49	0.94	1.60	39.5	2.69			
1.6	0.92	0.57	0.88	1.59	42.8	2.51		1.6	0.98	0.61	1.09	1.38	34.0	3.11			
1.9	1.10	0.68	1.15	1.20	32.4	3.28		1.9	1.17	0.73	1.30	0.91	22.4	3.69			
2.2	1.28	0.79	1.26	0.82	22.3	3.59		2.2	1.36	0.84	1.45	0.49	12.1	4.13			
2.5	1.46	0.90	1.44	0.41	11.2	4.09		2.5	1.55	0.96	1.47	0.22	5.4	4.20			
2.6	1.55	0.96	1.45	0.24	6.5	4.14		3.5	2.19	1.36	1.42	0.05	1.2	4.05			
3.8	2.24	1.38	1.40	0.05	1.3	4.00											

Figure 4-8a Normalized Depth-Velocity for steady uniform sand water mixture, particle D1, group 7.90, slope=28.6%, channel centre

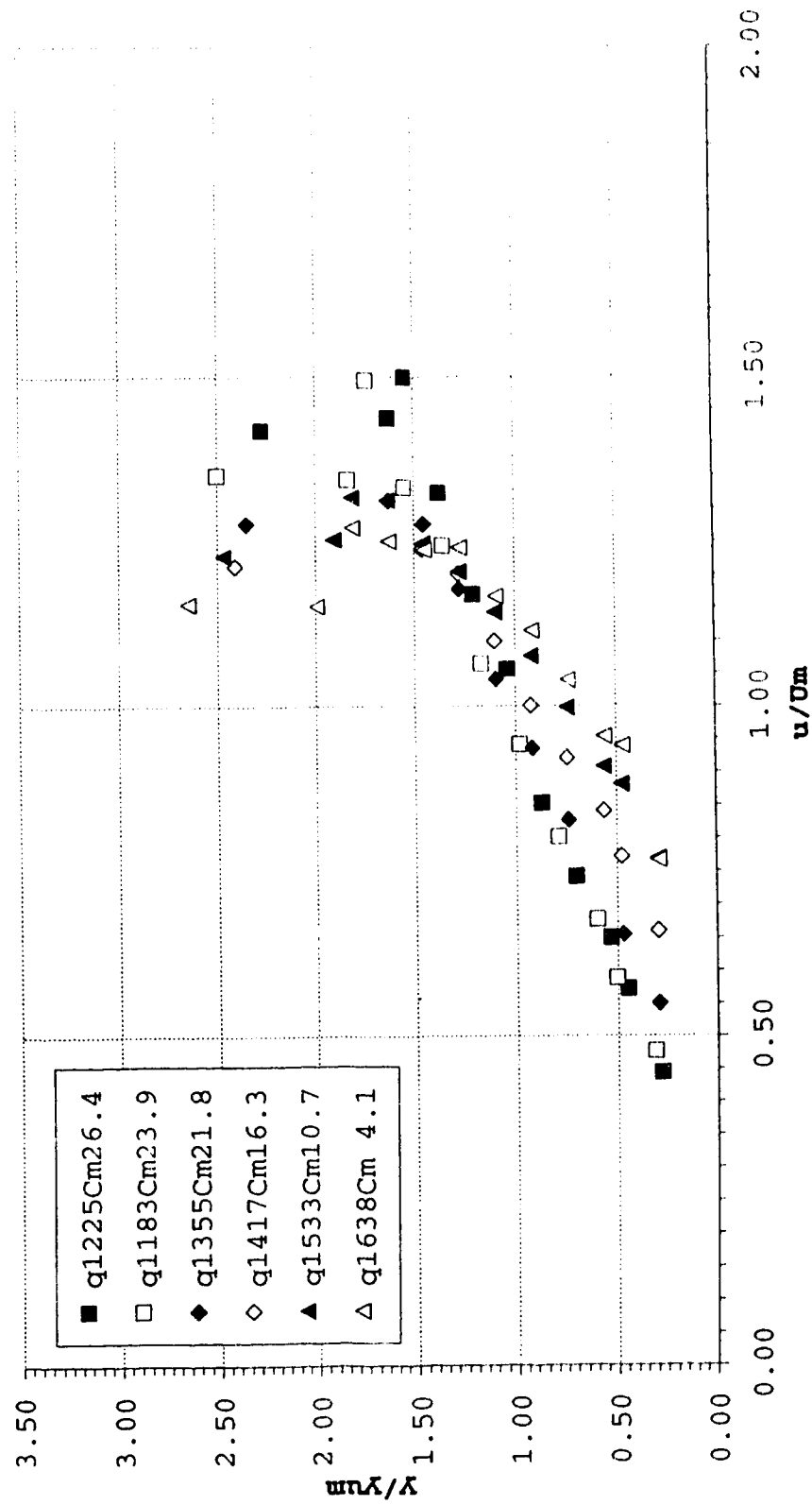


Figure 4-8b Normalized Depth-Concentration for steady uniform sand water mixture, particle D₁, group 7.90, slope=28.6%, channel centre

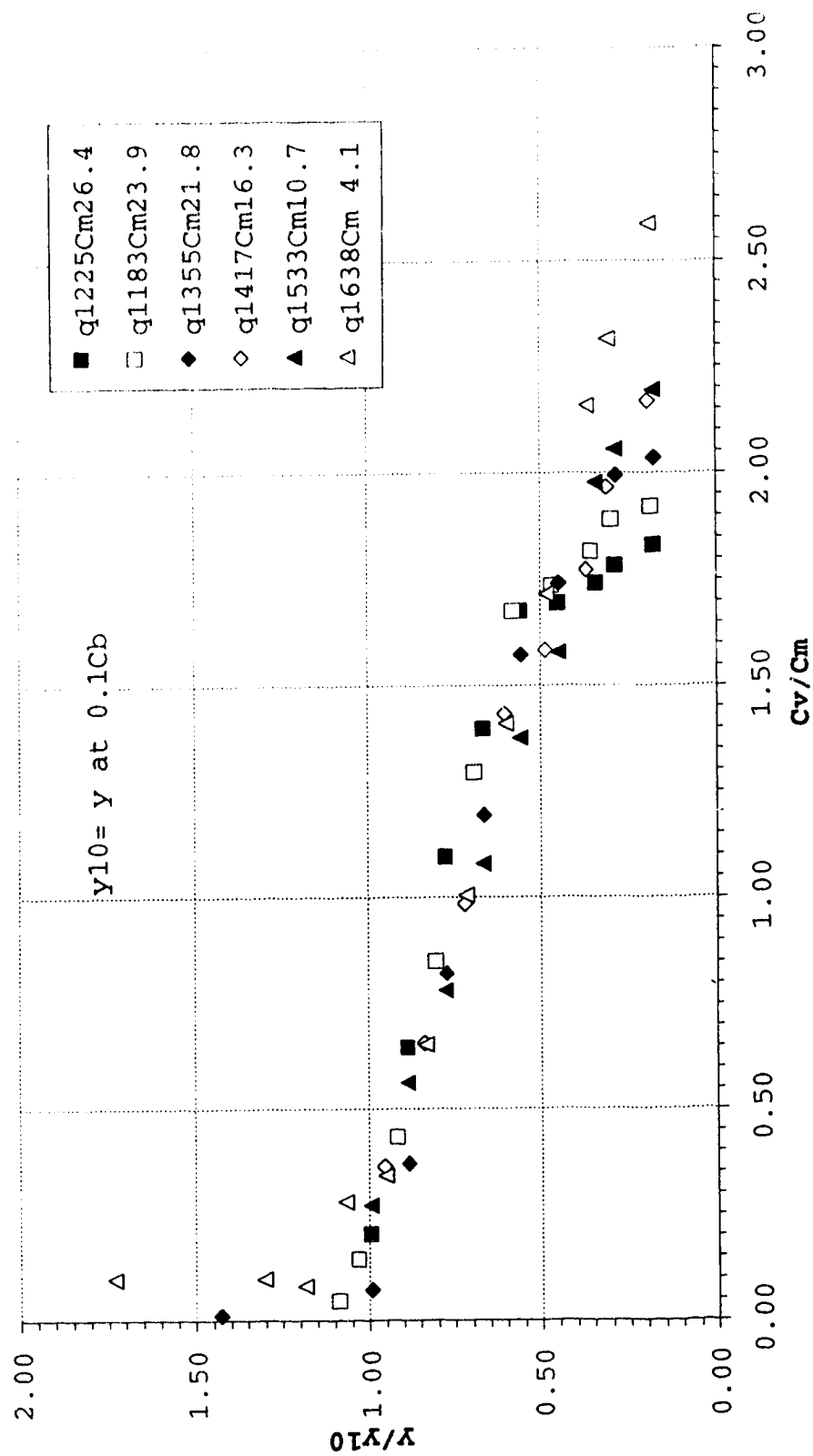


Table 4-5 Summary of Velocity and Concentration
profiles for Concentration set C1 to C6 Sediment D1
Group 7.90, Channel centre

q=1183sq cm/s Cm=23.9							h = 4.0			q=1225sq cm/s Cm=26.4							h = 4.1																								
Um= 2.96 Yum= 1.60 Y10= 2.70							Um= 2.99 Yum= 1.80 Y10= 2.80																																		
Y	Y/Yum	Y/Y10	u/Um	Cv/Cm	Cv	V	Y	Y/Yum	Y/Y10	u/Um	Cv/Cm	Cv	V	Y	Y/Yum	Y/Y10	u/Um	Cv/Cm	Cv	V																					
(cm)	(%)						(m/s)	(cm)	(%)						(m/s)	(cm)	(%)						(m/s)																		
q1183Cm23.9																					q1225Cm26.4																				
0.5	0.31	0.19	0.48	1.92	45.9	1.41	0.5	0.28	0.18	0.44	1.83	48.3	1.32	0.5	0.28	0.18	0.44	1.83	48.3	1.32																					
0.8	0.50	0.30	0.59	1.89	45.2	1.74	0.8	0.45	0.29	0.57	1.78	47.1	1.59	0.8	0.45	0.29	0.57	1.78	47.1	1.59																					
1.0	0.60	0.35	0.68	1.82	43.4	2.00	1.0	0.53	0.34	0.65	1.74	46.0	1.92	1.0	0.53	0.34	0.65	1.74	46.0	1.92																					
1.3	0.79	0.47	0.80	1.74	41.5	2.37	1.3	0.70	0.45	0.74	1.69	44.7	2.20	1.3	0.70	0.45	0.74	1.69	44.7	2.20																					
1.6	0.98	0.58	0.94	1.68	40.0	2.79	1.6	0.87	0.56	0.85	1.68	44.3	2.52	1.6	0.87	0.56	0.85	1.68	44.3	2.52																					
1.9	1.17	0.69	1.06	1.29	30.9	3.15	1.9	1.04	0.67	1.06	1.40	36.9	3.13	1.9	1.04	0.67	1.06	1.40	36.9	3.13																					
2.2	1.36	0.81	1.24	0.85	20.3	3.68	2.2	1.21	0.78	1.17	1.09	28.9	3.46	2.2	1.21	0.78	1.17	1.09	28.9	3.46																					
2.5	1.55	0.92	1.33	0.43	10.4	3.95	2.5	1.38	0.89	1.32	0.65	17.1	3.92	2.5	1.38	0.89	1.32	0.65	17.1	3.92																					
2.8	1.74	1.03	1.49	0.14	3.4	4.42	2.8	1.55	1.00	1.50	0.20	5.3	4.44	2.8	1.55	1.00	1.50	0.20	5.3	4.44																					
2.9	1.84	1.09	1.34	0.05	1.1	3.98	2.9	1.63	1.05	1.44	0.08	2.1	4.3	2.9	1.63	1.05	1.44	0.08	2.1	4.3																					
4.0	2.50	1.48	1.35	0.04	1.0	4.0	4.1	2.28	1.46	1.42	0.04	1.0	4.2	4.1	2.28	1.46	1.42	0.04	1.0	4.2																					

Table 4-5 Summary of Velocity and Concentration profiles for Concentration set C1 to C6 Sediment D1 Group 7.90, Channel centre

q=1417sq cm/s Cm=16.3				h = 4.1				q=1533sq cm/s Cm=10.7				h = 4.2			
Um= 3.46 yUm= 1.70 y10= 2.60								Um= 3.65 yUm= 1.70 y10= 2.80							
Y	y/yUm	Y/Y10	u/Um	Cv/Cm	Cv	V		Y	y/yUm	Y/Y10	u/Um	Cv/Cm	Cv	V	
(cm)	q1417Cm16.3						(%)	(m/s)	(cm)	q1533Cm10.7					
0.5	0.29	0.19	0.66	2.17	35.3	2.28		0.5	0.29	0.18	0.77	2.19	23.5	2.66	
0.8	0.47	0.31	0.77	1.97	32.0	2.67		0.8	0.47	0.29	0.88	2.05	22.0	3.05	
1.0	0.56	0.37	0.84	1.77	28.9	2.91		1.0	0.56	0.34	0.91	1.98	21.1	3.14	
1.3	0.74	0.49	0.92	1.58	25.8	3.15		1.3	0.74	0.45	1.00	1.58	16.9	3.45	
1.6		0.60	1.00	1.43	23.4	3.46		1.6	0.92	0.56	1.08	1.37	14.7	3.72	
1.9		0.72	1.10	0.99	16.1	3.80		1.9	1.10	0.67	1.14	1.08	11.5	3.95	
2.2		0.84	1.20	0.66	10.7	4.16		2.2	1.28	0.78	1.20	0.78	8.4	4.17	
2.5	1.46	0.95	1.24	0.36	5.9	4.29		2.5	1.46	0.89	1.25	0.56	6.0	4.32	
4.1	2.41	1.58	1.21	0.07	1.2	4.20		2.8	1.64	1.00	1.31	0.27	2.9	4.54	
								3.1	1.82	1.10	1.32	0.13	1.4	4.56	
								3.2	1.91	1.16	1.25	0.09	1.0	4.3	
								4.2	2.47	1.50	1.23	0.07	0.7	4.3	

Table 4-5 Summary of Velocity and Concentration
profiles for Concentration set C1 to C6 Sediment D1
Group 7.90, Channel centre

q=1638sq cm/s Cm= 4.1				h = 4.5				q=1355sq cm/s Cm=21.8				h = 4.0			
Um= 3.64 y _{um} =				1.70 y ₁₀ = 2.50				Um= 3.39 y _{um} = 1.70 y ₁₀ = 2.60							
Y	y/y _{um}	Y/Y ₁₀	u/U _m	Cv/C _m	Cv	V		Y	y/y _{um}	Y/Y ₁₀	u/U _m	Cv/C _m	Cv	V	
(cm)	(%) (m/s)							(cm)	(%) (m/s)						
	q1638Cm 4.1								q1355Cm21.8						
0.5	0.29	0.19	0.77	2.59	10.6	2.65	0.5	0.29	0.18	0.55	2.03	44.3	1.90		
0.8	0.47	0.31	0.94	2.31	9.5	3.25	0.8	0.47	0.28	0.65	1.99	43.4	2.27		
0.9	0.56	0.36	0.95	2.16	8.8	3.30	1.3	0.74	0.45	0.83	1.74	37.9	2.86		
1.3	0.74	0.48	1.04	1.72	7.0	3.60	1.6	0.92	0.56	0.94	1.57	34.3	3.24		
1.6	0.92	0.60	1.11	1.41	5.8	3.86	1.9	1.10	0.67	1.04	1.19	26.0	3.60		
1.9	1.10	0.72	1.17	1.00	4.1	4.04	2.2	1.28	0.77	1.18	0.82	17.9	4.08		
2.2	1.28	0.83	1.24	0.65	2.7	4.29	2.5	1.45	0.88	1.28	0.37	8.1	4.42		
2.5	1.45	0.95	1.24	0.34	1.4	4.28	2.8	1.63	0.99	1.31	0.07	1.6	4.54		
2.8	1.63	1.07	1.25	0.28	1.1	4.33	4.0	2.35	1.43	1.28	0.01	0.3	4.42		
3.1	1.81	1.19	1.27	0.08	0.3	4.40									
3.4	1.99	1.30	1.15	0.10	0.4	4.0									
4.5	2.65	1.73	1.16	0.10	0.4	4.0									

Figures 4-9 to 4-10 and Tables 4-6 to 4-7 give the detail plots and data for the normalized velocity and concentration profiles for particle D2 ($\approx 0.335\text{mm}$).

Figures 4-11 to 4-12 and Tables 4-8 to 4-9 give the detail plots and data for the normalized velocity and concentration profiles for particle D3 ($\approx 0.215\text{mm}$). Another variable, y_{cm} , is introduced here to normalized the concentration profile. y_{cm} represents the height above the bed where the concentration is equal to the mean concentration for the profile, C_m . The normalizing variables in all the above plots have been chosen mainly to obtain the least scatter of data.

Figures 4-13 to 4-14 and Tables 4-10 to 4-11 give the detail plots and data for the normalized velocity and concentration profiles for particle D4 ($\approx 0.330\text{mm}$). It is important to note here that although the mean particle diameter of D4 is about the same as D1, D4 represents a sample with a much severe particle gradation than the other three sizes which are approaching uniform gradation. The consequences of this can be seen in the differing nature of the velocity and concentration profiles between particles D1 and D4. This will be discussed later.

Figure 4-9a Normalized Depth-Velocity for steady uniform sand water mixture, particle D2, group 6.45, 28.6%, channel centre

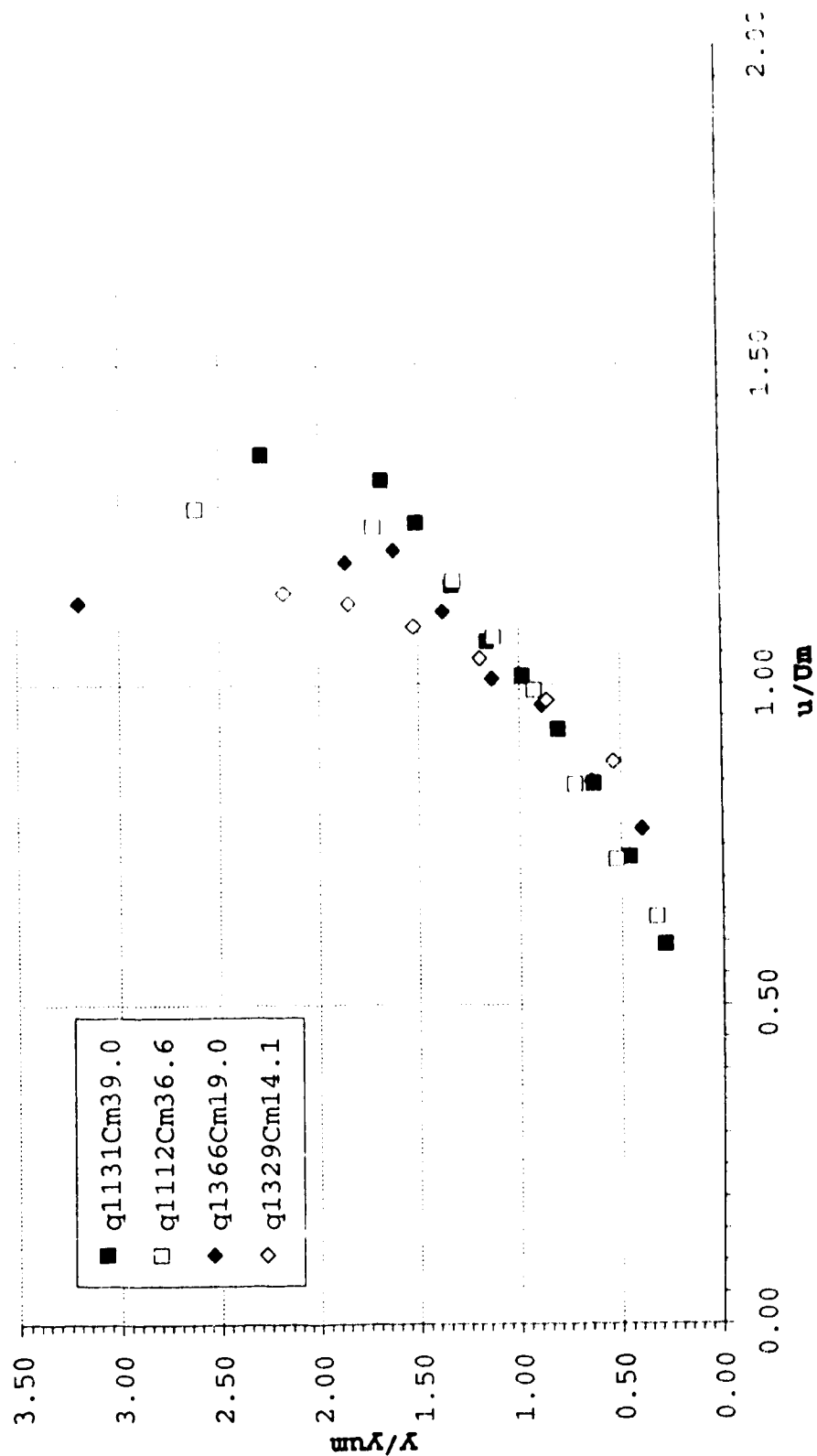


Figure 4-9b Normalized Depth-Concentration for steady uniform sand water mixture, particle D2, group 6.45,slope=28.6%, channel centre

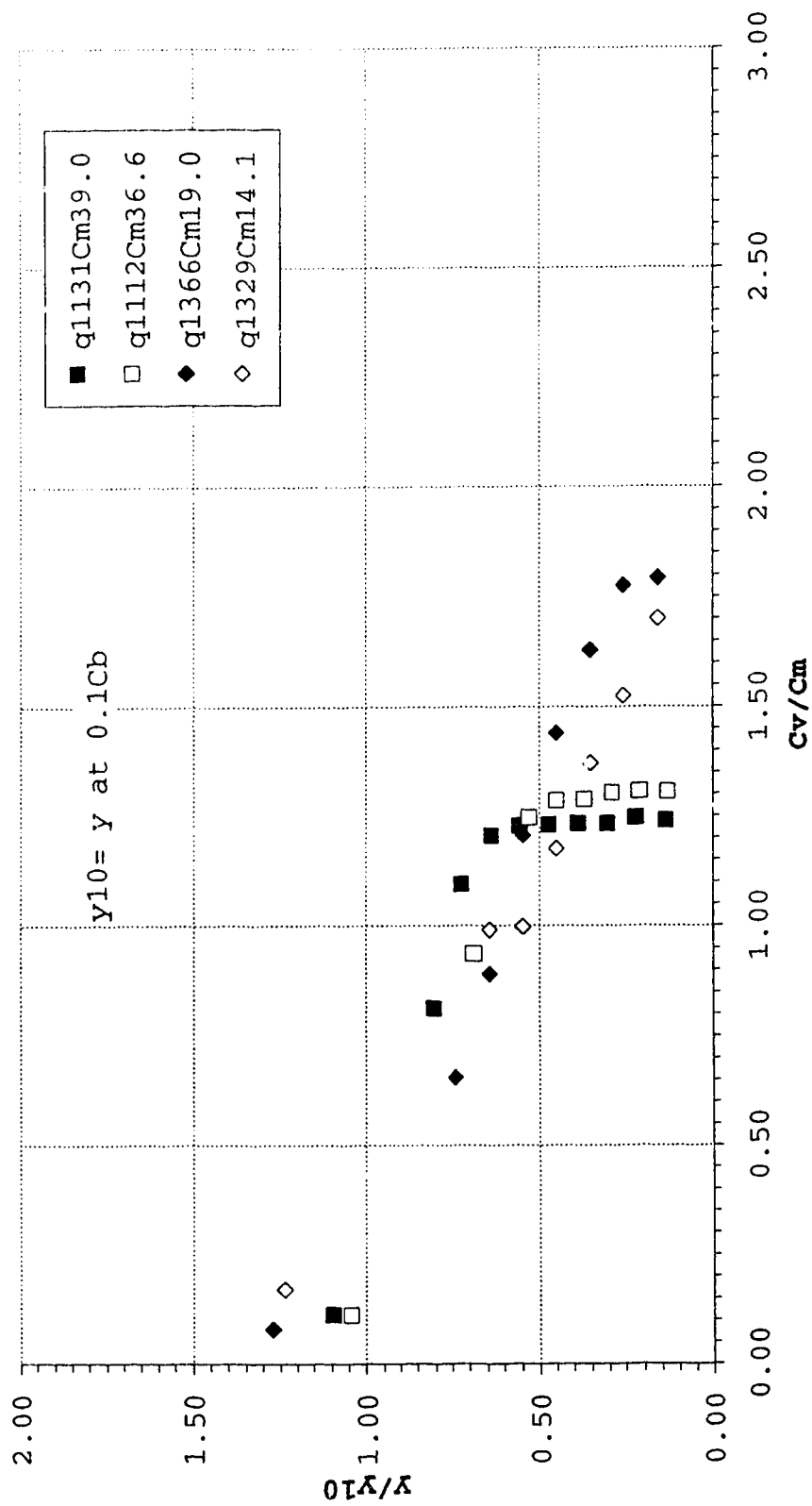


Table 4-6 Summary of Velocity and Concentration profiles for Group 6.45,
set C1 to C4, Sediment D2, Channel centre

q=1366sq cm/s Cm=19.0						q=1112sq cm/s Cm=36.6						h= 4.0					
Um= 3.41 ycm= 1.90 yum= 1.25 y10= 3.15						Um= 2.78 ycm= 2.55 yum= 1.53 y10= 3.83											
Y	Y/yum	Y/y10	u/Um	Cv	u	Y	Y/yum	Y/y10	u/Um	Cv	u	Y	Y/yum	Y/y10	u/Um	Cv	u
(cm)				(%)	(m/s)	(cm)				(%)	(m/s)					(%)	(m/s)
ql366Cm19.0																	
0.5	0.40	0.16	0.26	0.77	1.79	34.1	2.64	0.5	0.33	0.13	0.20	0.64	1.31	47.8	1.77	0.5	0.33
0.8	0.64	0.26	0.42	0.85	1.78	33.7	2.89	0.8	0.53	0.21	0.32	0.73	1.31	47.8	2.02	0.8	0.53
1.1	0.89	0.35	0.58	0.97	1.63	30.9	3.30	1.1	0.73	0.29	0.44	0.84	1.30	47.7	2.34	1.1	0.73
1.4	1.13	0.45	0.74	1.01	1.44	27.4	3.44	1.4	0.92	0.37	0.55	0.99	1.29	47.1	2.75	1.4	0.92
1.7	1.38	0.55	0.90	1.12	1.20	22.9	3.81	1.7	1.12	0.45	0.67	1.07	1.28	47.0	2.99	1.7	1.12
2.0	1.62	0.64	1.07	1.21	0.89	16.9	4.13	2.0	1.32	0.53	0.79	1.16	1.25	45.6	3.23	2.0	1.32
2.3	1.86	0.74	1.23	1.19	0.66	12.4	4.07	2.6	1.72	0.69	1.03	1.25	0.94	34.3	3.47	2.6	1.72
4.0	3.20	1.27	2.11	1.13	0.08	1.5	3.85	4.0	2.61	1.04	1.57	1.28	0.11	4.1	3.55	4.0	2.61
q=1329sq cm/s Cm=14.1																	
h= 3.9																	
q=1131sq cm/s Cm=39.0						Um= 2.83 ycm= 2.77 yum= 1.75 y10= 3.65						Um= 3.41 ycm= 1.67 yum= 0.93 y10= 3.15					
Y	Y/yum	Y/y10	u/Um	Cv	u	Y	Y/yum	Y/y10	u/Um	Cv	u	Y	Y/yum	Y/y10	u/Um	Cv	u
(cm)				(%)	(m/s)	(cm)				(%)	(m/s)	(cm)				(%)	(m/s)
ql131Cm39.0																	
0.5	0.29	0.14	0.18	0.59	1.24	48.3	1.68	0.5	0.54	0.16	0.30	0.88	1.70	24.0	3.00	0.5	0.54
0.8	0.46	0.22	0.29	0.73	1.25	48.6	2.07	0.8	0.87	0.26	0.48	0.98	1.52	21.5	3.33	0.8	0.87
1.1	0.63	0.30	0.40	0.84	1.23	48.1	2.39	1.1	1.19	0.35	0.66	1.04	1.37	19.3	3.55	1.1	1.19
1.4	0.81	0.39	0.51	0.93	1.23	48.1	2.63	1.4	1.52	0.45	0.85	1.09	1.18	16.6	3.72	1.4	1.52
1.7	0.98	0.47	0.62	1.01	1.23	47.9	2.87	1.7	1.85	0.55	1.03	1.13	1.00	14.1	3.85	1.7	1.85
2.0	1.16	0.55	0.73	1.07	1.23	47.8	3.02	2.0	2.18	0.64	1.21	1.15	0.99	14.0	3.91	2.0	2.18
2.3	1.33	0.64	0.84	1.16	1.20	47.0	3.27	3.9	4.19	1.24	2.34	1.07	0.17	2.4	3.65	3.9	4.19
2.6	1.50	0.72	0.95	1.25	1.09	42.7	3.55										
2.9	1.68	0.81	1.06	1.32	0.81	31.7	3.74										
4.0	2.29	1.10	1.44	1.36	0.11	4.4	3.85										

Figure 4-10a Normalized Depth-Velocity for steady uniform sand water mixture, particle D2, group 7.90, slope=28.6%, channel centre

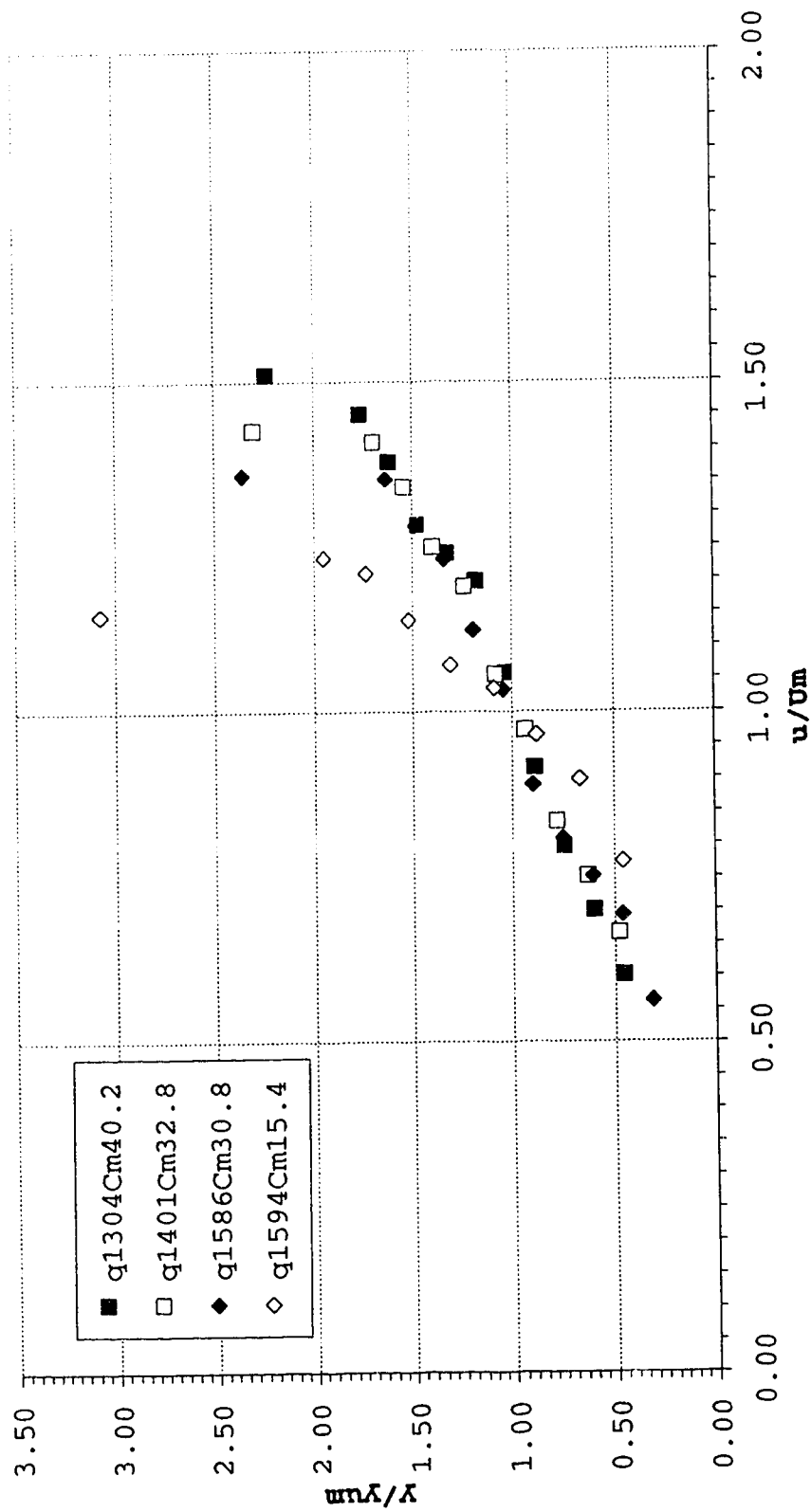


Figure 4-10b Normalized Depth-Concentration for steady uniform sand water mixture, particle D2, group 7.90, slope=28.6%, channel centre

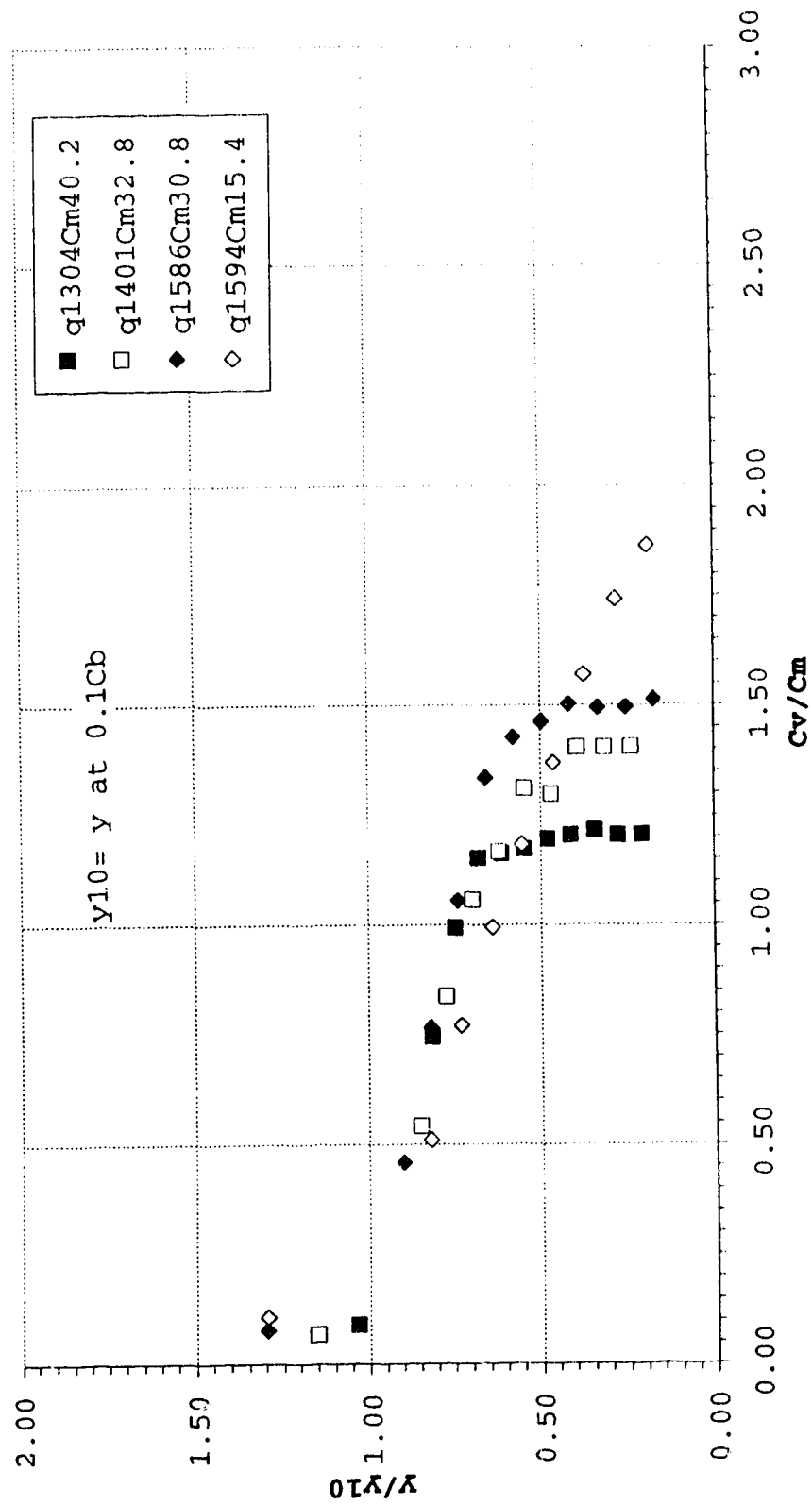


Table 4-7 Summary of Velocity and Concentration profiles
for Group 7.90, set C1 to C4, Sediment D2
Channel centre

q=1304sq cm/s Cm=40.2										q=1401sq cm/s Cm=32.8										h = 4.7										h = 4.6													
Um= 2.78 ycm= 3.40 yum= 2.10 y10= 4.55										Um= 3.05 ycm= 2.85 yum= 2.00 y10= 4.00																																	
Y	y/yum	y/y10	y/ycm	u/Um	Cv/Cm	Cv	u			Y	y/yum	y/y10	y/ycm	u/Um	Cv/Cm	Cv	u			Y	y/yum	y/y10	y/ycm	u/Um	Cv/Cm	Cv	u			Y	y/yum	y/y10	y/ycm	u/Um	Cv/Cm	Cv	u						
(cm)	(%)										(cm)	(%)										(cm)	(%)										(m/s)	(m/s)									
	q1304Cm40.2											q1401Cm32.8																															
1.0	0.46	0.21	0.28	0.60	1.21	48.5	1.67			1.0	0.48	0.24	0.34	0.67	1.40	46.1	2.03			1.0	0.48	0.24	0.34	0.67	1.40	46.1	2.03			1.0	0.48	0.24	0.34	0.67	1.40	46.1	2.03						
1.3	0.60	0.28	0.37	0.70	1.20	48.4	1.95			1.3	0.63	0.32	0.44	0.75	1.40	46.0	2.29			1.3	0.63	0.32	0.44	0.75	1.40	46.0	2.29			1.3	0.63	0.32	0.44	0.75	1.40	46.0	2.29						
1.6	0.75	0.34	0.46	0.80	1.22	48.9	2.22			1.6	0.78	0.39	0.55	0.83	1.40	46.1	2.54			1.6	0.78	0.39	0.55	0.83	1.40	46.1	2.54			1.6	0.78	0.39	0.55	0.83	1.40	46.1	2.54						
1.9	0.89	0.41	0.55	0.92	1.20	48.4	2.55			1.9	0.94	0.47	0.66	0.97	1.30	42.6	2.97			1.9	0.94	0.47	0.66	0.97	1.30	42.6	2.97			1.9	0.94	0.47	0.66	0.97	1.30	42.6	2.97						
2.2	1.04	0.48	0.64	1.06	1.20	48.1	2.94			2.2	1.09	0.54	0.76	1.06	1.31	43.0	3.22			2.2	1.09	0.54	0.76	1.06	1.31	43.0	3.22			2.2	1.09	0.54	0.76	1.06	1.31	43.0	3.22						
2.5	1.18	0.55	0.73	1.20	1.17	47.2	3.33			2.5	1.24	0.62	0.87	1.19	1.17	38.3	3.63			2.5	1.24	0.62	0.87	1.19	1.17	38.3	3.63			2.5	1.24	0.62	0.87	1.19	1.17	38.3	3.63						
2.8	1.33	0.61	0.82	1.24	1.16	46.8	3.45			2.8	1.39	0.70	0.98	1.25	1.06	34.7	3.81			2.8	1.39	0.70	0.98	1.25	1.06	34.7	3.81			2.8	1.39	0.70	0.98	1.25	1.06	34.7	3.81						
3.1	1.47	0.68	0.91	1.28	1.15	46.3	3.57			3.1	1.55	0.77	1.08	1.34	0.84	27.5	4.09			3.1	1.55	0.77	1.08	1.34	0.84	27.5	4.09			3.1	1.55	0.77	1.08	1.34	0.84	27.5	4.09						
3.4	1.62	0.75	1.00	1.38	0.99	39.9	3.83			3.4	1.70	0.85	1.19	1.41	0.54	17.8	4.29			3.4	1.70	0.85	1.19	1.41	0.54	17.8	4.29			3.4	1.70	0.85	1.19	1.41	0.54	17.8	4.29						
3.7	1.76	0.81	1.09	1.45	0.74	29.9	4.03			4.6	2.30	1.15	1.61	1.43	0.07	2.2	4.4			4.6	2.30	1.15	1.61	1.43	0.07	2.2	4.4			4.6	2.30	1.15	1.61	1.43	0.07	2.2	4.4						
4.7	2.24	1.03	1.38	1.51	0.09	3.6	4.2																																				

Table 4-7 Summary of Velocity and Concentration profiles
for Group 7.90, set C1 to C4, Sediment D2
Channel centre

q=1594sq cm/s Cm=15.4					q=1586sq cm/s Cm=30.8				
Um= 3.62 ycm= 2.13 yum= 1.43 y10= 3.40					Um= 3.24 ycm= 2.85 yum= 2.08 y10= 3.78				
h = 4.4					h = 4.9				
y	y/yum	y/y10	y/ycm	u/U _m	Cv	Cv/Cm	u/U _m	Cv	u
(cm)	(m/s)				(%)	(cm)	(m/s)		
q1594Cm15.4									
0.7	0.46	0.19	0.31	0.77	1.86	28.7	2.80		
1.0	0.67	0.28	0.45	0.90	1.74	26.8	3.25		
1.3	0.88	0.37	0.59	0.97	1.57	24.2	3.50		
1.6	1.10	0.46	0.74	1.04	1.37	21.1	3.75		
1.9	1.31	0.55	0.88	1.07	1.18	18.2	3.88		
2.2	1.52	0.64	1.02	1.14	0.99	15.3	4.12		
2.5	1.74	0.73	1.16	1.21	0.77	11.9	4.38		
2.8	1.95	0.82	1.31	1.23	0.51	7.8	4.46		
4.4	3.08	1.29	2.07	1.15	0.11	1.7	4.15		
q1586Cm30.8									
0.7	0.31	0.17	0.23	0.56	1.51	46.6	1.82		
1.0	0.46	0.25	0.34	0.69	1.50	46.1	2.24		
1.3	0.61	0.33	0.44	0.75	1.49	46.0	2.43		
1.6	0.75	0.41	0.55	0.81	1.50	46.3	2.62		
1.9	0.90	0.50	0.66	0.89	1.46	45.1	2.88		
2.2	1.05	0.58	0.76	1.03	1.43	44.0	3.35		
2.5	1.19	0.66	0.87	1.12	1.34	41.1	3.64		
2.8	1.34	0.74	0.98	1.23	1.06	32.5	3.99		
3.1	1.49	0.82	1.08	1.28	0.77	23.6	4.15		
3.4	1.63	0.90	1.19	1.35	0.46	14.1	4.38		
4.9	2.36	1.30	1.72	1.36	0.08	2.4	4.4		

Figure 4-11a Normalized Depth-Velocity for steady uniform sand water mixture, particle D3, group 6.45, slope=28.6%, channel centre

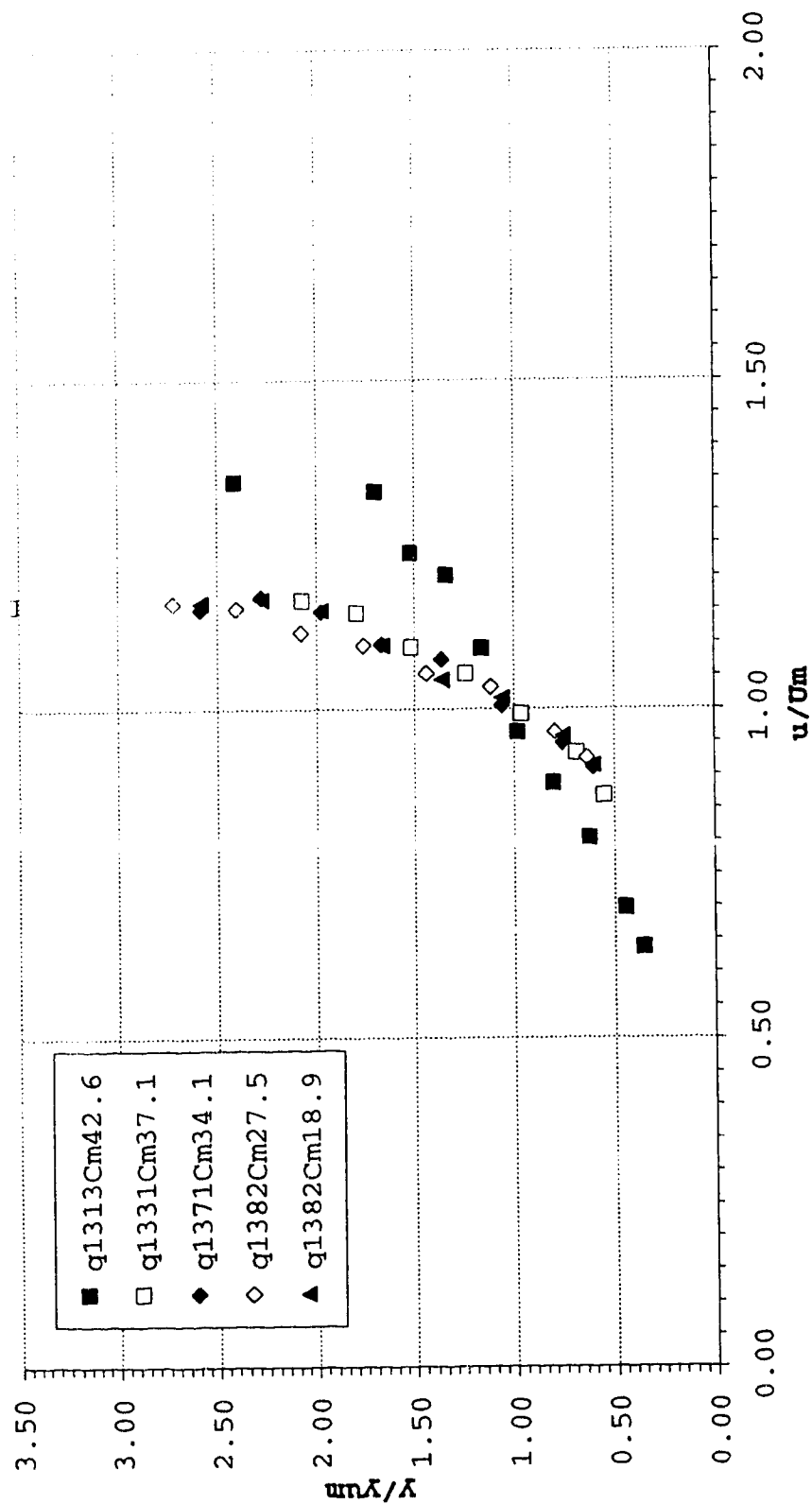


Figure 4-11b Normalized Depth-Concentration for steady uniform sand water mixture, particle D3,group 6.45,slope=28.6%, channel centre

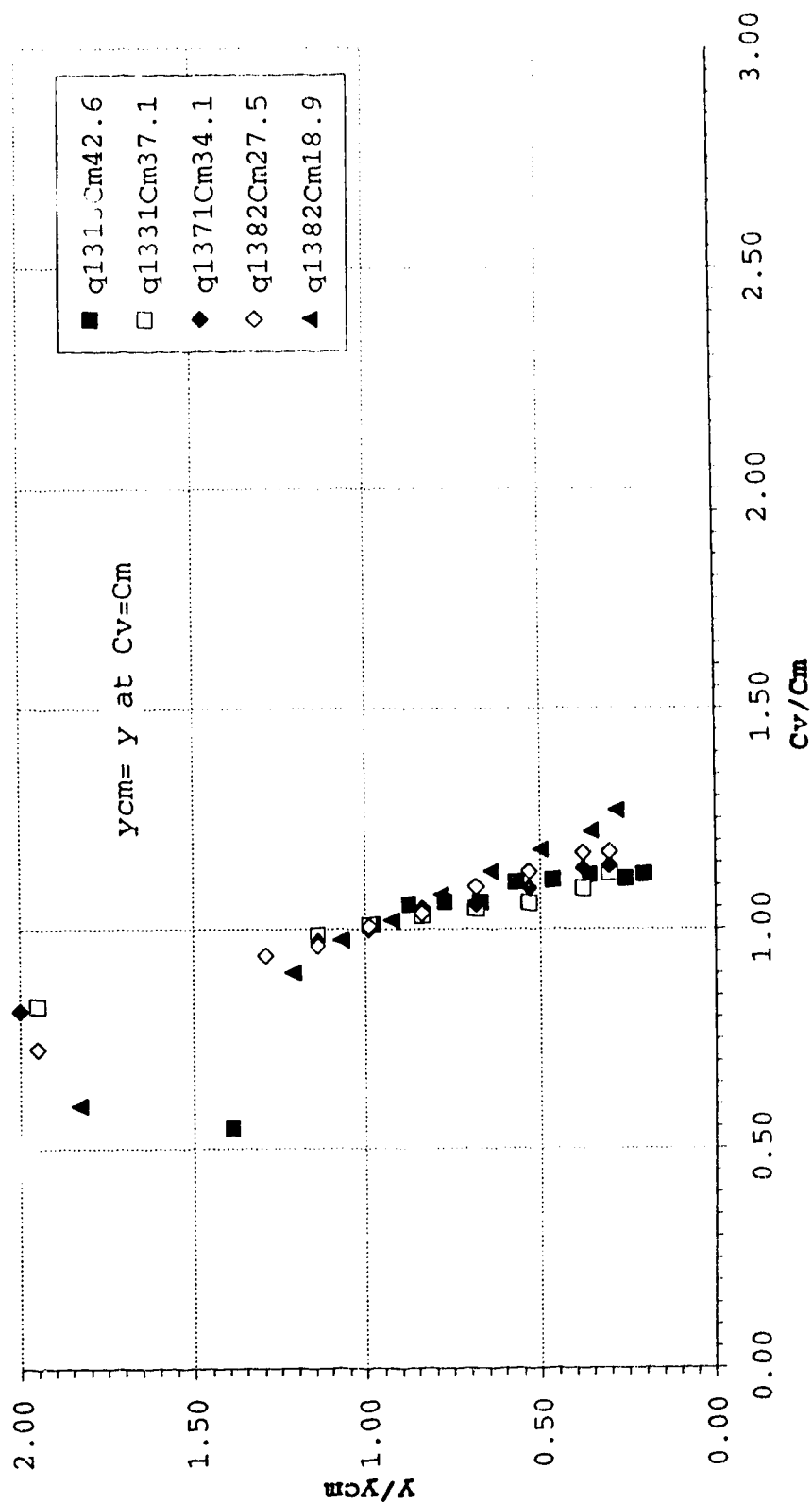


Table 4-8 Summary of Velocity and Concentration profiles
for Group 6.45, set C1 to C5, Sediment D3
Channel centre

q=1382sq cm/s Cm=27.5					q=1331sq cm/s Cm=37.1					h = 3.9				
Um= 3.54 ycm= 2.00 yum= 0.95					Um= 3.41 ycm= 2.00 yum= 1.10					h = 3.9				
Y	Y/yum	Y/ycm	u/Um	Cv	u	Y	Y/yum	Y/ycm	u/Um	Cv	Cv	u		
(cm)					(m/s)	(cm)					(%)	(m/s)		
					ql382Cm27.5						ql331Cm37.1			
0.6	0.64	0.30	0.92	1.17	32.3	0.6	0.55	0.30	0.87	1.13	41.8	2.96		
0.8	0.80	0.38	0.96	1.17	32.2	0.8	0.69	0.38	0.93	1.09	40.5	3.18		
1.1	1.12	0.53	1.03	1.13	31.1	1.1	0.96	0.53	0.99	1.06	39.2	3.38		
1.4	1.44	0.68	1.05	1.10	30.1	1.4	1.24	0.68	1.05	1.05	38.8	3.59		
1.7	1.76	0.84	1.10	1.03	28.4	1.7	1.52	0.84	1.09	1.03	38.3	3.72		
2.0	2.08	0.99	1.12	1.01	27.7	2.0	1.80	0.99	1.15	1.01	37.4	3.90		
2.3	2.40	1.14	1.15	0.96	26.5	2.3	2.07	1.14	1.16	0.99	36.6	3.97		
2.6	2.72	1.29	1.16	0.94	25.9	3.9	3.55	1.95	1.16	0.83	30.7	3.95		
3.9	4.11	1.95	1.12	0.73	20.0									

Table 4-8 Summary of Velocity and Concentration profiles
for Group 6.45, set C1 to C5, Sediment D3
Channel centre

q=1382sq cm/s		Cm=18.9		h =		3.9
Um=		3.54	ycm=	2.13	yum=	1.00
Y	Y/yum	Y/ycm	u/Um	Cv/Cm	Cv	u
(cm)						(m/s)
	q1382Cm18.9					
0.6	0.60	0.28	0.91	1.27	24.0	3.23
0.8	0.76	0.36	0.96	1.22	23.1	3.39
1.1	1.06	0.50	1.02	1.18	22.3	3.59
1.4	1.37	0.64	1.04	1.13	21.3	3.70
1.7	1.67	0.78	1.10	1.08	20.4	3.88
2.0	1.98	0.93	1.15	1.02	19.3	4.06
2.3	2.28	1.07	1.17	0.98	18.5	4.13
2.6	2.59	1.21	1.16	0.90	17.0	4.11
3.9	3.90	1.83	1.12	0.60	11.3	3.95

Figure 4-12a Normalized Depth-Velocity for steady uniform sand water mixture, particle D3, group 7.95, slope=28.6%, channel centre

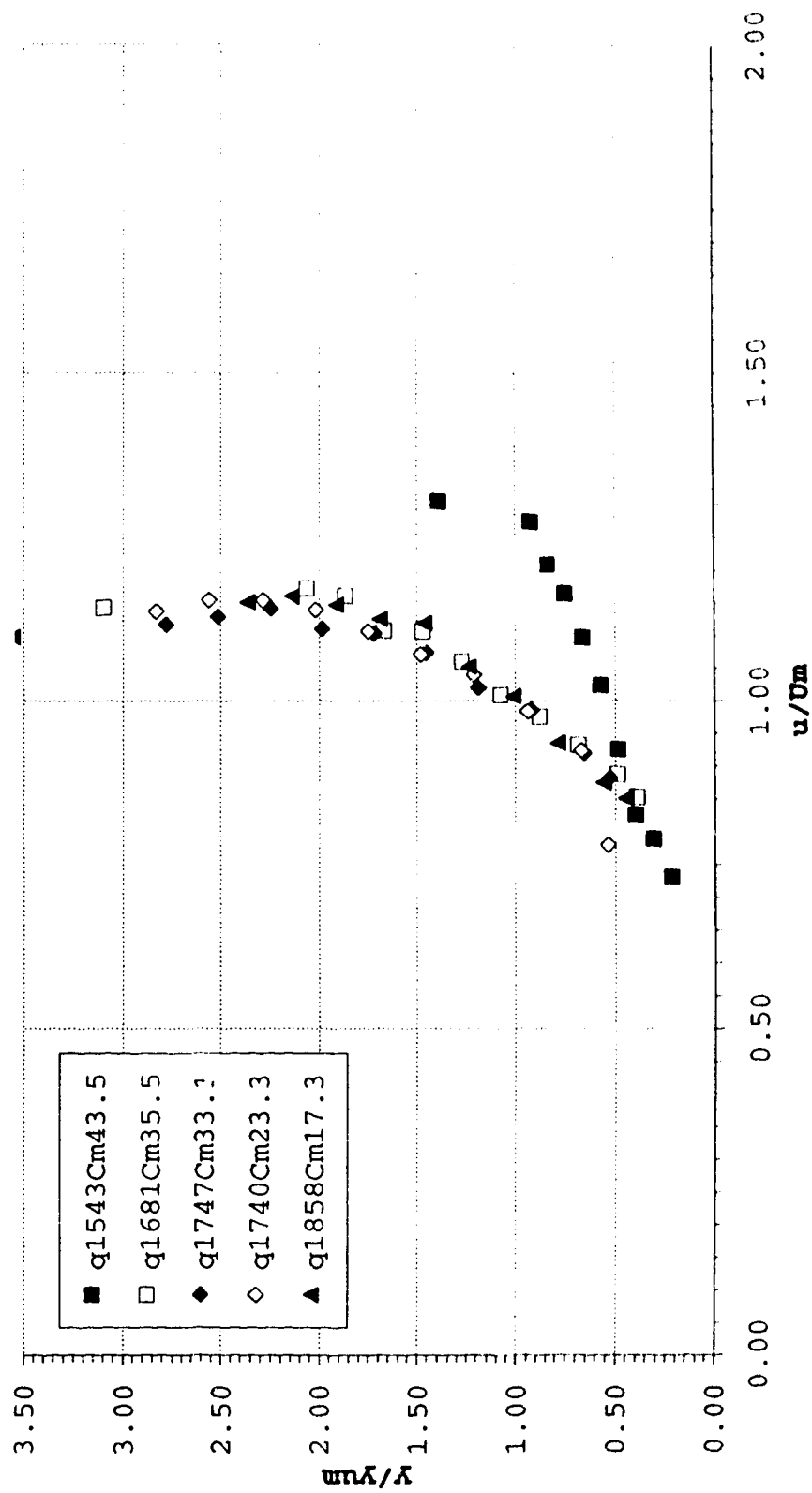


Figure 4-12b Normalized Depth-concentration for steady uniform sand water mixture, particle D3,group 7.95,slope=28.6%,channel centre

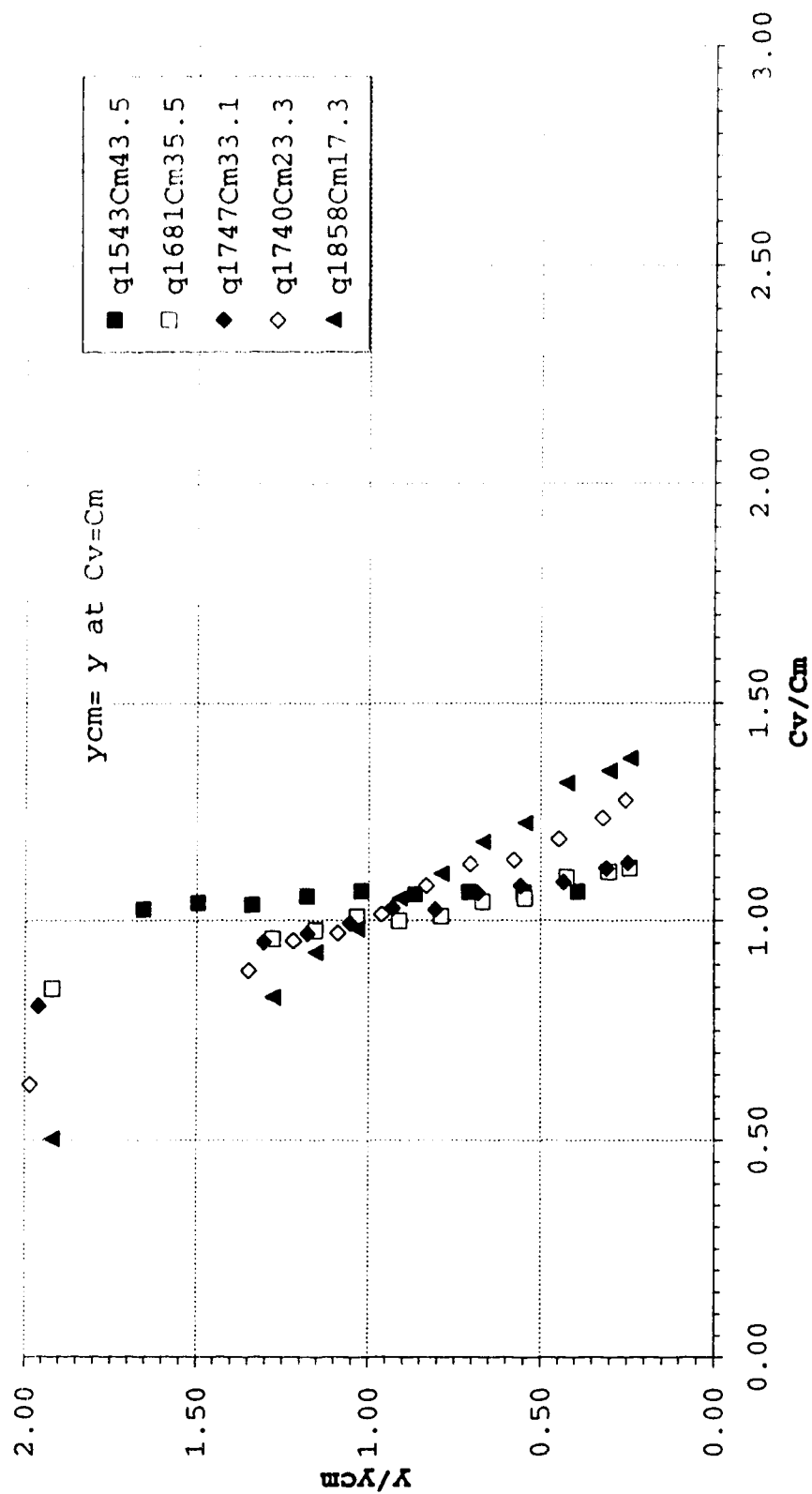


Table 4-9 Summary of Velocity and Concentration profiles
for Group 7.95, set C1 to C5, Sediment D3
Channel centre

q=1581sq cm/s Cm=35.5				h= 4.8 q=1543sq cm/s Cm=43.5				h= 4.0					
Um= 3.50 ycm= 2.50 yum= 1.55				Um= 3.22 ycm= 1.93 yum= 3.45									
Y	Y/yum	Y/ycm	u/Um	Cv	Cv/Cm	u	Y	Y/yum	Y/ycm	u/Um	Cv	u	
(cm)				(%)		(m/s)	(cm)				(%)	m/s	
				ql681Cm35.5				ql543Cm43.5					
0.6	0.39	0.24	0.85	1.12	39.8	2.98	0.8	0.22	0.39	0.73	1.07	46.4	2.35
0.8	0.49	0.30	0.89	1.11	39.5	3.10	1.1	0.31	0.55	0.79	1.07	46.4	2.54
1.1	0.68	0.42	0.93	1.10	39.1	3.26	1.4	0.40	0.71	0.82	1.07	46.4	2.65
1.4	0.88	0.55	0.98	1.05	37.3	3.41	1.7	0.48	0.87	0.93	1.06	46.1	2.98
1.7	1.08	0.67	1.01	1.04	37.0	3.53	2.0	0.57	1.02	1.02	1.07	46.5	3.30
2.0	1.27	0.79	1.06	1.01	35.9	3.71	2.3	0.66	1.18	1.10	1.06	45.9	3.53
2.3	1.47	0.91	1.11	1.00	35.5	3.87	2.6	0.75	1.34	1.16	1.04	45.1	3.75
2.6	1.67	1.03	1.11	1.01	35.8	3.88	2.9	0.84	1.50	1.21	1.04	45.3	3.89
2.9	1.86	1.16	1.16	0.98	34.7	4.07	3.2	0.93	1.66	1.27	1.02	44.6	4.10
3.2	2.06	1.28	1.17	0.96	34.0	4.10	4.8	1.39	2.49	1.39	0.74	32.1	4.20
4.8	3.10	1.92	1.14	0.85	30.0	4.0							

Table 4-9 Summary of Velocity and Concentration profiles
for Group 7.95, set C1 to C5, Sediment D3
Channel centre

q=1740sq cm/s Cm=23.3				h= 4.7				q=1747sq cm/s Cm=33.1				h= 4.8			
Um= 3.70 ycm= 2.37 yum= 1.13								Um= 3.64 ycm= 2.45 yum= 1.15							
Y	Y/yum	Y/ycm	u/Um	Cv/Cm	Cv	u		Y	Y/yum	Y/ycm	u/Um	Cv/Cm	Cv	u	
(cm)					(%)	(m/s)		(cm)				(%)	(m/s)		
q1740Cm23.3								q1747Cm33.1							
0.6	0.53	0.25	0.78	1.28	29.7	2.89	0.6	0.53	0.25	0.88	0.88	1.13	37.5	3.21	
0.8	0.67	0.32	0.92	1.24	28.8	3.42	0.8	0.66	0.31	0.92	0.92	1.12	37.1	3.35	
1.1	0.94	0.45	0.98	1.19	27.7	3.64	1.1	0.92	0.43	0.99	0.99	1.09	36.1	3.59	
1.4	1.21	0.58	1.04	1.14	26.6	3.85	1.4	1.19	0.56	1.02	1.02	1.08	35.8	3.71	
1.7	1.48	0.70	1.07	1.13	26.3	3.96	1.7	1.45	0.68	1.07	1.07	1.06	35.2	3.91	
2.0	1.75	0.83	1.11	1.08	25.2	4.10	2.0	1.72	0.81	1.10	1.10	1.03	33.9	4.02	
2.3	2.02	0.96	1.14	1.01	23.6	4.22	2.3	1.98	0.93	1.11	1.11	1.03	34.1	4.04	
2.6	2.29	1.09	1.15	0.97	22.6	4.27	2.6	2.25	1.06	1.14	1.14	0.99	32.9	4.16	
2.9	2.56	1.22	1.15	0.95	22.2	4.27	2.9	2.51	1.18	1.13	1.13	0.97	32.1	4.11	
3.2	2.83	1.35	1.14	0.89	20.7	4.21	3.2	2.78	1.30	1.12	1.12	0.95	31.5	4.07	
4.7	4.16	1.98	1.11	0.63	14.6	4.1	4.8	4.17	1.96	1.10	1.10	0.81	26.7	4.0	

Table 4-9 Summary of Velocity and Concentration profiles
for Group 7.95, set C1 to C5, Sediment D3
Channel centre

q=1858sq cm/s		Cm=17.3		h=		4.8	
Um=		3.87 ycm=	2.50 yum=	1.35			
Y	Y/yum	Y/ycm	u/Um	Cv/Cm	Cv	u	
(cm)						(%)	(m/s)
q1858Cm17.3							
0.6	0.45	0.24	0.85	1.37	23.8	3.29	
0.8	0.56	0.30	0.87	1.34	23.3	3.39	
1.1	0.79	0.42	0.93	1.32	22.8	3.62	
1.4	1.01	0.55	1.01	1.22	21.2	3.89	
1.7	1.24	0.67	1.05	1.18	20.4	4.07	
2.0	1.46	0.79	1.12	1.11	19.2	4.33	
2.3	1.69	0.91	1.13	1.05	18.2	4.36	
2.6	1.91	1.03	1.15	0.98	17.0	4.44	
2.9	2.14	1.16	1.16	0.93	16.1	4.49	
3.2	2.37	1.28	1.15	0.83	14.3	4.45	

Figure 4-13a Normalized Depth-Velocity for steady uniform sand water mixture, particle D4, group 6.45, slope=28.6%,channel centre

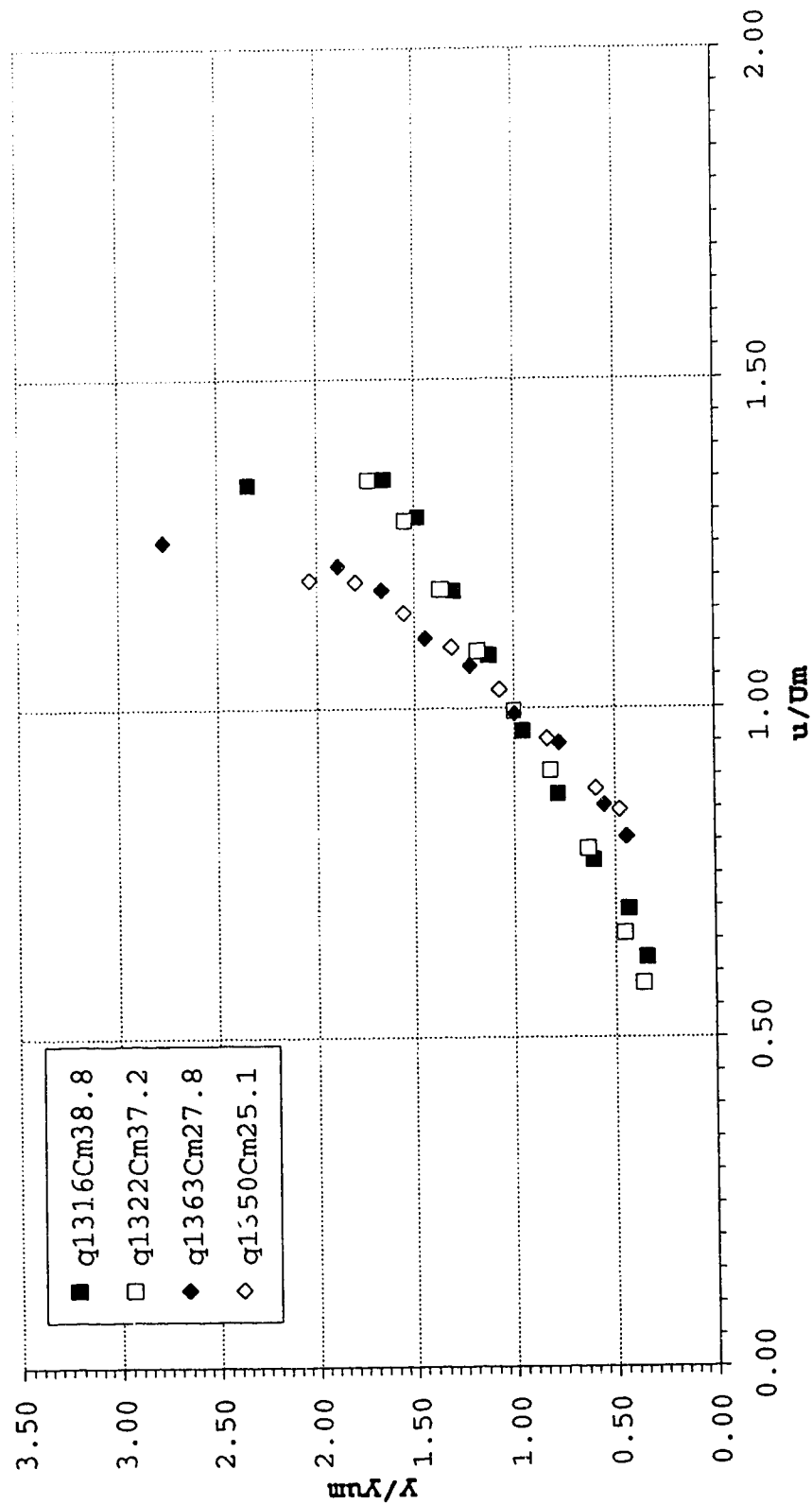


Figure 4-13b Normalized Depth-Concentration for steady uniform sand water mixture, particle D4, group 6.45, slope=28.6%, channel centre

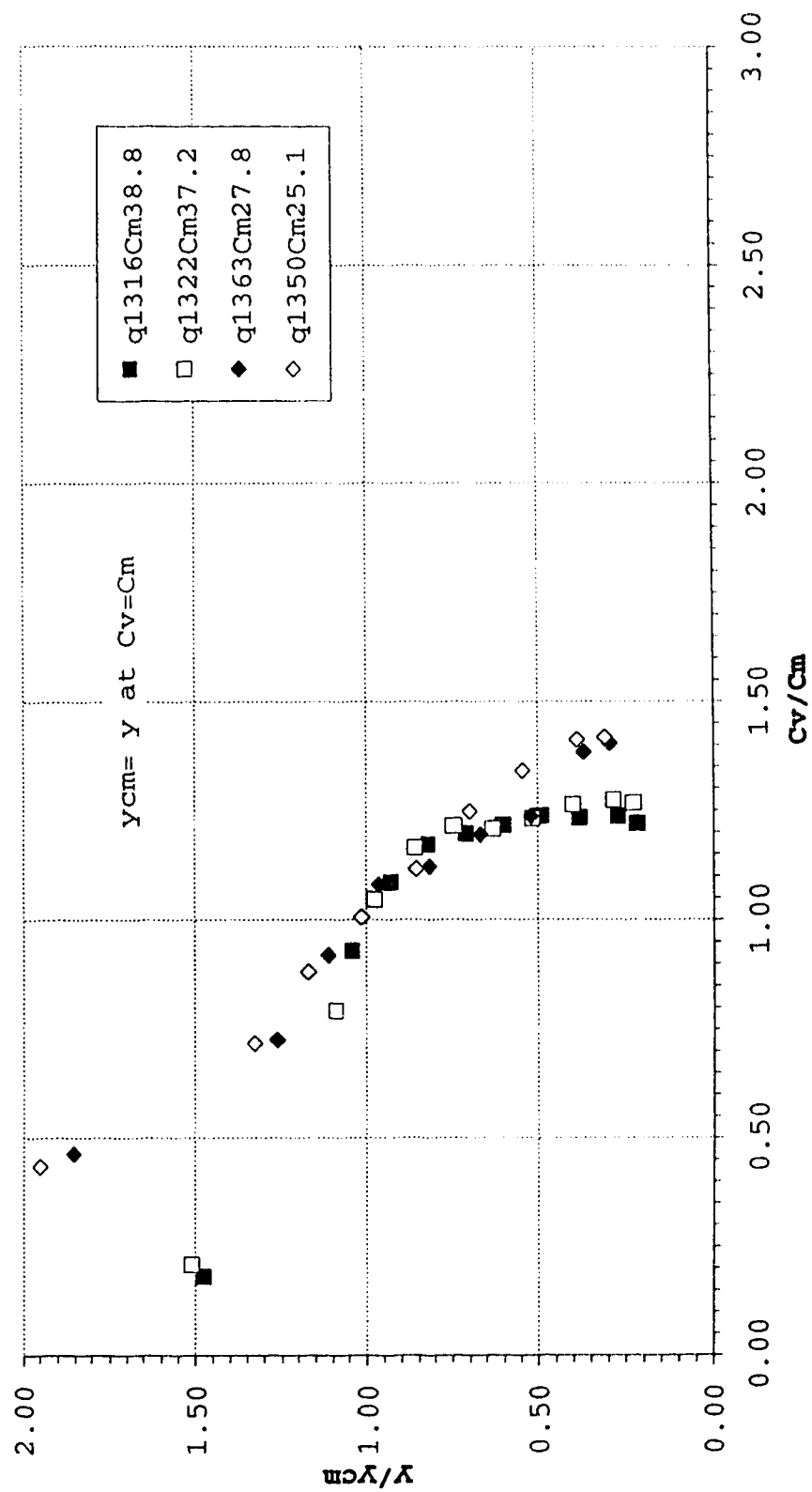


Table 4-10 Summary of Velocity and Concentration profiles
for Group 6.45, set C1 to C4, Sediment D4
Channel centre

q=1316sq cm/s Cm=38.8						h = 4.1		q=1322sq cm/s Cm=37.2						h = 4.0		
Um= 3.21 ycm= 2.78 yum= 1.75								Um= 3.31 ycm= 2.65 yum= 1.67								
Y	Y/yum	Y/ycm	u/U _m	Cv/Cm	Cv	u		Y	Y/yum	Y/ycm	u/U _m	Cv/Cm	Cv	u		
(cm)						(%)		(cm)						(%)		(m/s)
						q1316Cm38.8								q1322Cm37.2		
0.6	0.35	0.22	0.62	1.22	47.3	1.99		0.6	0.36	0.23	0.58	1.27	47.1	1.93		
0.8	0.43	0.27	0.69	1.24	47.9	2.23		0.8	0.45	0.29	0.66	1.27	47.4	2.18		
1.1	0.61	0.38	0.77	1.23	47.8	2.47		1.1	0.64	0.40	0.79	1.26	47.0	2.60		
1.4	0.78	0.49	0.87	1.24	48.0	2.79		1.4	0.82	0.52	0.91	1.23	45.8	3.00		
1.7	0.95	0.60	0.97	1.22	47.1	3.10		1.7	1.00	0.63	0.99	1.21	44.9	3.29		
2.0	1.13	0.71	1.08	1.20	46.4	3.46		2.0	1.18	0.75	1.09	1.21	45.2	3.59		
2.3	1.30	0.82	1.18	1.17	45.5	3.78		2.3	1.37	0.86	1.18	1.16	43.3	3.90		
2.6	1.48	0.93	1.29	1.08	42.1	4.14		2.6	1.55	0.98	1.28	1.05	38.9	4.25		
2.9	1.65	1.04	1.35	0.93	36.0	4.32		2.9	1.73	1.09	1.35	0.79	29.5	4.45		
4.1	2.34	1.47	1.34	0.18	7.0	4.30		4.0	2.40	1.51	1.39	0.21	7.7	4.60		

Table 4-10 Summary of Velocity and Concentration profiles
for Group 6.45, set C1 to C4, Sediment D4
Channel centre

q=1363sq cm/s Cm=27.8				h = 3.8				q=1350sq cm/s Cm=25.1				h = 3.8			
Um= 3.59 ycm= 2.05 yum= 1.37								Um= 3.55 ycm= 1.95 yum= 1.27							
Y	y/yum	y/ycm	u/Um	Cv	Cv	u		Y	y/yum	y/ycm	u/Um	Cv	Cv	u	
(cm)				(%)	(m/s)			(cm)				(%)	(m/s)		
							q1363Cm27.8								q1350Cm25.1
0.6	0.44	0.29	0.81	1.40	39.0	2.89		0.6	0.48	0.31	0.85	1.42	35.6	3.00	
0.8	0.55	0.37	0.85	1.38	38.5	3.06		0.8	0.60	0.39	0.88	1.41	35.4	3.12	
1.1	0.77	0.52	0.95	1.24	34.4	3.40		1.1	0.84	0.54	0.95	1.34	33.6	3.39	
1.4	1.00	0.67	0.99	1.19	33.2	3.56		1.4	1.08	0.70	1.03	1.25	31.3	3.65	
1.7	1.22	0.81	1.06	1.12	31.2	3.82		1.7	1.32	0.86	1.09	1.12	28.0	3.87	
2.0	1.44	0.96	1.11	1.08	30.1	3.97		2.0	1.56	1.01	1.14	1.01	25.2	4.06	
2.3	1.66	1.11	1.18	0.92	25.5	4.23		2.3	1.80	1.17	1.19	0.88	22.1	4.23	
2.6	1.89	1.26	1.22	0.73	20.2	4.36		2.6	2.04	1.33	1.19	0.72	18.0	4.24	
3.8	2.77	1.85	1.25	0.46	12.9	4.50		3.8	2.99	1.95	1.20	0.43	10.9	4.25	

Figure 4-14a Normalized Depth-Velocity for steady uniform sand water mixture, particle D4, group 7.95, slope=28.6%, channel centre

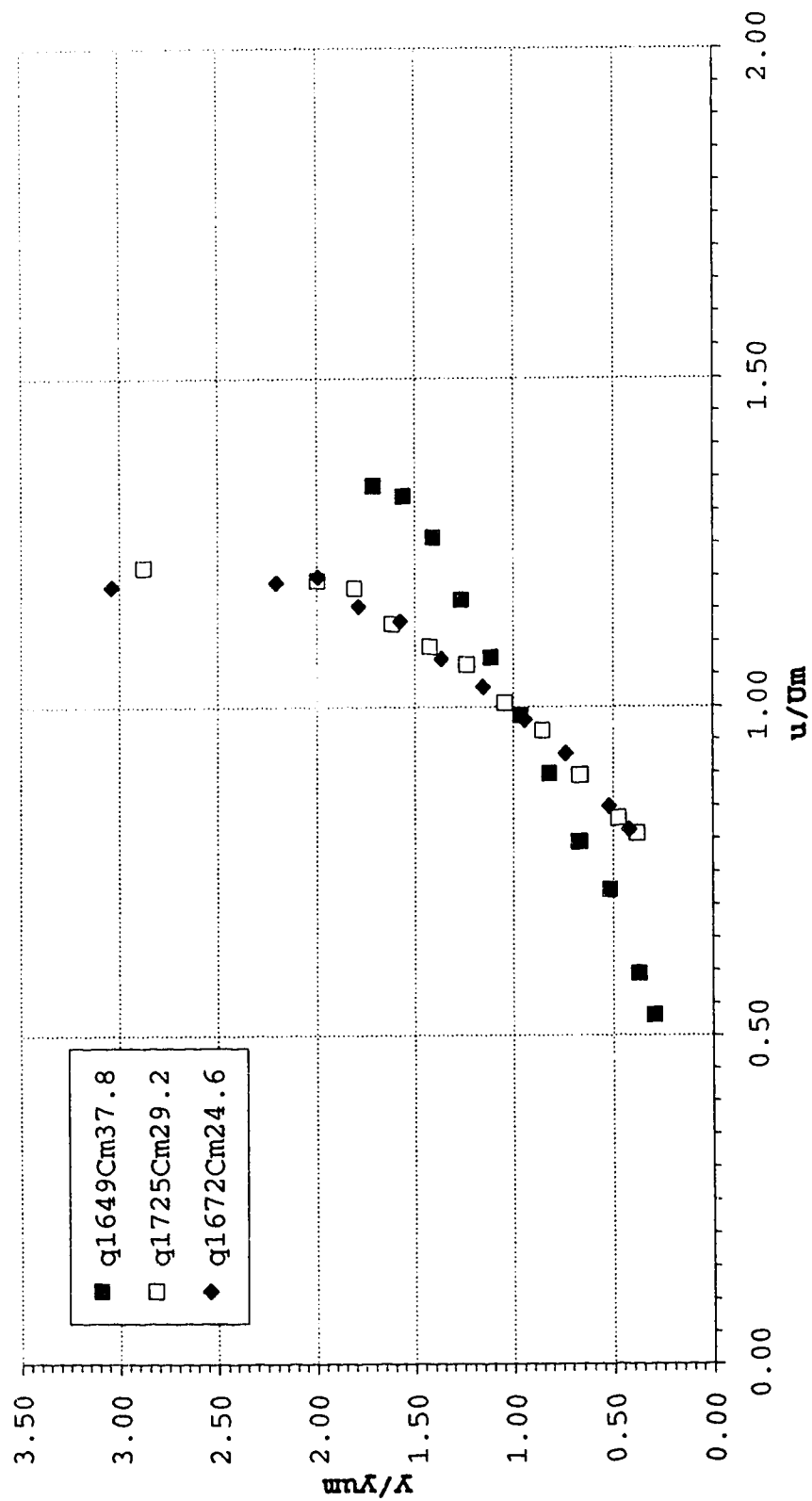


Figure 4-14. Normalized Depth-concentration for steady uniform sand water mixture, particle D4, group 7.95, slope=28.6%, channel centre

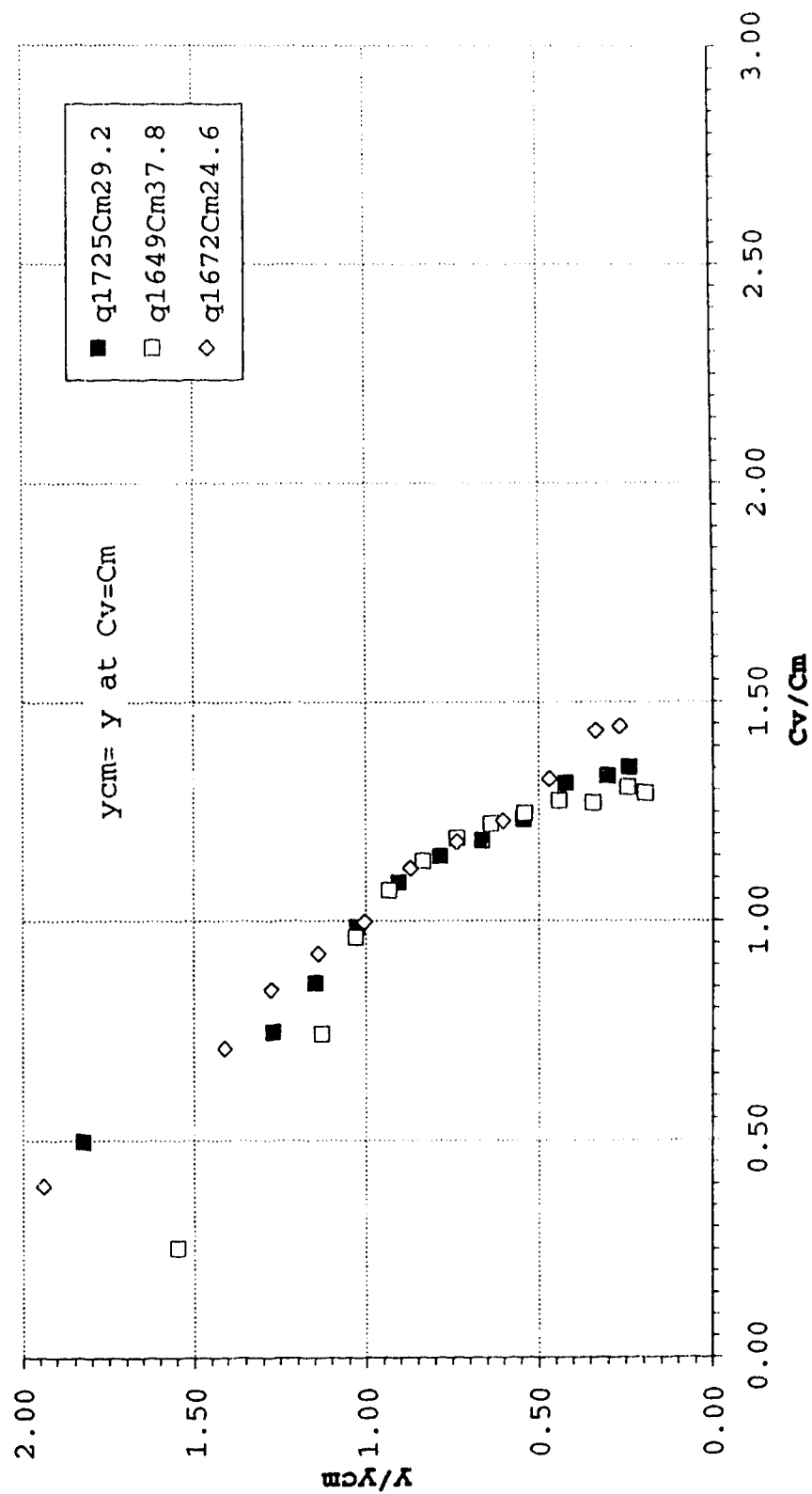


Table 4-11 Summary of Velocity and Concentration profiles
for Group 7.95, set C1 to C3, Sediment D4
Channel centre

q=1649sq cm/s Cm=37.8							q=1725sq cm/s Cm=29.2							h=		4.6	
Um= 3.44 ycm= 3.10 yum= 2.05							Um= 3.75 ycm= 2.52 yum= 1.60										
Y	y/yum	Y/Ycm	u/Ucm	Cv/Cm	Cv	u	Y	y/yum	Y/Ycm	u/Ucm	Cv/Cm	Cv	u				
(cm)				(%)	(m/s)		(cm)				(%)	(m/s)					
q1649Cm37.8							q1725Cm29.2										
0.6	0.29	0.19	0.53	1.29	48.9	1.83	0.6	0.38	0.24	0.81	1.35	39.5	3.03				
0.8	0.37	0.24	0.59	1.31	49.4	2.05	0.8	0.47	0.30	0.83	1.33	38.9	3.11				
1.1	0.52	0.34	0.72	1.27	48.0	2.48	1.1	0.66	0.42	0.90	1.32	38.4	3.36				
1.4	0.67	0.44	0.79	1.28	48.2	2.73	1.4	0.85	0.54	0.96	1.23	36.0	3.61				
1.7	0.81	0.54	0.90	1.25	47.1	3.09	1.7	1.04	0.66	1.01	1.19	34.6	3.77				
2.0	0.96	0.64	0.99	1.22	46.2	3.39	2.0	1.23	0.78	1.06	1.15	33.6	3.99				
2.3	1.11	0.74	1.08	1.19	45.0	3.70	2.3	1.43	0.90	1.09	1.09	31.8	4.09				
2.6	1.26	0.83	1.16	1.14	43.0	4.00	2.6	1.62	1.03	1.13	0.99	28.8	4.23				
2.9	1.41	0.93	1.26	1.07	40.5	4.33	2.9	1.81	1.15	1.18	0.86	25.0	4.43				
3.2	1.56	1.03	1.32	0.96	36.4	4.55	3.2	2.00	1.27	1.19	0.75	21.8	4.47				
3.5	1.71	1.13	1.34	0.74	28.0	4.6	4.6	2.88	1.83	1.21	0.50	14.5	4.6				
4.8	2.34	1.55	1.35	0.25	9.5	4.7											

Table 4-11 Summary of Velocity and Concentration profiles
for Group 7.95, set C1 to C3, Sediment D4
Channel centre

q=1672sq cm/s		Cm=24.6		h=		4.4
Um=		3.80 ycm=	2.27 yum=	1.45		
Y	Y/Yum	Y/Ycm	u/Um	Cv/Cm	Cv	u
(cm)				(%)	(m/s)	
0.6	0.42	0.27	0.81	1.44	35.5	3.09
0.8	0.52	0.33	0.85	1.44	35.3	3.22
1.1	0.73	0.47	0.93	1.33	32.6	3.53
1.4	0.94	0.60	0.98	1.23	30.3	3.72
1.7	1.15	0.74	1.03	1.18	29.1	3.92
2.0	1.36	0.87	1.07	1.12	27.6	4.08
2.3	1.57	1.00	1.13	1.00	24.6	4.30
2.6	1.78	1.14	1.15	0.92	22.8	4.39
2.9	1.99	1.27	1.20	0.84	20.7	4.56
3.2	2.20	1.41	1.19	0.71	17.4	4.52
4.4	3.03	1.94	1.18	0.40	9.7	4.50

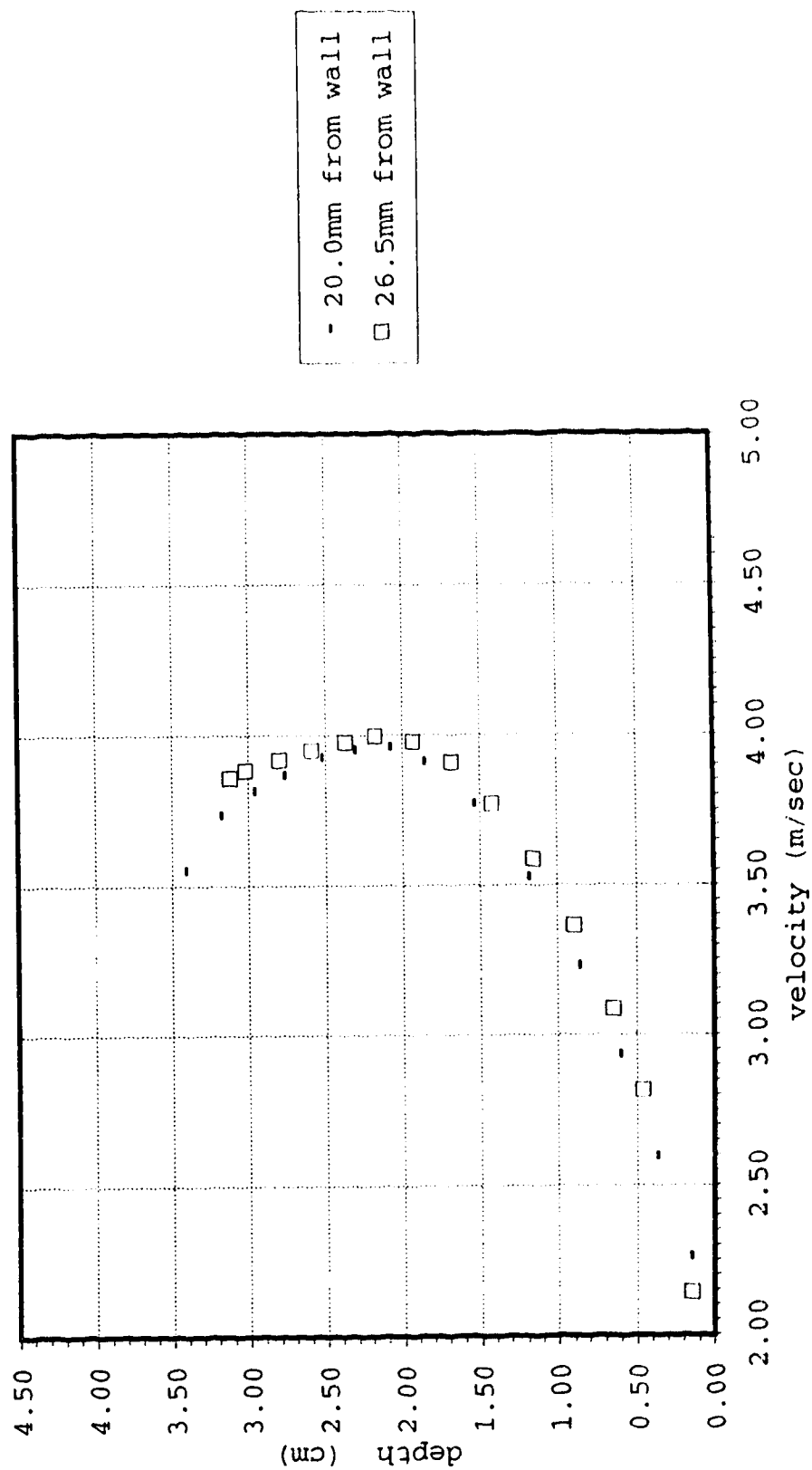
4.5 Limitations and Discussions

In order to get an adequate depth of flow, the width of the channel used was small. However, the velocity profile at the centre and at 6.5mm from the centre (Fig. 4-15) show a very small change in the profile. This shows that at high velocities the effect of the side wall was confined to the immediate wall region and the centreline profile could approximate a wide channel behavior. This was also observed by Takahashi (1980) in his study.

The question as to whether the calibration was adequate using water will have to be studied further. The ideal method would be to calibrate it using the fluid under consideration. But this posed a practical problem and a simple technique has yet to be developed.

One other variable that was not explored was the slope of the channel. All the experiments were carried out at a slope of 28.6%. There were two reasons for this. The first reason was that it was the intention to make measurements at a slope close to the slope at which deposition started. This slope of 28.6% proved to be very close to this equilibrium slope. The second reason was the shortage of head room in the laboratory. Any slope larger than above required headroom in the laboratory at least a foot which was not available.

Figure 4-15 Depth vs Velocity for Steady Uniform water Flow using pitot tube at channel centre and close to the channel centre



4.6 Error Analysis

The present measuring technique involves possible errors at several stages of measurement before the final velocity and concentration are evaluated. These are

- 1 measurement of sampler opening area (a)
- 2 measurement of volume of sample collected (V)
- 3 measurement of sampling time (t)
- 4 representativeness of the sample (possible error due to position and size of the sampler)

The sampler opening involved uncertainty in the measurement of two lengths to give the area. The uncertainty in time is assumed equal for turning the stop watch "on" and "off". In order to perform a sensitivity analysis, several possible differences in reaction time can be tried. An equally important contributor of error is the sampler position and size. Since the measured velocity is assumed to be at the centre of the sampler, error could be introduced as a result of the flow having a vertical velocity gradient ($\partial u / \partial y$). The difference in velocity (Δu) between the centre and the side of the sampler of width d' can be written in a Taylor expansion as

$$\Delta u = \frac{\partial u}{\partial y} \left(\frac{d'}{2} \right) + \frac{\partial^2 u}{\partial y^2} \left(\frac{d'^2}{8} \right) \quad (4-6.1)$$

In this experiment with a typical $\partial u / \partial y = 130/\text{sec}$, $\partial^2 u / \partial y^2 = 20/\text{m sec}$ and $d' = 0.005\text{m}$, the second term is negligible compared to the first. However, this error above the centre would

approximately be balanced by the error (equal but opposite in the case of a straight line velocity profile) below the centre of the sampler. Therefore, the resulting error is probably very small but quite difficult to quantify. We assume that in the process of calibrating the sampler and taking at least the mean of three measurements, this error has been minimized. For uncorrelated variables in the function $u = u(a, V, t)$ and $C_v = C_v(V, m)$, where m is the mass of the sample collected, the deviations can be written as (Bevington, 1969)

$$\sigma_u^2 = \sigma_a^2 \left(\frac{\partial u}{\partial a} \right)^2 + \sigma_v^2 \left(\frac{\partial u}{\partial V} \right)^2 + \sigma_t^2 \left(\frac{\partial u}{\partial t} \right)^2 \quad (4-6.2)$$

$$\sigma_{C_v}^2 = \sigma_v^2 \left(\frac{\partial C_v}{\partial V} \right)^2 + \sigma_m^2 \left(\frac{\partial C_v}{\partial m} \right)^2 \quad (4-6.3)$$

where $u = \frac{V}{a \cdot t} \quad (4-4.1)$

$$C_v = \frac{1}{1.65} \left[\frac{m}{V} - 1 \right] \quad (4-4.2)$$

with m in gm and V in mL. σ is the standard deviation for the variables shown as subscripts. The normalized variances can be written as

$$\frac{\text{Var}(u)}{u^2} = \frac{\text{Var}(V)}{V^2} + \frac{\text{Var}(a)}{a^2} + \frac{\text{Var}(t)}{t^2} \quad (4-6.4)$$

$$\frac{\text{Var}(C_v)}{C_v^2} = \frac{1}{(m-V^2)^2} \text{Var}(m) + \frac{m^2}{(m-V^2)^2} \text{Var}(V) \quad (4-6.5)$$

The typical values of each variable and their corresponding variances are given in Table 4-12.

Table 4-12

V	Var(V)	a	Var(a)	t	Var(t)	m	Var(m)	$\frac{\text{Var}(u)}{u^2}$	$\frac{\text{Var}(C_V)}{C_V^2}$
(ml)	(ml) ²	(cm ²)	(cm ²) ²	(sec)	(sec) ²	(gm)	(gm) ²		
700	25	0.98	1.6E-5	1.75	0.03	1000	1	0.0099	0.0001

5 DISCUSSION OF EXPERIMENTAL RESULTS

5.1 Introduction

The results of the experiments presented earlier show a range of behavior of slurry at different mean concentration, the size of particles as well as the grading of the particles. The three sizes of nearly uniform particles used were D1 to D3 with D1 the coarsest(0.430mm), D2 in the mid size(0.335mm) and D3 the finest(0.215mm). The size D4 was more or less an equal proportion mixture of all these three sizes(0.330mm).

General trends in the concentration and velocity distributions will first be discussed before analyzing the data.

5.2 General Trends

5.2.1 Concentration distribution

One of the primary reasons for selecting three different sizes of uniform particles and one non-uniform mixture was to see if there was significant difference in the dispersibility of these sediments. It is essential to see if the expected trend is displayed by the general distribution of velocity and concentration before they can be reflected in the constitutive behavior. One such trend is how the concentration profile responds to the particle size and the mean concentration.

On examining Fig 4-4 to 4-8 which represent measurements made next to the wall as well as the centreline for particle D1, the largest size, a consistent bottom layer of high sediment concentration is present. The concentration is higher in this layer and very quickly the profile tapers off near the surface. For smaller mean concentration this bottom layer is not as prominent (Fig.5-1b to 5-7b) and the profiles lose their similarity as shown by the scatter in the dimensionless concentration profiles. This separation of the profile is more apparent in Figures 4-4b, 4-5b, 4-7b and 4-8b. The separation is such that the profile with the smallest mean concentration appears to separate the most. This trend is observed in the concentration profiles for all the other particle sizes but in varying degree. This trend appears to be the result of a difference in the dispersibility of particles at low concentrations. The relatively larger concentration of the particles near the bed with almost linear and rapid tapering off of the profiles indicate a considerable reduction in the dispersion of these large particles at low concentrations. This indicates a "bed load" type movement similar to that seen in sediment transport. At this stage, because the supply of sediment is small, most of the sediment stays close to the bed. As the supply of sediment increases i.e. the concentration gets higher, a better dispersion is indicated by more rounded profiles.

Figure 5-1a Depth-Velocity for steady uniform sand water mixture, particle D1, Slope=28.6%, group C1, channel side

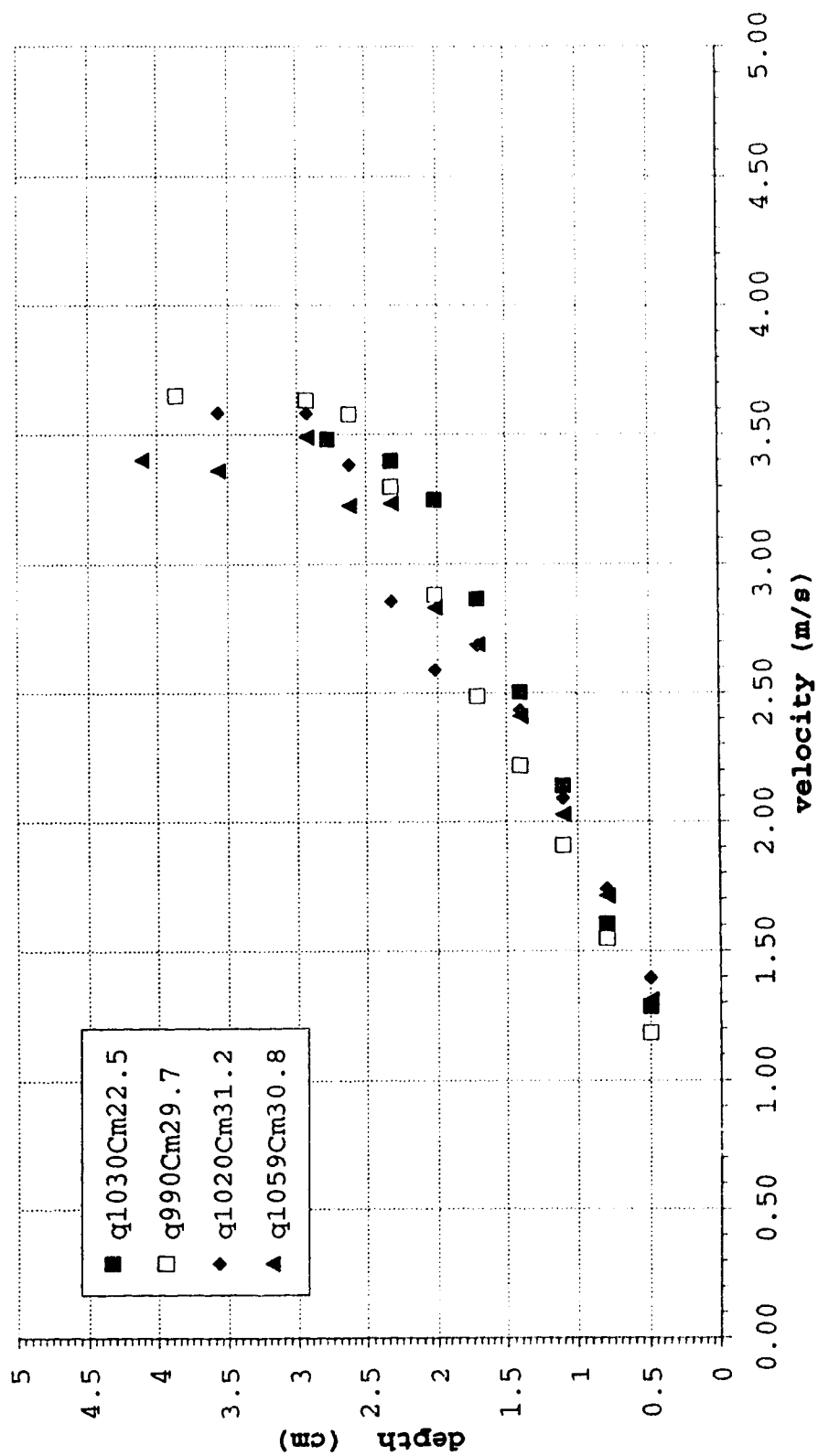


Figure 5-1b Depth-Concentration for Steady Uniform sand water mixture Particle D₁, Slope=28.6%, group C1, channel side

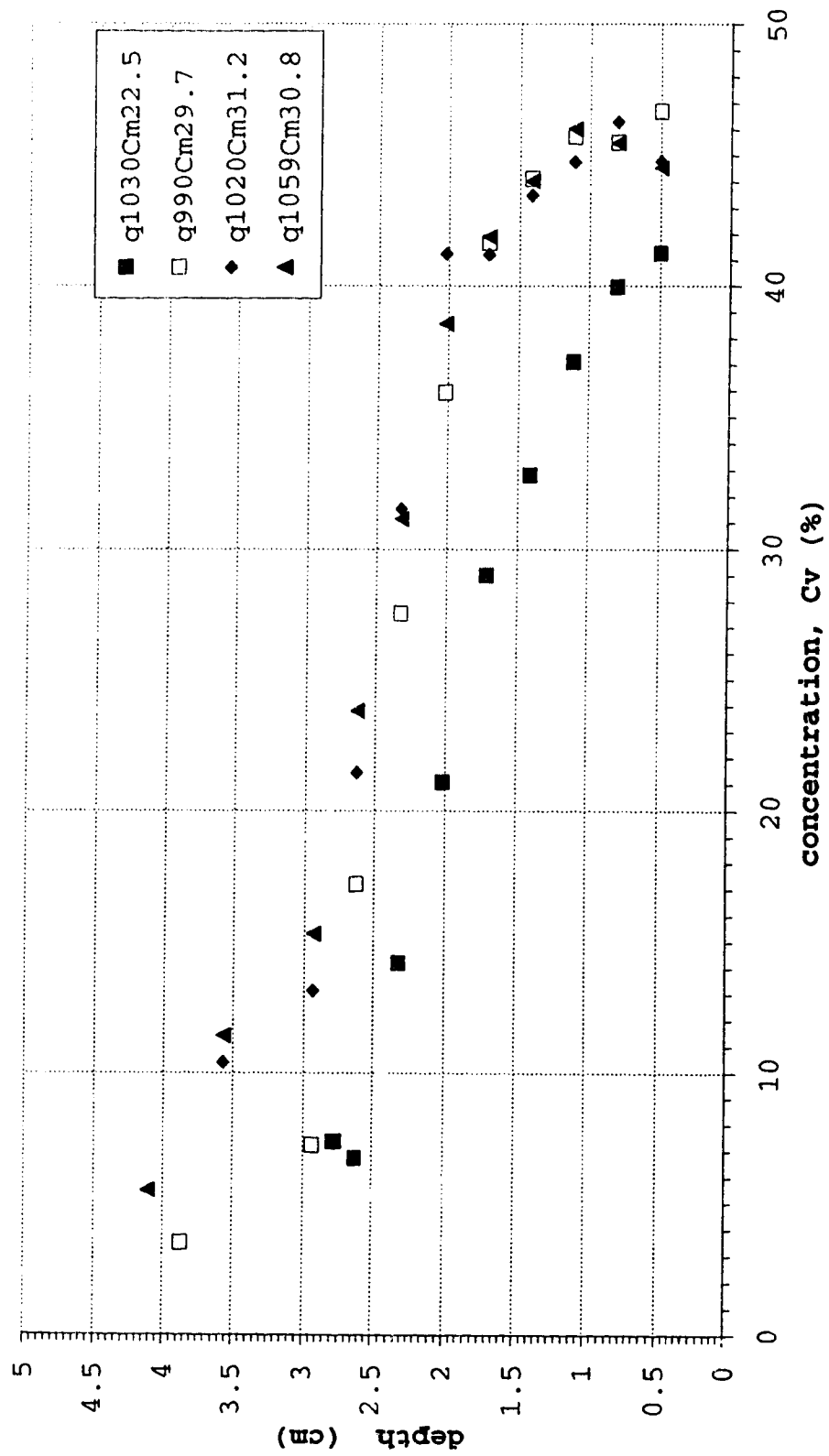


Figure 5-2a Depth-Velocity for steady uniform sand water mixture
particle D1, Slope=28.6%, group C2, channel side

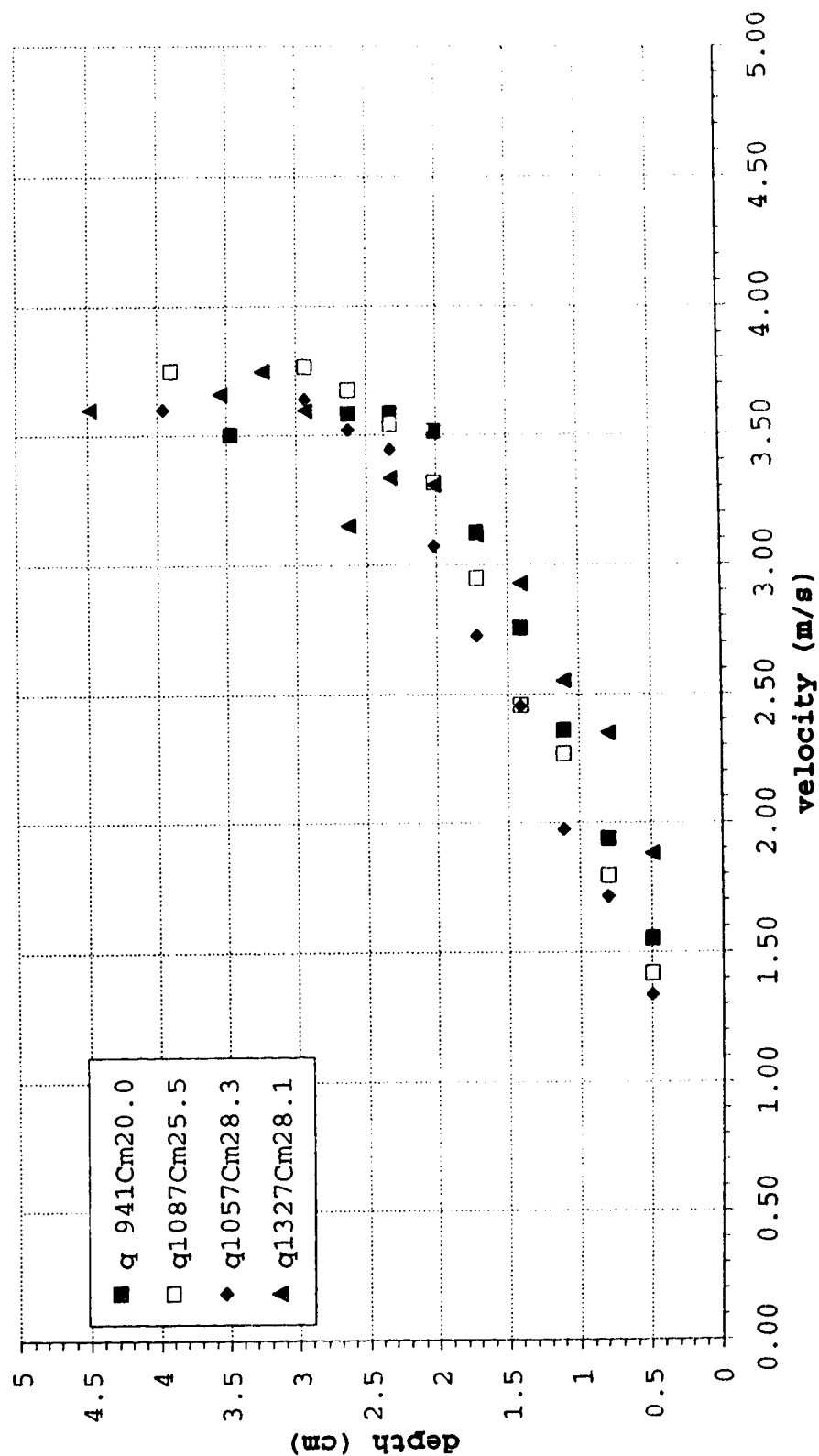


Figure 5-2b Depth-Concentration for Steady Uniform sand water mixture Particle D1, Slope=28.6%, group C2, channel side

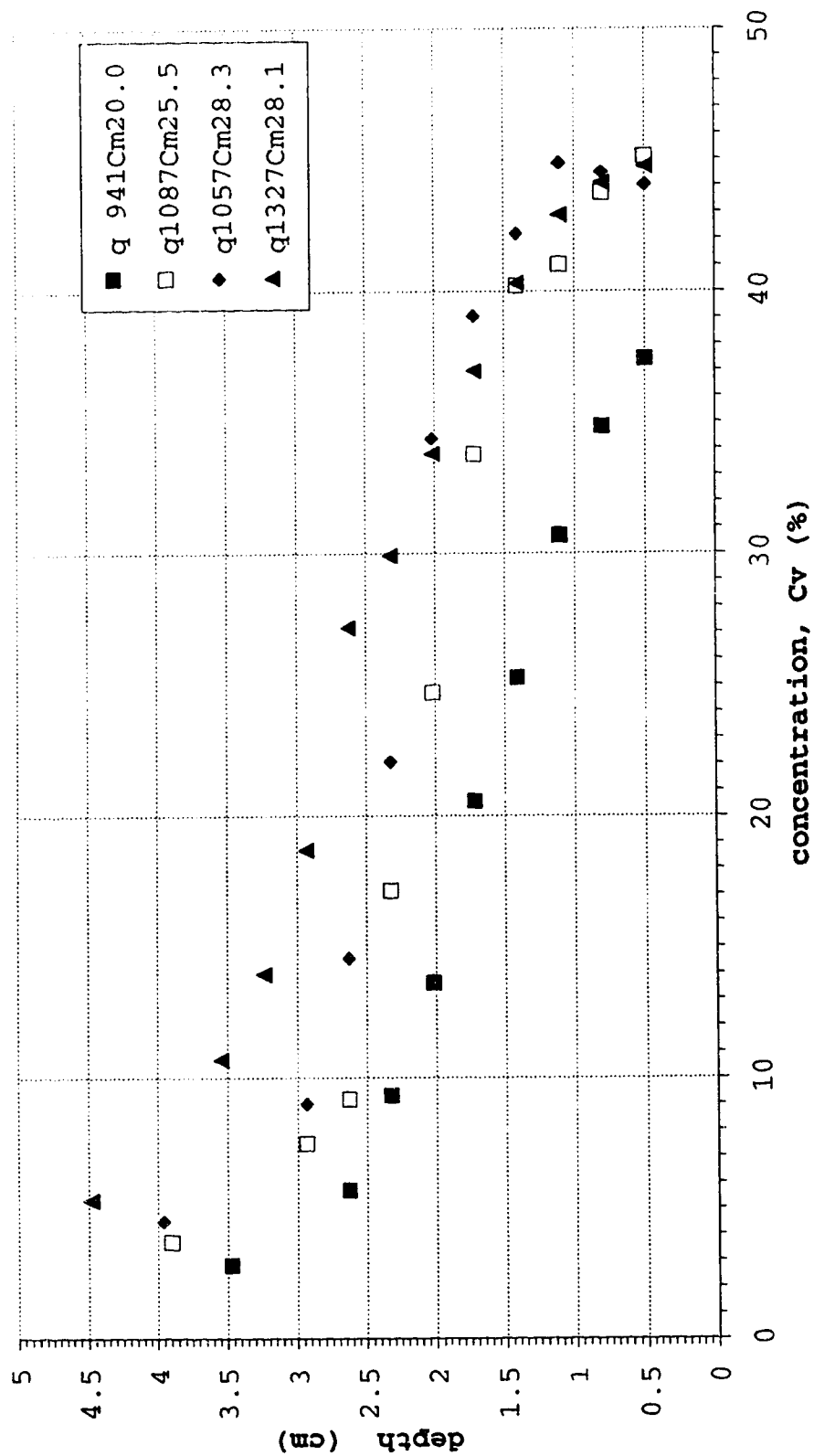


Figure 5-3a Depth-Velocity for steady uniform sand water mixture
particle D1, Slope=28.6%, group C3-C6, channel side

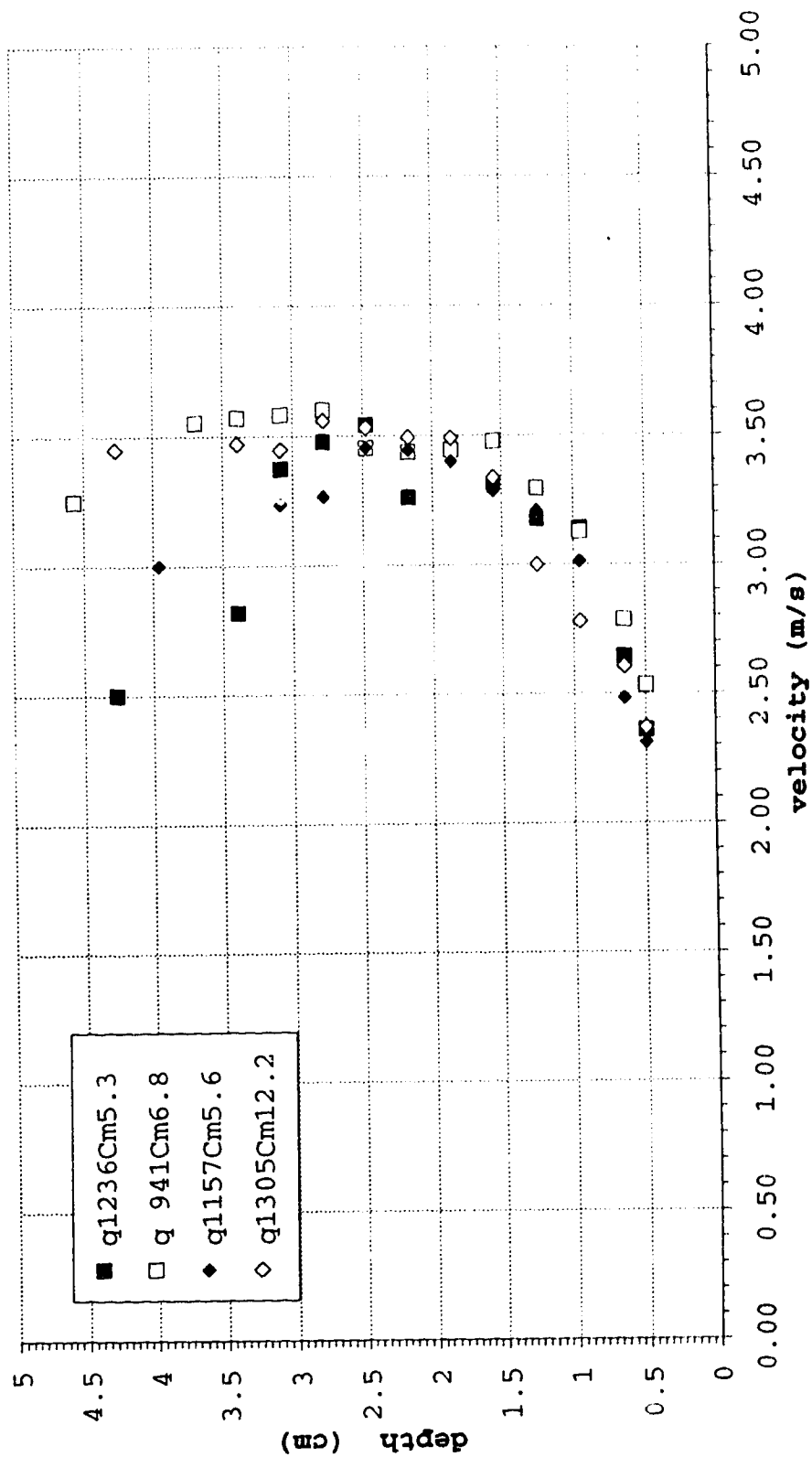


Figure 5-3b Depth-Concentration for Steady Uniform sand water mixture Particle D1, Slope=28.6%, group C3, channel side

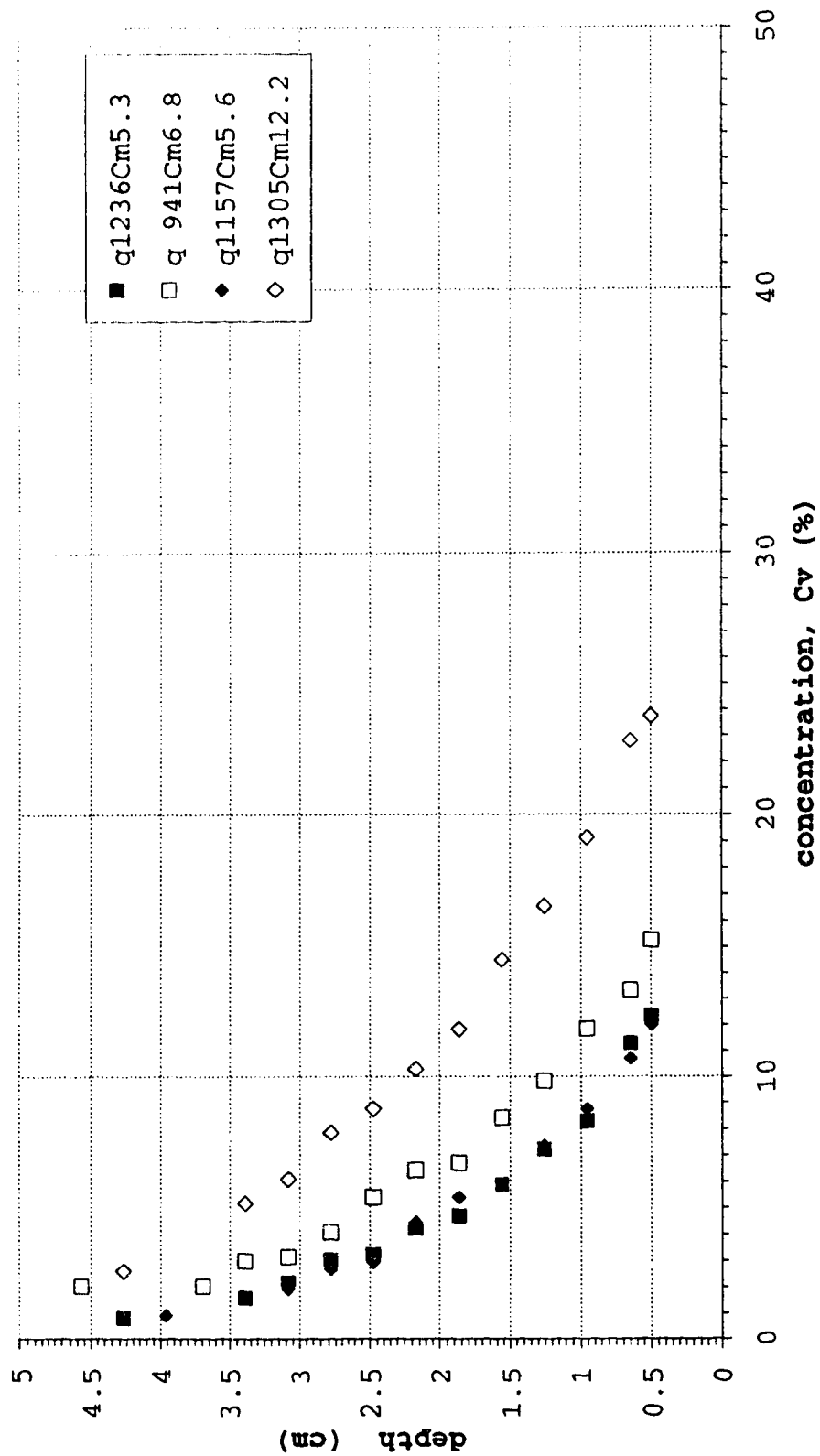


Figure 5-4a Depth-Velocity for steady uniform sand water mixture, particle D₁, S= 28.6%, group 6.45, channel centre

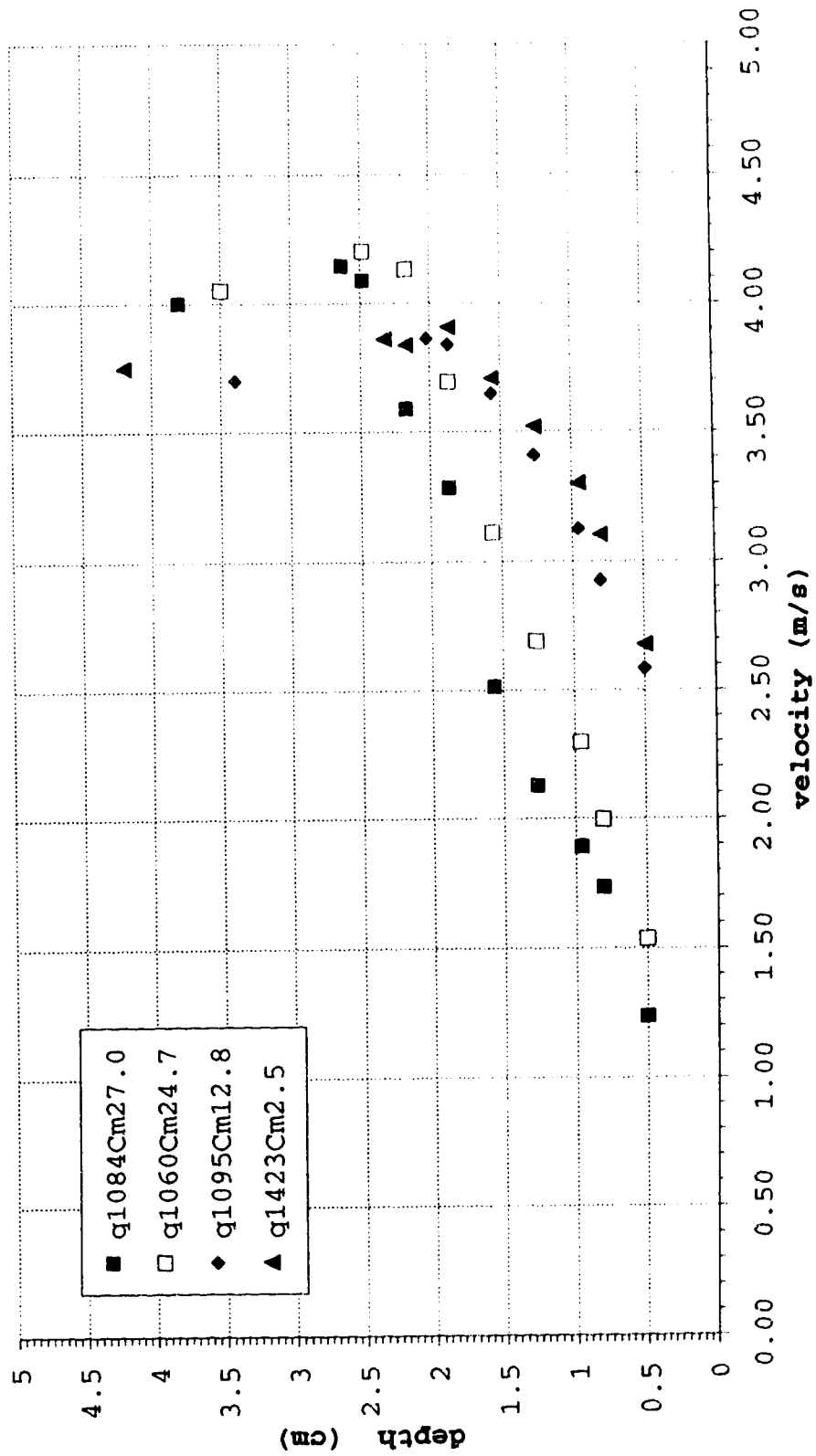


Figure 5-4b Depth- Concentration for Steady Uniform sand water mixture Particle D1, Slope=28.6%, group 6.45, channel centre

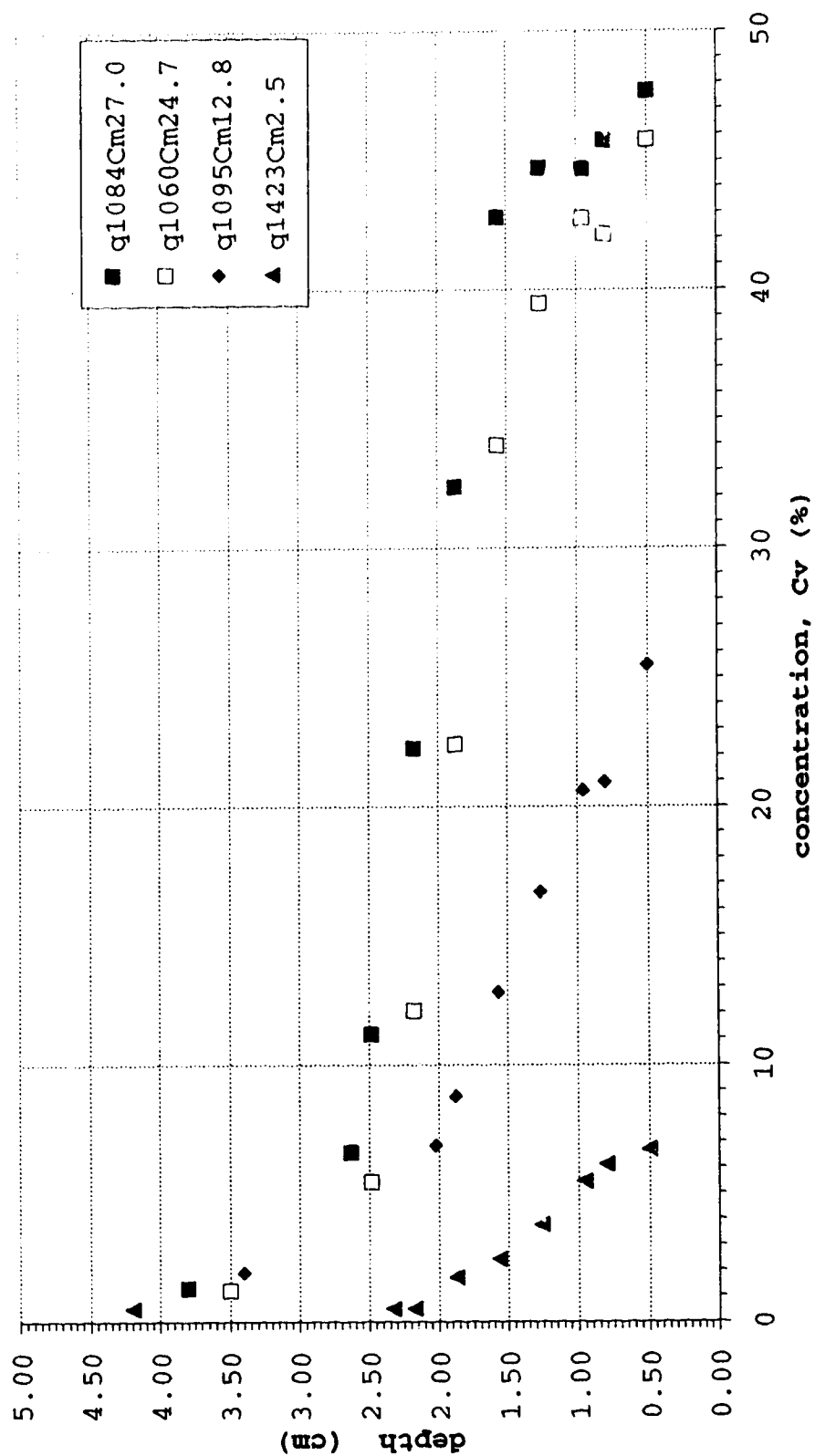


Figure 5-5a Depth-Velocity for steady uniform sand water mixture, particle D₁, Slope=28.6%, group 7.90, channel centre

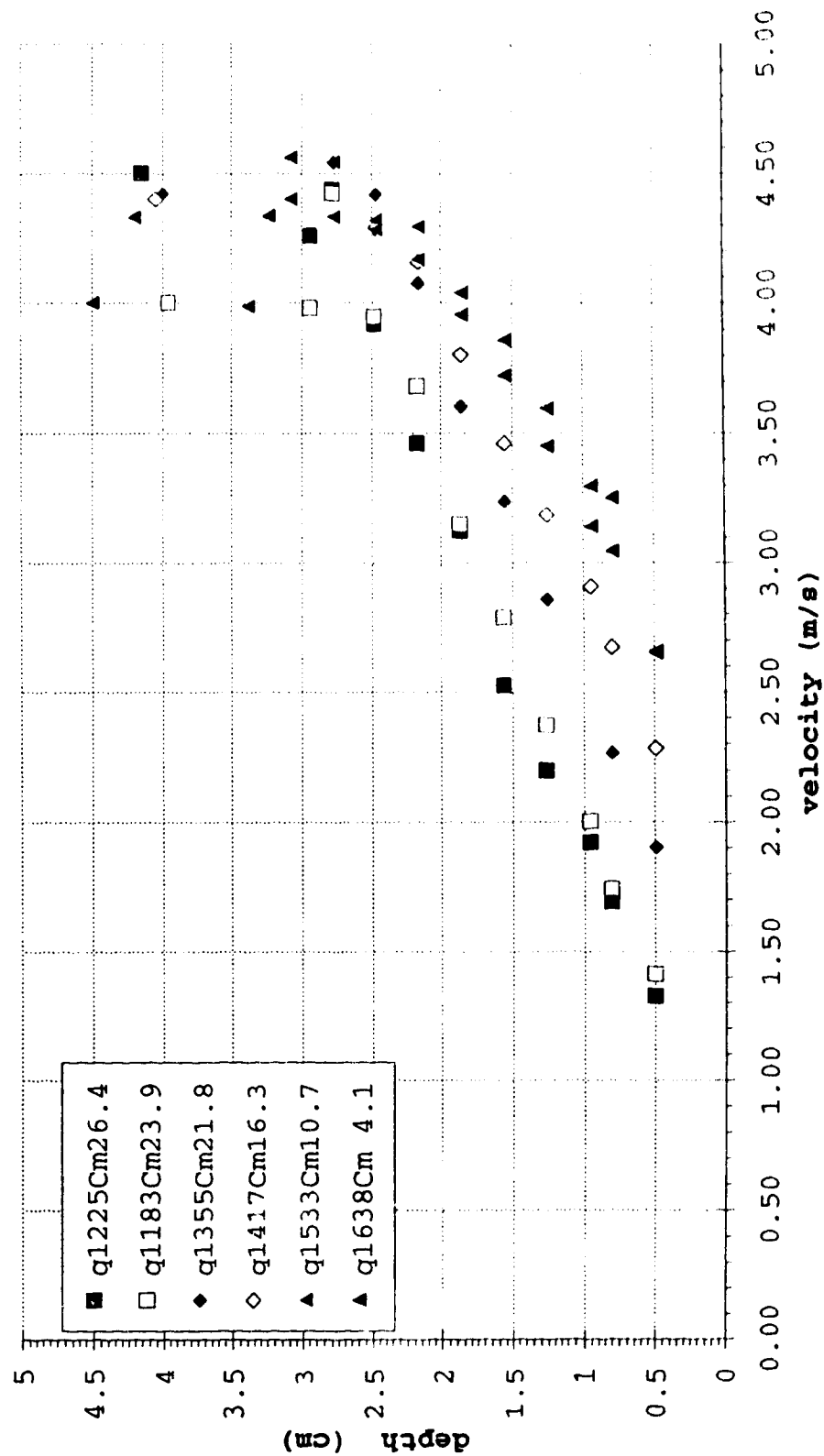


Figure 5-5b Depth-Concentration for steady uniform sand water mixture, particle D1, Slope=28.6%, group 7.90, channel centre

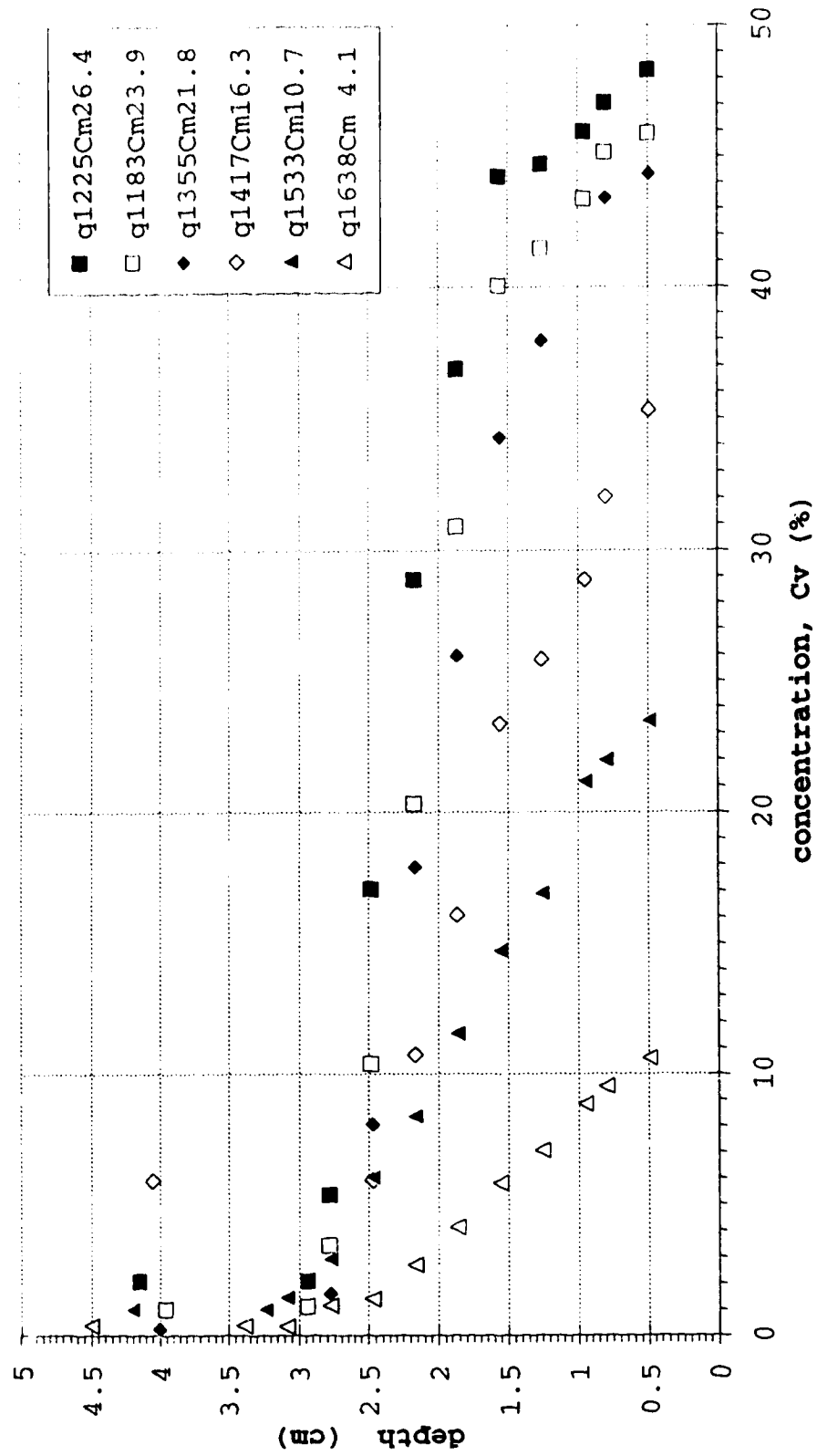


Figure 5-6a Depth-Velocity for steady uniform sand water mixture, particle D2, Slope=28.6%, group 6.45, channel centre

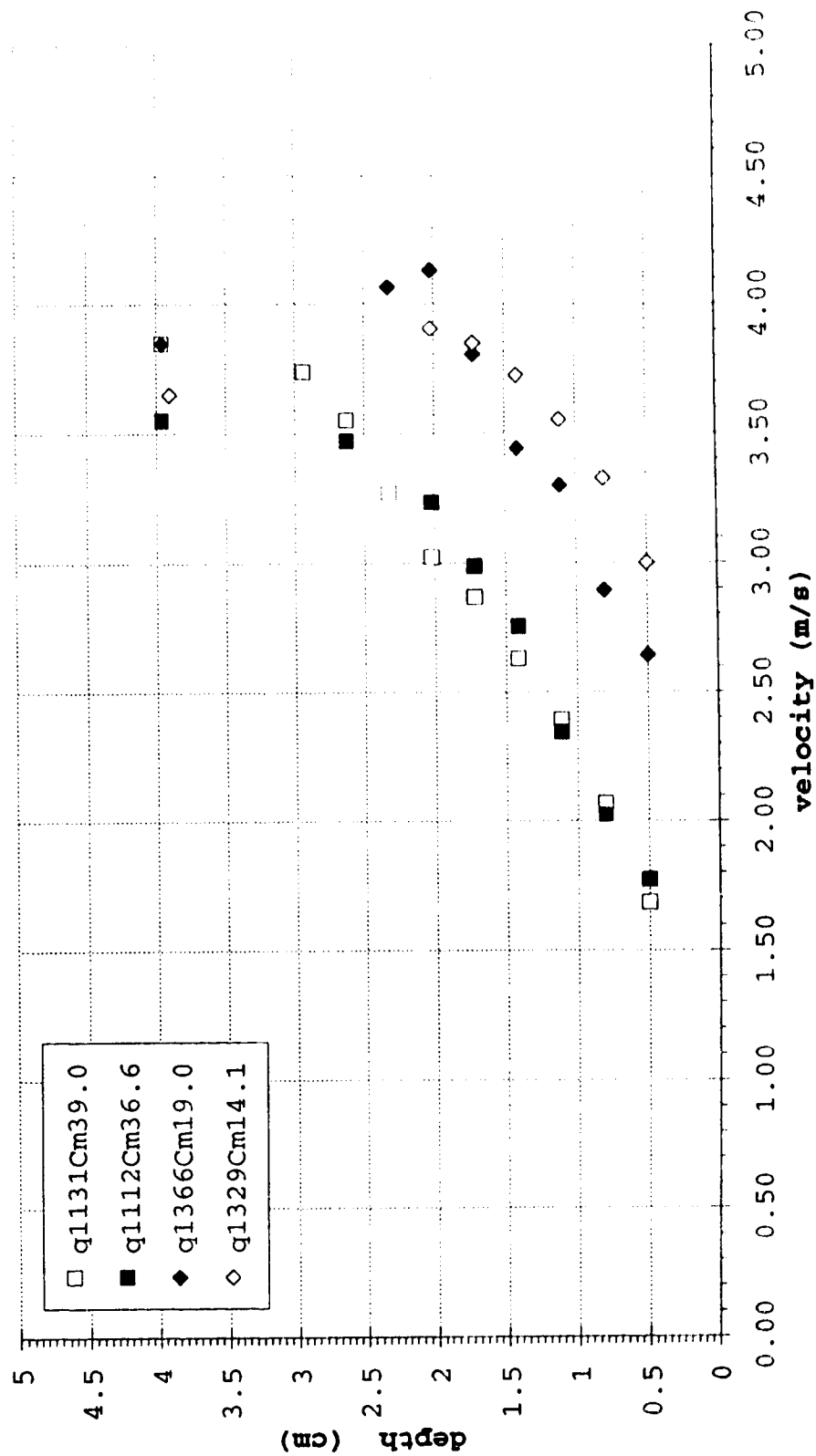


Figure 5-6b Depth-Concentration for steady uniform sand water mixture, particle D2, Slope=28.6%, group 6.45, channel centre

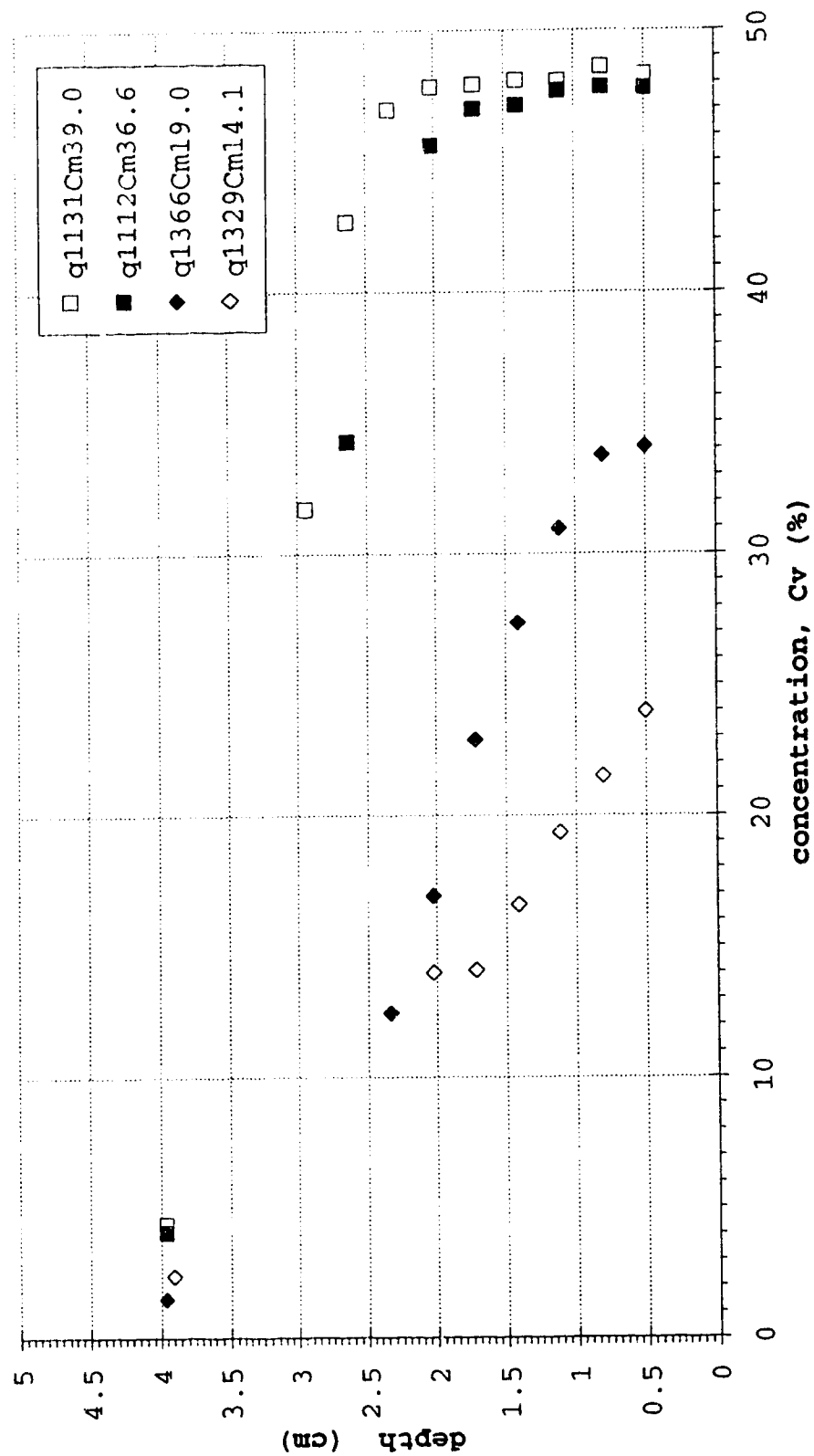


Figure 5-7a Depth-Velocity for steady uniform sand water mixture, particle D2, Slope=28.6%, group 7.90, channel centre

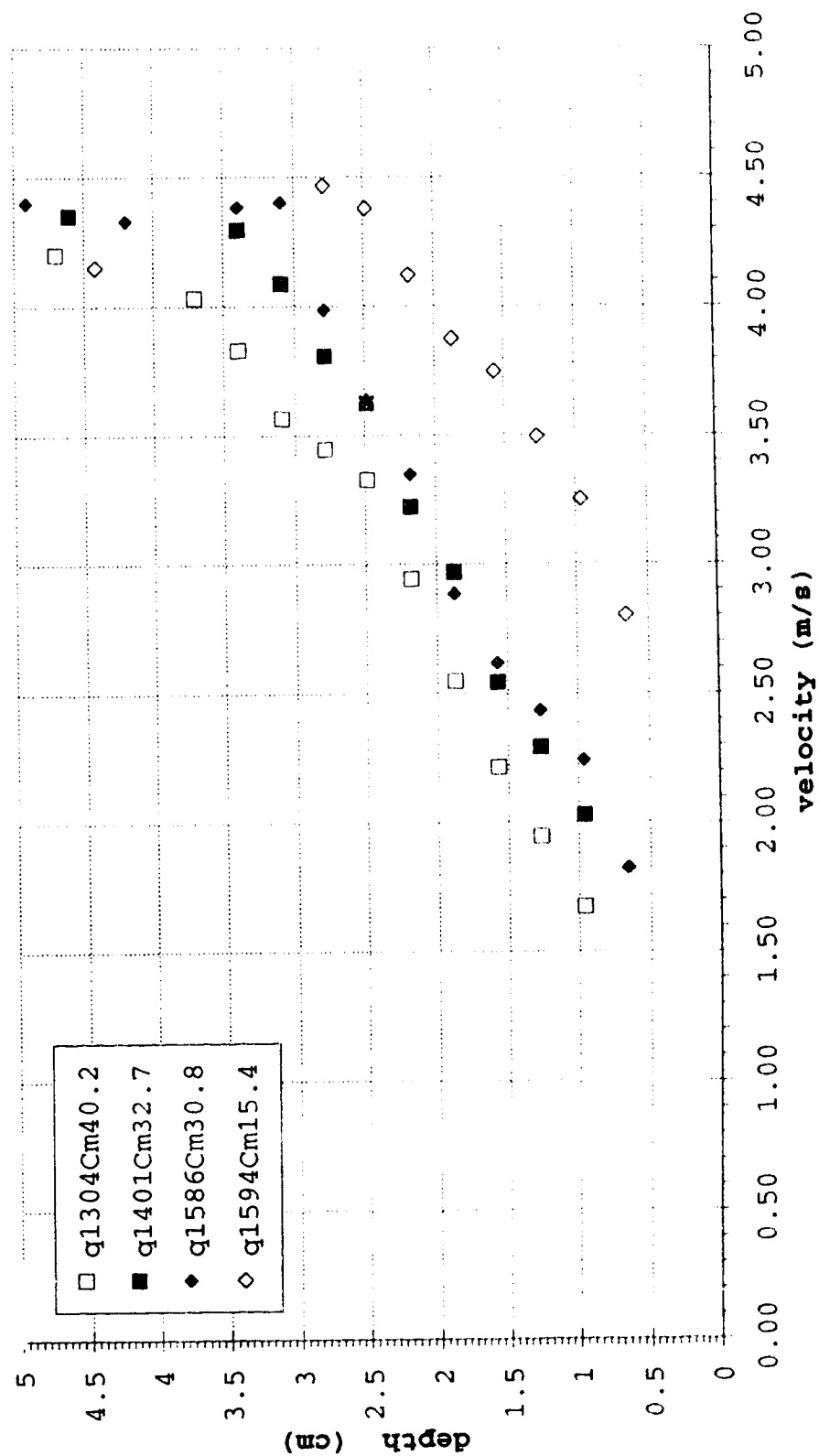
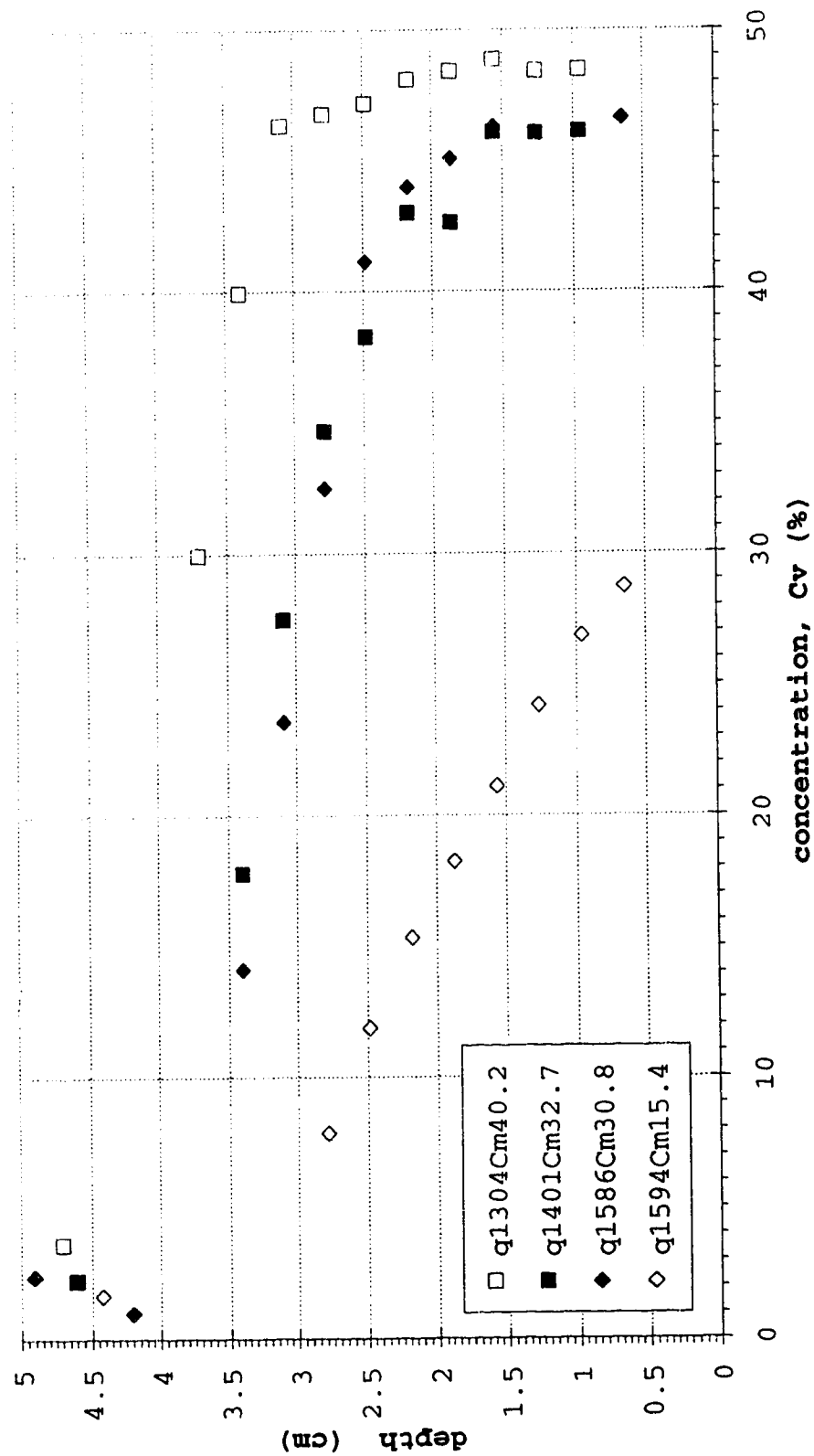


Figure 5-7b Depth velocity for steady uniform sand water mixture, particle D₅₀, slope=28.6%, group 7.90, channel centre



Dispersion is also directly related to the particle size. Fig. 5-8b and 5-9b show significantly better dispersion of particles D3, even in the case of larger concentration which show considerable thickening of the bottom layer. These profiles show relatively smaller concentration gradients even in the lower mean concentration ranges which suggests a possibility of more than one dispersing mechanisms in effect. There is a possibility in this particle range that turbulence is also responsible for dispersion.

The last particle size D4 displays some interesting behavior as a result of a more severe particle gradation. If the concentration profiles q1060Cm24.7 (Fig. 5-4b), q1183Cm23.9 (Fig. 5-5b) for particle D1 as well as profile q1112Cm36.6 (Fig. 5-6b) for particle D2 is compared to the D4 profiles with similar mean concentrations q1672Cm24.6 (Fig. 5-11b) and q1322Cm37.2 (Fig. 5-10b), it can be observed that the D4 profiles show a smaller concentration near the bed but better dispersion away from the bed. This is more obvious if the dimensionless plots Fig. 4-7b to 4-10b is compared to Fig. 4-13b and 4-14b. The better dispersion of D4 mixture is possibly due to the presence of the D3 fines which may have changed the properties of the interstitial fluid and thus increased dispersion.

Figure 5-8a Depth-Velocity for steady uniform sand water mixture, particle D3, Slope=28.6%, group 6.45, channel centre

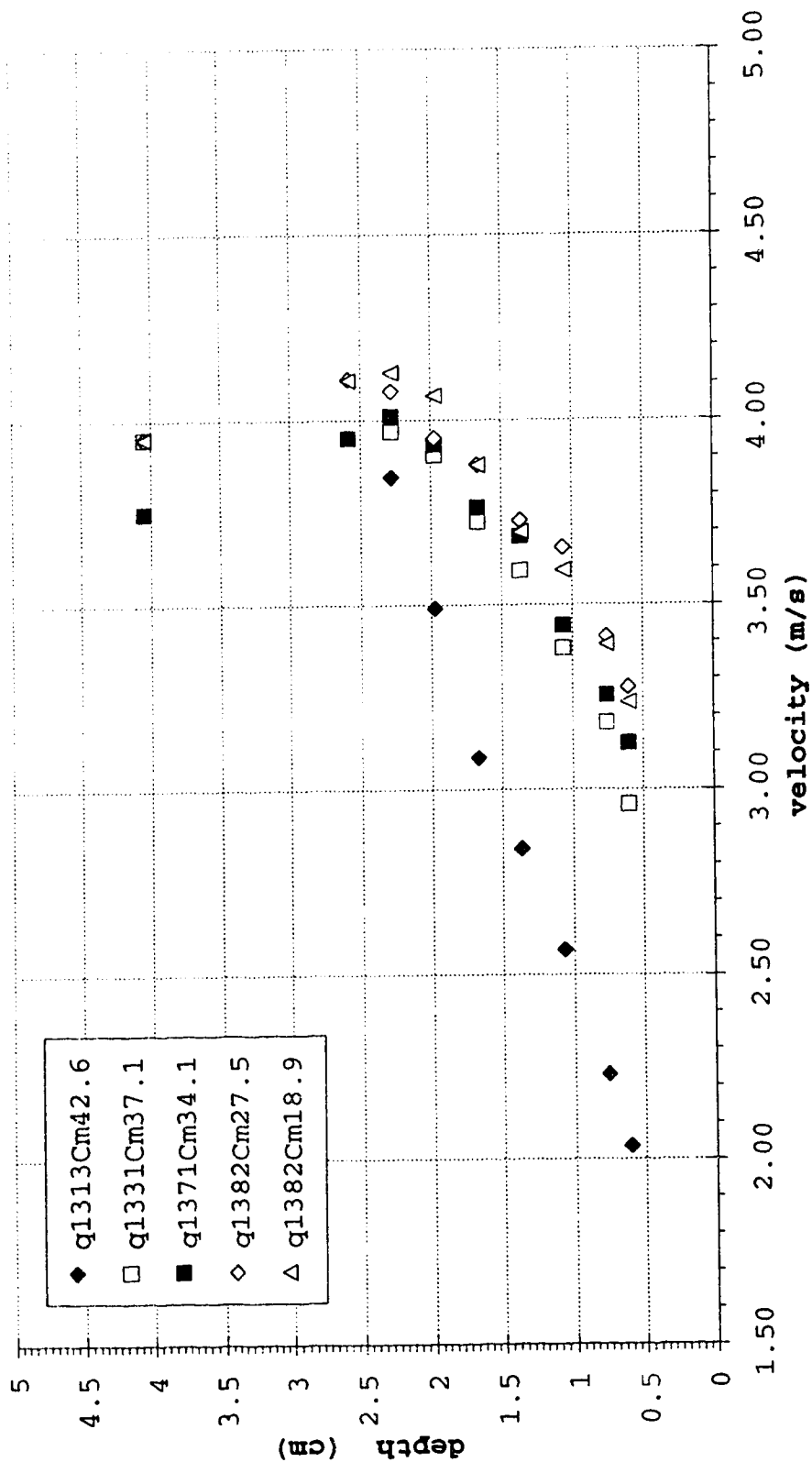


Figure 5-8b Depth-Concentration for steady uniform sand water mixture, particle D3, Slope=28.6%, group 6.45, channel centre

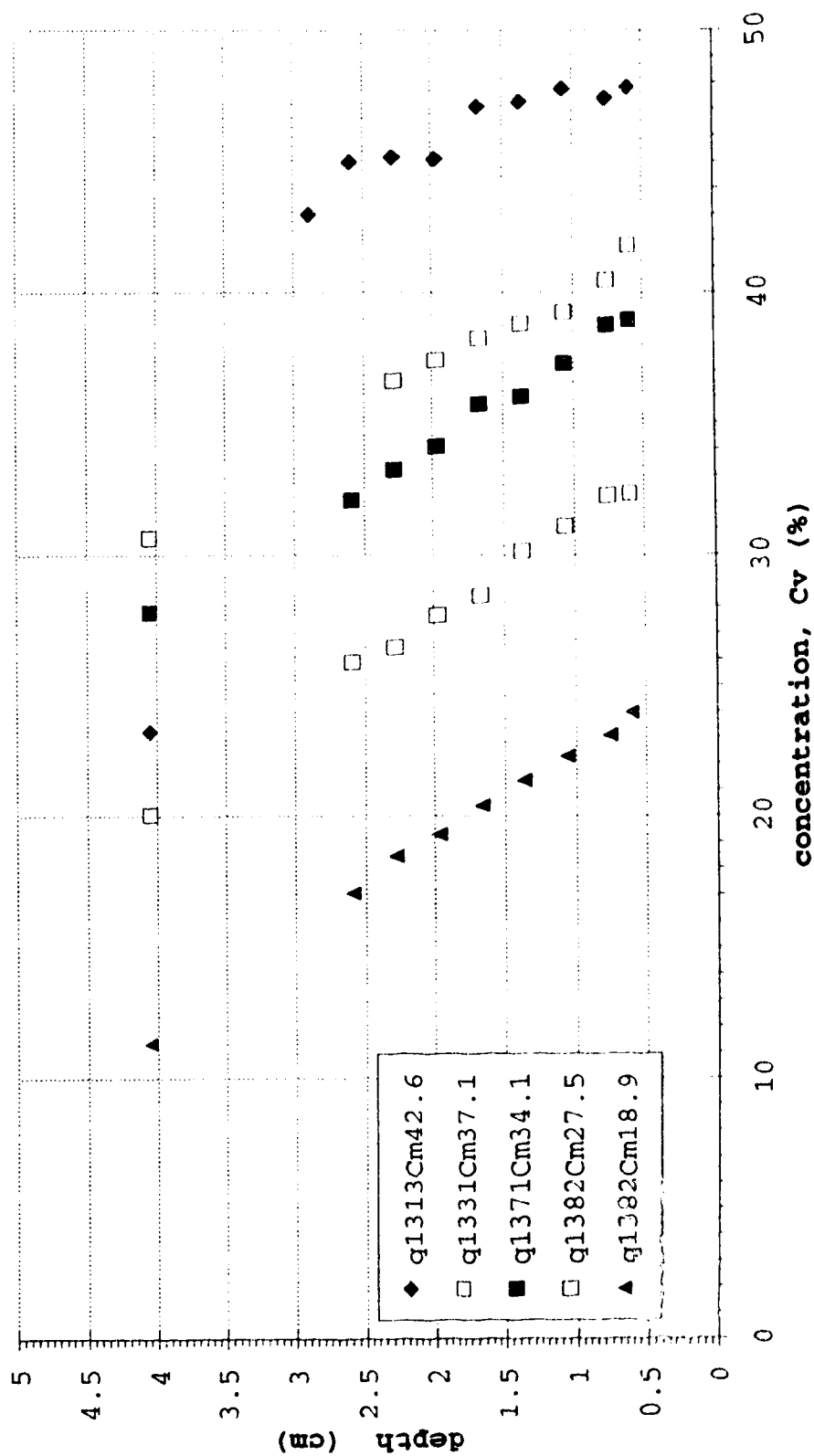


Figure 5-9a Depth-Velocity for steady uniform flow in water mixture, particle D3, Slope=28.6%, group 7.90, channel centre

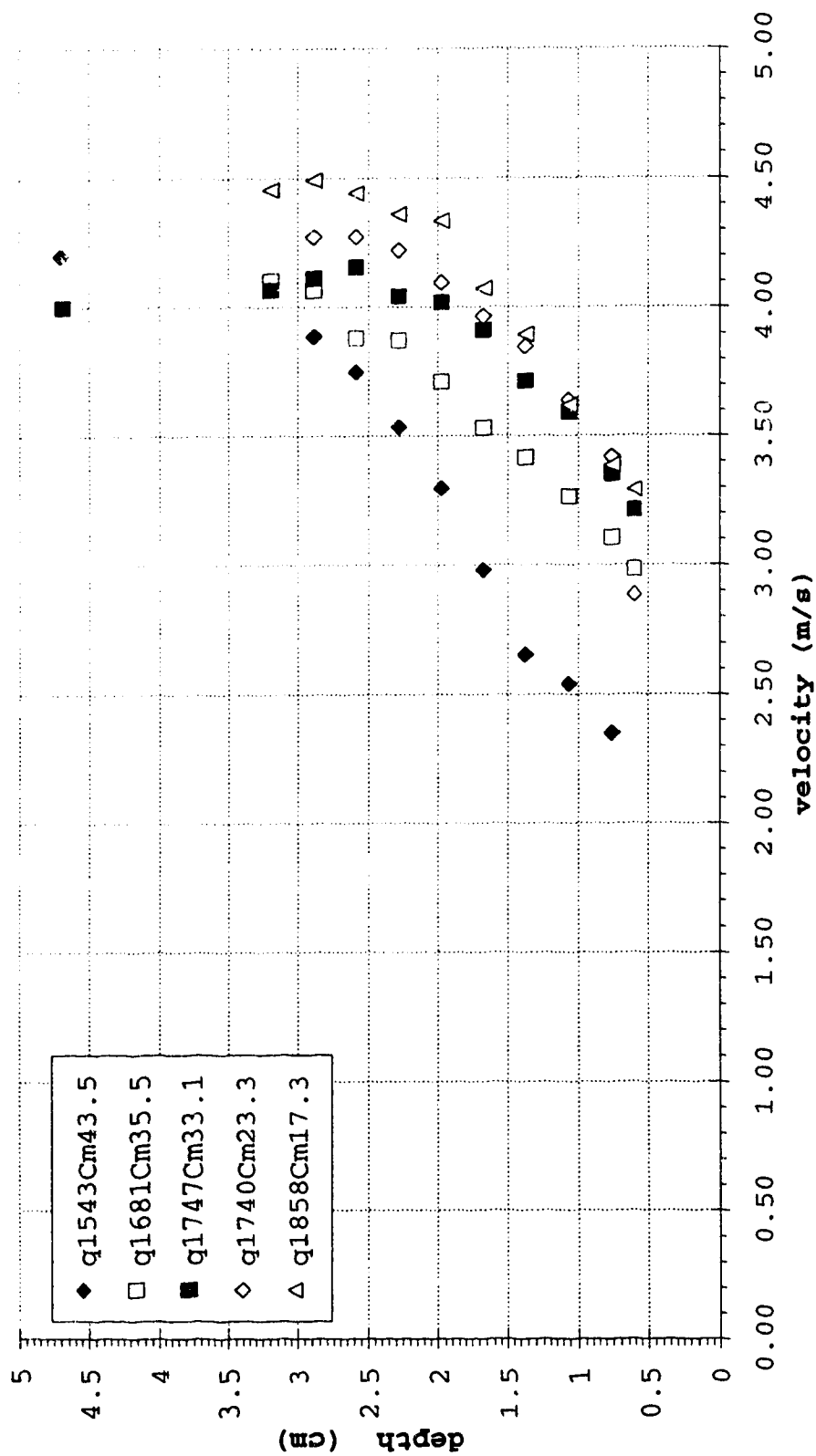


Figure 5-9b Depth-Concentration for steady uniform sand water mixture, particle D3, Slope=28.6%, group 7.90, channel centre

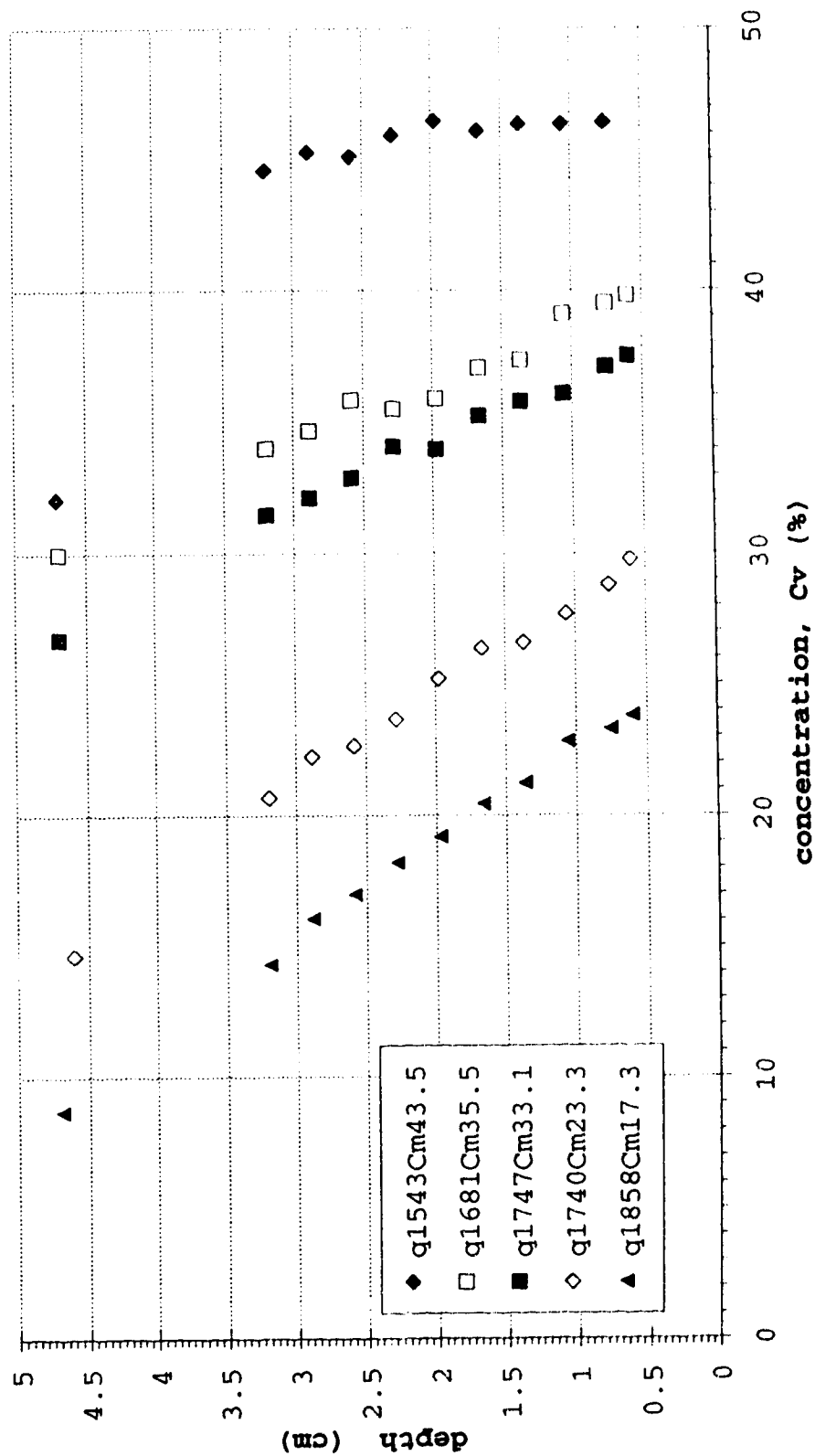


Figure 5-10a Depth-Velocity for steady uniform sand water mixture, particle D4, Slope=28.6%, group 6.45, channel centre

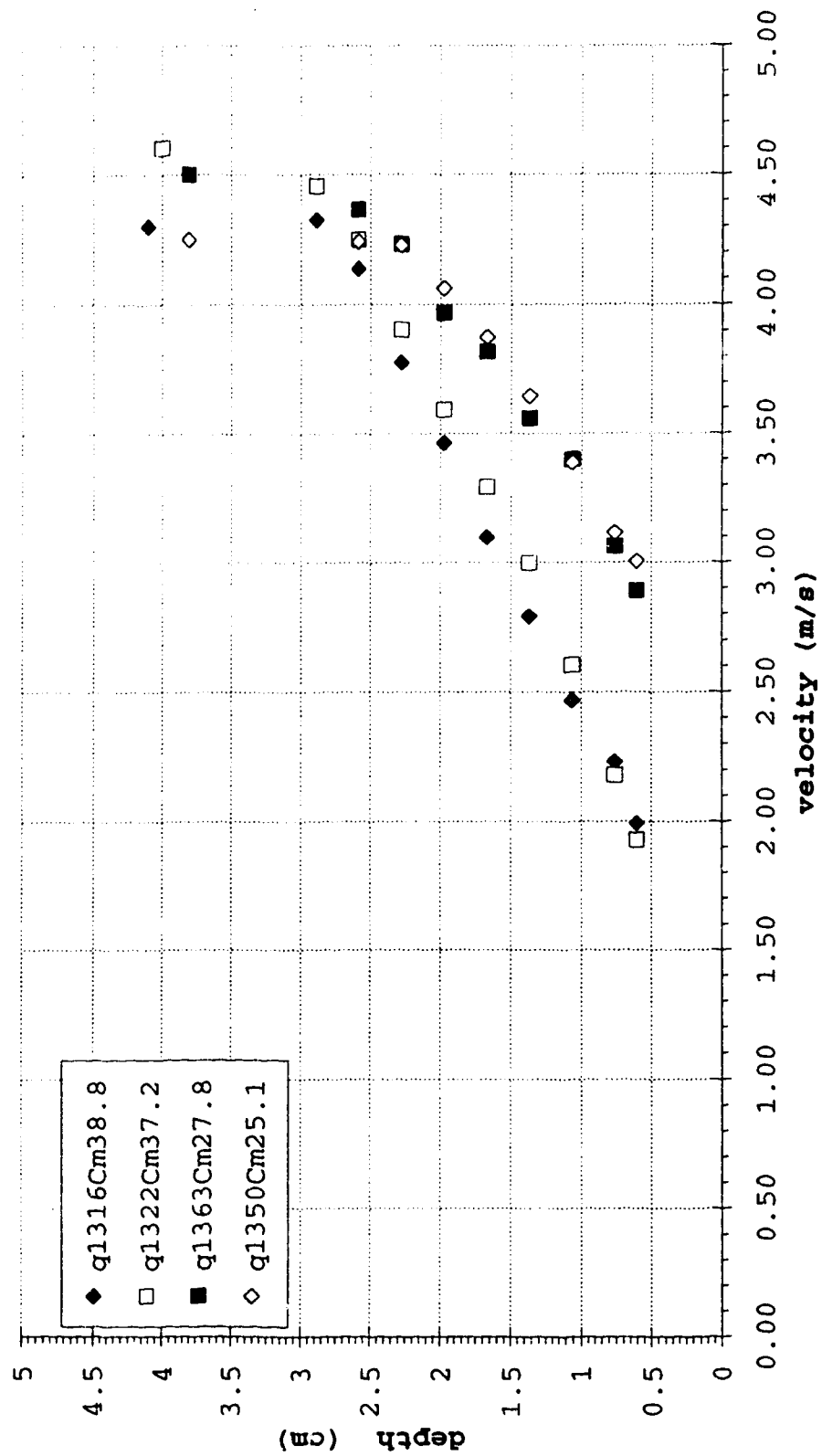


Figure 5-10b Depth-Concentration for steady uniform sand water mixture, particle D4, Slope=28.6%, group 6.45, channel centre

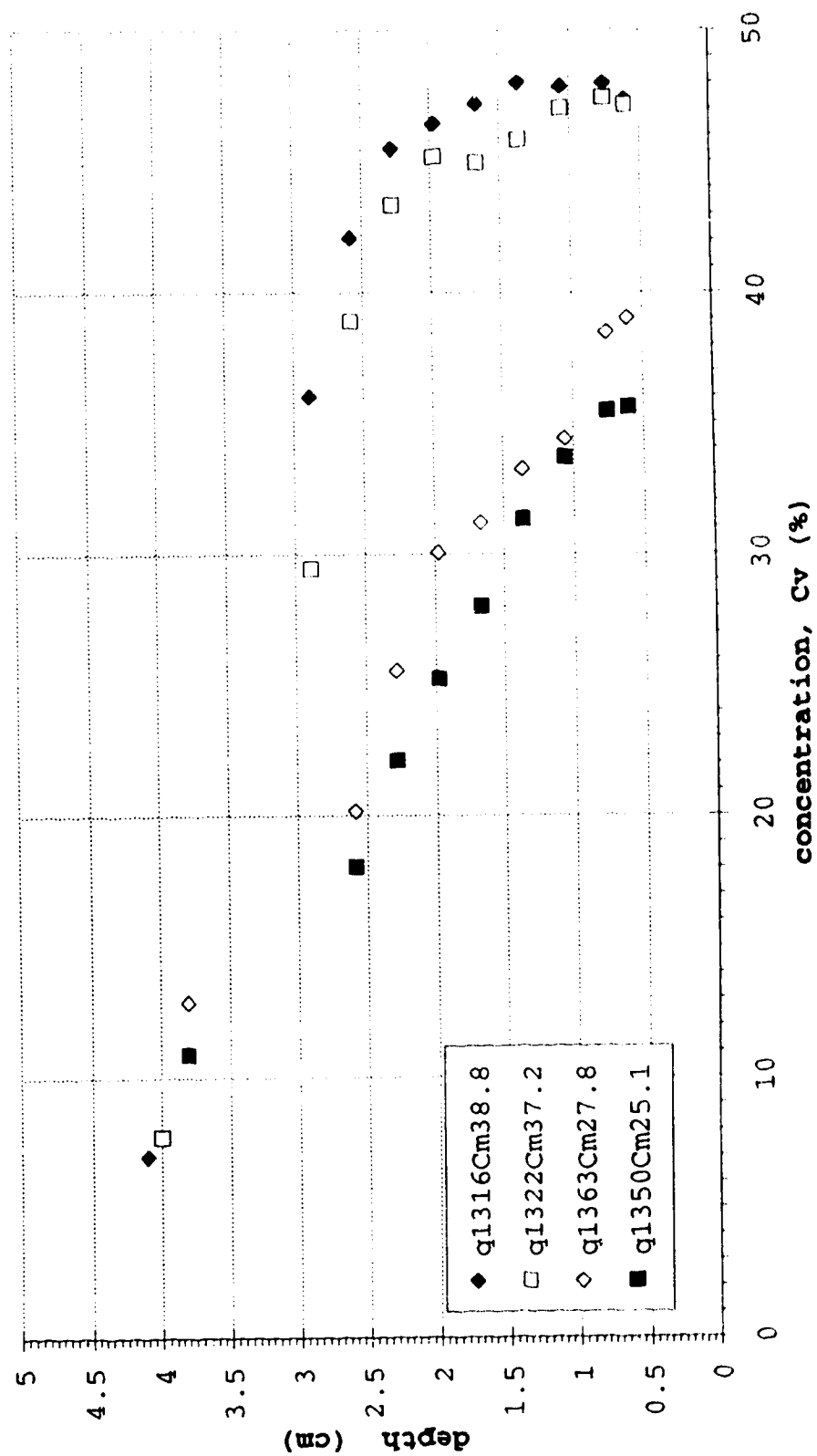


Figure 5-11a Depth-Velocity for steady uniform sand water mixture, particle D4, Slope=28.6%, group 7.90, channel centre

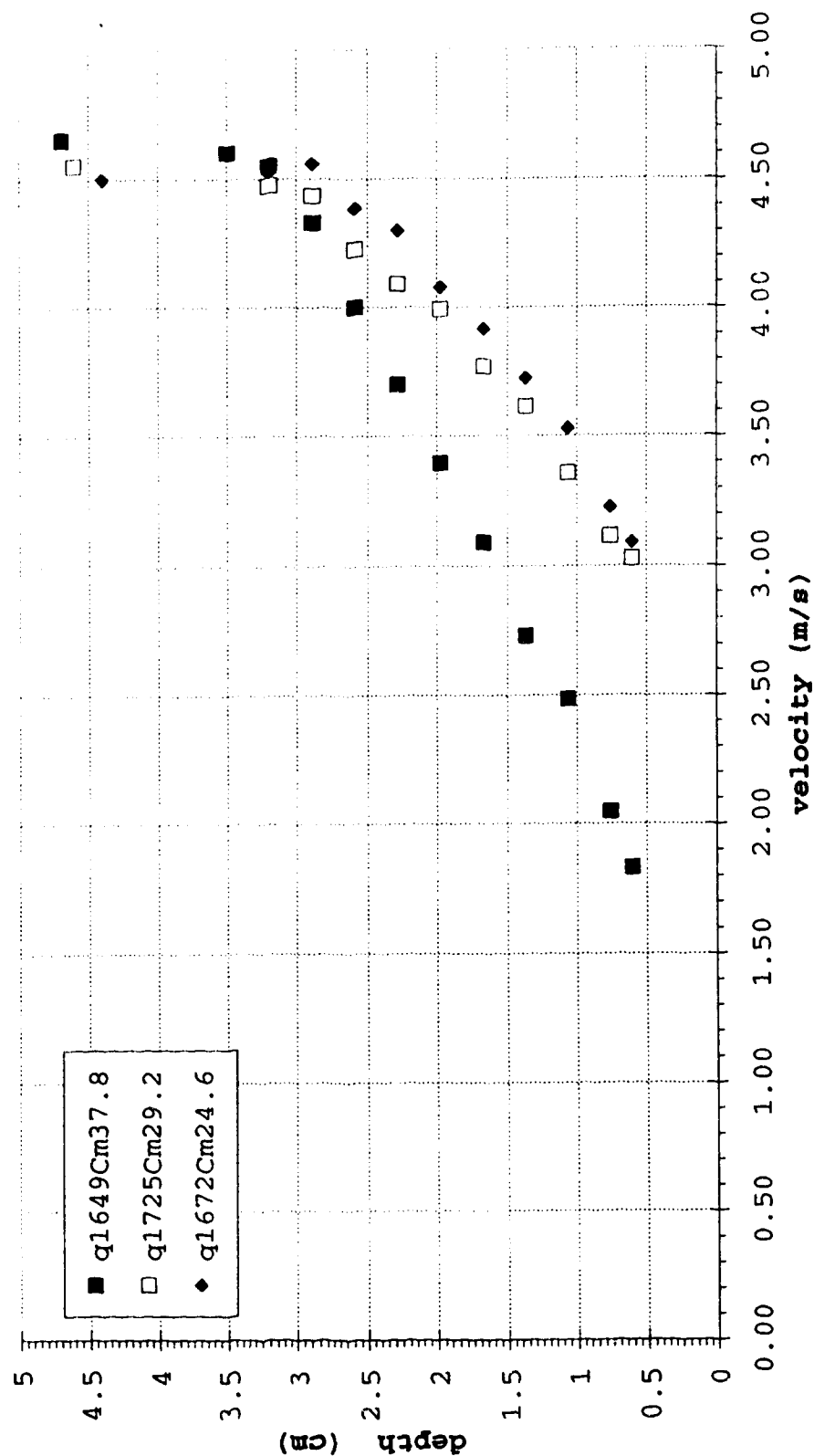
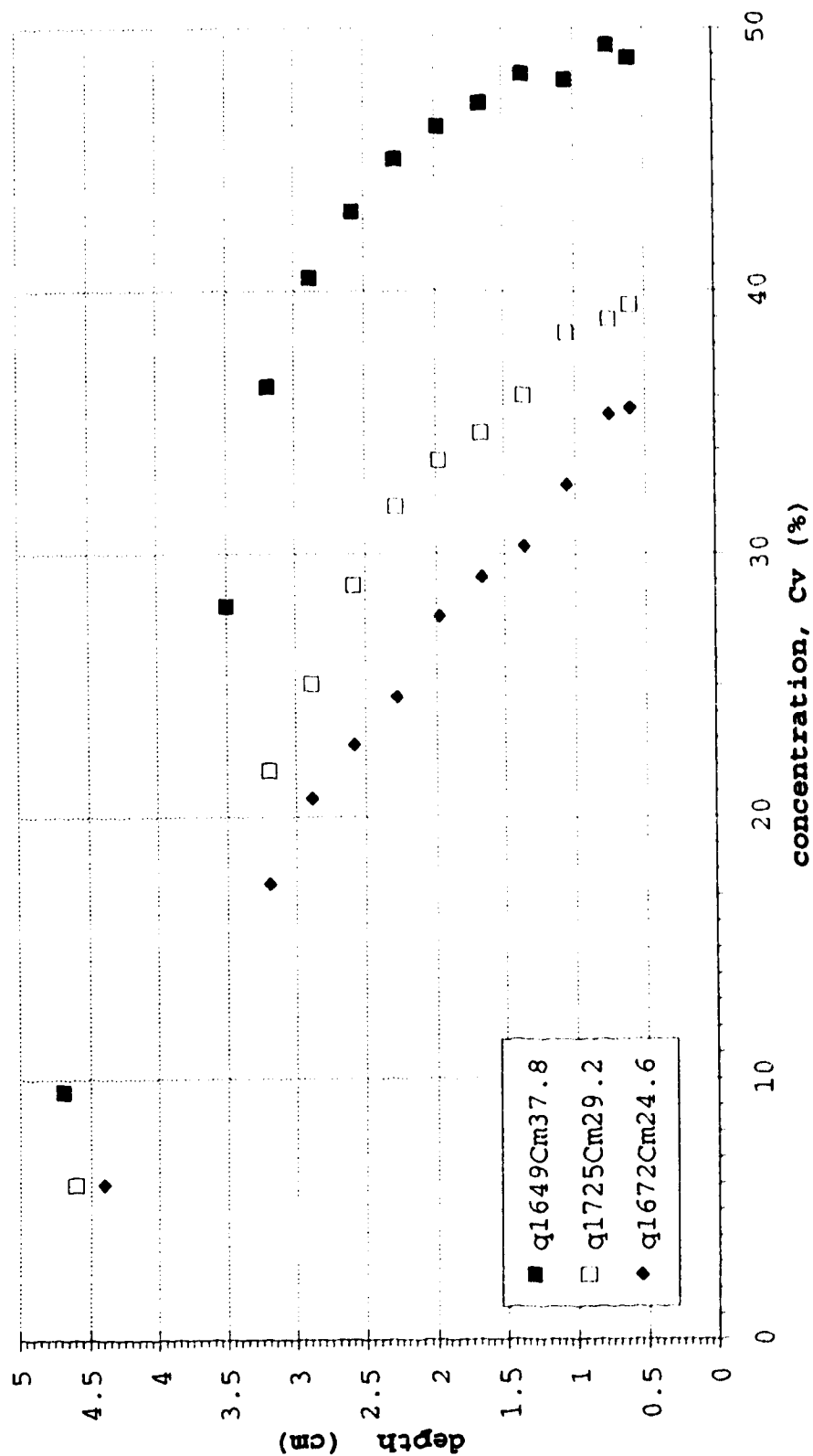


Figure 5-11b Depth-Concentration for steady uniform sand water mixture, particle D4, Slope=28.6%, group 7.90, channel centre



5.2.2 Velocity distribution

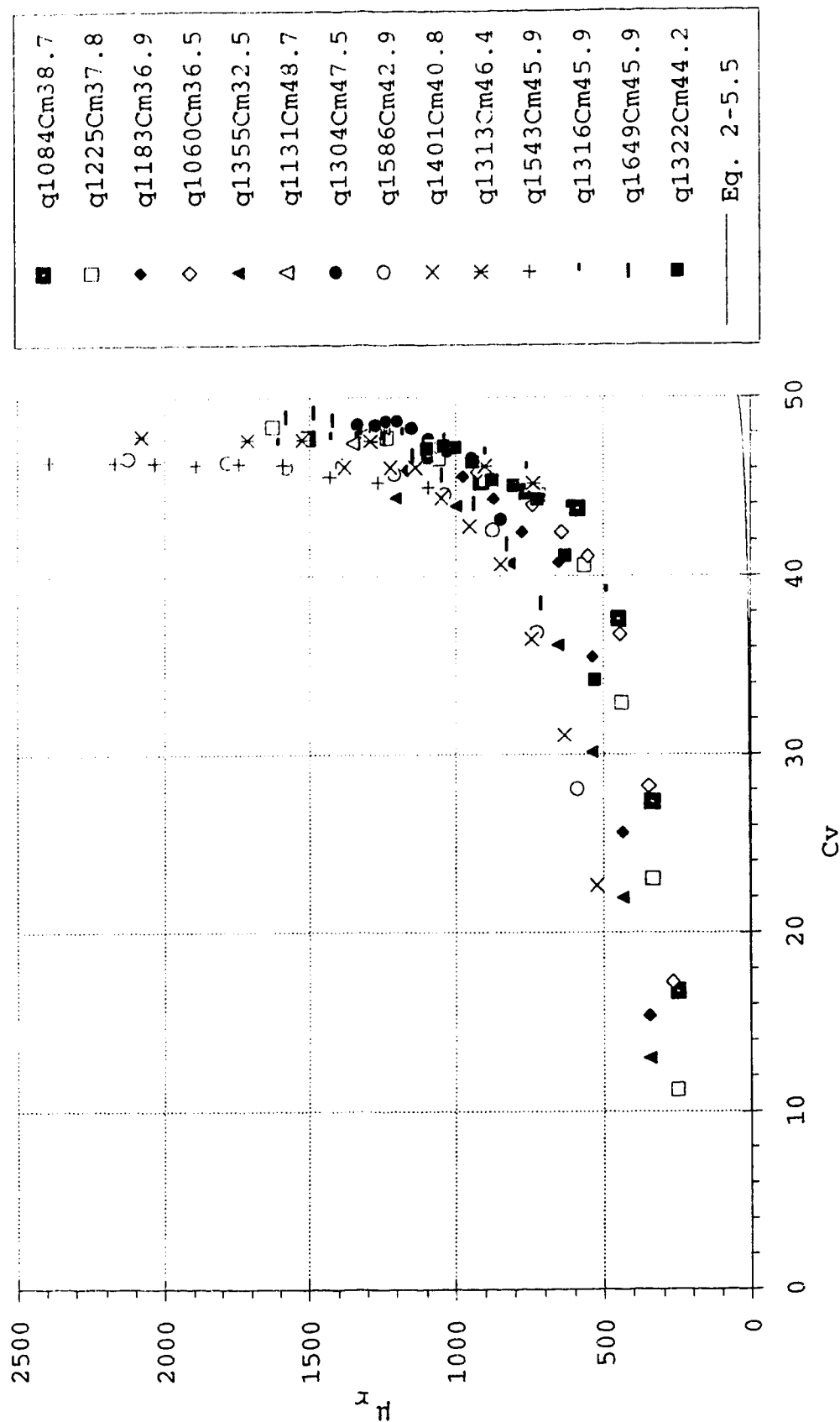
Dimensional velocity profiles are presented in Figures 5-1a to 5-11a. A closer examination of these profiles gives us some indication of the general behavior of the slurry when the mean concentration and the particle sizes are changed. It can be seen in these distributions that the velocity gradients are larger in high concentration flows. The low concentration mixtures show smaller gradients. The velocity profiles also show a trend towards approaching constant velocity gradients for larger concentrations. This is more obvious for larger particle size. As the particles get smaller, this trend to approach constant velocity gradient is apparent only at much higher mean concentrations. The velocity distributions for the particle size D4 show a behavior that is in between what is observed for particles D1, D2 and D3. These obvious dual behavior that can be confirmed in the dimensionless plots Fig. 4-6a to 4-14a are the similarities in the velocity profiles in the high concentration and the lower concentration ranges.

In summary, the velocity profiles in Figures 5-1a to 5-11a display two distinct behaviors. As the mean concentration is increased to a certain value, the velocity profiles become nearly linear. The concentration at which the velocity profile begins to get linear appears to increase with a decrease in particle size. This nature indicates that above a certain mean concentration the dominant dispersing mechanism changes for each particle size.

The nearly linear measured velocity profiles (which means constant velocity gradients) suggest that the total shear stress is independent of shear rates. This would suggest that the viscosity is increasing with depth to account for the increase in shear stress. This will be examined in Appendix E. Below a certain concentration (19% for D1, 30% for D2, 40% for D3 and 35% for D4) the velocity profiles are nonlinear indicating that the total shear is dependent on the velocity gradient. Most conceptual models describing debris flow in the inertial regime comprise of a rate dependent part and a comparatively less important rate independent part in defining a constitutive behavior. In order to estimate a shear-strain rate relations some curve fitting attempts have been made in the Appendix E.

All the profiles from Figures E-21 to A-24 that display distinct positive exponential trends have been plotted in Figure 5-12. The data covers the range of volume concentration from 10% to almost 50% and is displayed in an exponential band. Figure 5-12 also shows the concentration according to Equation 2-5.5. The band of data distinctly shows that the apparent viscosity from velocity and concentration measurement is 60 to 70 times that given by Do Ik Lee (1969) at a mean volumetric concentration of 40 %. This high viscosity which appears to be much larger than the

Figure 5-12 C_v vs μ_r , particle D1 to D4



laminar viscosity suggest that a significant portion of it is probably of turbulent viscosity.

The results from the measurements presented in this thesis clearly indicates that the viscosity of a mixture is not only dependent on the particle concentration of the mixture but also on the mechanism of dispersion.

The velocity profiles also experienced a negative velocity gradient, similar to the velocity profiles exhibited by clear water, for lower mean concentrations in the regions close to the surface. This trend is believed to be due to the secondary flow effects. For larger mean concentrations, the negative gradients usually turned slightly positive which showed a reduction in the secondary flow effects as concentration increased.

5.2.3 Shear distribution

Figures 5-13 to 5-16 show the normalized driving shear distribution calculated by integrating the concentration profiles. For larger particles i.e. D1 (Fig. 5-13) and D2 (Fig. 5-14) the shear profiles show a variation in the shear gradients which is indicated by the curvature in the profiles. The curvature increases with decreasing mean concentration where the distribution of the particles are not uniform throughout the depth. As the dispersion increases, the resulting concentration profiles becomes more uniform and the shear gradients approach a constant value. This is

Fig. 5-13 Dimensionless shear stress profiles for particle D1

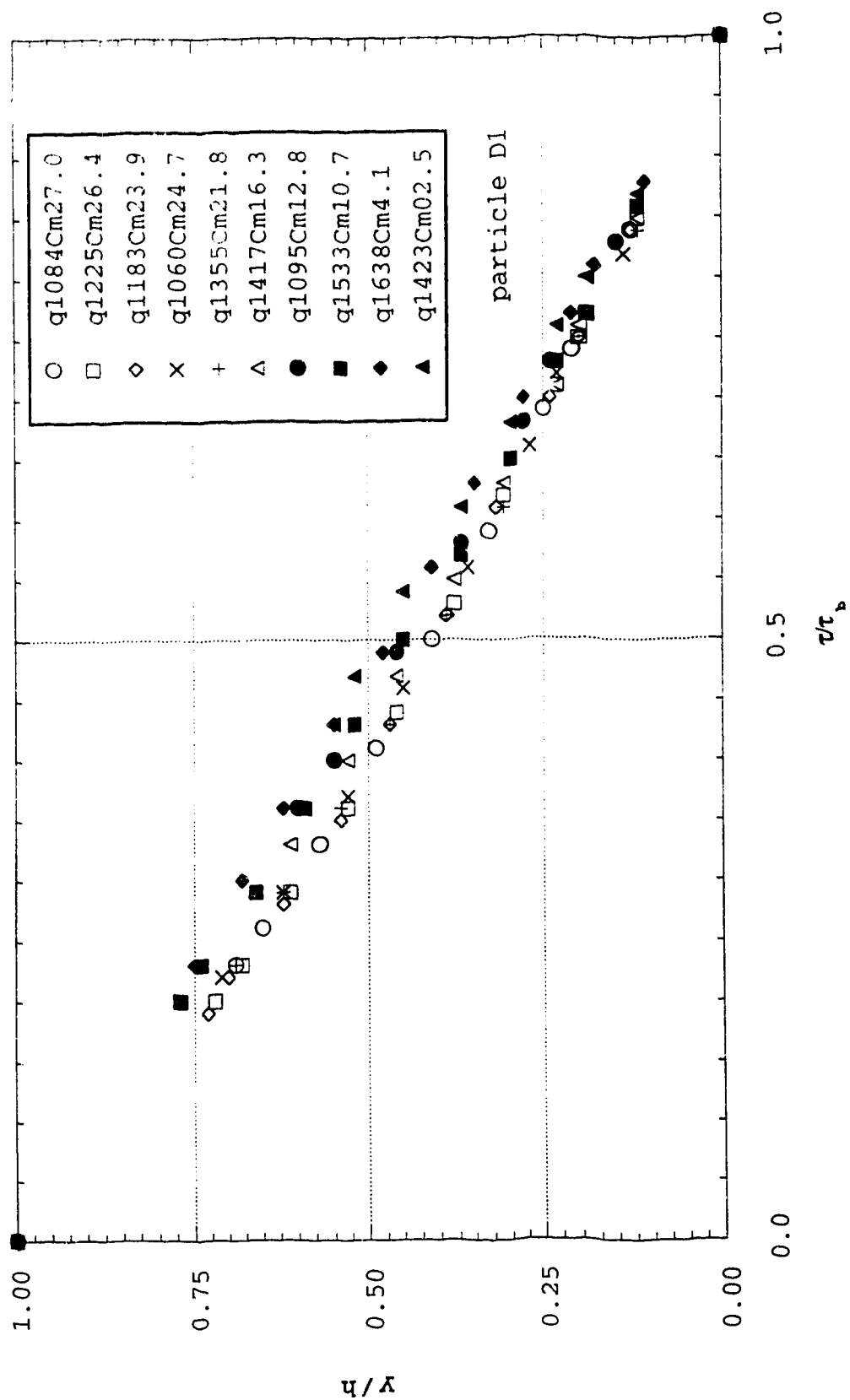


Fig. 5-14 Dimensionless shear stress profiles for particle D2

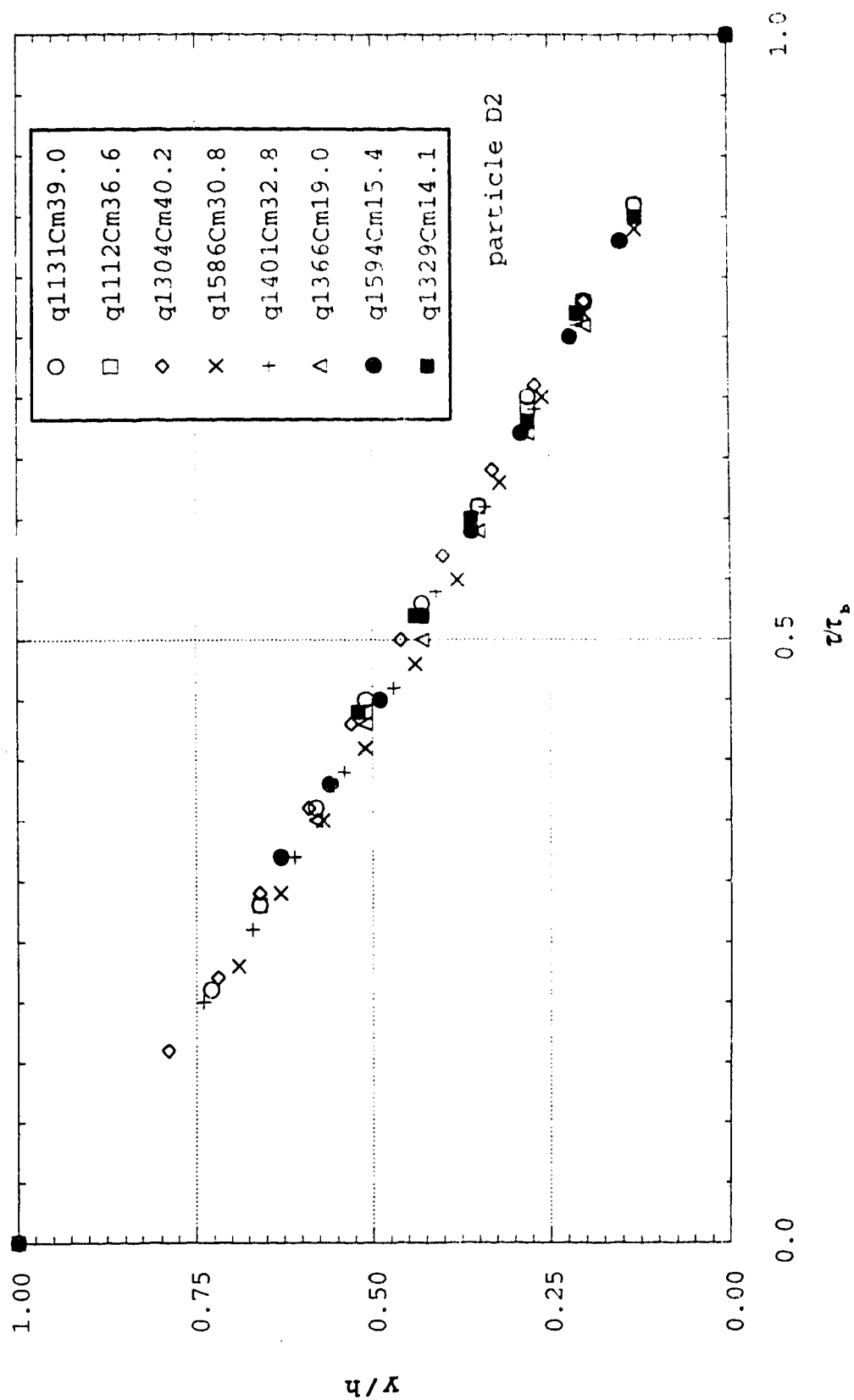


Fig. 5-15 Dimensionless shear stress profiles for particle D3

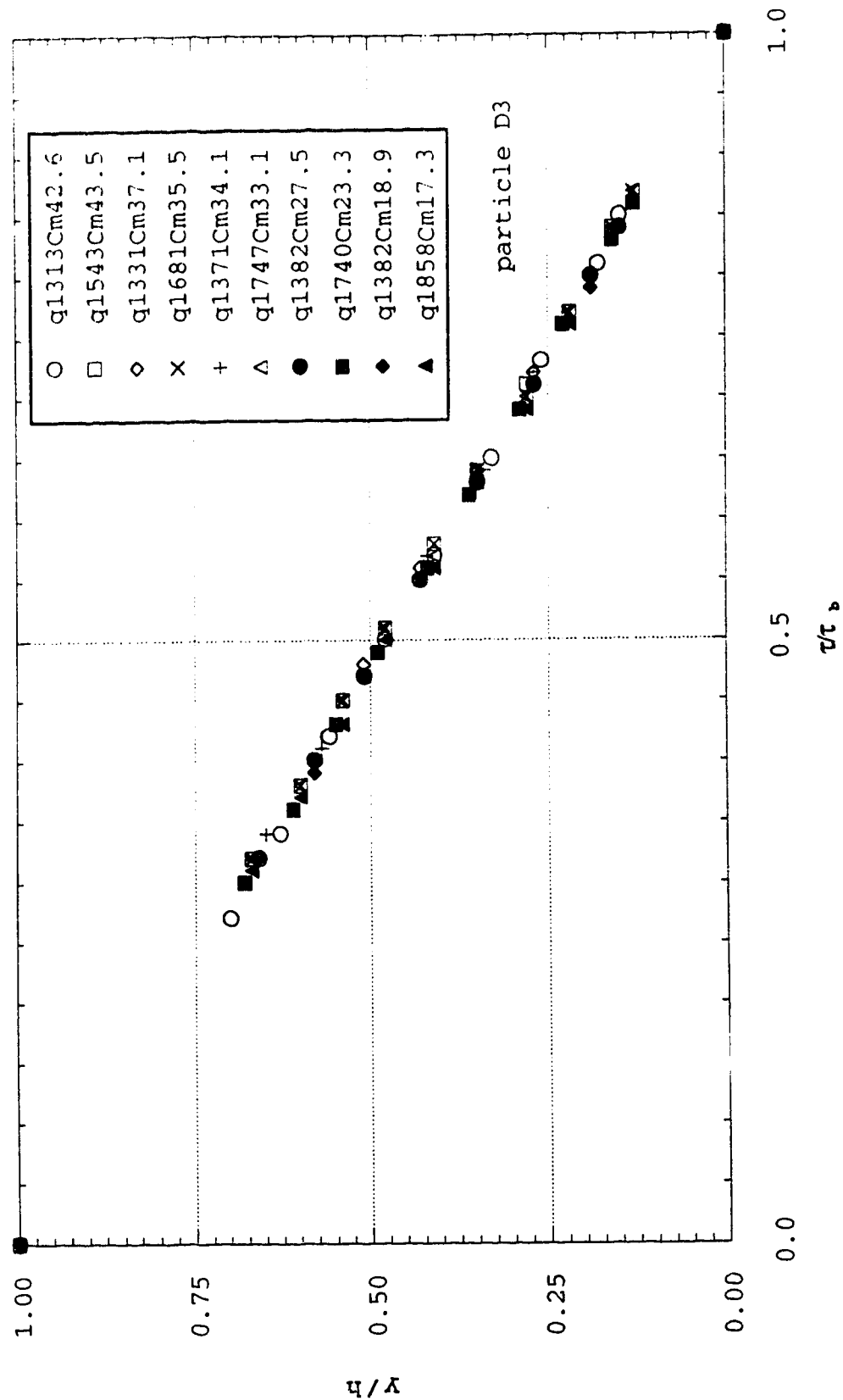
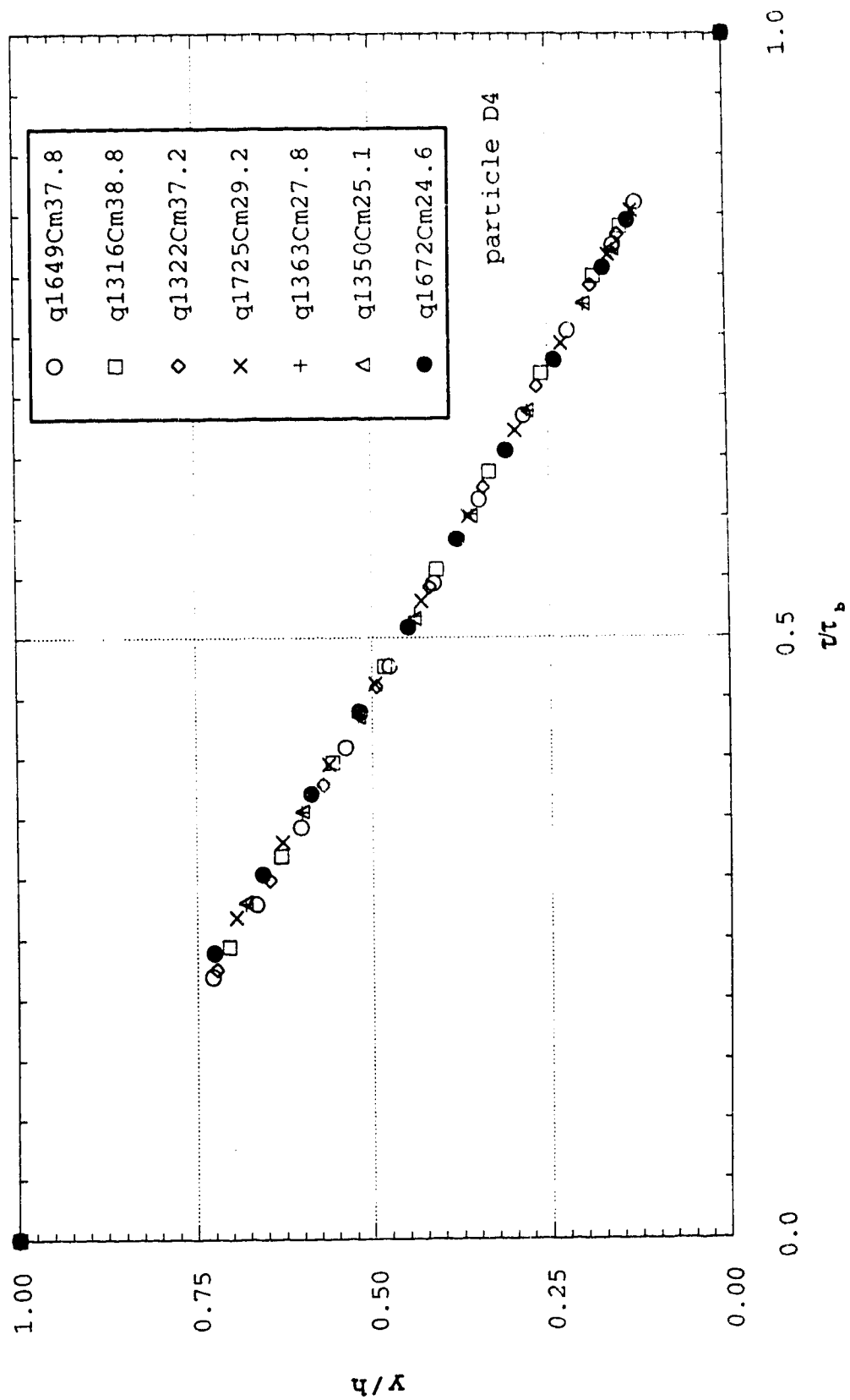


Fig. 5-16 Dimensionless shear stress profiles for particle D4



obvious in the case of D3 (Fig. 5-15). The mixture D4 also produced almost constant shear gradient with very little scatter (Fig. 5-16). The profiles for mixture D4 display a clear influence of the finer particles in enhancing dispersion.

5.3 Analysis of Experimental Data

5.3.1 Total shear versus grain shear

Equation(2-3.6b) was used to estimate the size of the grain shear for each measured profile. a_i was taken, as given by Bagnold, to be 0.042. ϕ_m was taken as 0.32. Figs. 5-17 to 5-20 show the ratio of grain shear velocity profiles for the four particle sizes. Although Bagnold's grain shear expression (2-3.6b) was for uniformly distributed particles, its use in the above figures is only to give estimate of at least an order of magnitude of the dispersive stresses in the measured profiles. It can be seen from Fig. 5-17 to 5-20 that the dispersive stress is less than 10% and ranges from 2 to 8% in most cases. This seems to show that dispersive stress is not the dominating dispersion mechanism in the present study.

If a flow with $C_v=40\%$ is considered the driving shear per unit width in terms of the flow depth h can be written as

$$\tau = 4657 h \quad (5-3.1)$$

Figure 5-17 Ratio of Bagnold's shear to the measured driving shear
particle D1

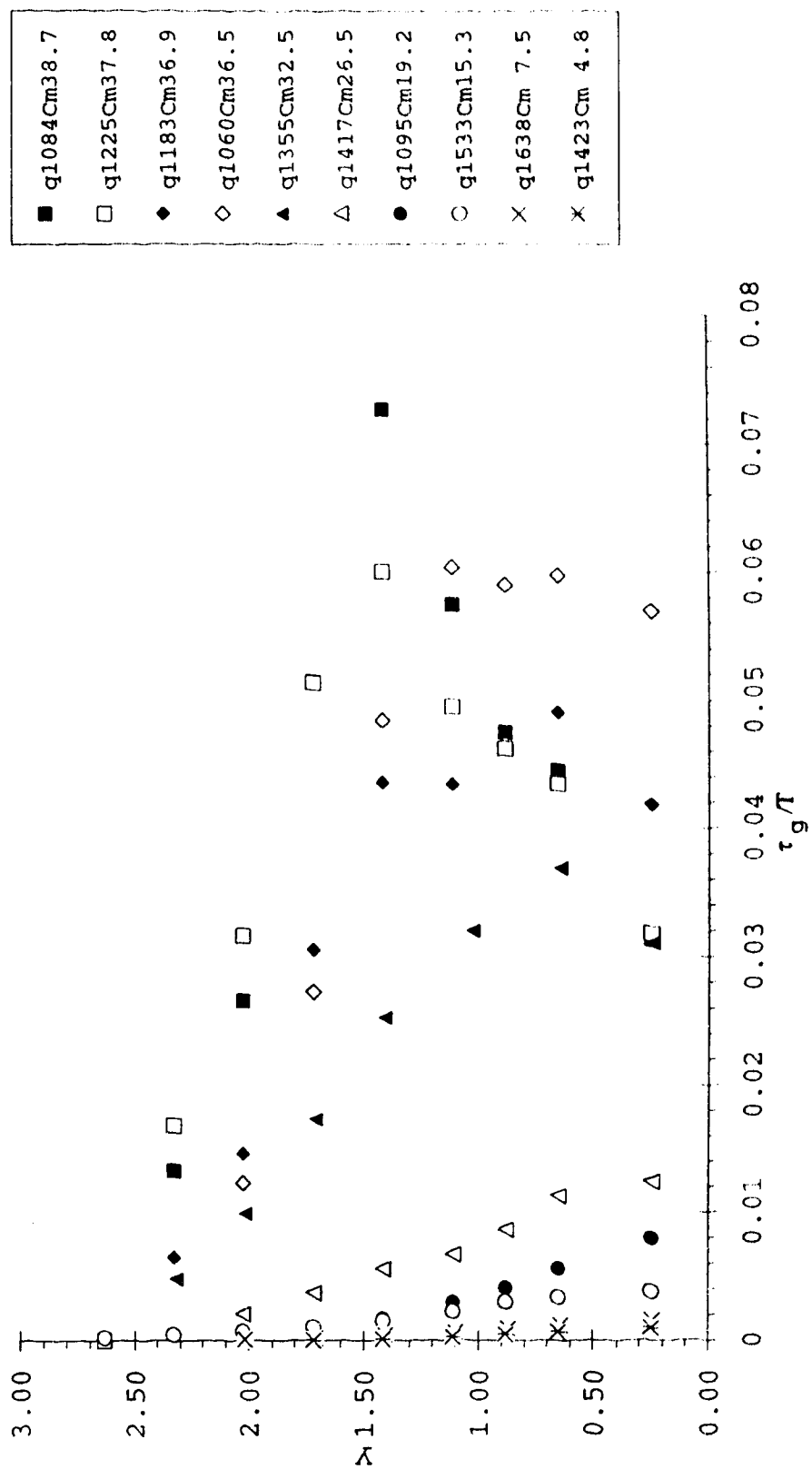


Figure 5-18 Ratio of Bagnold's shear to the measured driving shear
particle D2

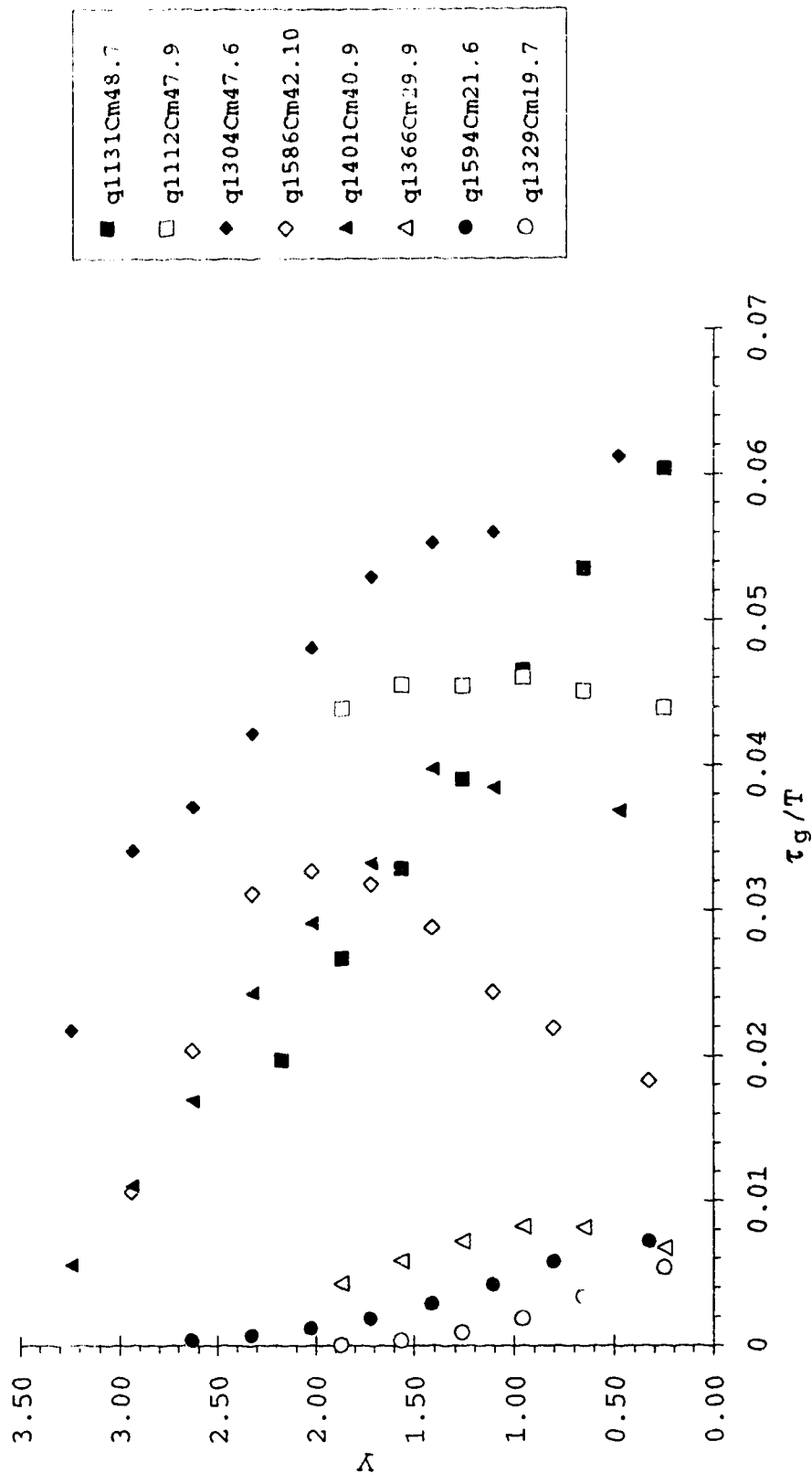


Figure 5-19 Ratio of Bagnold's shear to the measured driving shear
particle D3

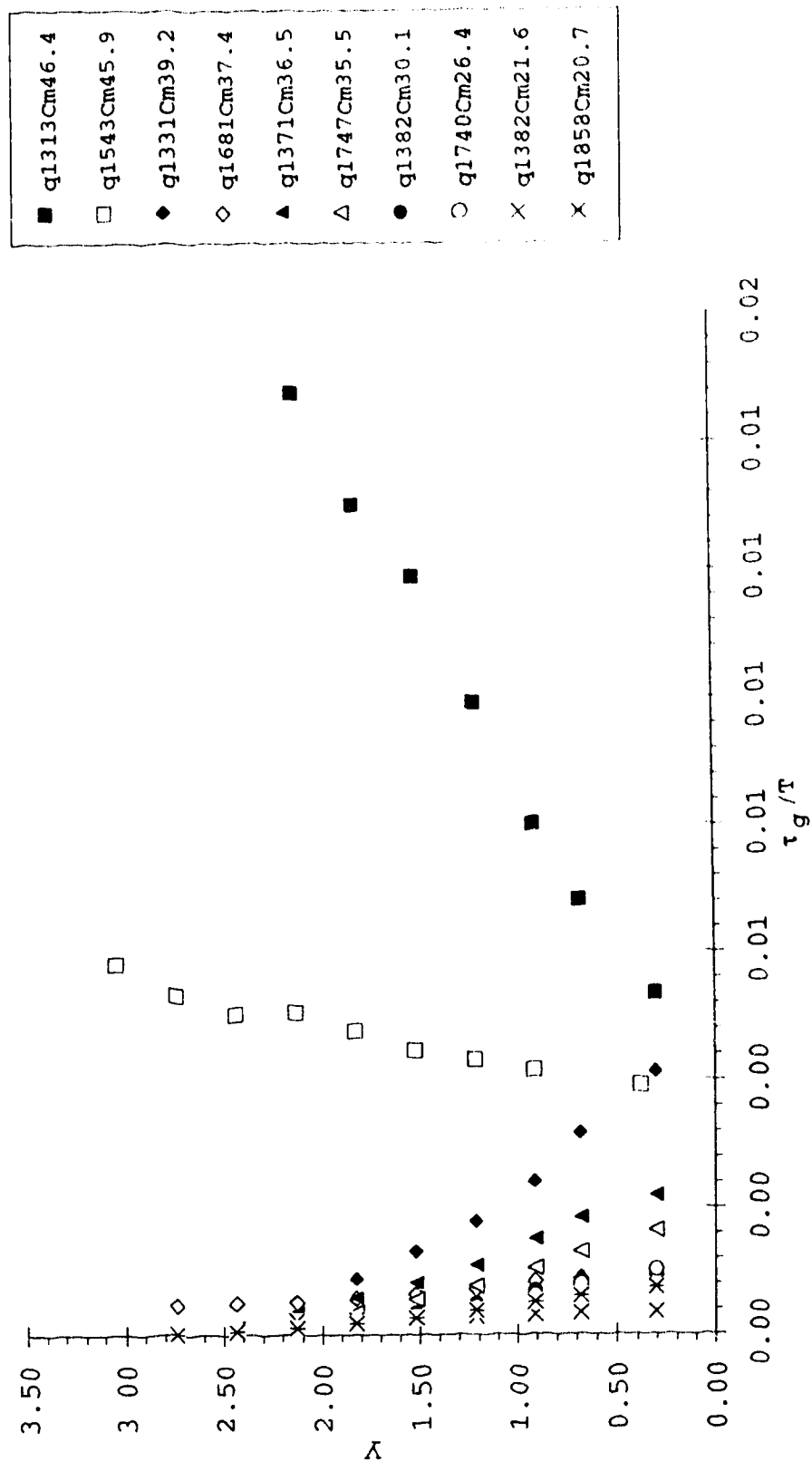
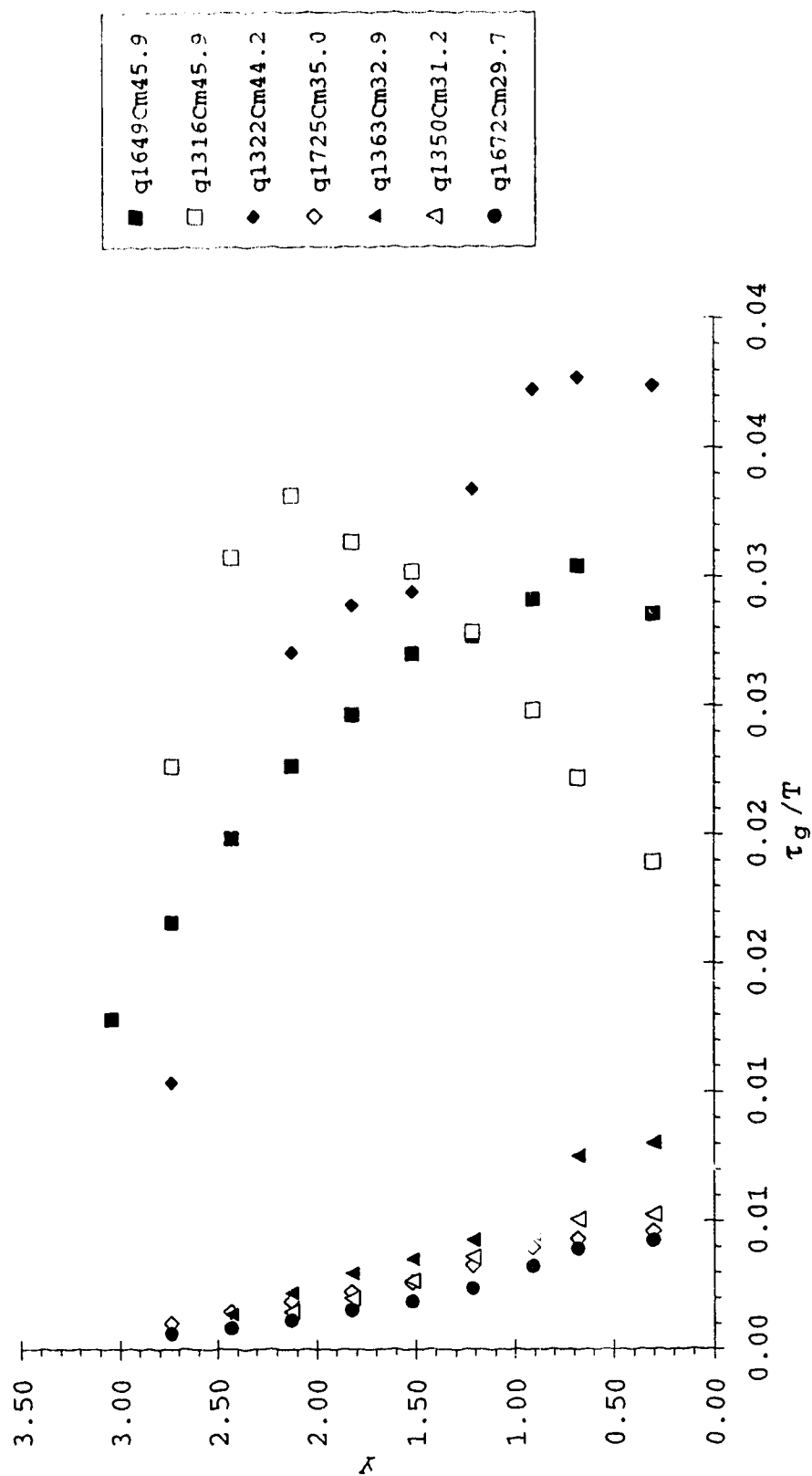


Figure 5-20 Ratio of Bagnold's shear to the measured driving shear
particle D4



and Bagnold's granular shear can be written in terms of velocity gradient $\partial u / \partial y$, and particle size D as

$$\tau_g = 1082 \left(\frac{\partial u}{\partial y} \right)^2 D^2 \quad (5-3.2)$$

For the grain shear stress to be 75% of the total shear Equations (5-3.1) and (5-3.2) give

$$\left(\frac{\partial u}{\partial y} \right)^2 D^2 = 3.23 h \quad (5-3.3)$$

If a 30 cm deep flow having a mean velocity of 3m/s with a mean gradient of 10^{-5} is considered, the particle size would have to be around 9cm for the grain shear to be 75% of the total shear. This flow depth and particle size is rather difficult to achieve in the laboratory setting. This suggests that larger flow depths and larger particles are essential for dispersive stress to be dominant which is more likely to be found in field condition.

5.3.2 Velocity distribution

Figs. 5-21 to 5-24 show the normalized velocity profiles for the four particle sizes. Table 5-1 gives the details of all the normalizing variables. The velocity profiles have been truncated at the top to neglect the changes in the

Figure 5-21 Comparison of dimensionless velocity profiles for particle D1

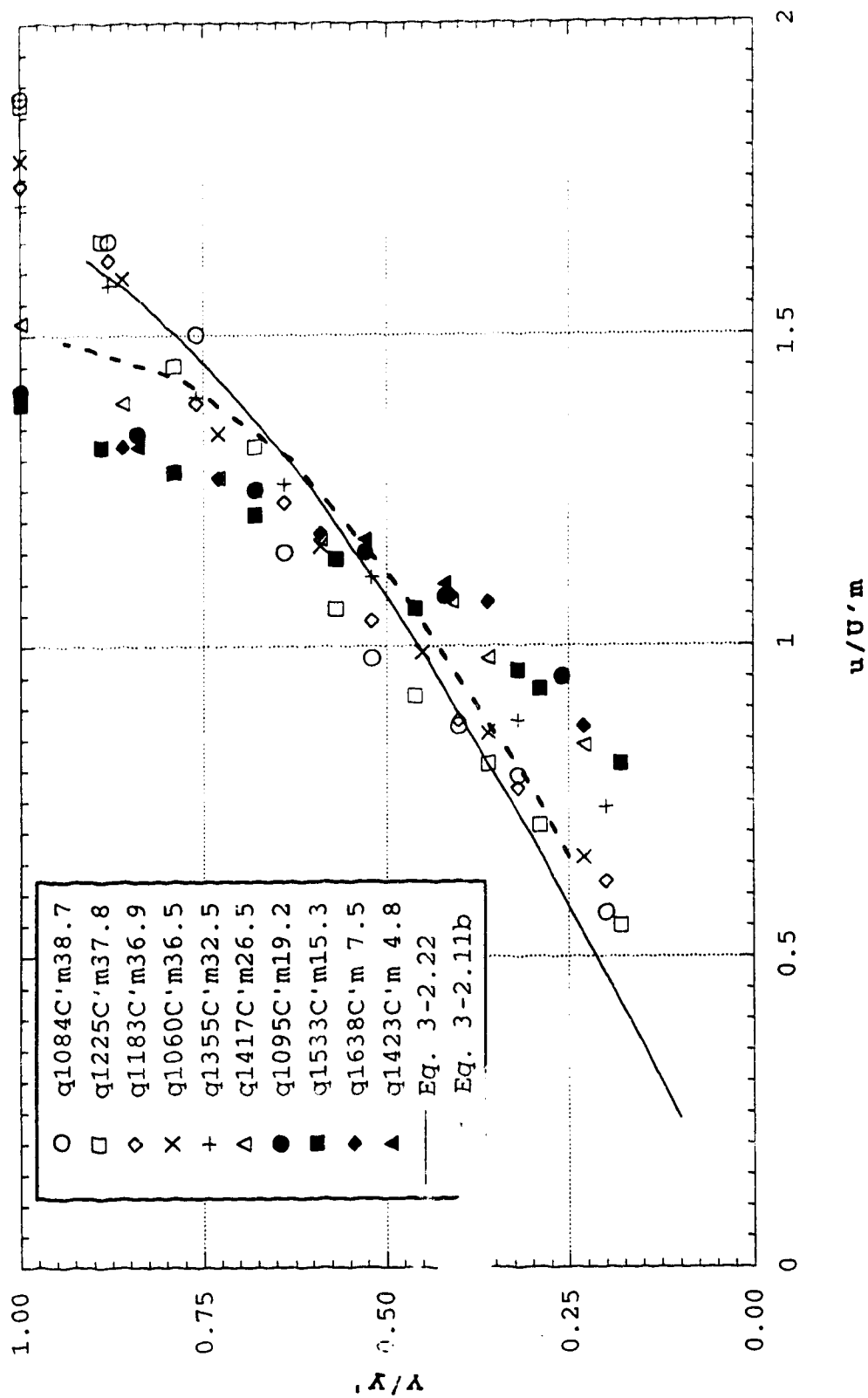


Figure 5-22 Comparison of dimensionless velocity profiles for particle D2

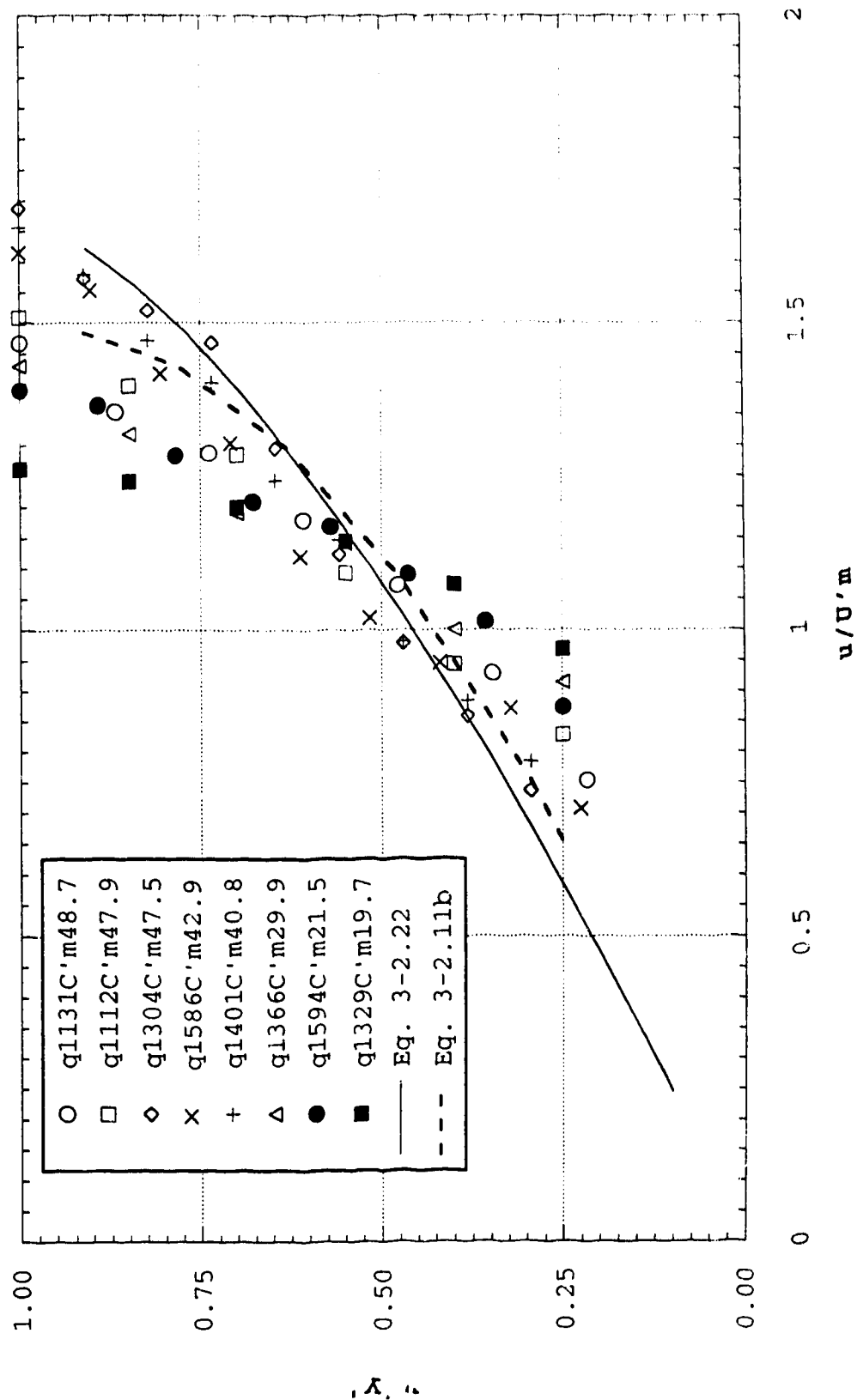


Figure 5-23 Comparison of dimensionless velocity profiles for particle D3

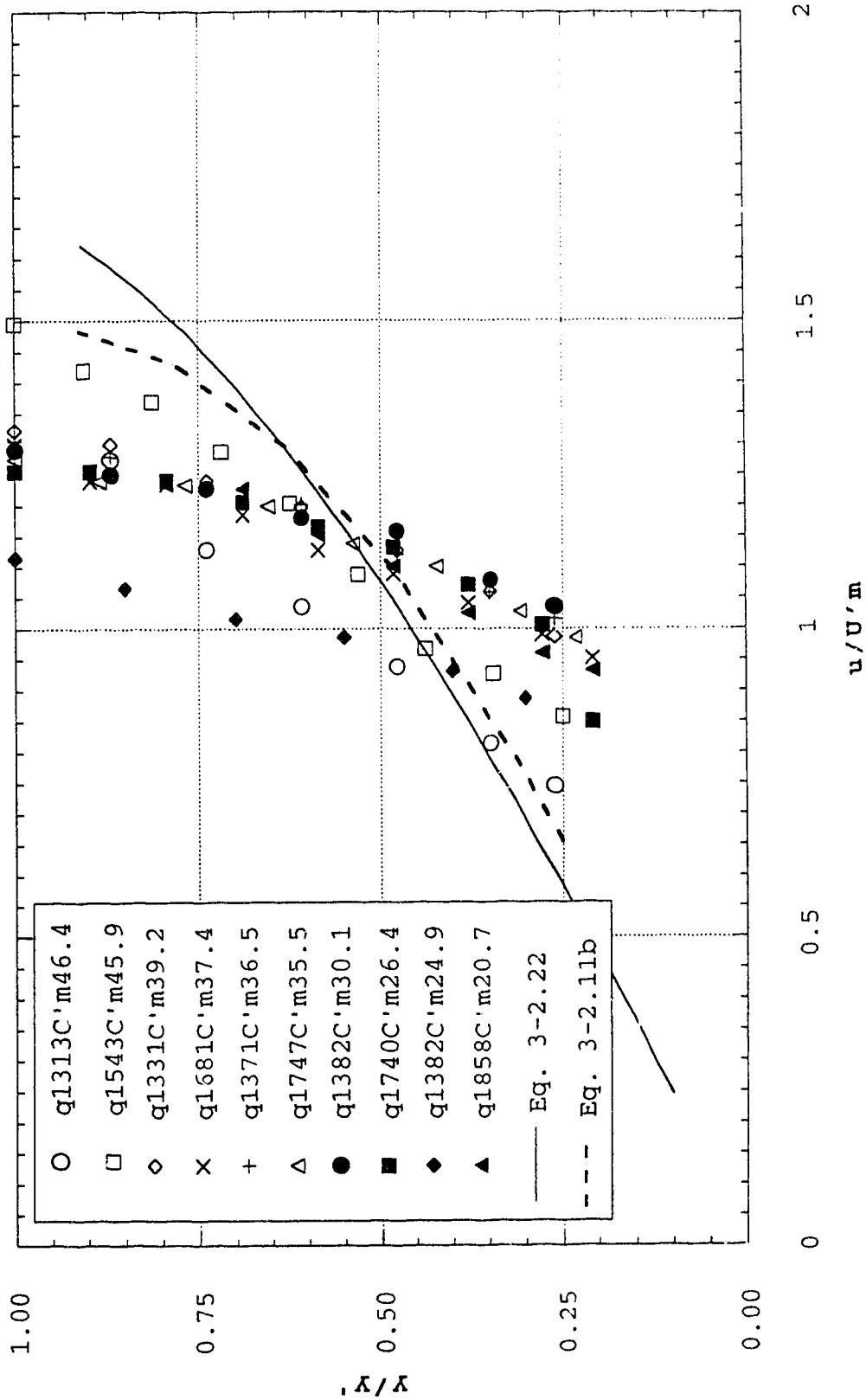


Figure 5-24 Comparison of dimensionless velocity profiles for particle D₄

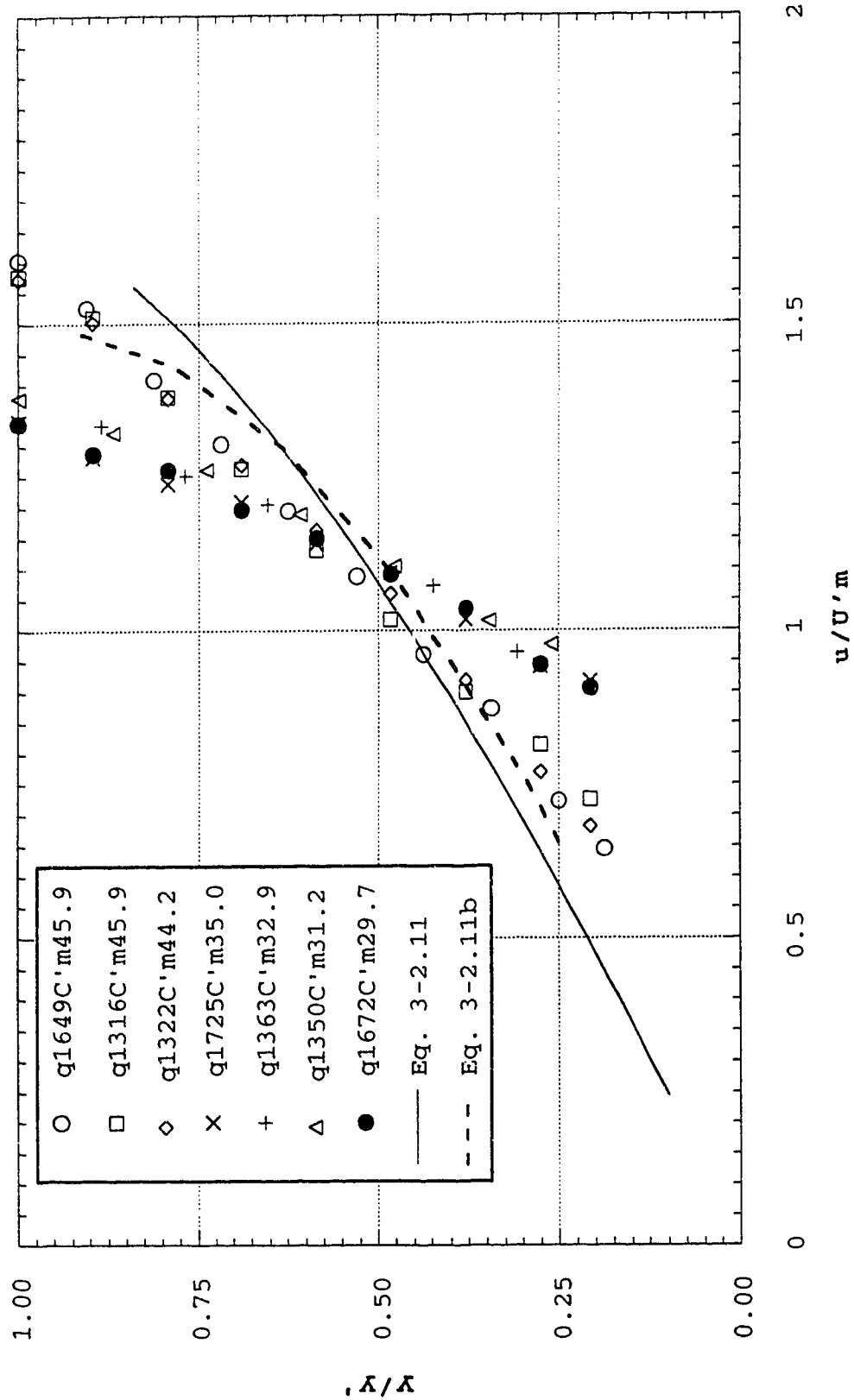


Table 5-1 Details of the measurements

Particle D1

$q(\text{cm}^2/\text{s})$	1084	1225	1183	1060	1355	1417	1095	1533	1638	1423
Cm	27	26	24	25	22	16	13	11	4	3
$\mu(\text{Ns}/\text{m}^2)$	3.1E-03	3.0E-03	2.5E-03	2.7E-03	2.2E-03	1.7E-03	1.5E-03	1.4E-03	1.1E-03	1.1E-03
h(cm)	3.8	4.1	4	3.5	4	4.1	3.4	4.2	4.5	4.2
$y'(\text{cm})$	2.5	2.8	2.5	2.2	2.5	2.2	1.9	2.8	2.2	1.9
$y_{10}(\text{cm})$	2.8	2.8	2.7	2.6	2.6	2.6	2.3	2.8	2.5	2.1
$\tau_b(\text{N}/\text{m}^2)$	148.4	158.9	150.7	133	146.8	140.4	111.2	133.3	129.7	118.1
$U'm(\text{m}/\text{s})$	2.18	2.1	2.27	2.32	2.58	2.73	2.72	3.27	3.05	2.81
$Um(\text{m}/\text{s})$	2.85	2.92	2.96	3.03	3.39	3.46	2.85	3.65	3.64	3.03
Re_*	84.0	90.2	101.4	91.1	111.5	138.1	138.7	161.7	187.0	184.1
Re	50697	59346	65210	56151	82175	105207	79190	131471	156899	124316

Particle D2

$q(\text{cm}^2/\text{s})$	1131	1112	1304	1586	1401	1366	1594	1329		
Cm	39	37	40	31	33	19	15	14		
$\mu(\text{Ns}/\text{m}^2)$	8.9E-03	6.9E-03	1.0E-02	4.1E-03	4.8E-03	1.9E-03	1.6E-03	1.6E-03		
h(cm)	4	4	4.7	4.9	4.6	4	4.4	3.9		
$y'(\text{cm})$	2.3	2	3.4	3.1	3.4	2	2.8	2		
$y_{10}(\text{cm})$	3.67	3.8	4.6	3.8	4	3.2	3.4	3.2		
$\tau_b(\text{N}/\text{m}^2)$	177.5	173.2	211.1	199.6	191.3	141.8	149	129.7		
$U'm(\text{m}/\text{s})$	2.23	2.14	2.27	2.57	2.59	2.89	3.21	3.1		
$Um(\text{m}/\text{s})$	2.83	2.78	2.78	3.24	3.05	3.41	3.62	3.41		
Re_*	33.9	42.8	32.4	75.1	62.9	124.6	147.1	143.6		
Re	20868	25836	21243	58548	44758	92364	121370	105103		

Particle D3

$q(\text{cm}^2/\text{s})$	1313	1543	1331	1681	1371	1747	1382	1740	1382	1858
Cm	43	44	37	36	34	33	28	23	19	17
$\mu(\text{Ns}/\text{m}^2)$	1.4E-02	1.5E-02	7.3E-03	6.2E-03	5.4E-03	5.0E-03	3.2E-03	2.4E-03	1.9E-03	1.8E-03
h(cm)	4.1	4.8	3.9	4.8	4	4.8	3.9	4.7	3.9	4.8
$y'(\text{cm})$	2.9	3.2	2.3	2.9	2.3	2.6	2.3	2.9	2.3	2.9
$y_{cm}(\text{cm})$	3	1.9	2	2.5	2	2.5	2	2.4	2.1	2.5
$\tau_b(\text{N}/\text{m}^2)$	188.5	222.5	169.7	205.5	168.7	200.3	153.1	175.7	138.2	166.6
$U'm(\text{m}/\text{s})$	2.74	2.74	3	3.13	3.07	3.26	3.16	3.4	3.64	3.53
$Um(\text{m}/\text{s})$	3.2	3.22	3.41	3.5	3.43	3.64	3.54	3.7	3.54	3.87
Re_*	23.1	22.3	40.3	51.6	53.0	62.8	82.7	113.0	123.5	144.8
Re	16240	17137	29507	43041	39522	54472	62793	98541	93829	133432

Particle D4

$q(\text{cm}^2/\text{s})$	1649	1316	1322	1725	1363	1350	1672			
Cm	38	39	37	29	28	25	25			
$\mu(\text{Ns}/\text{m}^2)$	7.8E-03	8.7E-03	7.3E-03	3.6E-03	3.3E-03	2.7E-03	2.6E-03			
h(cm)	4.8	4.1	4	4.6	3.8	3.8	4.4			
$y'(\text{cm})$	3.2	2.9	2.9	2.9	2.6	2.3	2.9			
$y_{cm}(\text{cm})$	3.1	2.8	2.7	2.5	2.1	2	2.3			
$\tau_b(\text{N}/\text{m}^2)$	210.3	181.5	174.3	183.9	149.6	145.1	167.1			
$U'm(\text{m}/\text{s})$	2.84	2.74	2.83	3.3	3.17	3.07	3.41			
$Um(\text{m}/\text{s})$	3.44	3.21	3.31	3.75	3.59	3.55	3.8			
Re_*	41.8	35.0	40.5	80.9	80.1	93.1	102.7			
Re	34282	24758	29102	70732	60962	69987	88973			

profiles due to the secondary flow effects. U'_m represents the mean velocity of the truncated profile, y is the position above the bed, y' is the height above the bed to the point where the velocity profile is truncated. The profiles were truncated primarily to remove scatter as well as to study only the region with consistent trends.

Figures 5-21 to 5-24 include the velocity profiles for a dilatant fluid, Equation (3-2.22) (Takahashi, Shen and Ackermann), and a laminar Newtonian fluid equivalent to the Bingham plastic fluid with $\tau_y=0$ (Equation 3-2.11b). The plots show that the dilatant fluid model as well as the laminar Newtonian model fail to reproduce the steeper gradients observed in the measured profiles. The measured velocity profiles with lower mean concentrations show a significant transfer of streamwise momentum to the slower bed region resulting in a more uniform profile reminiscent of turbulent flow.

Generalized Reynolds' criteria have been suggested to apply to non-Newtonian fluids to define laminar and turbulent flow conditions. It is more appropriate in non-Newtonian fluids to appeal to experiments to establish the validity of turbulence criteria. However, visualization presents a problem in slurry flow. When departure from Newtonian behavior is small, Reynolds' criteria based on an apparent viscosity may sometimes be adequate. Table 5-1 shows apparent viscosities for each mean concentration calculated

using Eq. (2-5.5). Note that q is the integrated unit discharge at a section. Roughness Reynolds number Re_* ($=u_* k_s \rho_m / \mu$) and Reynolds number (R) given by $U_m h \rho_m / \mu$ are also presented in Table 5-1. The large Reynolds number and Re_* suggest that the measured flows are rough turbulent or, in some cases, transitional turbulent. As discussed earlier, at a certain mean concentration turbulent dispersion of sediment appears to dominate over other dispersion mechanisms resulting in a nonlinear velocity distribution. For large Reynolds number when the particles are small (D3), or when the particles are graded with fines present (D4), turbulent dispersion persists even at large concentrations (Fig. 5-23 and Fig 5-24).

Figure 5-25 to 5-28 show semi-log plots for the particles D1 to D4. Some of the velocity profiles display logarithmic behavior typical of turbulent flow shown by Eq. (5-2.29). The slopes, however are different than that observed in clear water flows. These semi-log plots display a continuous shift of the profiles to the right indicating increasing bed friction with concentration. Figure 5-29 shows the variation of κ with C_v calculated from Figures 5-25 to Figure 5-28. Although Figure 5-29 shows a large scatter, there is a decline in the value of κ with concentration.

Figure 5-25 Semi-log velocity distribution for particle D1

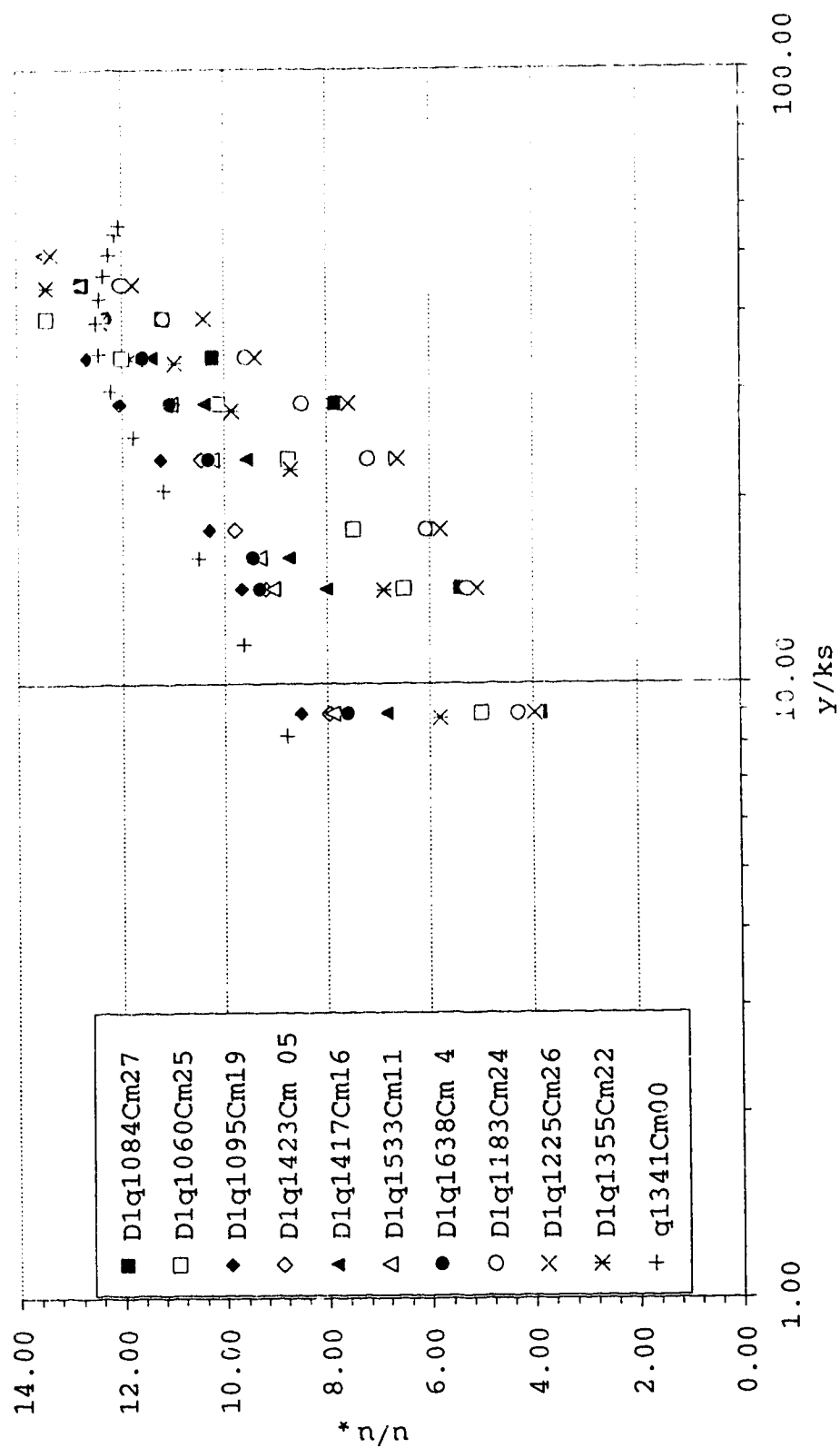


Figure 5-26 Semi-log velocity distribution for particle D2

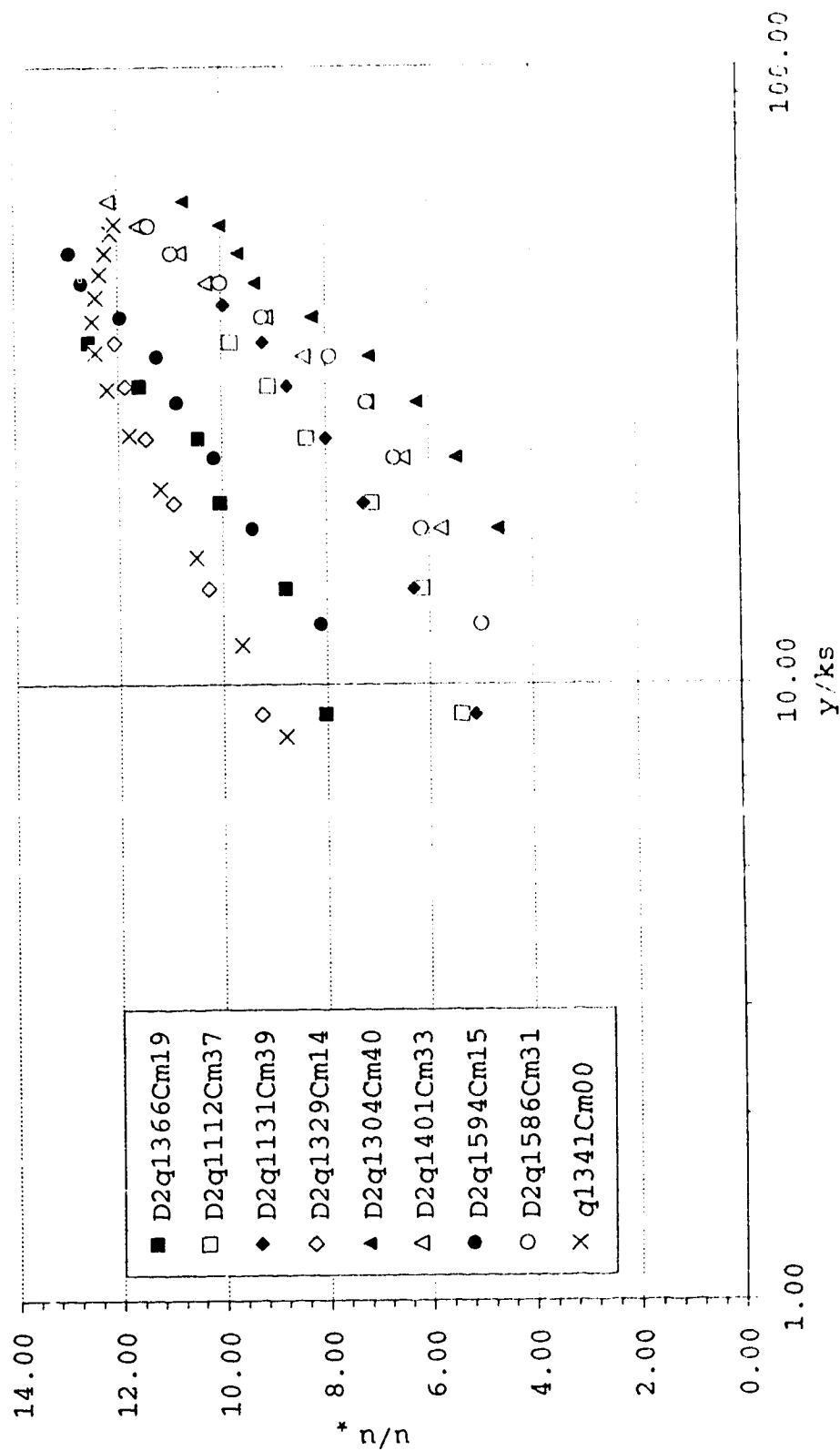


Figure 5-27 Semi-log velocity distribution for particle D3

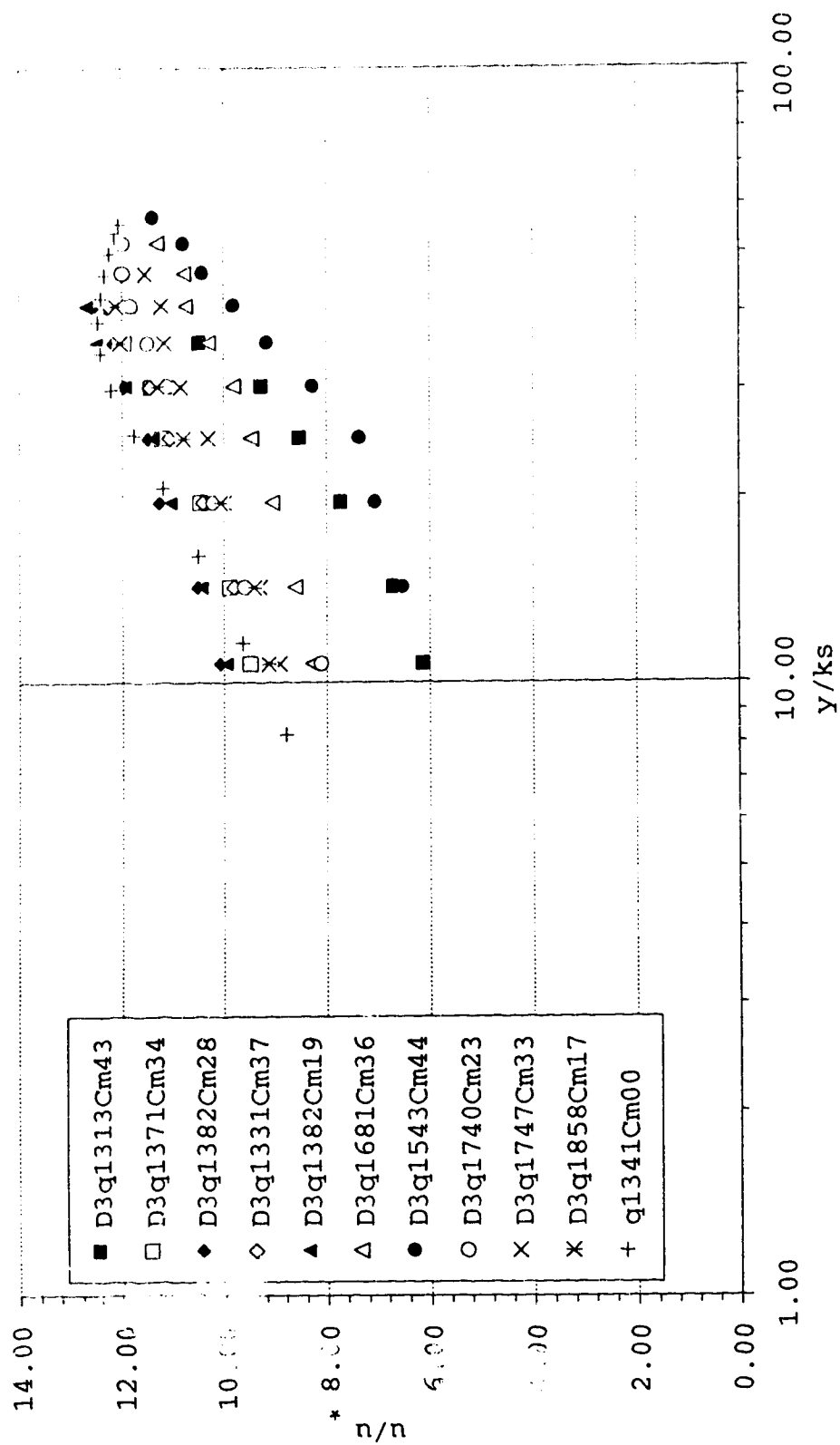


Figure 5-28 Semi-log velocity distribution for particle D4

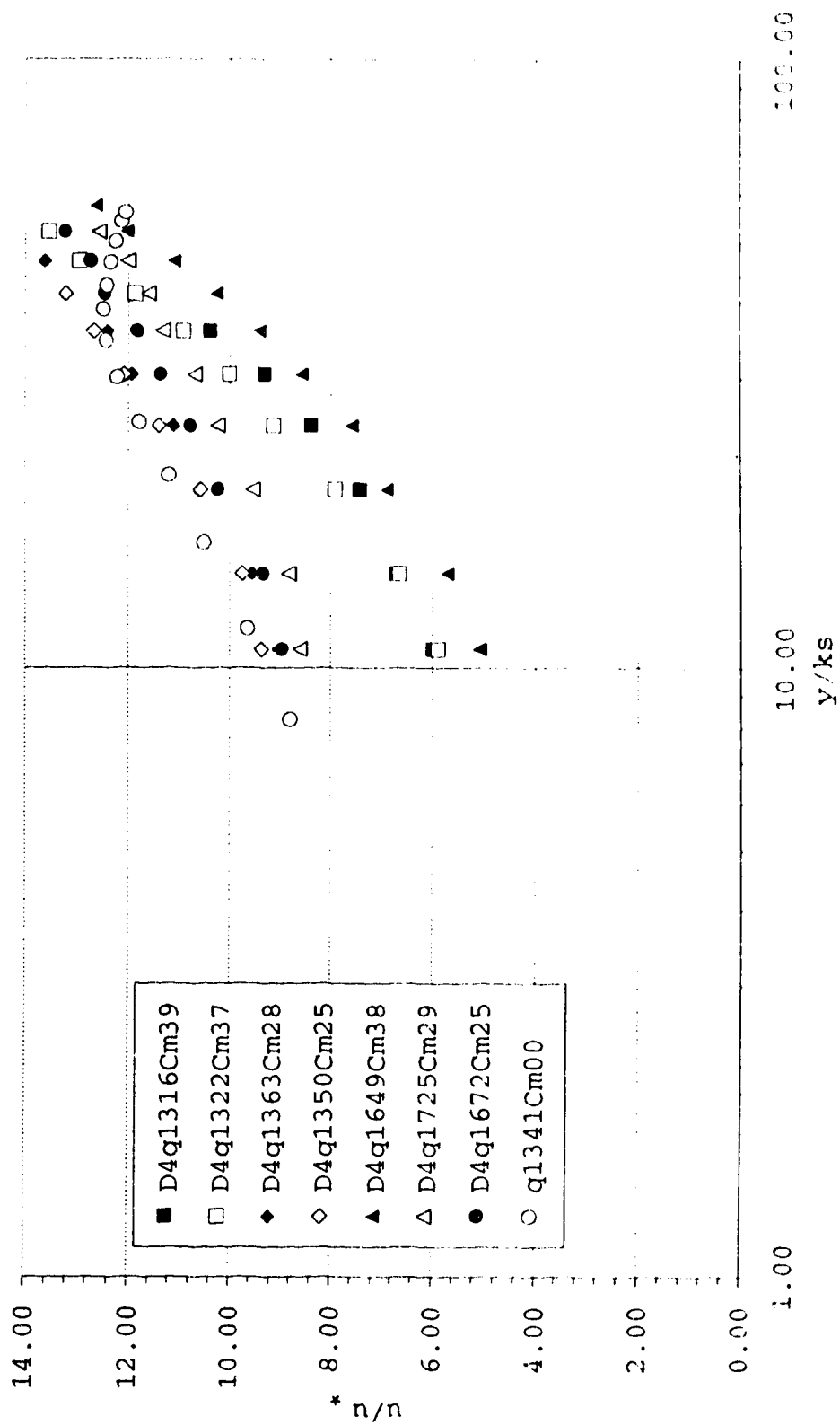
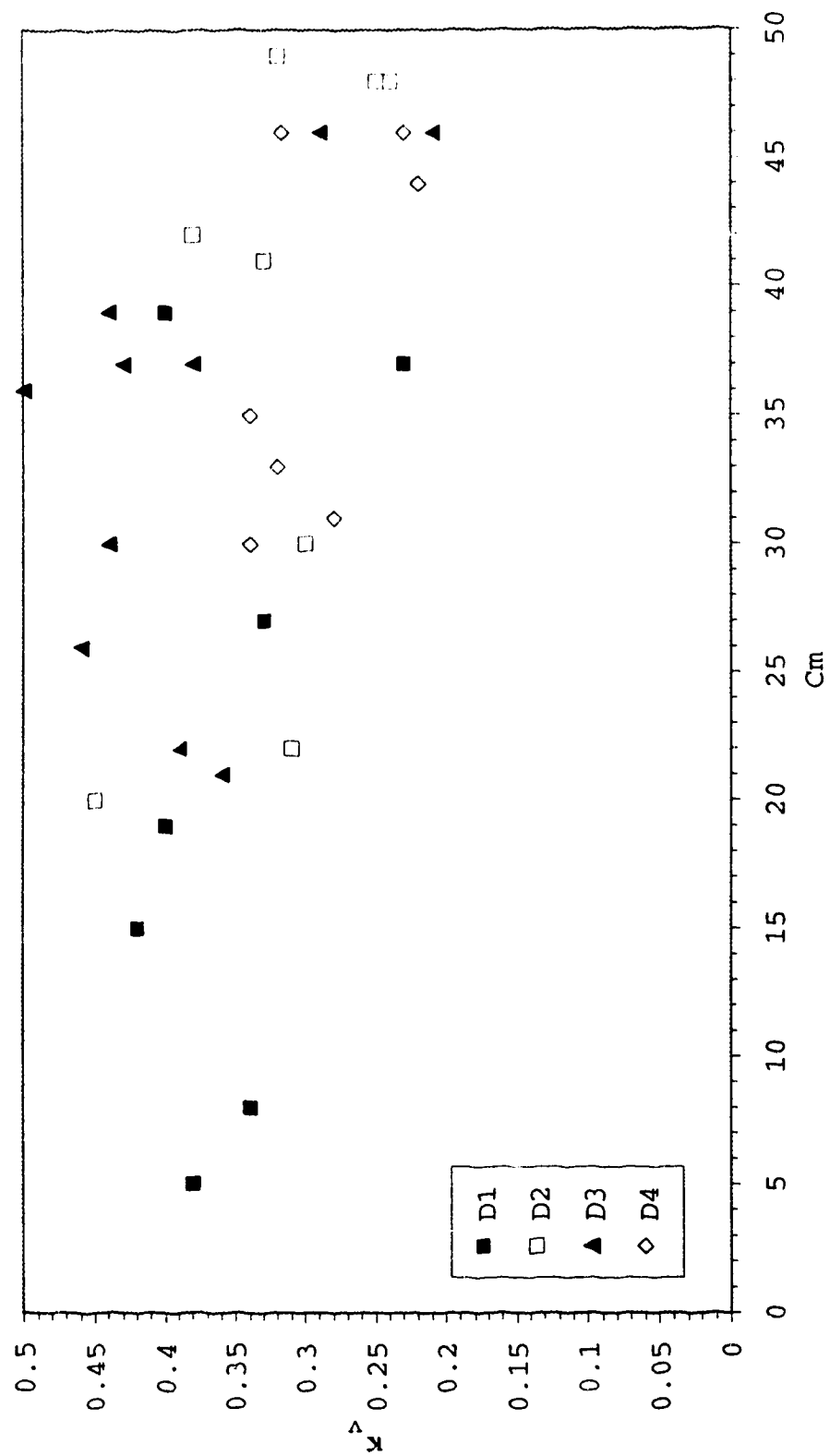


Figure 5-29 C_m vs von Karman's constant for high concentration flows



5.3.3 Concentration distribution

The concentration profiles for the large particle sizes (D1 and D2), although continuous in nature, display some stratification with a large mixing zone (Fig. 5-1b to Fig. 5-7b). For these cases, density stratification has the effect of suppressing turbulence which probably explains why the velocity profiles are linear at lower mean concentration (27% for D1 and 30% for D2) as compared to the finer particles (46% for D3 and 44% for D4). The dependence of particle size on stratification and turbulence suppression was also observed by Winterwerp et. al (1990).

In all the analyses presented so far the evidences indicate that the flows studied in the laboratory were turbulent. In other words, turbulence was mainly responsible for the dispersion of particles in the fluid. In order to further illustrate this, the vertical distribution of sediment particles given by Equation(3-2.31), according to Rouse(1937), is plotted together with the measured data in Figures 5-30(a-b) to 5-37(a-b). In Figures 5-30a to 5-37a the fall velocities have been calculated using the mean concentration for each of these profiles. As Rouse's equation is for small concentration, it fails to reproduce the shape of the measured concentration profiles. However, if the fall velocity due to hindered settling is considered as given by Equation(3-2.32), Rouse's equation is plotted in Figures 5-30b to 5-37b. These distributions show a better fit

Figure 5-30a Concentration distribution using Rouse's equation,
particle D1, group 6.45, channel centre

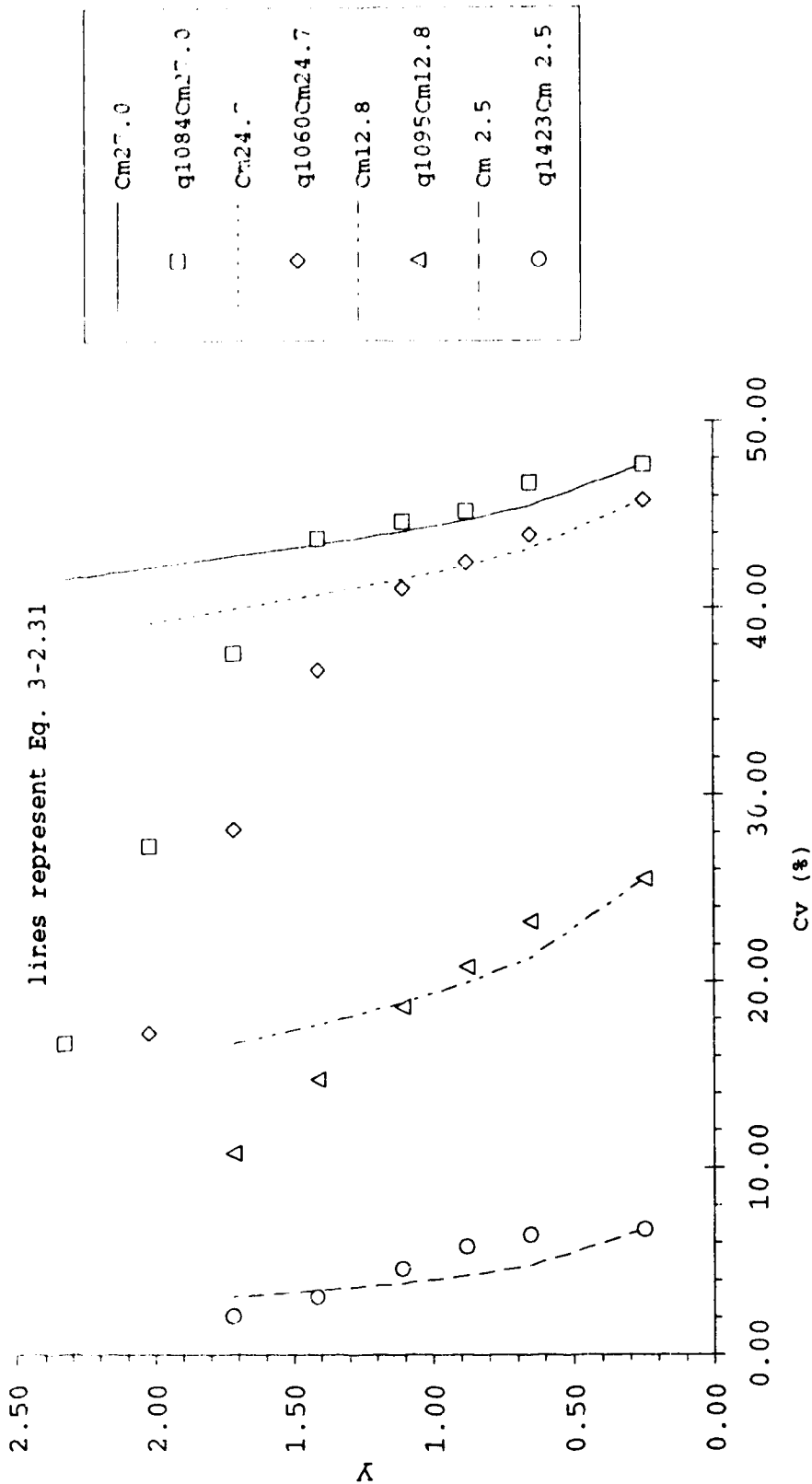


Figure 5-30b Concentration distribution using modified Rouse equation particle D1, group 6.45, channel centre

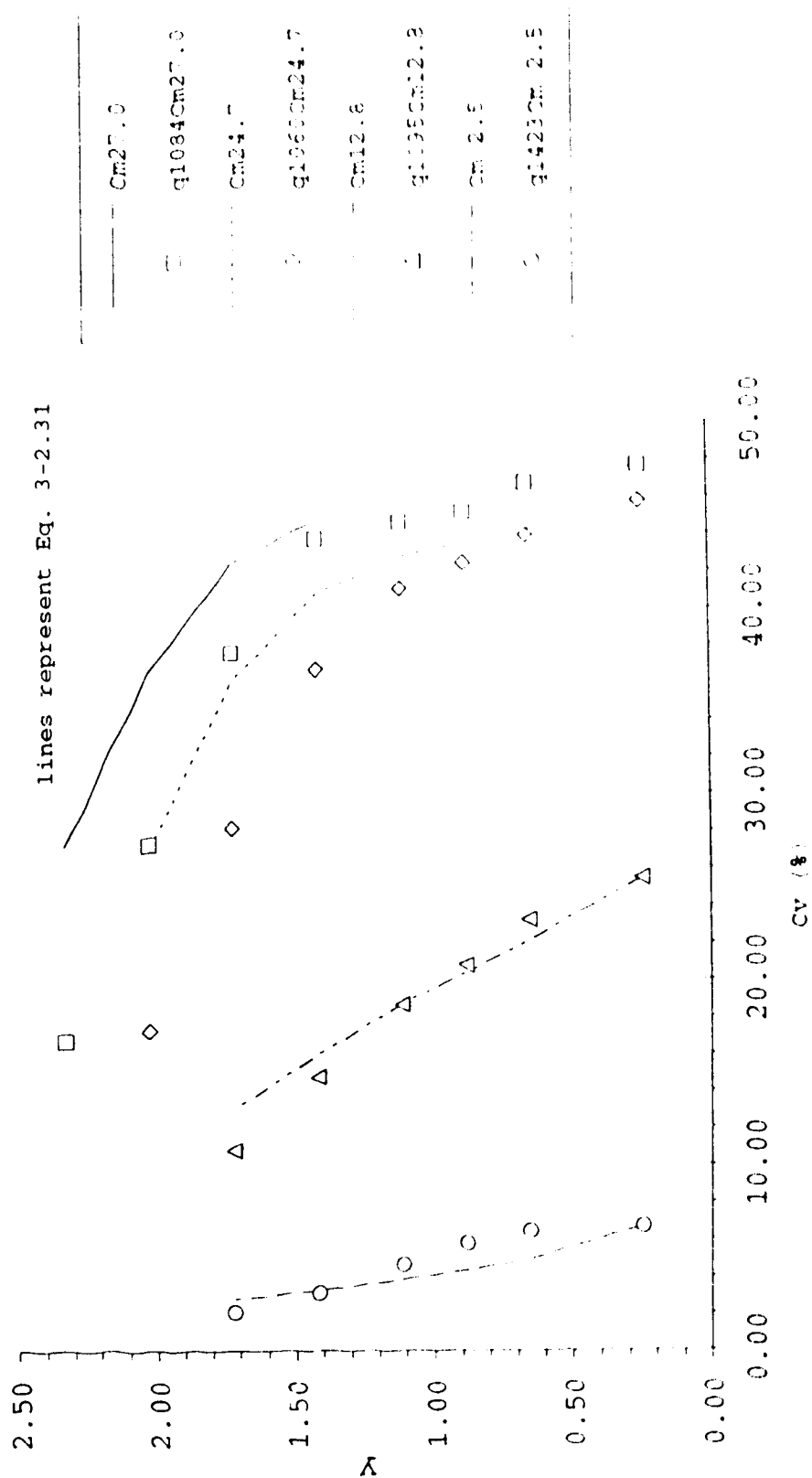


Figure 5-31a Concentration distribution using Rouse's equation,
particle D1, group 7.90, channel centre

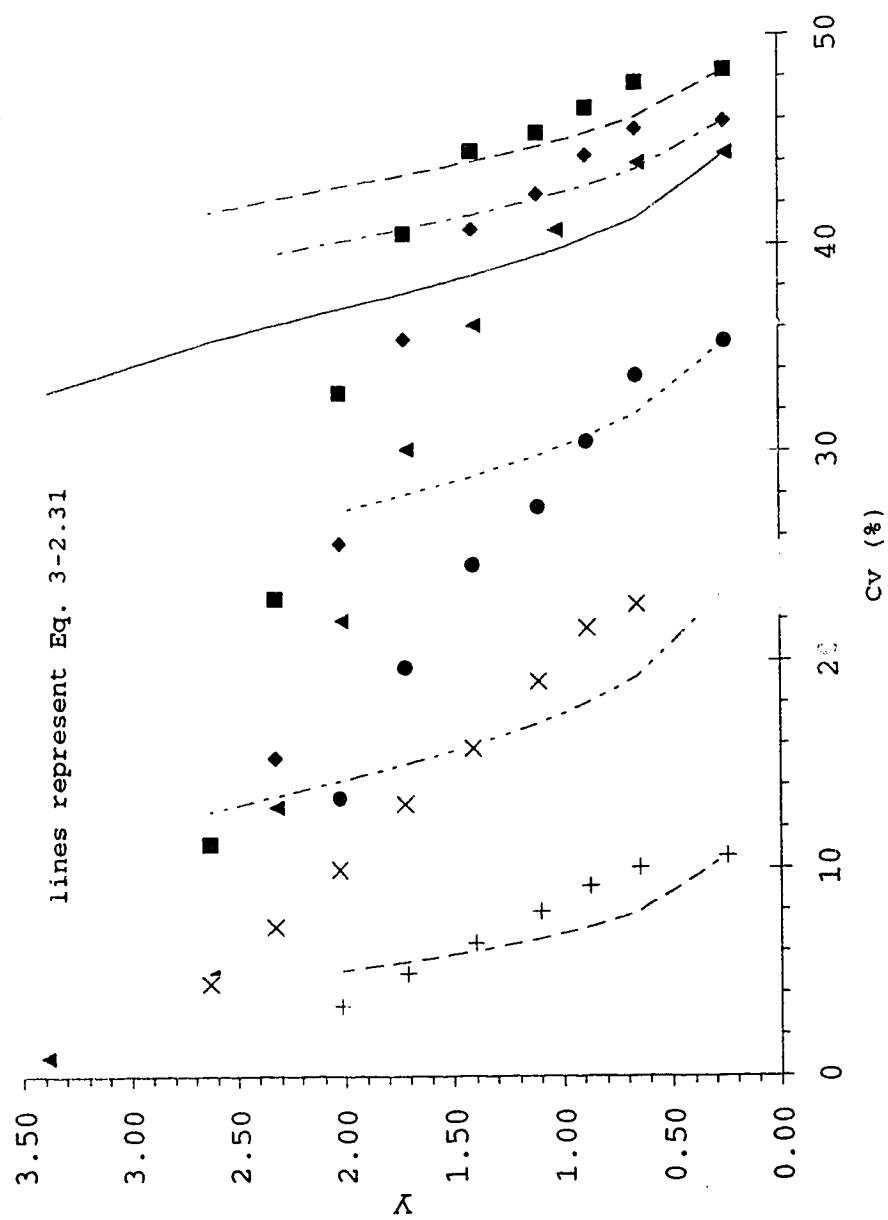


Figure 5-31b Concentration distribution using modified Rouse equation, particle D1, group 7.90, channel centre

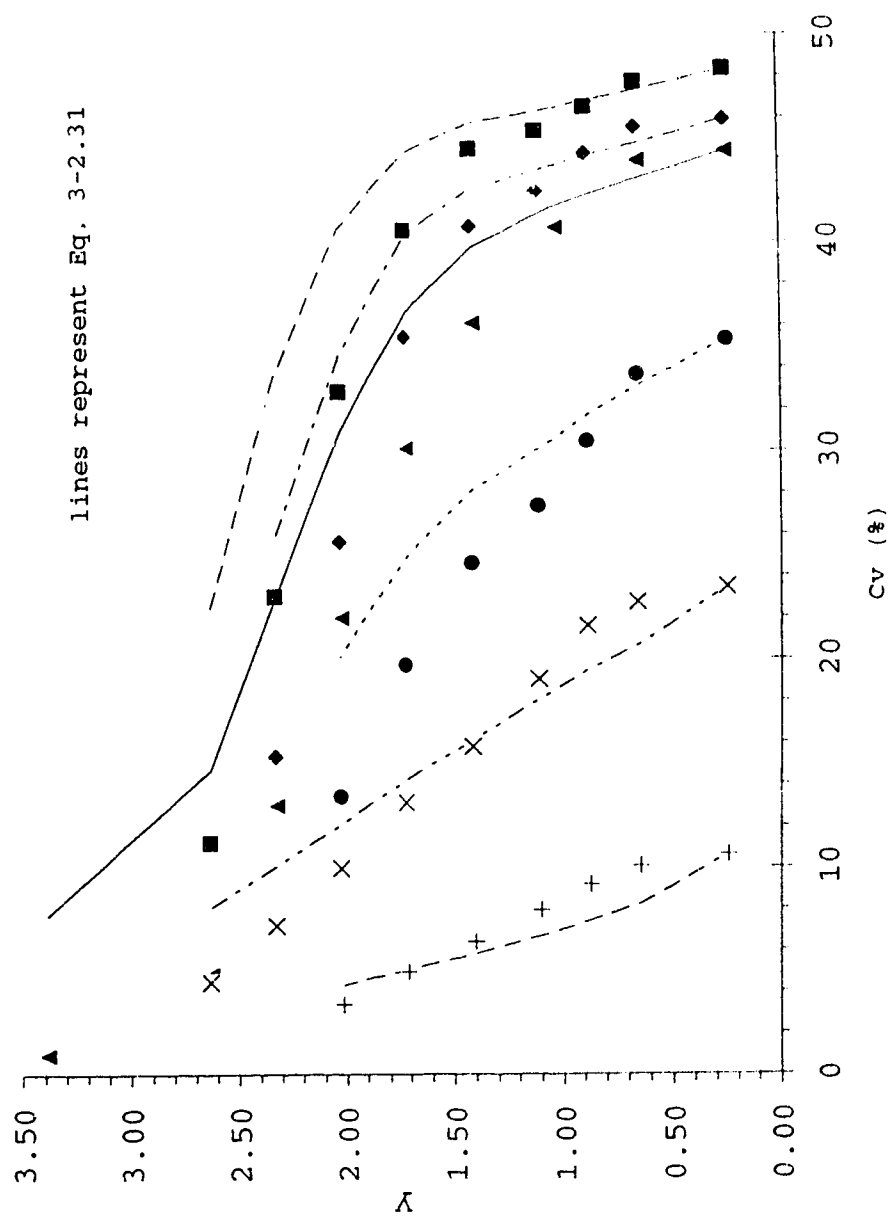


Figure 5-32a Concentration distribution using Rouse's equation,
particle D2, group 6.45, channel centre

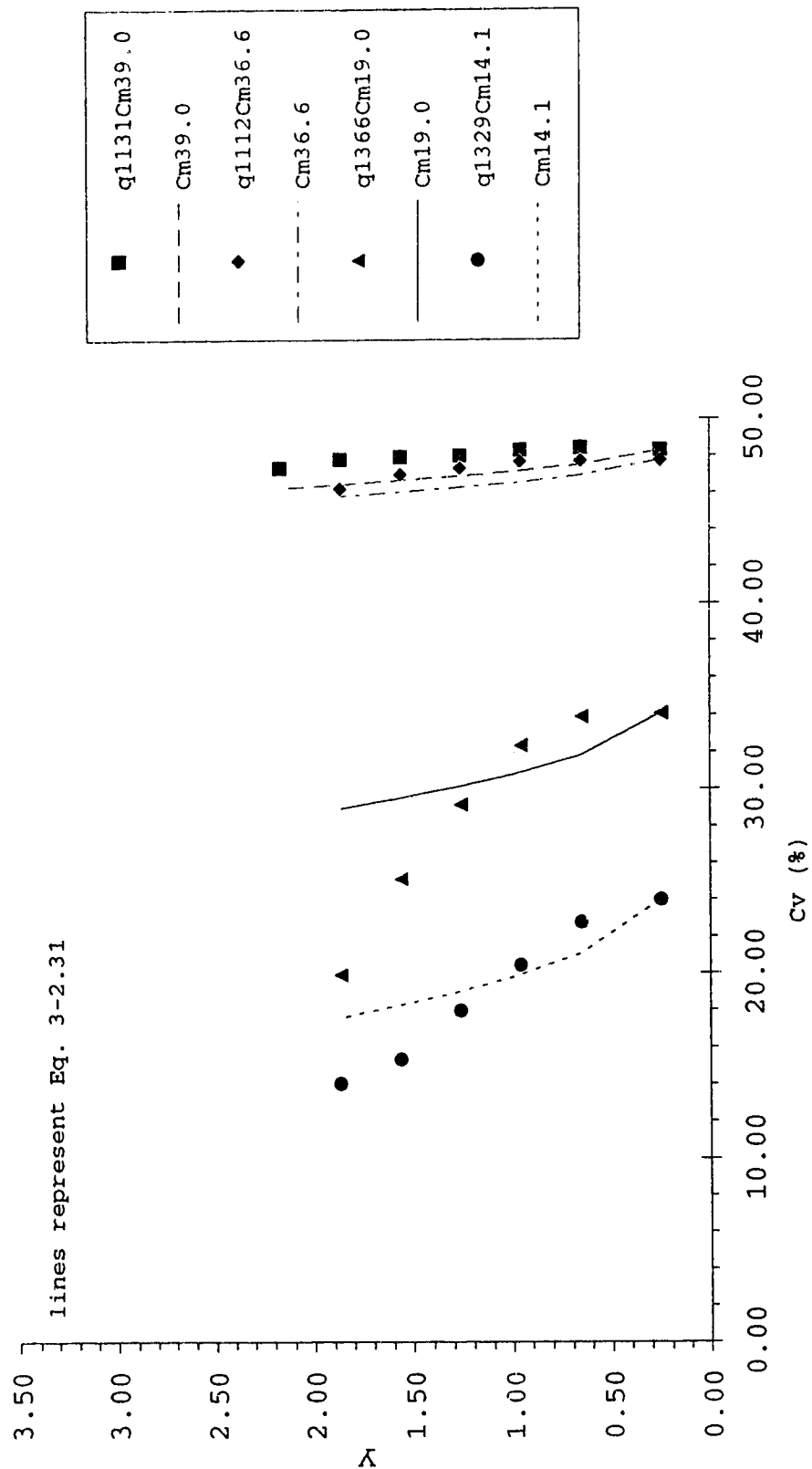


Figure 5-32b Concentration distribution using modified Rouse equation, particle D2, group 6.45, channel centre

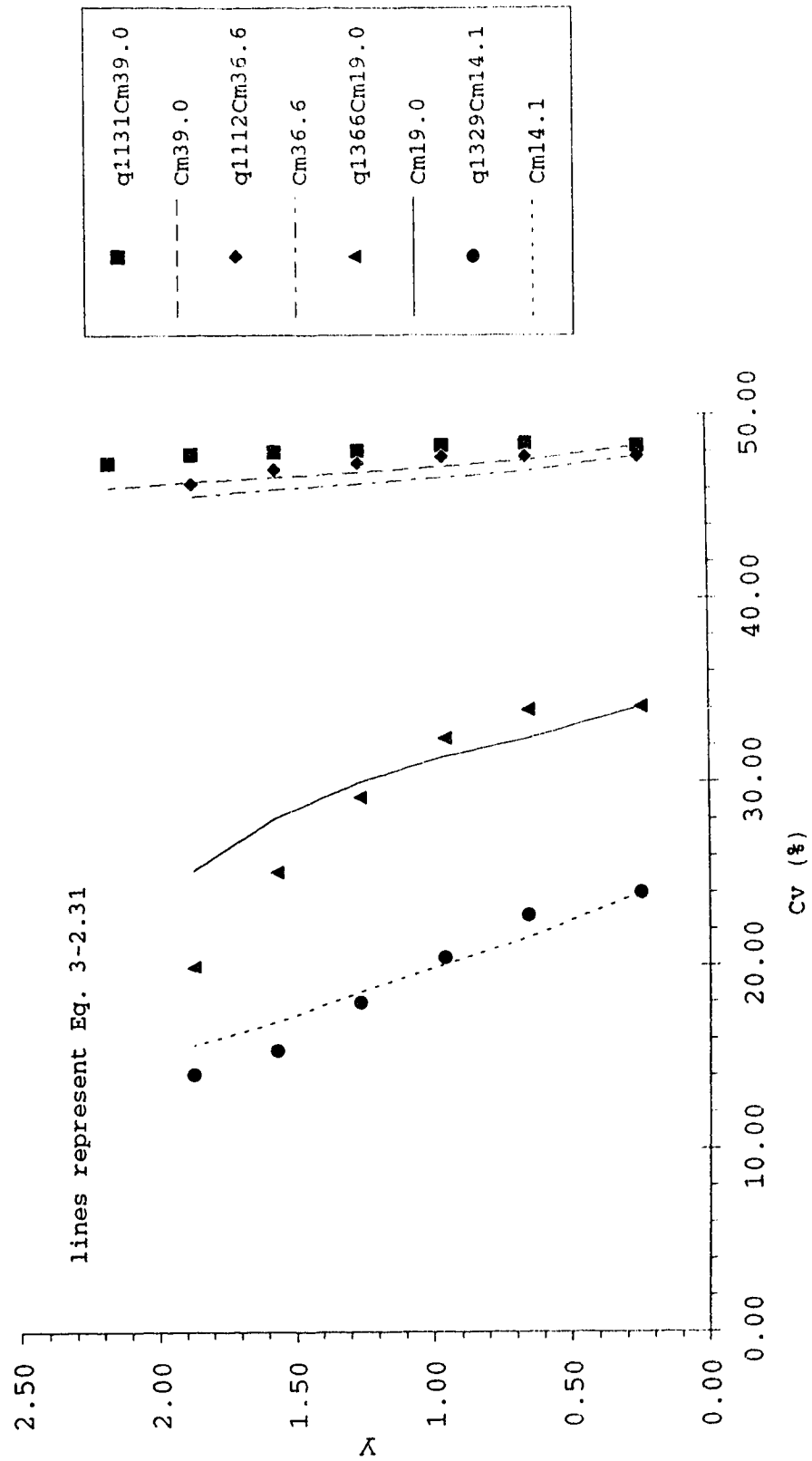


Figure 5-33a Concentration distribution using Rouse's equation,
particle D2, group 7.90, channel centre

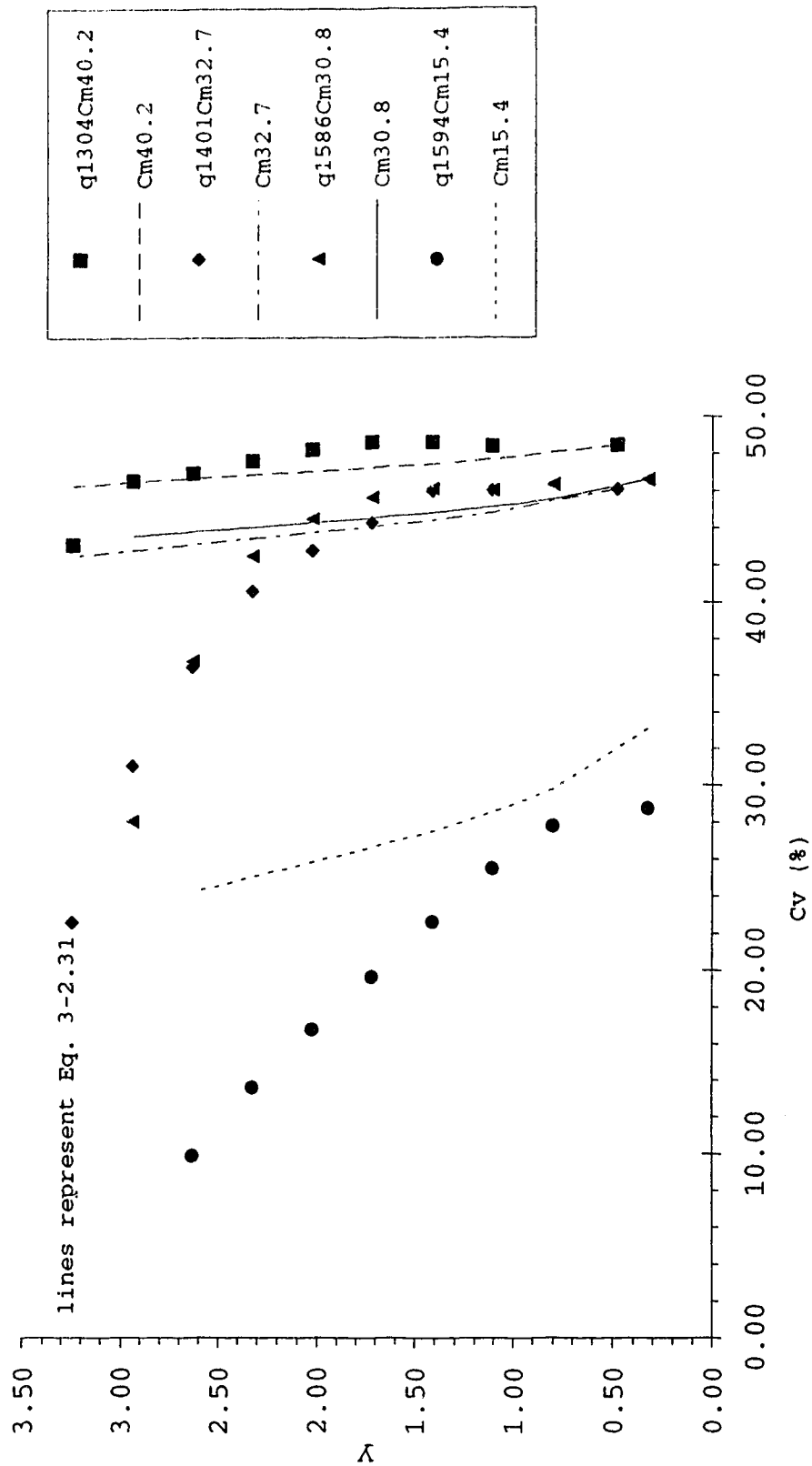


Figure 5-33b Concentration distribution using modified Rouse equation, particle D2, group 7.90, channel centre

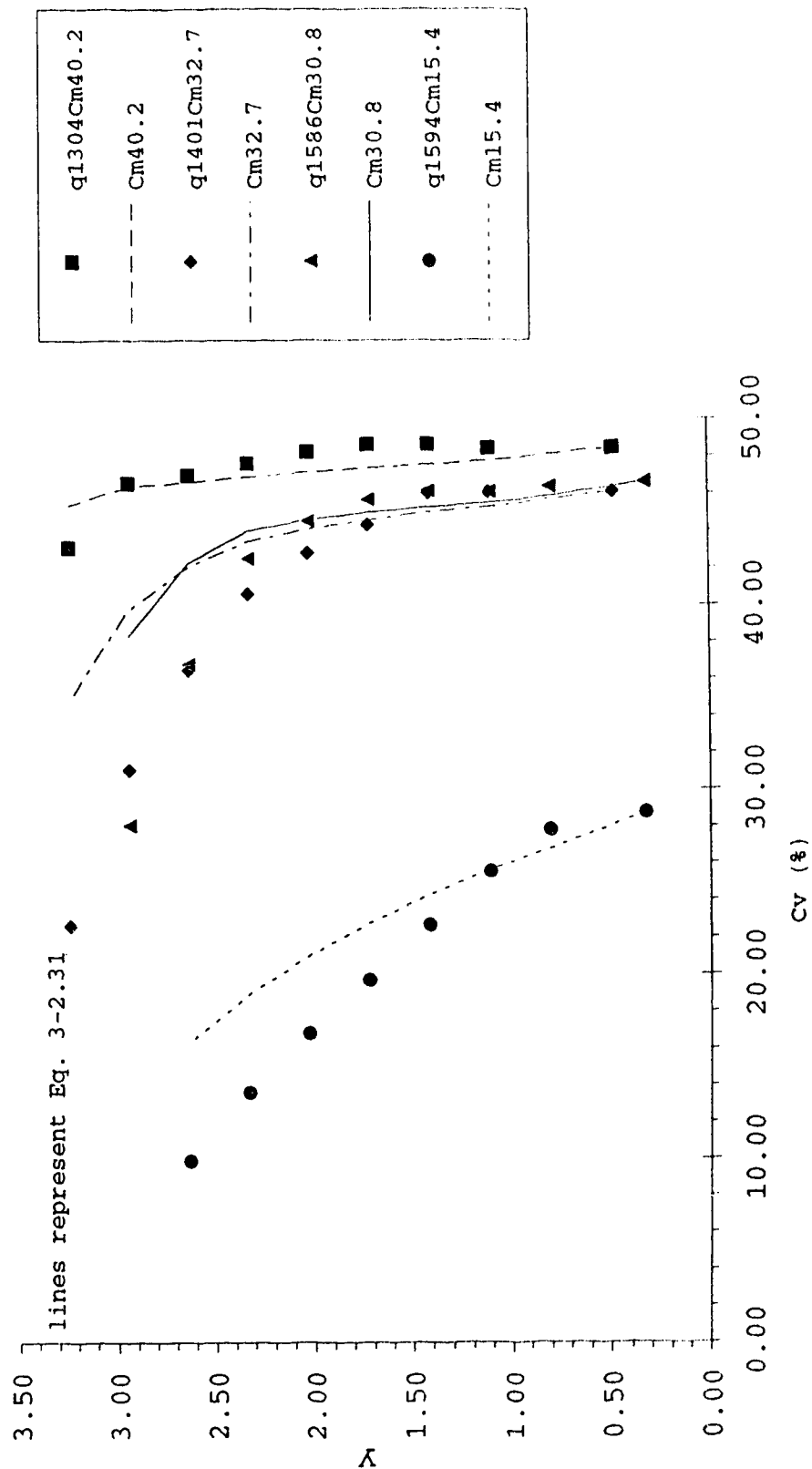


Figure 5-34a Concentration distribution using Rouse's equation,
particle D3, group 6.45, channel centre

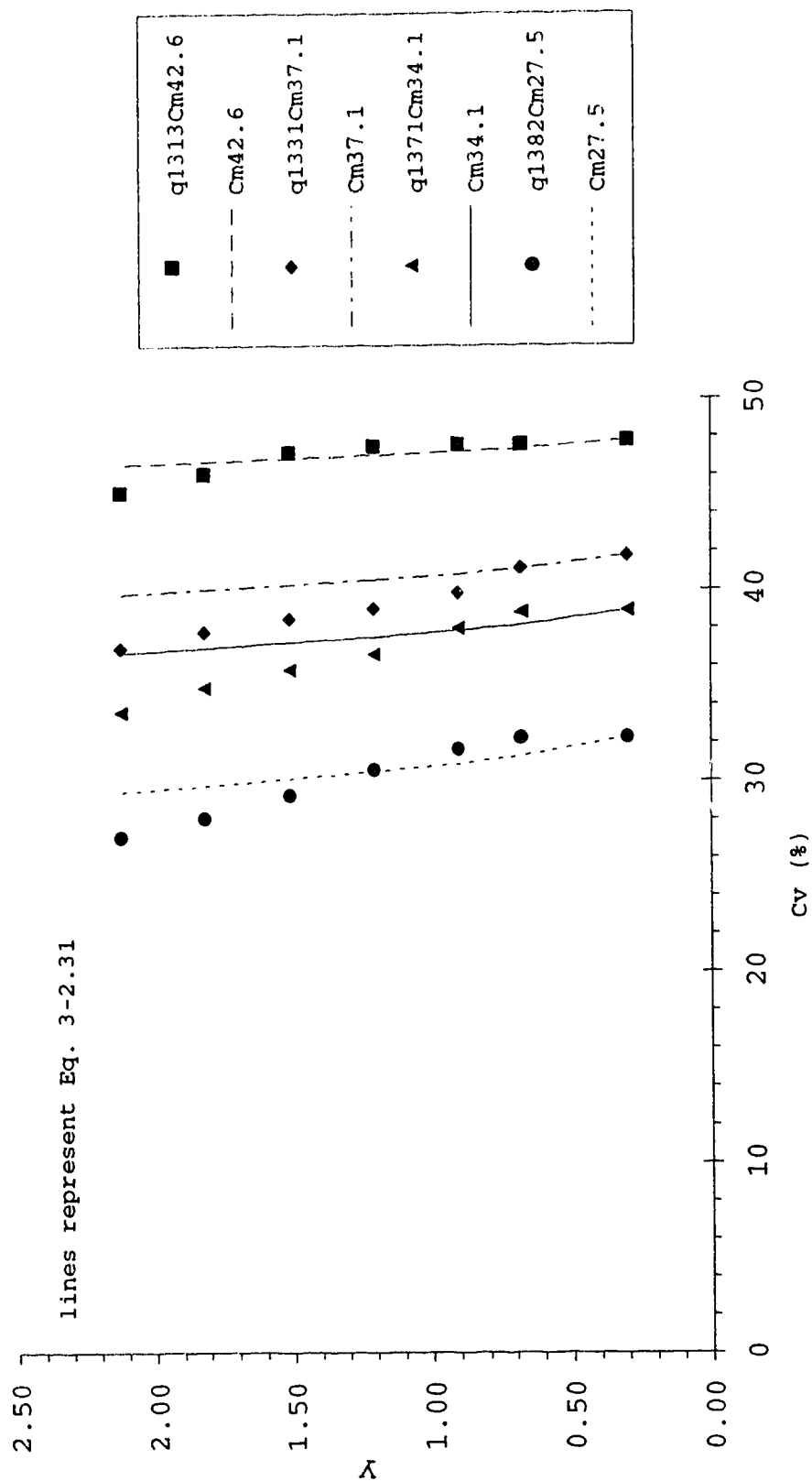


Figure 5-34b Concentration distribution using modified Rouse equation, particle D3, group 6.45, channel centre

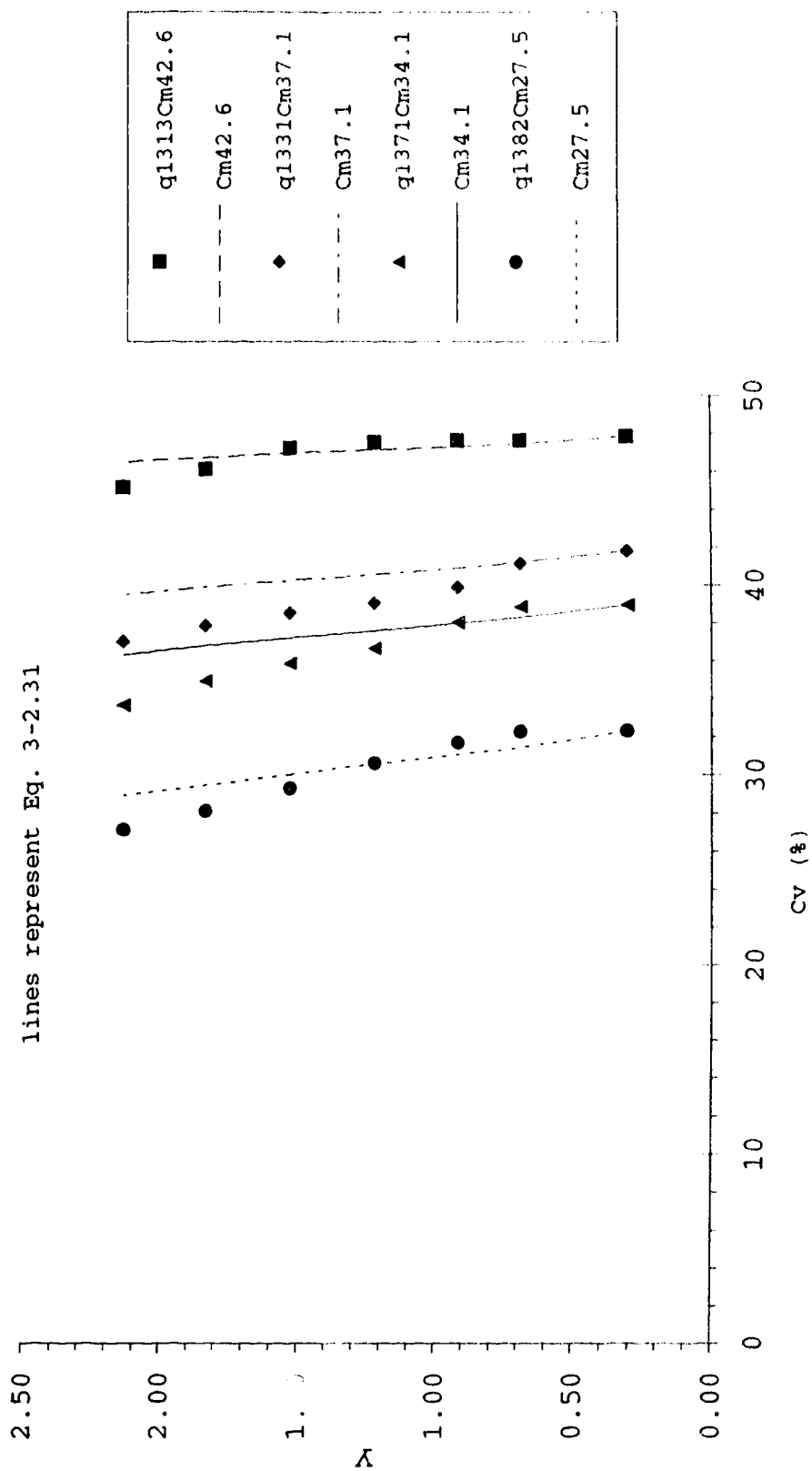


Figure 5-35a Concentration distribution using Rouse's equation,
particle D3, group 7.90, channel centre

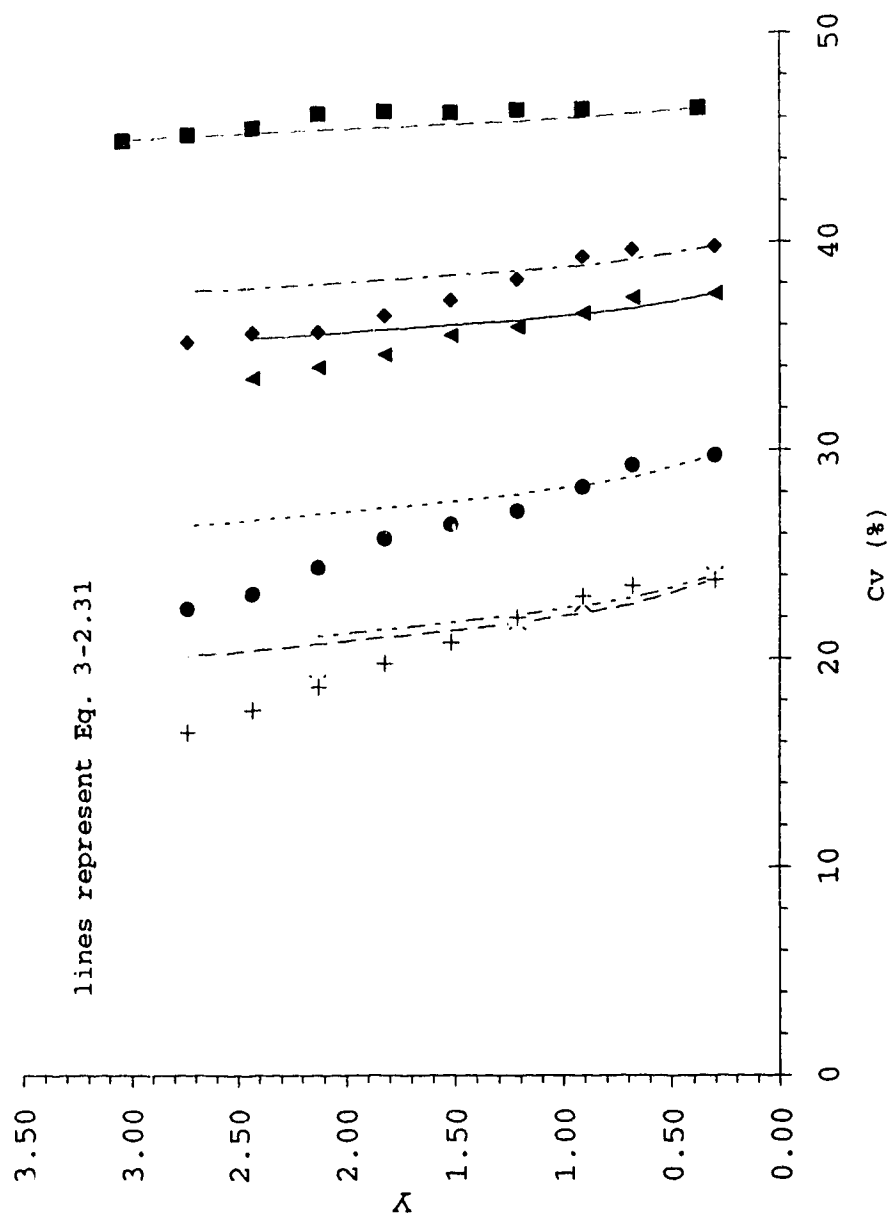


Figure 5-35b Concentration distribution using modified Rouse equation, particle D3, group 7.90, channel centre

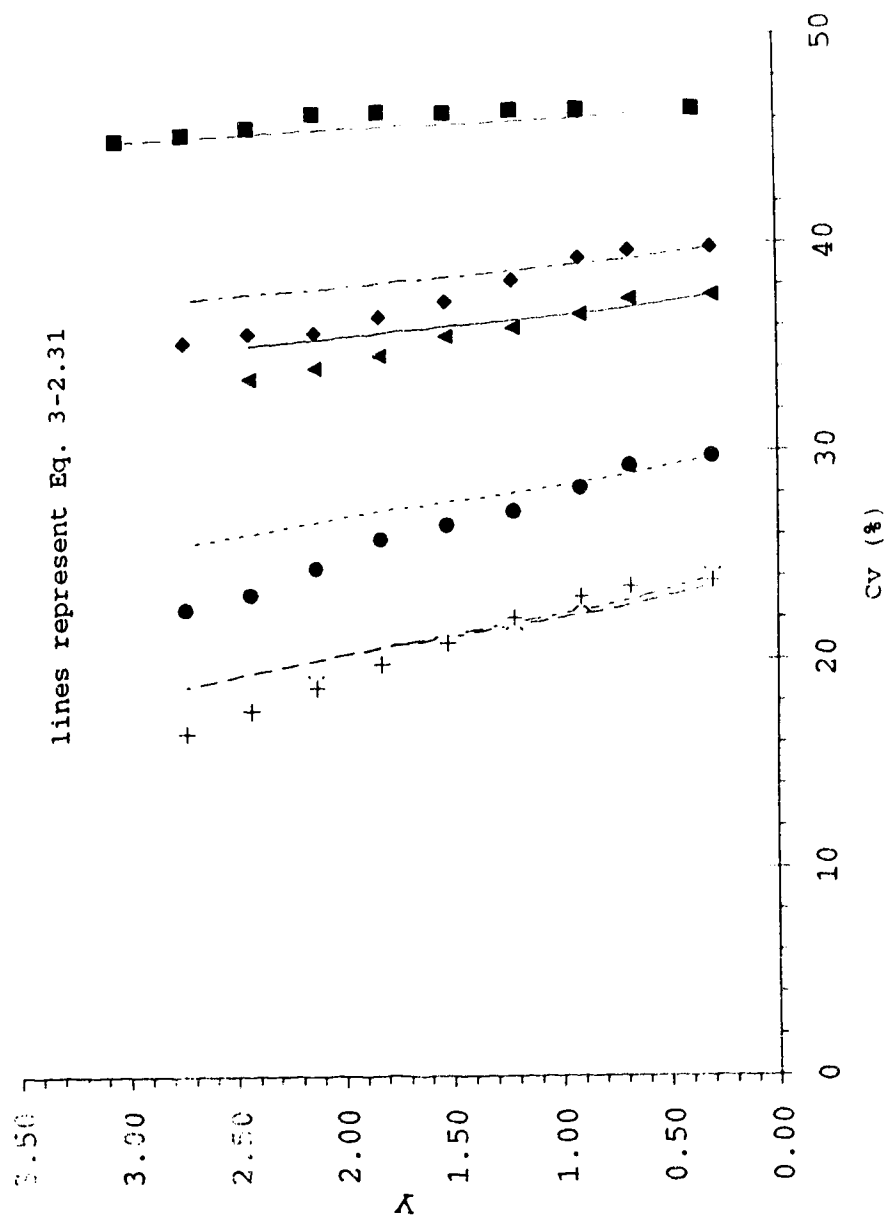


Figure 5-36a Concentration distribution using Rouse equation,
particle D4, group 6.45, channel centre

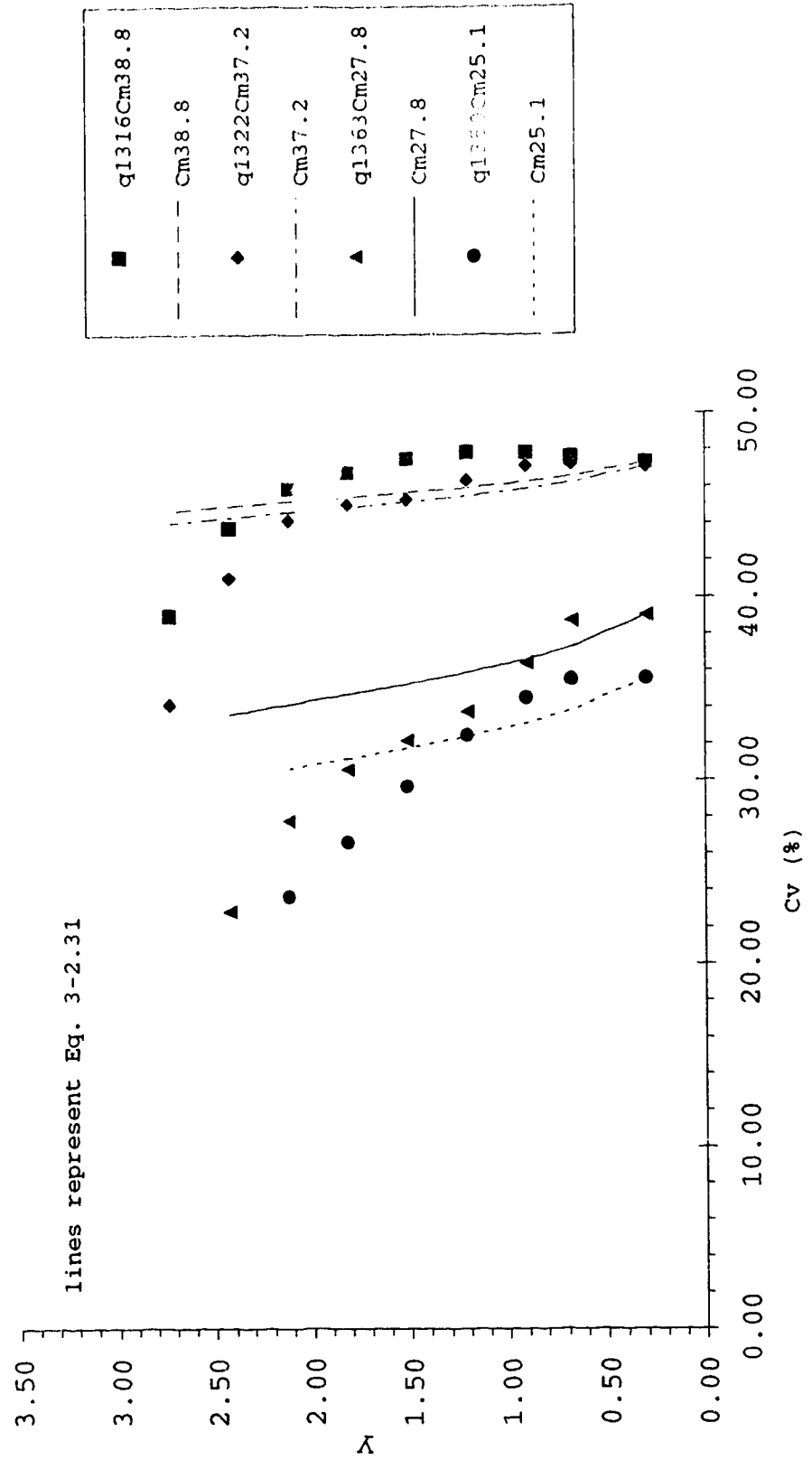


Figure 5-36b Concentration distribution using modified Rouse equation, particle D4, group 6.45, channel centre

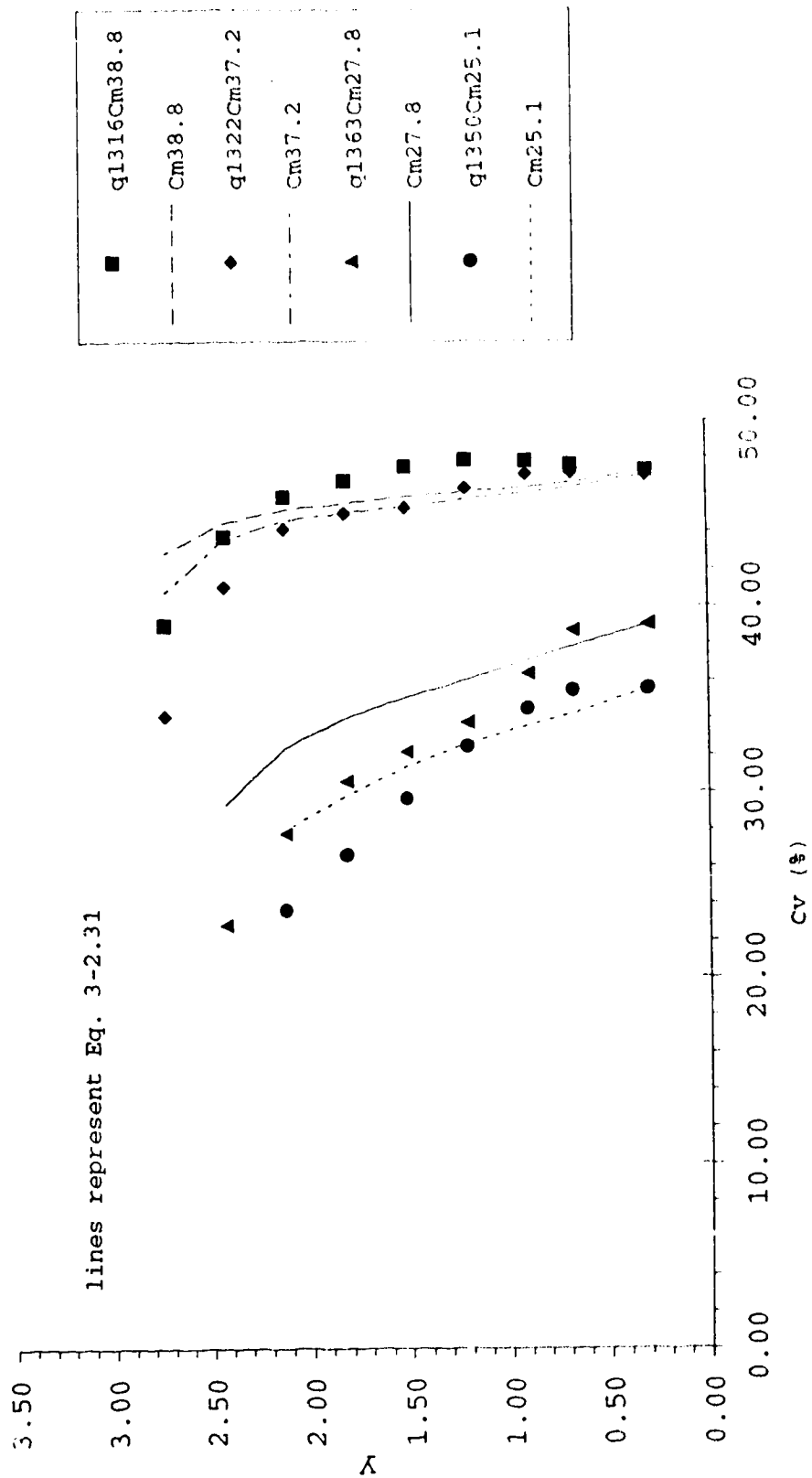


Figure 5-37a Concentration distribution using Rouse's equation,
particle D4, group 7.90, channel centre

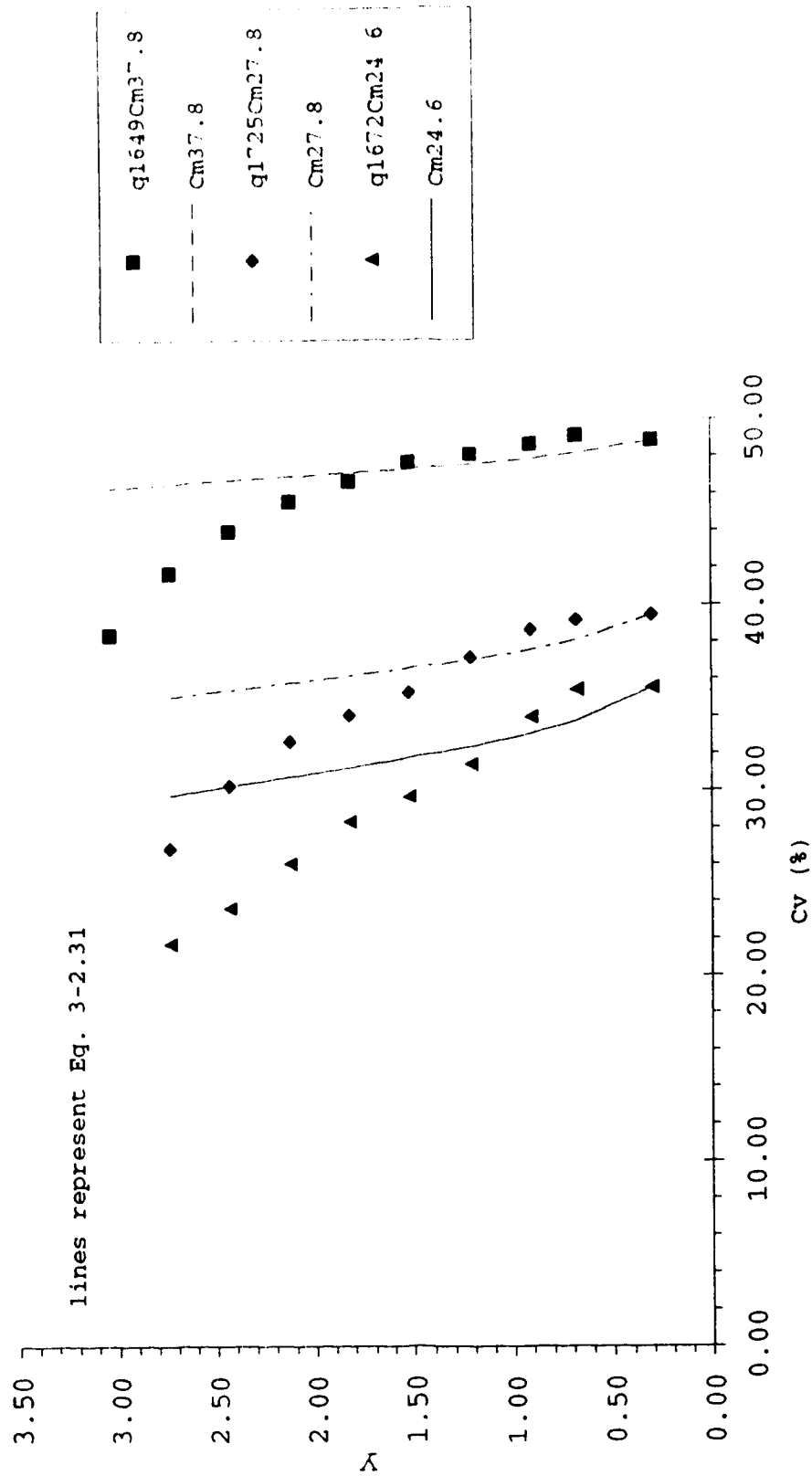
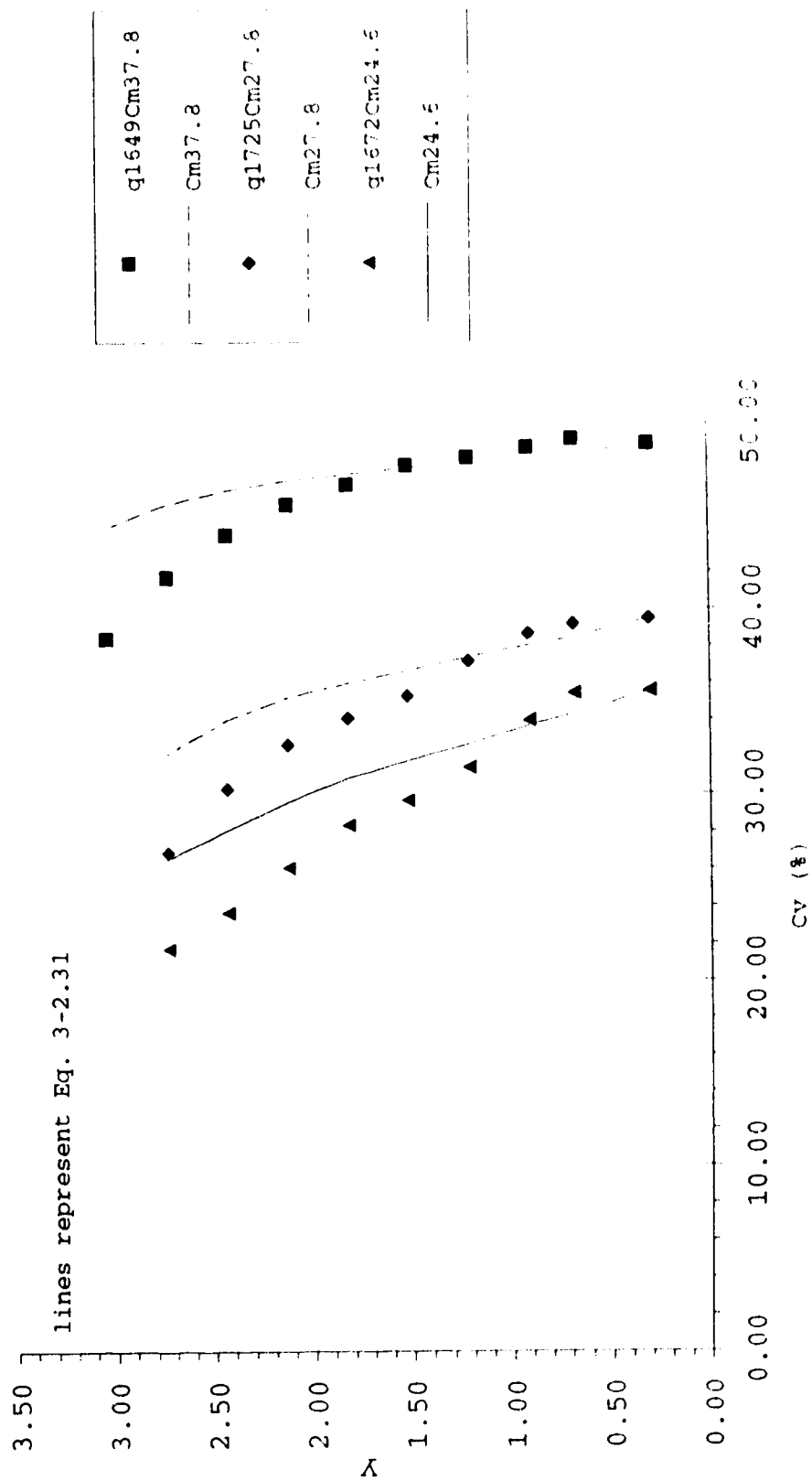


Figure 5-37b Concentration distribution using modified Rouse equation, particle D4, group 7.90, channel centre



of the measured concentration profiles. This exercise is merely to show that turbulent diffusion theory with some approximation is able to describe the measured quantities. The more suitable procedure would be to incorporate Equation(3-2.32) into (3-2.30) and solve the differential equation for the concentration distribution.

5.3.4 Manning's equation

The equivalent sand grain roughness for the bed in this study was 0.56mm. This was estimated from velocity distribution measurements made with water flowing in a wide channel with the sandpaper glued to the bed. The Manning's roughness n^* calculated using Equation(3-1.8) is 0.0112.

As discussed earlier, the flow of high concentration fluid in a channel has the effect of increased bed roughness. This was observed in the study of semi-logarithmic profiles Figures 5-25 to 5-28. Manning's roughness n^* can be calculated for the flows in the present study using Equation(3-1.7). Figures 5-38 and 5-39 show the variation of Manning's n^* with specific discharge q and the mean volume concentration C_v . Although n^* appears to scatter between 0.017 to 0.024, there is no obvious increase with q . However, n^* appears to increase slightly with C_v .

Figure 5-38 Mean Concentration Cv vs Manning's roughness coefficient n^* for sand water mixture, Slope 28.6*

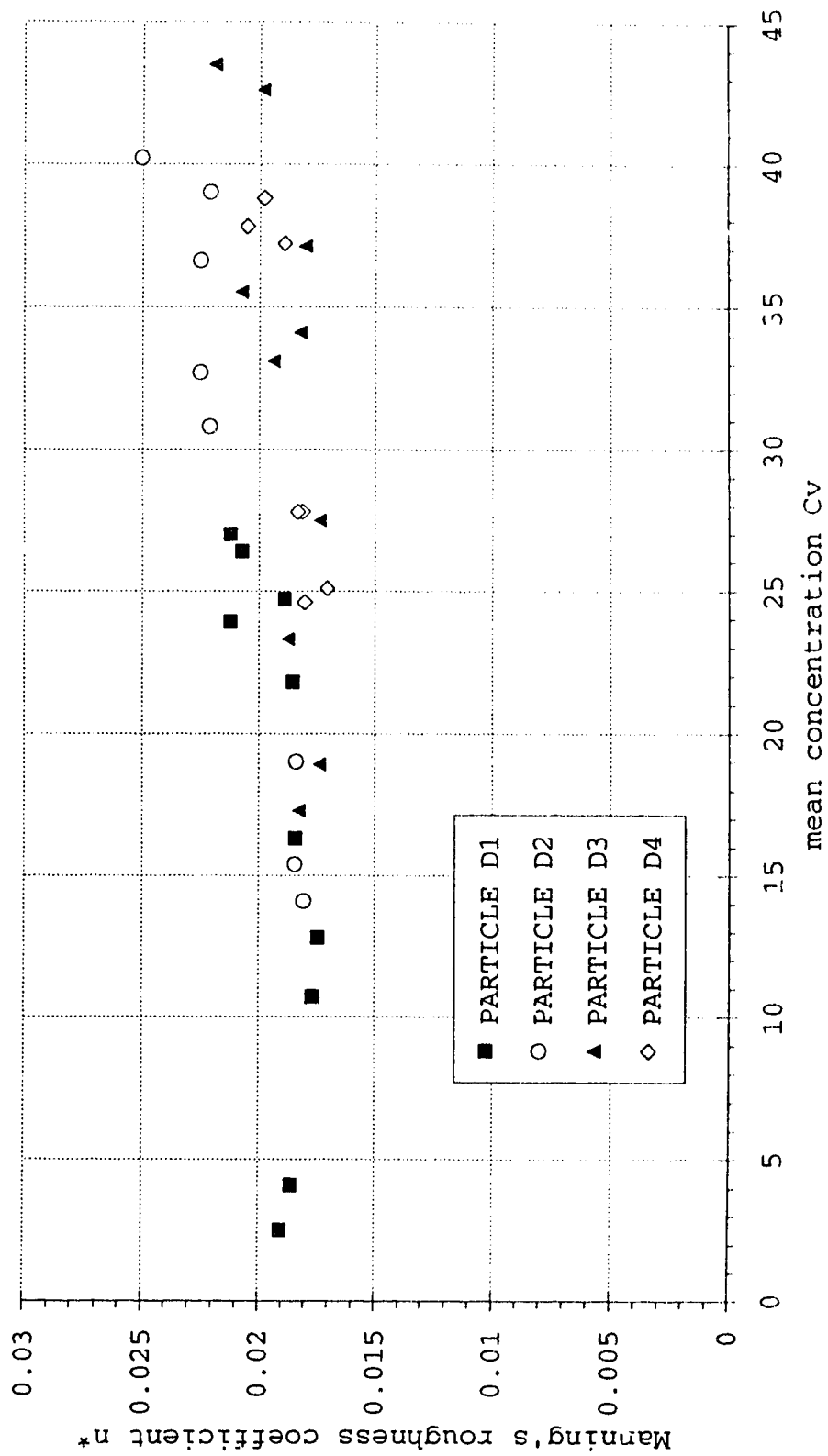
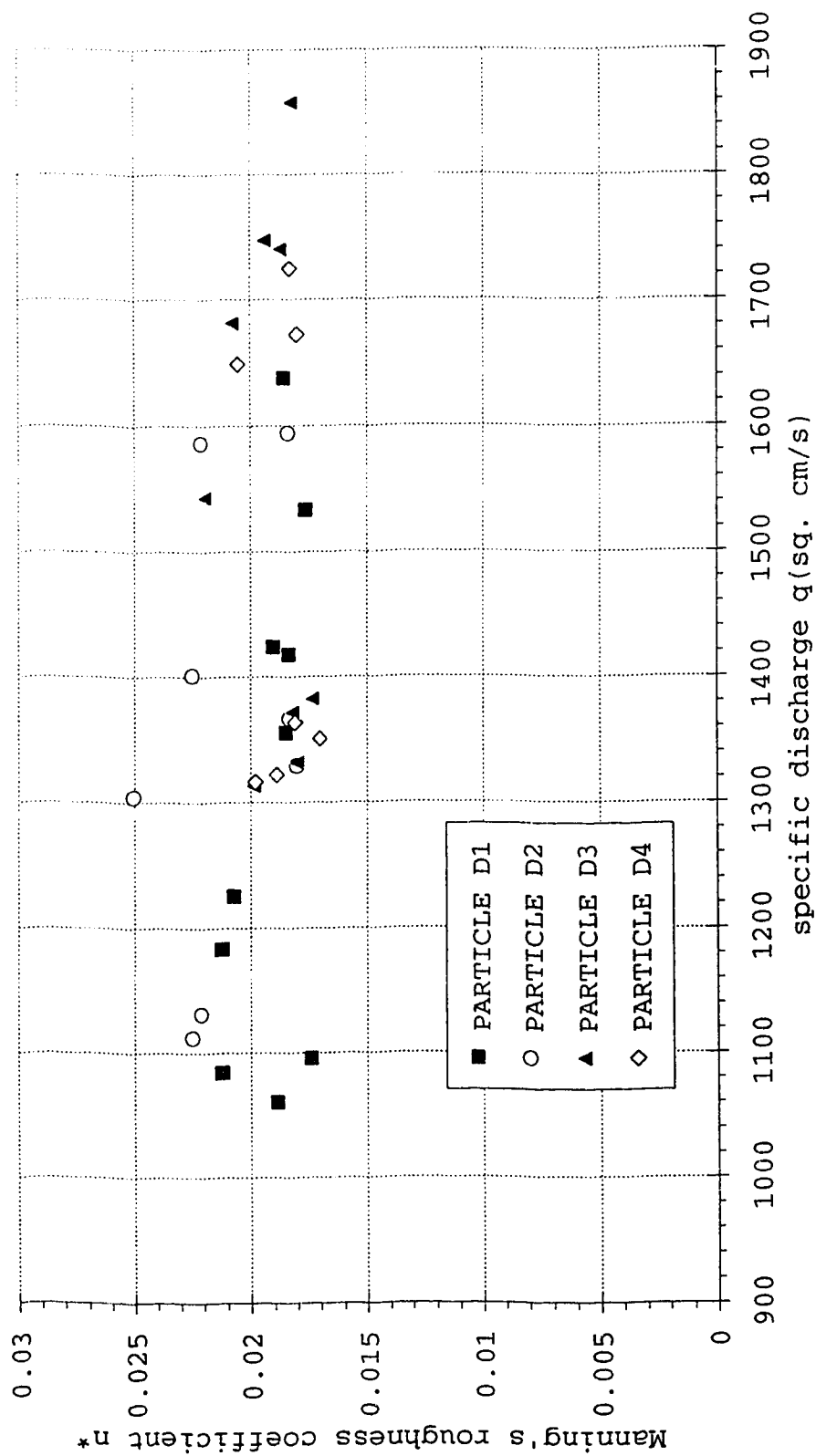


Figure 5-39 Specific discharge vs Manning's roughness coefficient n^* for sand water mixture, Slope 28.6*



6 DISCUSSIONS AND CONCLUSIONS

A review of the previous chapters in the field of debris flows shows that there still is a wide area of this field that needs more conclusive research. Though the physical process appears to be known well, there are many aspects of the mechanics of debris flow processes that still have to be understood better. The study of the mechanics of debris flows especially presents some difficulty in that it overlaps other areas like geomorphology, geology, hydrology, fluid flow, rock and soil mechanics in considerable detail. Key concepts from these areas as well as the mechanics of granular flows have to be understood well in order to explain debris flow mechanics to a satisfactory detail. The following areas of debris flow mechanics has attracted the attention of researchers for some time:

- i The particle support mechanism
- ii The reverse grading mechanism
- iii The development of constitutive relations
- iv The mechanics of debris flow in channels

Each of these areas can be examined by considering research from the standpoint of theoretical, experimental and field work.

6.1 Theoretical

Previous studies of the theoretical aspects of particle support mechanism and the reverse grading in debris flows have attempted to explain these processes with a few inconclusive theories among which some do merit considerable attention. However, further research is needed to identify more sound and conclusive explanations for these mechanisms.

The development of constitutive equations is one area of debris flow which has received considerable attention. Most attempts have focussed on rheologic approaches that are varying in their degree of complexity. The rheological approaches have resulted in equations that require a variety of parameters, the numbers and types of which depend on the the degree of complexity of the constitutive equations. These equations provide ample room for the determination of these parameters for a range of flow situations, if one desires. An alternate avenue of research that can be pursued is to investigate the use of simpler models and and their sensitivity when applied to channel flows. There is a need to incorporate the rheological formulations in the conservation equations in a compatible form such that the flow parameters that define resistance are represented realistically for the case of open channel routing. This leads to the next approach of research which is inevitable if any of these parameters are to be evaluated or tested.

6.2 Experimental

A review of previous works show that there is an extreme dearth of reliable experimental data against which some of the constitutive models that have been proposed can be tested. There is also a need for experiments to determine the different parameters like the viscosity and yield strengths. Experiments designed to provide a relation between the particle concentration and the flow parameters are essential. Other experiments that focus on the channel flow both on the straight and the curved reaches have yet to be investigated. The experimental aspect of the research of debris flow faces a bigger problem in the design of accurate measuring techniques as well as in representing actual flow situations in the laboratory without introducing the problems of scale effects. This needs careful study.

6.3 Field studies

This aspect of the research is probably more difficult to conduct than the above two. Debris flow events are episodic events and therefore considerable time may pass by before a researcher gets the opportunity to witness an actual event. This demands preparedness and, therefore, is expensive. As discussed earlier, a complete study of debris flow involves several areas of material science. Therefore,

research in this area is better accomplished by a joint effort of a multi-discipline-research team with a broad base of cooperation between the various groups.

Field data is invaluable in determining the accuracy of the mathematical models. Therefore, field measurements of velocity, discharge, concentration, yield, viscosity and particle size distribution are some of the measurements that are required. There is a need also for research in designing appropriate field measuring strategies as well as instruments for measuring these properties.

6.4 CONCLUSIONS

This study gives an overview of the present understanding in the field of debris flow. The need for measurements, either in the laboratory or the field, under a variety of conditions is identified. The difficulty in designing a measuring device which is suitable for the abrasive environment probably is one of the main reasons for this dearth in debris flow measurement.

The experimental portion of this study is presented in three stages. The first stage involves the setting-up of a continuous, high concentration sand-water mixture pumping system for generating a steady uniform flow. In the second stage a sampling device is developed to sample the mixture from the flow. Finally, this sampler is used to make

velocity and concentration distribution measurements in a open channel flow of sand-water mixture for four particle sizes and several mean particle concentrations. As the sampler was calibrated using water, there is sufficient room for the improvement in the calibration procedure of this measuring device.

The velocity profiles appear linear above a certain mean concentration which is strongly dependent on grain size. The influence of the velocity gradient in any particular flow, especially in a large mean concentration, appears to be less than that suggested by dilatant fluid models. Large Reynolds number suggests that the flows are turbulent which are also confirmed by some semi-logarithmic velocity profiles. The role of turbulence in dispersing the particles are more pronounced for smaller grain size (D3). The presence of the fines in the graded particles (D4) enhances dispersion. The shift in the semilogarithmic profiles with increasing mean concentration is reminiscent of rough turbulent flows with increasing roughness. Preliminary results show a gradual decline in the value of k from the clear water value with increasing concentration. The concentration profiles are similar, more uniform and show less scatter for the finer grain size and the graded particles. For the larger particles there is a tendency towards stratification resulting in the suppression of turbulence.

The vertical shear stress approaches a linear distribution as the concentration profiles become uniform. Otherwise the distribution displays some curvature.

CITED REFERENCES

- Ackermann, N. L., Shen, H. (1982) Stresses in rapidly sheared fluid-solid mixtures, *J. Eng. Mech. Div. ASCE* 108, pp. 95-123.
- Arai, M. and Takahashi, T. (1983). A method for measuring velocity profiles in mud flows, *Proc. of 20th IAHR Congress*, vol.3, pp. 279-286.
- Arai, M. and Takahashi, T. (1986) The Karman constant of the flow laden with high sediment, Third International Symposium on River Sedimentation, Univ. of Mississippi, pp. 824-833.
- Bagnold, R. A., (1954) Experiments in a gravity-free dispersion of large solid spheres in a Newtonian fluid under shear, *Proc. Royal Soc. London, Ser A*, Vol 225, pp. 49-63.
- Beverage, J. P. and J. K. Culbertson, (1964) *Hyperconcentrations of suspended sediments*, ASCE vol 90, HY 6, pp. 117-128.
- Bevington, P. R., (1969) Data Reduction and error analysis for the physical sciences, McGraw-Hill.
- Blackwelder, E., (1928) Mudflow as a geologic agent in semiarid mountain, *Bull. Geol. Soc. Am.*, vol. 39, pp. 465-487.
- Bradley, J. B. & S.C. McCutcheon, (1985) The effects of high sediment concentration on transport processes and flow phenomenon, *Proceedings, International Symposium on Erosion, Debris Flow and Disaster Prevention*, Tsukuba, Japan, pp. 219-225.
- Broscoe, A. J. & S. Thompson, (1969) Observations on an alpine mudflow, Steele Creek, Yukon, *Canadian Journal of Earth Sciences*, vol. 6.
- Chen, C. L., (1983) On frontier between rheology and mud flow mechanics, *Proceedings on the 1983 Hydraulic Division Specialty Conference on Frontiers in Hydraulic Engineering*, ASCE, MIT, Cambridge, MA pp. 113-118.
- (1985a) Present status of research in debris flow modelling, *Proceedings of the 1985 Hydraulic Division Specialty Conference of Hydraulics and Hydrology in Small Computer Age*, ASCE, Lake Buena Vista, Florida pp. 733-741.

- (1986) Chinese concepts of modelling hyperconcentrated streamflow and debris flow, *Third International Symposium on River Sedimentation, The University of Mississippi*, pp. 1647-1657.
 - (1987) Comprehensive review of debris flow modelling concepts in Japan., *Geol Soc. Am., Reviews in Engineering Geology vol VII*, pp. 13-29.
 - (1988a) Generalized Viscoplastic modelling of debris flow, *Transc. ASCE*, vol. 114, No.3, pp. 237-258.
 - (1988b) General solutions for viscoplastic debris flow, *Transc. ASCE*, vol. 114, No.3, pp. 259-279.
 - (1988c) Issues in debris flow research-personal views, *U.S. Geological Survey Water Supply Paper Series Selected Papers in Hydrologic Sciences*, WSP 2340.
- Chi-Hai Ling, Cheng-lung Chen, and Chyan-Deng Jan, (1990), Rheological properties of simulated debris flows in the laboratory environment, *Hydraulics/ Hydrology of Arid Lands, Proceedings of the International Symposium, San Diego, ASCE*, (ed) Richard French, July 30-August 2, pp.218-224.
- Church, M. & M. J. Miles, (1987) Meteorological antecedents to debris flow in Southwestern British Columbia; some case studies, *Reviews in Engineering Geology*, vol. VII, *geol Soc of Am.* pp. 63-79.
- Costa, J. E., (1984) Physical geomorphology of debris flows, *Developments and Applications of Geomorphology*, Ed. J. E. Costa & P. J. Fleisher, pp. 268-317.
- Cruden, D. M. and J. Krahn, (1978) *Frank Rockslide, Alberta, Canada, Rockslides and Avalanches*, Voight. B., Ed., Elsevier, vol. 1, pp. 97-112.
- Curry, R. R., (1966) Observations of alpine mudflows in the Tenmile Range, Central Colorado, *Bull. Geol. Soc. Am.*, vol. 77, pp. 771-776.
- Davies, R.H., (1986) Large debris flows: A macroviscous phenomenon, *Acta Mechanica* 63, pp. 161-178.
- Davies, R.H., (1988) Debris flow surges - a laboratory investigations, *Mitteilungen der Versuchsanstalt fur Wasserbau, Hydrologie und Glaziologie, Zurich*

- Davis, R.H., Serayssol, J-M. and Hinch, E. J. (1986) The elastohydrodynamic collision of two spheres, *J. Fluid Mech.*, 163, pp. 479-497.
- DeLeon, A.A, & R. W. Jeppson, (1982), *Hydraulics & numerical solutions of steady-state but spatially varied debris flow*, report, *Utah Water Research Laboratory, Logan, Utah.*
- De Matos, M., (1987) *Mobility of Rock Soil and Rock Avalanches*, Ph. D. thesis, Department of Civil Engineering, -University of Alberta, Edmonton, Alberta.
- Do Ik Lee, (1969) The viscosity of concentrated suspensions, *Transactions of the society of Rheology*, vol. 3, No. 2, pp. 273-288.
- Eilers, H., (1941) *Kolloid Z.*, vol. 97, p313
- Einstein, A., (1906), Eine neue bestimmung der molekuldimensionen, *Annslen der Physik, Leipzig* (4) 19.
- Einstein, H. A. and Chien, N., (1955), Effects of heavy sediment concentration near the bed on velocity and sediment distribution, *MRD series*, no. 8, University of California, Inst. of Engrg. Res and U.S. Army Engrg. Div., Missouri River, Corps of Engrs., Omaha, Nebr.
- Embly, R. W., (1976) New Evidence for occurrence of debris flow deposits in the deep sea, *Geology* vol 4, pp.371-374.
- Enos, Paul, (1977) Flow regimes in debris flow, *Sedimentology*, vol. 24, pp. 133-142.
- Fan, J. and Dou, G., (1980) General Report Theme B (I), *Sediment transport mechanics, including hyperconcentration transportation*, *Proceedings of the International Symposium on River Sedimentation*, Beijing, China, pp. 1167-1170.
- Fei, X., (1983) Grain composition and flow properties of heavily concentrated suspension, *Proceeding of the Second International Conference on River Sedimentation, Nanjing, China*, pp.296-308 (in Chinese with abstract in English).
- Fink J. H., M. C. Malin, R. E. D'Alli, R. Greeley, (1981), *Rheological properties of mudflows associated with*

- spring 1980 eruptions of Mt. St Helens volcano, Washington. *Geophys. Res. Lett.* 8(1):43-46.
- Fisher, R. V., (1971) Features of coarse-grained, high concentration fluids and their deposits, *Journal of Sedimentary Petrology*, vol. 41, No. 4, pp. 916-927.
- Fisher, R. V. & J. M. Mattinson, (1968) Wheeler-George turbidite-conglomerate series, California; inverse grading, *Journal of Sedimentary Petrol.*, vol. 38, No. 4, pp. 1013-1023.
- Ghahramani-Wright, V., (1987) Laboratory and numerical study of mud and debris flow (vol.1 & 2), Ph. D. Dissertation, Dept of Civil Engineering, University of California, Davis.
- Gol'din, B. M. & L. S. Lyubashevskiy, (1966) Computation of the velocity of mudflows for Crimean rivers, *Soviet Hydrol.* vol. 2, pp. 179-181.
- Goodman, M. A., and Cowin, S. C., (1972) A continuum theory for granular materials, *Archive for Rational Mechanics and Analysis*, vol. 44, pp. 249-266.
- Govier, G. W., Shook, C. A., and Lilge, E. O. (1957). "The properties of water suspension of finely subdivided magnetite, galena and ferrosilicon." *Trans. Can. Inst. Mining and Met.*, 60, 147-154.
- Hampton, M., (1972) The role of subaqueous sediment flow in the generation of turbidity currents, *J. Sediment. Petrol.*, vol. 42, pp. 775-793.
- (1975) Competence of fine-grained debris flows, *Journal of Sedimentary Petrology*, vol. 45, pp. 834-844.
- (1979) Buoyancy in debris flows, *Journal of Sedimentary Petrology*, vol 49, pp. 753-758.
- Hashimoto, H., and T. Tsubaki, (1983) Reverse grading in debris flow, *Transactions of the J.S.C.E.*, vol. 15, pp. 282-284.
- Hirano, M., and M. Iwamoto (1981) Experimental study on the grain sorting and the flow characteristics of a bore, *Memoirs of the Faculty of Engineering, Kyushu University*, vol. 1, No.3, Sept., pp. 193-202.

- Hopfinger, E. J., (1983) Snow avalanche motion and related phenomenon, *Ann. Rev. Fluid Mech.*, vol 15, pp. 47-76.
- Howard, K., (1973), Avalanche mode of motion: implications from lunar examples, *Science*, vol. 180, pp. 1052-1055.
- Hsu, Kenneth J., (1975) Catastrophic debris streams (Sturzstroms) generated by Rockfalls, *Bull. Geol Soc. Am.*, vol 86, pp. 129-140.
- Hungr, O., (1981) Dynamics of Rock avalanches and slope movements, Ph. D. thesis, Department of Civil Engineering, *University of Alberta*, Edmonton, Alberta.
- Hungr, O., G. C. Morgan, D. F. Vandine, D. R. Lester, (1987) Debris flow defences in British Columbia, *Reviews in Engineering Geology*, vol. VII, *geol Soc of Am.* pp. 201-222.
- Hungr, O. and Morgenstern, N., (1984a), Experiments on the flow behaviour of granular materials at high velocity in an open channel, *Geotechnique*, vol. 34, No. 3 , pp. 405-413.
- - (1984b), High velocity ring shear tests on sand, *Geotechnique*, vol. 34, No. 3., pp. 415-421.
- Hunt, J. N., (1954) The turbulent transport of suspended sediment in open channels, *Proc. Royal Society of London*, Series A., 224(1158), pp. 322-335.
- Hutchinson, J. N. & R. K. Bhandari, (1971) Undrained loading, a fundamental mechanism of mudflows and other mass movements, *Geotechnique* vol 21, No. 4, pp. 353-358.
- Jackson, L. E., Jr. (1979) A catastrophic glacial Outburst floods (Jökulhlaup) mechanism for debris flow generation at the Spiral Tunnels, Kicking Horse River Basin, B.C., *Canadian Geotechnical Journal*, vol. 16, pp. 806-813.
- Jackson, L. E., R. A. Kostaschuk & G. M. McDonald, (1987) Identification of debris flow hazard on alluvial fans in the Canadian Rocky Mountains, *Reviews in Engineering Geology*, vol. VII, *geol Soc of Am.* pp. 115-124.
- Jeppson, R. W., (1985) Mechanisms associated with Utah's 1983 slide and debris flow, Delineations of landslides, flash floods and debris flow hazards in Utah,

Proceedings of the Specialty Conference on Delineation of Landslide, Flash Flood and Debris Flow Hazard in Utah, Utah State University, pp. 197-234.

- Jeyapalan, J. K., J. M. Duncan & H. Bolton Seed, (1983a), Analysis of flow failures of mine tailings dams, *Journal of Geotechnical Engineering*, vol 107, No. 2, ASCE, pp. 172-189.
- (1983b), Investigation of flow failures of tailings dams, *Journal of Geotechnical Engineering*, vol 107, No. 2, ASCE, pp. 172-189.
- Johnson, A. M., (1970) Physical processes in geology, pp. 431-571, *Freeman, Cooper & Company.*
- Julien, P. Y., and Lan, Y. (1991) Rheology of hyperconcentrations, *J. Hyd. Engrg.*, ASCE, vol. 117, No. 3, pp. 346-353.
- Kanatani, K., (1982) A plasticity theory for the Kinematics of ideal granular materials, *International Journal of Engineering Science*, vol. 20, pp. 1-13.
- Kang, Z., and Zhang, Shucheng, (1980) A preliminary analysis of the characteristics of debris flow, *Proceedings of the International Symposium on River Sedimentation, Beijing, China*, vol. 1, pp. 213-226 (in Chinese with abstract in English).
- Kojan, E. & J. N. Hutchinson, (1978) Mayunmarca Rockslide and debris flow, Peru, *Rockslides and Avalanches, Natural Phenomena 1*, Ed. B. Voight, pp. 315-361.
- Kreiger, I. M. and T. J. Dougherty, (1959) A mechanism for non-Newtonian flow in suspension of rigid spheres, *Trans. of the Society of Rheology*, vol. 3, pp. 137-152.
- Kurdin, R. D., (1973) Classifications of mudflows, *Soviet Hydrology selected papers, Issue No., 4*, pp. 310-316.
- Lang, T. E. and J D. Dent, (1987) Kinematic properties of mudflows on Mt. ST. Helens, *Transactions ASCE*, vol 113, HY 5.
- Legowo, D., (1985) On the recent technical development of Sabo works in Indonesia, *Proceedings, International Symposium on Erosion, Debris flow and Disaster Prevention, Tsukuba, Japan*, pp. 439-443.

- Li, J. and Luo Defu, (1981), The formation and the characteristics of mudflows and flood in the mountain area of the Dachao River and its prevention, *Z. Geomorphol* 25: 470-484.
- Li Jian, Yuan Jianmo, Bi Cheng, Luo Defu, (1983) The main features of the mudflow in Jiang Jia Ravine, *Z. Geomorphol* 27: 325-341.
- Lun, C.K.K., Savage, S.B., Jeffery D.J. and Chepurniy, N. (1984). "Kinetic theories for granular flow: inelastic particles in couette flow and slightly inelastic particles in a general flowfield," *J. Fluid Mech.* 140, 223-256.
- Maa, P.-Y (1990) Discussion of Laboratory Analysis of Mudflow Properties, *Journal of hydraulic Engineering*, vol. ,No. , ASCE, pp. 299-301.
- MacArthur, R. C. and D. R. Schamber, (1986) Numerical methods for simulating mudflows, *Third International Symp. on River Sedimentation, The Univ. of Mississippi*, pp. 1615-1623.
- Mainali, A. and Rajaratnam, N.(1991) "Laboratory measurements of debris flows," *Proc. 1991 Annual Conf. of the Canadian Soc. for Civil Engrg.*, vol.1, 146-154.
- Major, J. J. and Pierson, T. C. (1990), Rheological analysis of fine grained natural debris flow material, *Hydraulics/Hydrology of Arid Lands, Proceedings of the International Symposium, ASCE, SanDeigo*, pp. 225-231.
- Major, J. J. and Pierson, T. C. (1992), Debris flow rheology:experimental analysis of fine-grained slurries, *Water Resources Research*, vol. 28. pp
- McGee, W. J., (1897) Sheet Flood Erosion, *Bull. Geol. Soc. Am.*, vol. 8, 1897, pp. 87-112.
- McTigue, D: F. (1978) A model for stresses in shear flow of granular materials, *Proceedings of the U.S. Japan Seminar on Continuum Mechanical and Statistical Approaches in the Mechanics of Granular Materials*, S. C. Cowin and M. Satake, eds., Gakujutsu Bunken Fukyukai, Tokyo, Japan, pp. 266-271.
- (1982) A nonlinear constitutive model for granular material, application to gravity flows, *Journal of Applied Mechanics, ASME*, vol. 49, pp. 291-296.

- Mellor, M., (1978) Dynamics of Snow Avalanches, *Rockslides and Avalanches, Natural Phenomena 1*, Ed. B. Voight, pp. 753-791.
- Middleton, G. V. (1970) Experimental studies related to problems of flysch sedimentation, *The geological Association of Canada, Special Paper Number 7*, pp. 253-272.
- and Hampton M. A., (1976) Subaqueous sediment transport and deposition by sediment gravity flows in Stanley, D. J. and Swift, J. P., eds., *Marine Sediment Transport and Environmental Management*, New York, John Wiley, pp. 197-218.
- Midriak, R., (1985) Debris flow and their occurrences in the Czechoslovak high mountain West Carpathians, *Proceedings, International Symposium on Erosion, Debris flow and Disaster Prevention, Tsukuba, Japan*, pp. 175-180.
- Miles, M. J. & R. Kellerhals, (1981) Some engineering aspects of debris torrents, *5th Canadian Hydrotechnical Conference, May 1981, Canadian Society of Civil Engineering*, pp. 395-420.
- Morgenstern, N., (1967) Submarine slumping and the Initiation of turbidity currents, in: A. F. Richards ed. *marine Geotechnique*, Urbana, Univ. of Illinois Press, pp. 189-220.
- Morton, D. M. and R. H. Campbell, (1974), Spring mudflows at Wrightwood, Southern California, *Q. J. Eng. Geol.* 7:377-384.
- Nash, D. F. T., D. K. Brunsden, R. E. Hughes, D. K. C. Jones, B. F. Whalley, (1987), A catastrophic debris flow near Gupis, Northern areas, Pakistan, in *Proceedings of the Eleventh International Conference on Soil Mechanics and Foundational Engineering: San Francisco, California*, pp. 1163-1166.
- Nasmith, H. W., and Mercer, A. G. (1979) Design of dykes to protect against debris flows at Port Alice, British Columbia, *Canadian Geotechnical Journal*, vol 16, pp 748-757.
- O'Brien, J. S. & P. Y. Julien, (1985) Physical Properties and mechanics of hyperconcentrated sediment flows, *Proceedings of the Specialty Conference on*

Delineation of Landslide, Flash Flood and Debris Flow Hazard in Utah, Utah State University, Utah, pp. 260-279

--- (1986) Rheology of non-Newtonian fine sediment mixtures, *Proc., ASCE Specialty Conference on Aerodynamics, Fluid Mechanics and Hydraulics*, Minneapolis, Minn., pp. 989-996.

--- (1988) Laboratory analysis of mudflow properties, *Tr. ASCE, HY 8*, vol 114, pp. 877-887.

Ogawa, S., (1978) Multitemperature theory of granular materials, *Proceedings of the U.S. Japan Seminar on Continuum Mechanical and Statistical Approaches in the Mechanics of Granular Materials*, S. C. Cowin and M. Satake, eds., Gakujutsu Bunken Fukyukai, Tokyo, Japan, pp. 208-217.

Okuda, S., H. Suwa, K. Okinishu, K. Yokoyama and M. Nakano, (1980) Observations on the motions of Debris flow and its geomorphical effects, *Z. Geomorph. N. F., Supp.1* vol 35, pp. 142-163.

Phillips, C. J. and Davies, T. R. (1989). Debris flow material rheology-direct measurement, *Proceedings of International symposium on Erosion and volcanic debris flow Technology*, Yogyakarta, Indonesia, v13-1 to v13-13.

Phillips, C. J. and Davies, T. R. (1991). Determining rheological parameters of debris flow material, *Geomorphology*, v.4, pp.101-110.

Pierson, T. C., (1981) Dominant particle support mechanism in debris flow at Mt. Thomas, New Zealand, and implications for flow mobility, *Sedimentology*, vol 28, pp. 49-60.

Pierson, T. C., (1985) Field techniques for measuring debris-flow dynamics, *Proceedings of the International Symposium on Erosion, Debris Flow and Disaster Prevention*, Tsukuba, Japan, pp. 203-207.

Pierson, T. C. & J. E. Costa (1987) A rheological classification of subaerial sediment-water flows, *Reviews in engineering geology*, vol VII, *Geol Soc. Am.*, pp. 1-12.

Plafker, G. & G. E. Ericksen, (1978) Nevados Huascarán Avalanches, Peru, *Rockslides and Avalanches, Natural Phenomena 1*, Ed. B. Voight, pp. 277-314.

- Ranga Raju, K. G. (1981) Flow through open channels, *Tata McGraw-Hill Publishing Company Ltd.*, New Delhi.
- Replogle, J., (1964) Tractive-force distribution in sewers and channels, Ph. D. Thesis, University of Illinois.
- Reynolds, O., (1885) On the dilatancy of media composed of rigid particles in contact, *Phil. Mag. Ser. 520*, pp. 469-481.
- Richardson, J. F. and Zaki, W. N., (1954) Sedimentation and fluidization, part I, *Trans. Inst. of Chemical Engineers*, vol. 32, pp. 35-53.
- Rickenmann, D., (1991), Hyperconcentrated flow and sediment transport at steep slopes, *ASCE, Journal of Hydraulic Engineering*, vol. 117, No. 11, pp. 1419-1439.
- Rodine, J. D. and Johnson, A. M., (1976) The ability of Debris, heavily freighted with coarse clastic materials, to flow on gentle slopes, *Sedimentology*, vol. 23, pp. 213-234.
- Roscoe, R. (1952), The viscosity of suspensions of rigid spheres, *Brit. J. Appl. Phys.*, vol 3, pp. 267-269
- Rouse, H., (1937) Modern concepts of the mechanics of fluid turbulence, *Trans. ASCE*, vol 102, pp. 463-543.
- Russell, S. O. D., (1988), Debris torrents and engineering Responsibilities in: *1988 Annual Conference, Canadian Society of Civil Engineers*, pp. 1-7.
- Sassa, K., (1985) The mechanics of Debris Flows, *Proc. XI Int. Conf. Soil Mech. Found. Eng.*, San Francisco, pp. 1173-1176.
- Savage S. B., (1979) Gravity flow of cohesionless granular material in chutes and channels, *Journal of fluid mechanics*, vol. 92 part 1, pp. 53-96.
- (1984) The mechanics of rapid granular flows, *Advances in Applied Mechanics*, vol 24, pp. 289-366.
- (1987) Flow of granular material, *Laboratory for Hydraulic, Hydrology, and Glaciology*, Switzerland.
- Savage, S. B. and McKeown, S., (1983), Shear stresses developed during rapid shear of concentrated

- suspensions of large spherical particles between concentric cylinders, *J. Fluid Mechanics*, 127, pp 453-472.
- Savage S. B. and Lun, C.K.K., (1988) Particle size segregation in inclined chute flow of dry cohesionless granular solids, *J. Fluid Mech.*, 189, pp. 311-335.
- Sayed, M., (1981) Theoretical and experimental studies of the flow of cohesionless granular materials, Ph. D. Thesis, Mc Gill University, Montreal.
- Sayed, M. & S. B. Savage, (1983) Rapid gravity flow of cohesionless granular material down inclined chutes, *Journal of applied mathematics and Physics*, vol. 34, pp. 84-100.
- Schamber, D. R. and R. C. MacArthur, (1985) One dimensional model for mudflows, *Hydraulics and Hydrology in the Small Computer Age, Proceedings of the Specialty Conference*, ed. W. R. Waldorp, ASCE vol. 2, pp. 1334-1339.
- Schlichting, H., (1968) Boundary-Layer theory, McGraw-Hill Book Company.
- Sharpe, C. F. S. (1968) Landslides and related phenomenon, Cooper Square Publications Inc., New York.
- Sharpe, R. P. & L. H. Nobles, (1953) Mudflow of 1941 at Wrightwood, Southern California, *Bull. Geol. Soc. Am.*, vol. 64, pp. 547-560.
- Shen S. and Xie S., (1985) Structure mode and rheologic property of mud debris flow, *Proceedings, International Symposium on Erosion, Debris flow and Disaster Prevention, Tsukuba, Japan*, pp. 227-230.
- Shen, H. and Ackermann, N. L., (1982) Constitutive relations for fluid-solid mixtures, *J. Eng. Mech. Div., ASCE*, vol 108, pp. 748-763.
- Suwa, H. and S. Okuda, (1980) Dissection of valleys by debris flow, *Z. Geomorph. N. F., Suppl.1-Bd 35*, pp. 164-182.
- Suwa, H., S. Okuda & K. Ogawa, (1985) Size Segregation of large boulders in debris flow, *Proceedings, International Symposium on Erosion, Debris flow and Disaster Prevention, Tsukuba, Japan*, pp. 237-241.

- Swanston, D. N., (1971) Principal mass movement process influenced by; logging, road building and fire: in J. T. Krygler and J. D. Hall, eds., *Forest Landuse and Stream Environment, Oregon state University, Corvallis, Proceedings of conference, Oct. 19-21, 1970*, pp. 29-39.
- (1974) Slope stability problems associated with timber harvesting in mountainous regions of the western United States, *Pacific Northwest Forest and Range Experiment Station, U.S.D.A. Forest Service, General Technical Report PNW 21*.
- and F. J. Swanson, (1976) Timber harvesting mass erosion and steep land forest geomorphology in the pacific Northwest, in D. R. Coates ed. *Geomorphology and engineering, Strandsberg, Pennsylvania, Dowden, Hutchinson and Ross Inc.*, pp. 199-221.
- Takahashi, T., (1978) Mechanical characteristics of debris Flow, *Journal of the Hydraulic Div., ASCE*, vol 104, No. HY8, pp. 1153-1169.
- (1980) Debris flow on prismatic open channels, *Transactions ASCE*, vol 106, *Journal of Hydraulic Division*, pp. 381-396.
- (1981) Debris Flow, *Annual Reviews in Fluid Mechanics*, vol 13, pp. 57-77.
- Thomas, D. G., (1963) Non-Newtonian Suspensions, *Ind. & Engr. Chem.*, vol 55, No 11.
- Tsubaki, T., H. Hashimoto and T. Suetsugi, (1982) Grain stress and flow properties of debris flows, *Transactions of the J.S.C.E.*, vol. 14, pp. 413-416.
- Tsubaki, T., H. Hashimoto, (1983) Interparticle stresses and characteristics of debris flow, *Journal of Hydroscience and Hydraulic Engineering*, vol. 1, No. 2, pp. 67-82.
- VanDine, D. F., (1985) Debris flows and debris torrents in the Southern Canadian Cordillera, *Canadian Geotechnical Journal*, vol. 22, 1985, pp. 44-68.
- Vanoni, V. A.(ed.), (1975) Sedimentation engineering, *Task Committee for the Preparation of the Manual on Sedimentation, ASCE*

- Varnes, D. J., (1958) Landslide type and process, in landslide & engineering practice, Ed. Edwin B. Eckel, *Highway Research Board, special Report 21*.
- Waldron, H. H., (1967), Debris flow and erosion control problems caused by the ash eruptions of Irazu Volcano, Costa Rica, *US Geol Survey Bull.* 1241-I: 1-37.
- Wang, L. (1990). "Flume experiments on Debris flow," *Hydraulics/Hydrology of Arid Lands, Proceedings of the International Symposium, ASCE, SanDeigo*, 238-243.
- Ward, S. G. and Whitmore, R. L., (1950) Studies of the viscosity and sedimentation of suspensions, Part 1- The viscosity of suspensions of spherical particles, *Brit. J. Appl. Phys.*, vol 1, pp. 286-290.
- Winterwerp, J.C., M. B. de Groot, D.R. Masterbergen, AND H. Verwoert, (1990) Hyperconcentrated sand-water mixture flows over flat-bed, *ASCE- Journal of Hydraulic Engineering*, vol. 116, No. 1, pp. 36-54.
- Woo, H.S. and Julien, P.Y., (1988) Suspension of large concentrations of sand, *ASCE- Journal of Hydraulic Engineering*, vol. 114, No. 8, pp.888-898.
- Yano, K. & Daido, A., (1965) Fundamental study on mud-flow, Kyoto, Japan, Kyoto Univ., *Bulletin of the Disaster Prevention Research Institute*, vol. 14, pp. 69-83.
- Zhang, X., T. Liu, Y. Wang & J. Luo, (1995) The main feature of debris flow and control structures in Hunshein Gully, Yuannan Province, China, *Proceedings. International Symposium on Erosion, Debris flow and Disaster Prevention, Tsukuba, Japan*, pp. 181-186.

APPENDIX A

A.1 Favorable conditions for debris flows

A close observation of debris flow events seems to indicate that there are three particular regions where debris flows are more prevalent

1. semi arid regions
2. alpine regions
3. volcanic regions

In the semi arid regions the main source of moisture is the sudden "cloudburst" phenomenon that brings large amounts of rain in a small basin. The moisture seeps into the soil and the increased pore water pressure reduces the shear strength of the soil mass and helps mobilize the mostly unconsolidated soil and rock debris overlying a relatively stable bedrock.

The alpine mudflows appear to get most of their moisture from snowmelt and, in some cases, the bursting of glacial dammed lakes i.e. glacial lake outburst floods (GLOF) also known as Jokulhlaup (Jackson, 1979). In both the alpine as well as the semiarid debris flow events, sparse vegetation and intermittent water supply appear to be some of the favorable conditions.

The volcanic debris flows known as lahars normally originate on the slopes of volcanoes. These can be mobilized

accompanying an active eruption or shortly after one (Sharpe, 1968). Lahars can be formed, according to Costa (1984), by

1. mobilization by rainfall
2. rapid melting of snow and glaciers
3. rapid drainage of crater lakes by expulsion
4. pyroclastic flows that incorporate water
from melting eroded snow moving downwards
5. mobilizing of saturated material moving
down a volcano triggered by an earthquake

Normally, debris flows are the results of some form of slope failure. There isn't an unanimous opinion about the exact mechanism of how a slide develops into an active debris flow. But the general belief is that the material collects moisture and as it moves down the slope, it either liquefies or dilates further increasing its mobility (Hampton, 1972).

A.2 Definitions

A.2.1 Introduction

Mass transport with its broad implications requires clear distinctions between the various processes included in this topic. For our special interest it is appropriate to discuss those mass transport processes that move relatively faster and fall within the category of mud and debris flows. A general classification will be given later after the different terms are better understood.

In many instances, when these masses are transported from one point to the other, it is quite difficult to define clear cut boundaries between each of these different types of movements. This is mainly due to the variety of methods of transport and the material found in different locations. For instance the term **mudflows** and **debris flows** are very often used inter-changeably in the older literature. At what point can a mudflow be called debris flow and how this boundary can be recognized is a difficult task. But, however, depending on the nature of the flow and the composition, different terms have been coined and have remained in use.

A.2.2 Debris slides and debris avalanches

Debris slides have been explained as the movement of relatively unconsolidated material which consist of different kinds of rock fragments and other fines. They are unsaturated and what distinguishes them from debris avalanches is the fact that they have a lower moisture content. In both these cases the initial failure could be either rotational or translational resulting in an immediate disintegration of the mass. The early definitions of these terms were given by Varnes(1958) where debris slides and debris avalanches have been included as flows, presumably with the intrinsic assumption that these processes undergo continuous deformation.

A.2.3 Debris flows and debris torrents

As the mass of soil and debris moves down the slope, it accumulates moisture and becomes saturated, the terminology changes from debris avalanche to debris flow (Swanston, 1971, 1974 & Swanston and Swanson, 1976). An important distinction is made here by Swanston (1971) in between the flow of debris on a normal unconfined sloping surface and the flow in regular steep drainage channels. In the case of the channelized debris flows termed *debris torrents*, the mud and debris is confined in between the side walls and moves down the channel in regular pulses.

A.2.4 Mudflows

As the term indicates, mudflows, normally have come to represent the flow of fine cohesive material down a slope in almost the same manner as debris flows except that they do not contain the larger variation in particle sizes. Normally, the term debris flow indicates the presence of large variation in the particle fragments. Mudflows are distinguished by the presence of at least 50% sand, silt and clay size particles (Varnes, 1958).

It has to be pointed out that the earlier definition (Sharpe, 1968) of mudflows appears to be the same as debris flows defined here and, to a certain degree, this definition is still being used. This is partly because a clear cut boundary is hard to define.

APPENDIX B

B Classifications

B.1 Classification of Sediment-Water Flows

Most of the previous classifications of sediment gravity flows are based on type of material, movement mechanism, and the concentration of the sediment. This study will focus mainly on that group of sediment gravity flows which involves the mixtures of sediment and water flowing in high concentrations. One such classification based on this approach has been given by Pierson and Costa(1987). It is important to understand that for all flow phenomena it is not essential that the material be sediment or the interstitial fluid be water. There are many other flow situations where the interstitial fluid is air or, in the case of lunar slides, an absence of air (Howard, 1973). These types of flows are associated with granular material (Savage, 1987) where the interstitial fluid density is low and the main flow is governed by the interparticle stresses, friction and collision. Common examples of these flows are grain flows (Savage, 1979; Sayed and Savage, 1983), dry dense-snow avalanche and airborne powder snow avalanche (Hopfinger, 1983), flow of medicine tablets and other industrial granular flows.

Sediment-water flows can be grouped into three main bands

- i ordinary streamflow
- ii hyperconcentrated flow
- iii granular flow

Pierson and Costa(1987) further divide the above granular flows into slurry flows and granular flows. Since the basic constitutive laws for both of these flows can be conceptually put in the same class, it is quite sufficient to merely define the whole regime as granular flows. All the other forms of flows involving water and sediment can be accommodated in one of these basic bands.

B.1.1 Streamflow

In the strict sense, streamflow is water and entrained sediment and air flowing as a multiphase flow. For low sediment concentration, the flow behaves essentially as Newtonian fluid.

As the concentrations of the sediment increases, the particle interaction increases. If clay particles are present in the flow, they begin to form flocks due to the presence of electrochemical forces. These flocks tend to give strength to the fluid and, as a result, introduce yield strength i.e. the applied stress would have to break these bonds and alignments before any deformation of the fluid can take place. This initial stress is the yield stress typical of many non-Newtonian fluids. The concentration at which this occurs is dependent on the type of clay mineralogy as well as the particle size distribution. Yield strength has

been experienced in concentrations as low as 3% in smectite suspensions (Hampton, 1972) and at higher percentage in other clay minerals.

B.1.2 Hyperconcentrated flows

While studying high concentration stream flows, Beverage & Culbertson (1964) defined hyperconcentration as concentration with more than 40% sediment by weight. They suggested an upper limit of 80%. Different names like *mud floods* or *non-cohesive mudflows* (Kurdin, 1973) have been given to these flows. Often, especially in Chinese literature (Fan and Dou 1980, Fei 1983) the implications of higher concentrations is that the mixture possesses yield strength. They also prefer to classify debris flows as a type of hyperconcentrated flow. O' Brien and Julien (1985) prefer to do the same. In this text hyperconcentration will be referred to flows with suspension of fines with little or no shear strength and with sand size or larger particles allowed to settle and even move as bed load. This obviously would imply a reduction in the fall velocity as well.

B.1.3 Granular flows

This condition describes the flow which possesses high concentrations of solids. The mixture may be saturated, unsaturated or dry. In the unsaturated case it may be partially dry with air filling some of its voids. In the saturated case, they exhibit free draining nature during

continuous deformation. In other words, because they are in a process of continuous deformation, the pore water can freely maintain hydrostatic conditions throughout the flow. Any excess pressure will immediately be dissipated because water can flow freely.

A general classification according to Savage(1984) describes three limiting flow regimes for granular flows:

- i Quasi-static
- ii Macroviscous
- iii Grain Inertia

These classifications are extensions of the classification given earlier by Bagnold(1954). Bagnold defined a regime called macroviscous regime where the particle concentration and the strain rates are small and the interstitial fluid plays a prominent role in determining the viscous nature of the flow. Davies(1986 1988) hypothesizes that certain types of debris flows fall in this category of granular flows.

When sufficient stress is applied to a granular mass such that the frictional bonds are broken, the mass starts to flow. This flow, mainly confined to shear bands along the shear plane, involves multiparticle blocks moving relative to one another. This slow deformation maintained for a long period of time defines the quasistatic regime.

The grain inertia regime is where the strain rates are high enough that the momentum transfer is predominantly by grain to grain interaction. Friction plays a minor role. There are several suggestions (Bagnold, 1954; Takahashi,

1981; Chen 1985a) that debris flow is an inertial flow. Debris avalanche and debris slides fall in this region as well. Many of the high inertial flows such as rock avalanches called Sturzstroms (Hsu, 1975), are characteristic of this regime. Because of the high inertia Sturzstroms have a tendency to ride up the other side of the valley when a rockfall event does occur as witnessed in the Frank slide, Alberta (Cruden & Krahn, 1978)

APPENDIX C

C Characteristics Of Debris Flows

C.1 Debris Sources

Debris flows occur under the condition that there is an ample supply of unconsolidated mud and rock fragments, a large intermittent supply of water and, preferably, sparse vegetation. In many cases sparse vegetation may not be necessary for debris flows to occur. Since debris flows are the product of slope failures, the source of debris is either some kind of a slide, slump or a debris avalanche. There are many factors responsible for triggering these failures. Bursts of heavy rain and, in some cases, seismic forces are two main triggering factors.

Many of these mass wasting processes are exacerbated by logging, road building and forest fires (Swanston, 1971). This is prevalent in the Western Cordillera in North America. Many of the steep slopes and the high reliefs in this region have been further steepened by erosion creating a very unstable state. Logging, road building and residential developments disturb the delicate balance existing in these slopes which results in slides and avalanches that debris flows thrive on. Logging also contributes organic debris to the stream. An equally important source of debris is the massive erosive nature of the flowing debris. The highly

erosive movements have the ability to scour a few meters of material from the bed (Nasmith and Mercer, 1979).

C.2 Composition of Debris Flows

Very often debris flows have been described as resembling wet concrete. Even though the appearance is similar to concrete, the composition of a debris flow varies greatly in that it is a poorly sorted multiphase flow with air and water entrained in it. The particle sizes vary from finer materials to boulders supported in a matrix of dispersed fines. The matrix could also contain wood, bark from trees and anything it picks up on its way. Depending on the source of debris, the flow could be mudflow with predominantly fine material or it could be rock fragments dispersed in a matrix of water and fines. In the Myunmorea Rockslide, the debris ranged from clay size to blocks of at least several hundred cubic meters in volume which, in most part, were granular and with some cohesion (Kojan and Hutchinson, 1978). In the Nevados Huascaran avalanches of Peru the debris flow contained angular blocks of rocks constituting 10-15% of the total volume. The matrix material was typically medium-grey gravelly mud. A representative sample showed 10.6-39.1% gravel, 46.0-72.3% sand and 3.5 to 24.4% combined silt and clay (Plafker and Ericksen, 1978). The mudflow in Wrightwood, California had material that was light grey and consisted of silt, sand and pebbles less than

1 inch in diameter. The largest boulders were 6 ft. in diameter (Sharp & Nobles, 1953)

C.3 Nature of Flows

The similarity between debris flows and water flows is that they both flow as fluids. Besides that there are certain features of the flow of debris that are quite different from ordinary stream flow. These features can be studied by first examining the physical behavior, velocity of flow and the slope of the bed.

C.3.1 Physical Behavior

Debris flow has a characteristic way of moving down its path. The flow is made up of a succession of surges of a steep front loaded with bouldery fragments. In the mudflow of Wrightwood, California, at the time of maximum frequency, the surges came at intervals of a few seconds to tens of minutes (Sharp and Nobles, 1953). Later they were less frequent with a period of a few hours. There are also suggestions (Li et. al., 1983; Davies, 1986) that the surges are a result of some inherent properties of the fluid and open channel flow instabilities. Similar behavior of flow was observed by Curry(1966). The series of lobate pulses lasted for one hour with each unit of pulse having ten or more less distinct flow pulses. In the observations of Broscoe and

Thompson(1969), the mudflow moved into the fan in a series of arcs of circles with increasing radii. The fronts were observed to be 6-8 ft. high. In all these observations, the noise accompanying the release of the pulses of viscous rock-charged mud were characteristic of the failure of a dam which had impounded the material. The surges have been attributed to (Sharp & Nobles, 1953):

- i periodic sloughing of debris in source area
- ii temporary choking of channels
- iii caving of undercut banks
- iv friction between the moving debris and the channel

C.3.2 Velocity

The velocity of debris flow has been observed to vary from 0.5 m/s to 20 m/s. The reasons for this wide range of velocity is due to the fact that the sorting, the geometry of the channel including the slope, size and sinuosity can have large variations. Table C-1 gives the observed velocities of some of the debris flows. In one observation in Japan (Okuda, et al, 1980) the velocity on the upper reach was over 10 m/s but, in the fan area the velocity was rarely found to exceed 5 m/s.

The discussion of velocity leads us directly to the question of turbulence in debris flow. The large velocities would tend to indicate the possibility of turbulence in the flow. There have been only a few references to turbulence in

Table C-1 Physical properties of observed debris flows (after Costa, 1984)

Location	velocity (m/s)	slope (%)	Bulk density (g/cm ³)	μ (poise)	% clay	depth (m)	Solids (% wt.)	Reynolds No.	Reference
Rio Reventado, Costa Rica	2.9-10	4.6 to 17.4	1.13 to 1.98	-	1-10	8-12	20-79	-	Waldron, 1967
Hunshui Gully, China	10-13	-	2-2.3	15-20	3.6 (<.005mm)	3-5	80-85	40000	Li and Luo 1981
Bullock Creek, New Zealand	2.5-5.0	10.5	1.95 to 2.13	2100 to 8100	4	1.0	77-84	28.57	Pierson 1981
Pine Creek, Mt. St. Helens	10-31.1	7-32	1.97 to 2.03	200-3200	-	0.13 to 1.5	-	200	Fink et.al. 1981
Wrightwood Canyon Ca. (1941)	1.2-4.4	9-31	2.4	2100 to 6000	<5	1.2	79-85	23.8	Sharp and Nobles 1953
Wrightwood Canyon Ca. (1969)	0.6-3.8	9-31	1.62 to 2.13	100 to 60000	-	1.0	59-86	1.33	Mortan and Campbell 1974
Mayflower Gulch, Colorado	2.5	27	2.53	30000	1.1 (<.004mm)	1.5	91	3.2	Curry 1966
Dragon Creek, Arizona	7.0	5.9	2.0	27800	-	5.8	80	29.2	Cooley et.al. 1977
Jian-jia Ravine, China	8.0	0.06	2.3	15.5 to 1736	-	1.4	89	148 to 11561	Li et.al. 1983

debris flows. Bagnold(1954, p 60) indicates that the presence of clay size particle tends to dampen turbulent eddies. This is further emphasized by Johnson(1970, p 442) in the study of kaolin-water slurries. In their observations of debris flow in Wrightwood, California, Johnson(1970) suggests that the choppy surface seen in many mudflows was the result of "shear turbulence". In most cases the turbulence was dampened by the presence of suspended clay and silt. Johnson suggests that only muddy water flowed turbulently and the turbulence observed in the ordinary flow was mainly when the flow churned over a small fall or constriction. On reaching straight walled channels, the churning was observed to disappear entirely. In the study of debris flows as Bingham material, Enos (1977) has attempted to outline the threshold between laminar and turbulent flow. These observations, however, appear to lack any conclusive guidelines.

Turbulent flow was observed by Pierson(1981, 1985) in the debris flow at Mt. Thomas, Newzealand and Rudd Canyon, Utah. At Mt. Thomas once the velocity increased to 3 to 5 m/s, the flow turned distinctly turbulent with standing waves often throwing mud and stones in the air. In Rudd Creek, Utah the turbulence was apparent at a concentration by weight approaching 70%. In this flow a large percentage of fines and clay content was present. The turbulent flow was recognized in both these cases visually. There was no formal criteria set to define these boundaries.

C.3.3 Slopes

Although debris flow occurs in steep slopes, it is important to note that it has the ability to flow in very gentle slopes. Some observed slopes range from 2% to 32% (Costa, 1984). In the debris flow in Mt. Thomas, New Zealand (Pierson, 1981) the channel slopes ranged from 5-7°. In Steele Creek, Yukon (Broscoe and Thompson, 1969) the slope was 13-32° and in Wrightwood, California the slope was 1° to 9° (Sharpe & Nobles, 1953).

This is clearer if a simple stability analysis is performed in a unit width and length of saturated, cohesionless planar soil at height h , slope $\sin \theta$ with the soil having an internal angle of friction ϕ (Fig. C-1). According to Mohr-Coulomb friction criteria, the limiting shear strength τ_L for a non-cohesive soil material is

$$\tau_L = \bar{\sigma} \tan \phi \quad (C-3.1)$$

The effective normal stress $\bar{\sigma} = \sigma - u_p$ with

$$u_p = \gamma_w h \cos \theta \quad (C-3.2)$$

$$\sigma = W \cos \theta \quad (C-3.3)$$

W is the weight of the material concerned. The bulk unit weight of saturated material is given as

$$\gamma_{sat} = \gamma_w + (\gamma_s - \gamma_w)C_v \quad (C-3.4)$$

where γ_w is the unit weight of water and γ_s is the unit weight of solids and C_v is the volume concentrations of the mixture.

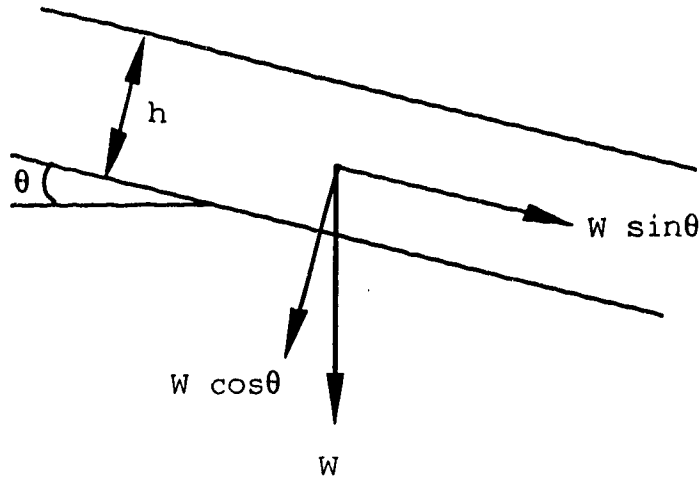


Figure C-1 Definition sketch of mass of debris flowing down a slope

The component of the weight of debris parallel to the bed is

$$W \sin \theta = \{ \gamma_w + C_v(\gamma_s - \gamma_w) \} h \sin \theta \quad (C-3.5)$$

For limiting equilibrium condition replacing τ_L by $W \sin \theta$ in Equation (C-3.1) yields

$$\tan \theta = \frac{C_v(\gamma_s - \gamma_w)}{C_v(\gamma_s - \gamma_w) + \gamma_w} \tan \phi \quad (C-3.6)$$

It can be observed from Eq. (C-3.6) that since the expression multiplying $\tan \phi$ is < 1 , $\tan \theta$ is always less than $\tan \phi$ i.e. the slope required for the flow of dispersed grains is always smaller than that required for frictional sliding of an undispersed grain aggregate.

The small slopes involved in debris flows have been evident in submarine conditions. In submarine debris flow deposits in the Canary Basin off the coast of Spanish Sahara the slope was estimated as 0.1° (Embly, 1976). Similarly, submarine slumps have also been found to occur in very gentle slopes (Morgenstern, 1967).

This tendency of mudflows to occur in slopes considerably flatter than those corresponding to limiting equilibrium for residual strength on the sliding surface was studied by Hutchinson and Bhandari (1971). They attribute this increased mobility to the undrained loading of the front of the mud slides by debris discharged from steeper slopes at the back.

C.4 Important Concepts in Particle Support Mechanism

The ability of debris flows to carry coarse particles of various sizes and move over far distances and small slopes with surprising competence has intrigued many researchers. Observations of actual mud and debris flows show surprisingly large boulders floating in the fluid matrix. Pierson (1981) observed boulders of up to half a meter floating at the flow surface. Broscoe & Thomson (1969) observed boulders 13 ft. across in the mudflow. Sharp & Nobles (1953) report boulders 2-3 ft. diameter moving with the debris front travelling for almost 15 miles before being deposited. In order to explain these observations, various mechanisms

including turbulence for particle support in debris flows have been suggested.

C.4.1 Dispersive stress

Much of the mechanisms behind debris flows were still unexplained until the concepts of dispersive stress was proposed by Bagnold(1954). Bagnold conducted experiments with particles sheared in a rotating cylinder and defined two flow regimes namely *macroviscous* and *grain inertia*. In the grain inertia regime stresses were generated as a result of collisions of particles as one layer moved to overtake the other adjacent layer of particles. The stresses generated in this process were a normal stress called the dispersive stress and a shear stress. With an analysis roughly similar to the kinetic theory of gases Bagnold showed that the normal stress was proportional to the square of the shear rate and the particle diameter. This was an attractive concept in that it attempted to give some rationale to the supporting mechanism for the coarse clasts in sediment-water gravity flow. There is some evidence in observations of actual debris flow (Pierson, 1981) that dispersive pressure is not the only mechanism involved in the support of particles. Solid clasts were observed to be floating even when the debris was static indicating the mobilization of some additional support mechanisms.

C.4.2 Matrix Strength in Debris Flows

When a particle is supported in a stationary slurry, it is observed that if it is pushed, it has a tendency to sink a little and remain in that position without either bobbing back up to the surface or sinking to the bottom. This was observed by Johnson (1970) whose inference from this was that there must be another support mechanism, beside dispersive force. Johnson called this support mechanism **matrix strength**.

The exact origin of matrix strength is still not very certain. It is, however, speculated (Hampton, 1975) that the network of flocculated clay particles throughout the fluid are responsible for this strength. Flocculation is the result of net attractive forces between two clay particles. The minimum strength required to break this network of flocculated particle has been defined as the *matrix strength*. The implication inherent to this theory is that it is essential for clay to be present in the flow. It has been pointed out (Hampton, 1975) that the strength of the matrix is also a function of clay mineralogy and other variables.

Hampton(1975) studied the stationary competence of slurry before and after it had been sheared at different rates and brought to rest. Hampton found that the competence decreased after shearing and concluded that there is a presence of matrix strength in debris flows even though the strength decreased after shearing. Shen and Xie(1985) inserted rotors 2.1 cm and 3.1 cm diameter into clay slurry

and calculated the bearing strength of the slurry both in static and in a state of being sheared. They found that the strength of the slurry was more than due to buoyancy in static case and decreased gradually as the shearing was started. At high shear rates, the yield strength virtually disappeared. This showed a shear rate dependence of the matrix strength.

Davies(1986, 1988) disagrees with this idea and argues that when the flow is stationary, the unyielding structure of the mixture transfers the excess weight of the particles to the bed. However, once the flow starts, then by definition, yield has been overcome and therefore there is no longer a matrix that can transfer the stress to the ground. Any excess weight would increase the shear rate of the flow. Davies argues that even in a case of a plug flow, the shear stress is not transferred to the ground through the rest of the unyielding matrix but, rather, results in the increase of the shear rate in the continuously deforming flow. A fluid is not able to act as both solid and fluid at the same time. This argument, in principle, appears quite reasonable. However, some serious investigation isolating buoyancy and yield strength needs to be done before confirming either of these arguments.

It is interesting to note at this point that according to Curry(1966) the flow in the Tenmile Range, Colorado had 2.5 ft. boulders in it but the clay content was as low as 1.1% and the water content was 9.1%. This raises the

question of how much clay is really required for yield strength to be of significance if that is indeed responsible for the large competence of debris flows

C.4.3 Buoyancy in Debris Flow

Among all the particle support mechanisms, buoyancy stands out as the most obvious mechanisms (Johnson, 1970; Hampton, 1975, 1979; Middleton & Hampton, 1976; Rodine and Johnson, 1976; Pierson, 1981; Sassa, 1985). The generally accepted theory was that the matrix was composed of a homogeneous mixture of clay, water and fine silt. The clasts present in the flow was dispersed in this fluid. The buoyancy, in the Archimedian sense is the weight of the displaced fluid. However, Rodine & Johnson(1976) suggested that the buoyancy was determined by the total displaced material which comprised of the matrix and particles of sizes smaller than the particular clast in question i.e. similar to a pyramid effect. One of the serious shortcomings of these analyses is that the contribution of dispersive pressure is not included. The presence of matrix strength and the failure to include dispersive pressure renders this analysis more suitable for a slurry at rest.

The other argument of Hampton and Pierson that is equally questionable is the increase in buoyancy due to pore pressure above hydrostatic(Sassa 1985, Davies 1986). They suggest that the increase in buoyancy is due to pore pressure being above hydrostatic. To demonstrate the effect of pore

pressure causing increased mobility and competence, Pierson (1981) measured pore pressure and its dissipation in containers following the mixing of slurry. In this measurement, because the pore pressure in a variety of mixes took 20 minutes to several hours to dissipate, Pierson concluded that for the time scale of a debris flow event, this was adequate mechanism to support clasts in addition to simple buoyancy and dispersive pressure. However, in a continuously deforming medium where the pores are continuously breaking and reforming, there is ample opportunity to immediately dissipate the excess pore pressure. The fluid and the grains would adjust to any excess pressure. In other words, the mixture would be free draining. In Pierson's (1981) case, the pore pressures were measured in a stationary mixture where there is indeed a possibility of excess pore pressure being present. This also questions the validity that excess pore pressure is responsible for the high mobility of debris flows. The liquefaction of stationary saturated mass due to pore pressure increase, on the other hand, is quite acceptable (Sassa, 1985). In other words, excess pore pressure is probably more important in reducing shear strength of the material during initiation but its contribution to mobility during continuous shear is questionable.

C.4.4 Inverse Grading

The snout of a surge of debris shows that the larger particles have a tendency to move laterally and vertically resulting in the reverse grading of the particles. This phenomenon of the migration of clasts to the margins is sometimes called **segregation**. Reverse grading is of interest not only in the case of subaerial flows but also in subaqueous flows (Middleton & Hampton, 1976; Middleton, 1970). In submarine environments one of the ongoing geological processes is the formation of sedimentary rocks. It has been observed in certain rocks that the sequence of particle grading is fine at the bottom to coarse on the top (Fisher & Mattinson, 1968). In subaerial flows the evidence of this reverse grading can be best observed in deposits of debris (Fisher, 1971). It is observed that inversely graded deposits of debris flows can be found where there are no planes of erosion. This helps to invalidate the theory that reverse grading may have been caused by a few sequences of debris flows.

There have been a few qualitative explanations given for the reason behind reverse grading. Bagnold's dispersive stress has been suggested as one of the main mechanisms for segregation. The expression for dispersive pressure shows that it is directly proportional to the second power of the particle diameter and the velocity gradient. Therefore an increase in diameter would mean an increase of dispersive pressure. Together with this, an increase in velocity

gradient increases the dispersive pressure. Since the velocity gradient is the largest near the bed, there is a large dispersive pressure there causing the particle to move upwards.

Middleton(1970) offered another mechanism for segregation and called it **kinetic sieving**. In kinetic sieving the finer particles move in between the larger particles and thus displace them upwards. Middleton has offered no further explanation. Suwa et. al.(1985) verified this experimentally as one of the causes for size segregation in debris flows.

There have been few attempts to explain segregation using analytical reasoning(Takahashi, 1980; Hashimoto & Tsubaki, 1983; Savage and Lun, 1988). Takahashi explains segregation using the dilatant fluid model(Bagnold, 1954) Hashimoto and Tsubaki use a concept which they proposed earlier (Tsubaki et al., 1982) to explain the mechanism involved in a solid-liquid shear flow at high concentrations and high shear rates. Their model proposes that a particle in such shear flows experiences two forces from the surrounding particles namely, the **collision force** and the **contact force**. Both these analyses write an equation of vertical motion of a particle larger than the surrounding particles. The analyses show that a particle with a diameter larger than the average diameter of the surrounding particles has a tendency to segregate upwards.

APPENDIX D

D.1 Rheological properties of debris flows

Most of the models described so far for defining debris flows involve two important parameters, viscosity and yield, in their equations. The models with higher order dependence on the shear rate require the determination of the nature of this dependence which has been termed the **flow-behavior index** (Chen, 1985a).

One very practical difficulty arises in determining the property of a debris flow. The debris flow is in the form of a slurry which may have large variation in clast sizes in a mixture of fine matrix. The measurement of viscosity of the actual mixture is very difficult mainly because the standard viscometer cannot use such mixtures. Johnson(1970) used the integrated form of the velocity profile in a semicircular channel to estimate a viscosity. This technique assumed that the boundary shear across the channel was uniform. This method is questionable because boundary shear in a semicircular channel varies across the section unlike a wide rectangular channel (Replogle, 1964).

In practice, the viscosity of the mixture is normally taken as the viscosity of the matrix fluid after the heavier clasts have been removed. The largest particle size that can be used for viscosity measurement is dependent on the method that is used to determine the viscosity and yield strength.

D.1.1 Fluid viscosity and shear strength under field conditions

The viscosity of debris flows with high sediment concentration is generally expressed in several different ways. Some of the earlier estimates (Sharp & Nobles, 1953, Curry, 1961) were made assuming the fluid to be Newtonian. The Newtonian friction law

$$\tau = \mu \frac{\partial u}{\partial y} \quad (D-1.1)$$

was integrated in a wide open channel of velocity U_{\max} at the top and zero at the bed with a flow depth of h . If the specific gravity of the fluid is γ_m and the channel is inclined at a slope of θ° , the equation used to estimate viscosity was:

$$\mu = \frac{\gamma_m h^2 \sin \theta}{2 U_{\max}} \quad (D-1.2)$$

Costa (1984) reported the viscosity of actual recorded debris flow in the range between 200 to 30000 poise. This represents viscosity 3 000 000 times the viscosity of water. An inflated Newtonian viscosity was used by Lang and Dent (1987) in their numerical simulation. One would have to be cautious in taking this approach especially in the light of the non-Newtonian nature of debris flows.

A field estimate of the viscosity can also be made from an equation derived from Bingham fluid approximation for fluid

flowing in an open channel with a plug. The following equation was given by Johnson(1970).

$$\mu = \frac{\tau_y W_p}{4U_{\max}} \left[\frac{W_c}{W_p} - 1 \right]^2 \quad (\text{D-1.3})$$

where

τ_y is the shear strength

W_p is the width of the plug

U_{\max} is the maximum velocity of the plug

W_c is the width of the channel

A simple rheological approach is to estimate the apparent viscosity, μ_a of the fluid

$$\mu_a = \tau / \frac{\partial u}{\partial y} \quad (\text{D-1.4})$$

which is usually estimated using one of the several viscometers available. Similarly, there have been some approximate relations presented for field conditions to estimate the shear strength. Costa(1984) has given a summary of the equations given by Johnson for the yield strength calculations. The first method was using the thickness of the equilibrium deposit (t_d) to estimate the yield strength:

$$\tau_y = t_d \gamma_m \sin \theta \quad (\text{D-1.5})$$

The second method uses the dimension of the plugged channel. The properties of the channel plugged by a debris flow can be used to estimate the yield strength:

$$\tau_y = \frac{d_p \gamma_m \sin \theta}{\left(\frac{2d_p}{W_p}\right)^2 + 1} \quad (D-1.6)$$

where d_p is the depth of the plug.

The third technique involves the use of the height of the largest deposited boulder D_L flowing and the volume fraction of the boulder submerged in debris(n). This assumes that the transport of large boulders is mainly due to the small density difference between the fluid and the solid, and the consolidation in the flowing matrix is negligible. This gives:

$$\tau_y = 0.219 D_L \gamma_m (1 - n) \quad (D-1.7)$$

If the boulder is flowing half submerged, $n=0.5$. The other symbols have their usual definitions.

D.2 Viscosity and yield measurements in debris flows

Our present state of knowledge in debris flows, suggests that the best approach to study debris flow is to examine an actual flow or at least a physically simulated flow. This would then give more confidence to our modelling efforts. Two parameters that have been examined by some researchers (O'Brien and Julien, 1986; Ghahramani-Wright, 1987; Phillips and Davies, 1989, 1991) are the viscosity and yield strength. O'Brien and Julien designed a concentric cylindrical viscometer to measure the viscosity and the yield strength using remolded mud from deposits from the Colorado Rocky

mountain. They compared their measurements to the Bingham plastic model. The experiment shows that when less than 20% by volume of sand <0.5mm in diameter is added to a fine slurry of mud, the viscosity of the mixture of the matrix fluid with silt and 5 to 6% clay is unaltered. Similar observation was made by Major and Pierson(1990) for shear rates $> 5 \text{ sec}^{-1}$.

Ghahramani-Wright(1987) studied the viscosity and yield strength of bentonitic slurry. Since this study involved a comparatively low concentration slurry i.e. 1.4 to 11.9% by wt., the use of the fairly sophisticated Weissenberg Rheogoniometer was possible. The measurement showed that after shearing was stopped, there was some retained stress. Ghahramani-Wright concluded that bentonitic slurry behaved as viscoplastic fluid and called this retained stress the yield stress defining the total stress as

$$\tau = \tau_y + \tau_v = \tau_y + m_p \left(\frac{\partial u}{\partial y} \right)^\eta \quad (\text{D-2.1})$$

where

τ is the total shear

τ_y is the yield stress

τ_v is the viscous stress

m_p and η are parameters which vary with concentration. For shear rate greater than 1, Ghahramani-Wright found that both the yield stress τ_y and the viscosity η could be expressed as:

$$\tau_y = a' - b' \ln \frac{\partial u}{\partial y} \quad (\text{D-2.2})$$

$$\mu = m_p \left(\frac{\partial u}{\partial y} \right)^{n-1} \quad (D-2.3)$$

where both τ_y and μ are functions of shear rates. At shear rates less than 1, both τ_y and μ are constants. Considering that actual debris flows are much higher in concentration than the range studied by Ghahramani-Wright, the result is of little consequence to our study. Other studies of viscosity and yield strength for fine particles can be found in the literature (Fei, 1983)

All these studies consider predominantly very fine particles. The sand added in O'Brien and Julien's study was below 0.5mm. Recognizing the poorly sorted nature of debris flow, Phillips and Davies (1989, 1991) studied the rheological properties of debris flow. This study was carried out in a large 30° inverted cone and plate type viscometer with actual debris flow samples. Clasts up to 35mm was tested in a small scale model and clasts up to 120mm in a large scale model. Yield stress measured by them was in the range of 15 to 300 Pa and depended on the volume concentration. The apparent viscosities which were shear rate dependent ranged from 0.4 to 1800 Pa s. Although they did not define an explicit relationship for apparent viscosity, they made several interesting observations. One of the comments was that their data envelope did not suggest either Bingham Plastic or viscoplastic behavior and at low shear rate the behavior was more likely yield dilatant.

One of the important outcomes from all these studies shows that debris flows display a range of behavior and it is quite difficult to describe one single model for the complete range of flows with our present state of knowledge. This view is also shared by Major and Pierson (1992). All the studies described above have emphasized the importance of conducting experiments in the shear rate range commonly found in the field, i.e. $<50 \text{ s}^{-1}$. One of the main reasons for the low shear rates has been to prevent overestimation of the yield stress which varies with shear rate. (Maa, 1990). This problem of overestimation has mostly been experienced in the case of cohesive sediment where yield stress is a result of electrochemical bonding. Therefore it is necessary to maintain appropriate shear rate in simulated debris flows where the clay content is high. However, in many debris flows, the clay content is normally found to be low.

In the case of non-cohesive granular flows, the important question is whether the constitutive behavior of a test debris flow is representative of a prototype. In other words, it has yet to be fully investigated what range of shear rate is any constitutive relation valid for and how critical is the shear rate in any relation. Another fact is that laboratory flows tend to have larger shear rates but considerably smaller normal and shear stresses than in the field. This is one of the most obvious limitations of simulated debris flows in the laboratory where it is not practical to generate flows of large scale.

APPENDIX E

E.1 Curve fit

Two important information were examined in the velocity distribution measurement. The nature of the profile was expected to provide some indication of the influence of the boundary. The nature of the vertical velocity gradient in the flow combined with the shear distribution acquired from the concentration distribution measurements should provide some reflection of the influence of the velocity gradient in the general constitutive behavior of the fluid.

Initially the velocity gradients were obtained by simply using the discrete measured values of the velocity. This, however, resulted in a highly discontinuous local gradients. The velocity gradients were, therefore, evaluated by first fitting a second order polynomial to the measured velocity profile (Figure E-1 to E-8) with u in cm/s and y in cm.

$$u = b_1 + b_2 y + b_3 y^2 \quad (E-1)$$

This was done after neglecting the top regions of the profiles which were influenced by the secondary flows. Table E1 to E4 give the details of the polynomial velocity fit. Tables E1 to E4 also give the velocity gradients obtained by differentiating the polynomial profiles.

$$\frac{\partial u}{\partial y} = b_2 + b_4 y \quad (E-2)$$

Figure E-1 Polynomial velocity fit for particle D1, group 6.45, channel centre

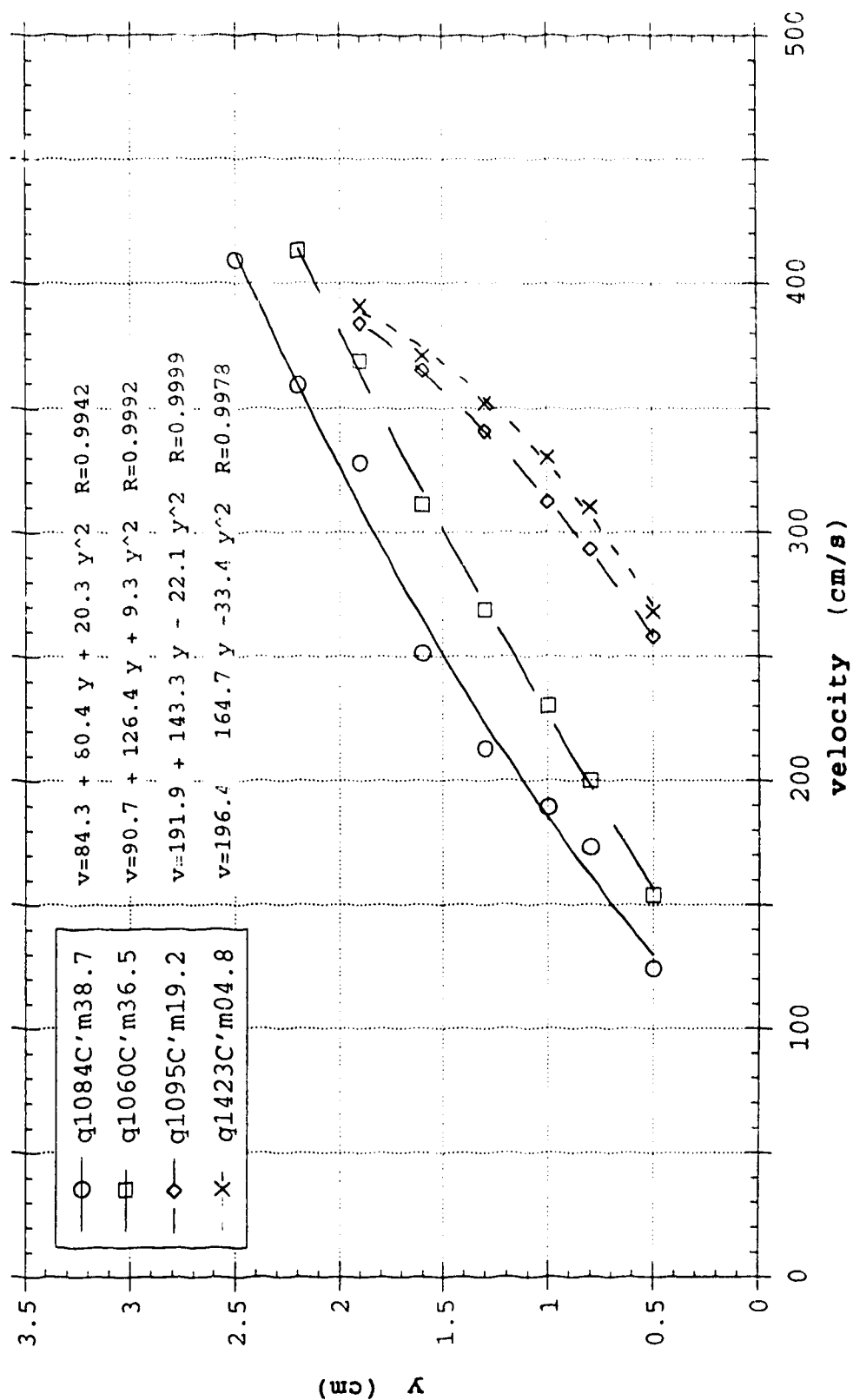


Figure E-2 Polynomial velocity fit for particle D1, group 7.90, channel centre

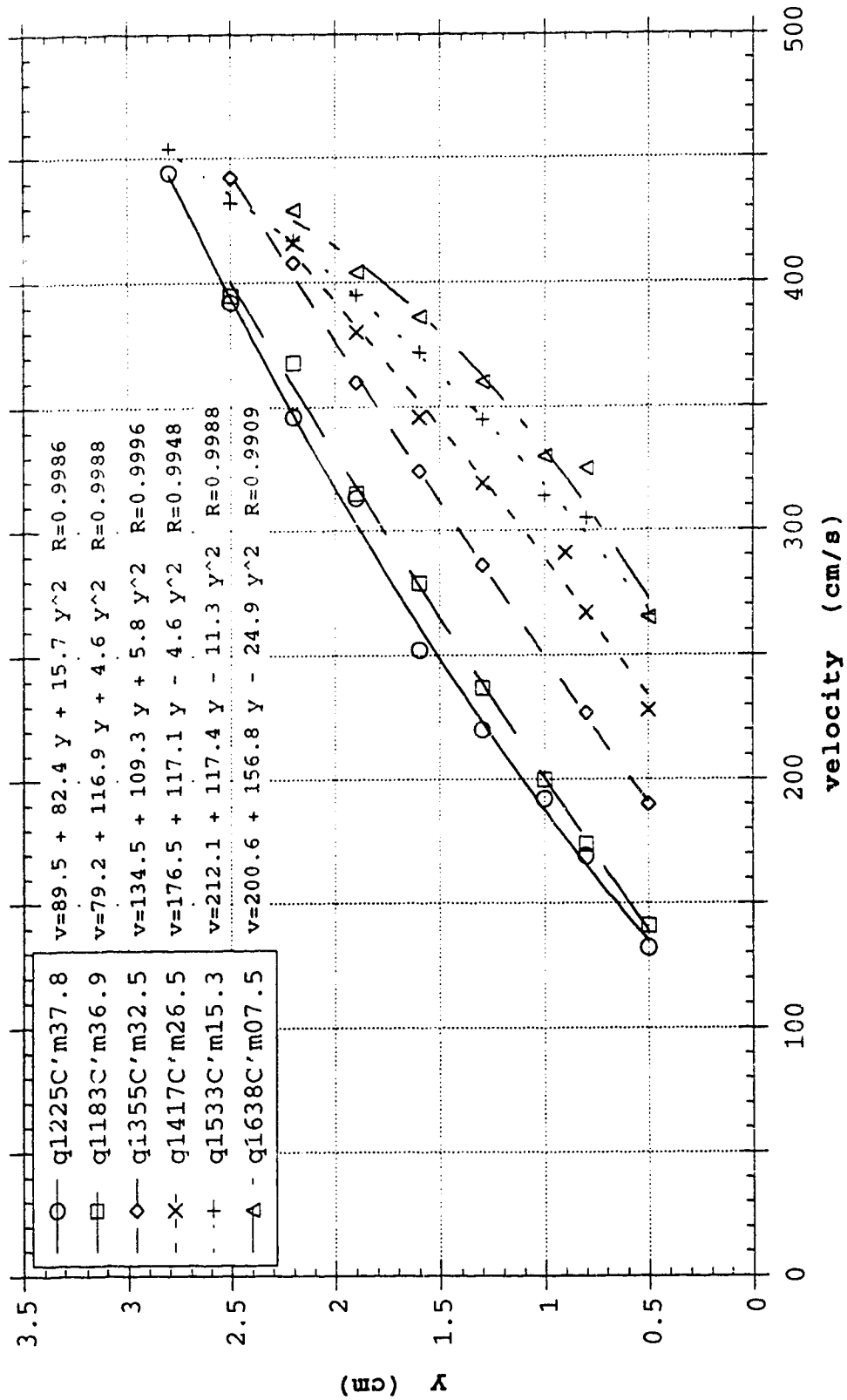


Figure E-3 Polynomial velocity fit for particle D2, group 6.45, channel centre

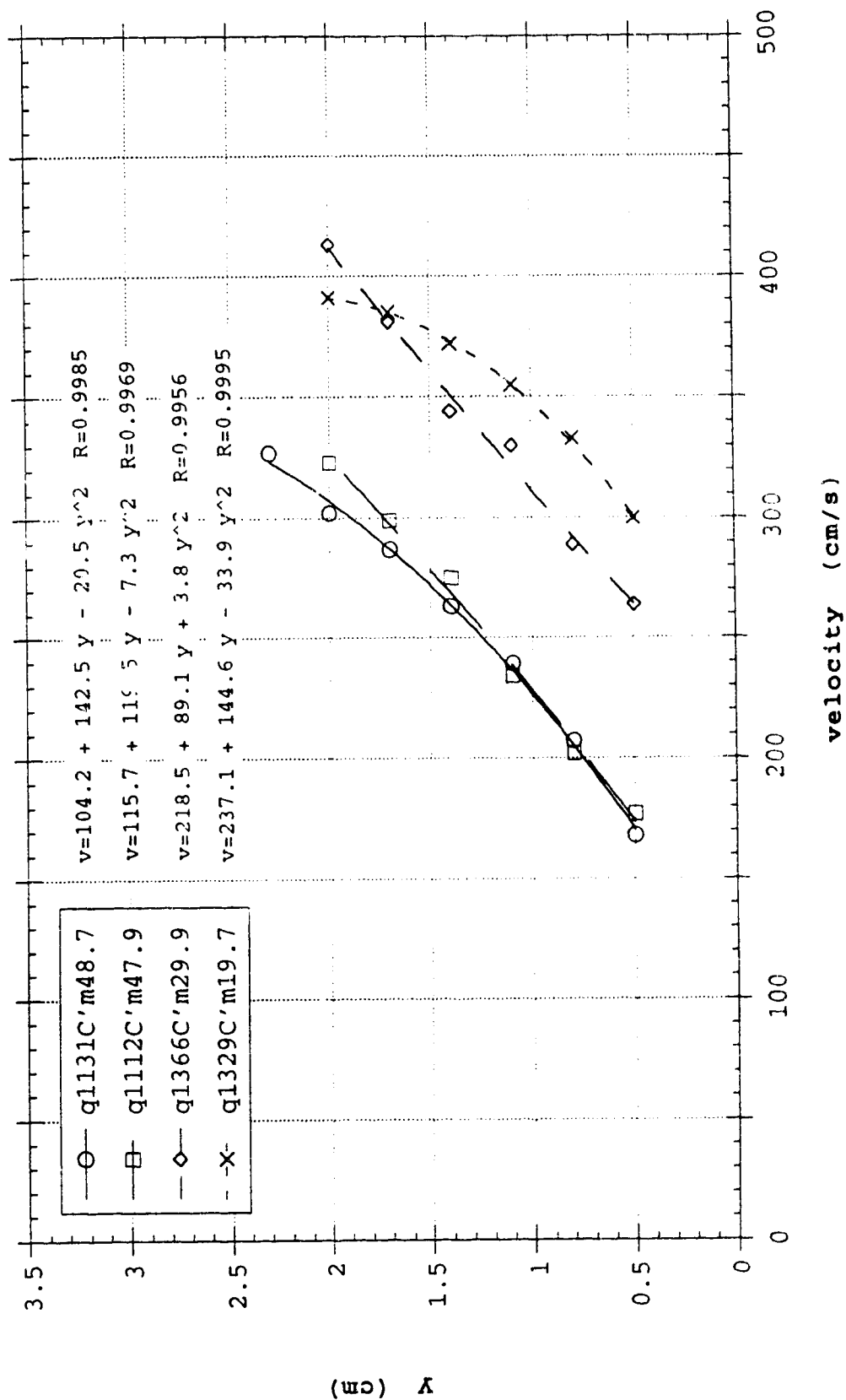


Figure E-4 Polynomial velocity fit for particle D2, group 7.90, channel centre

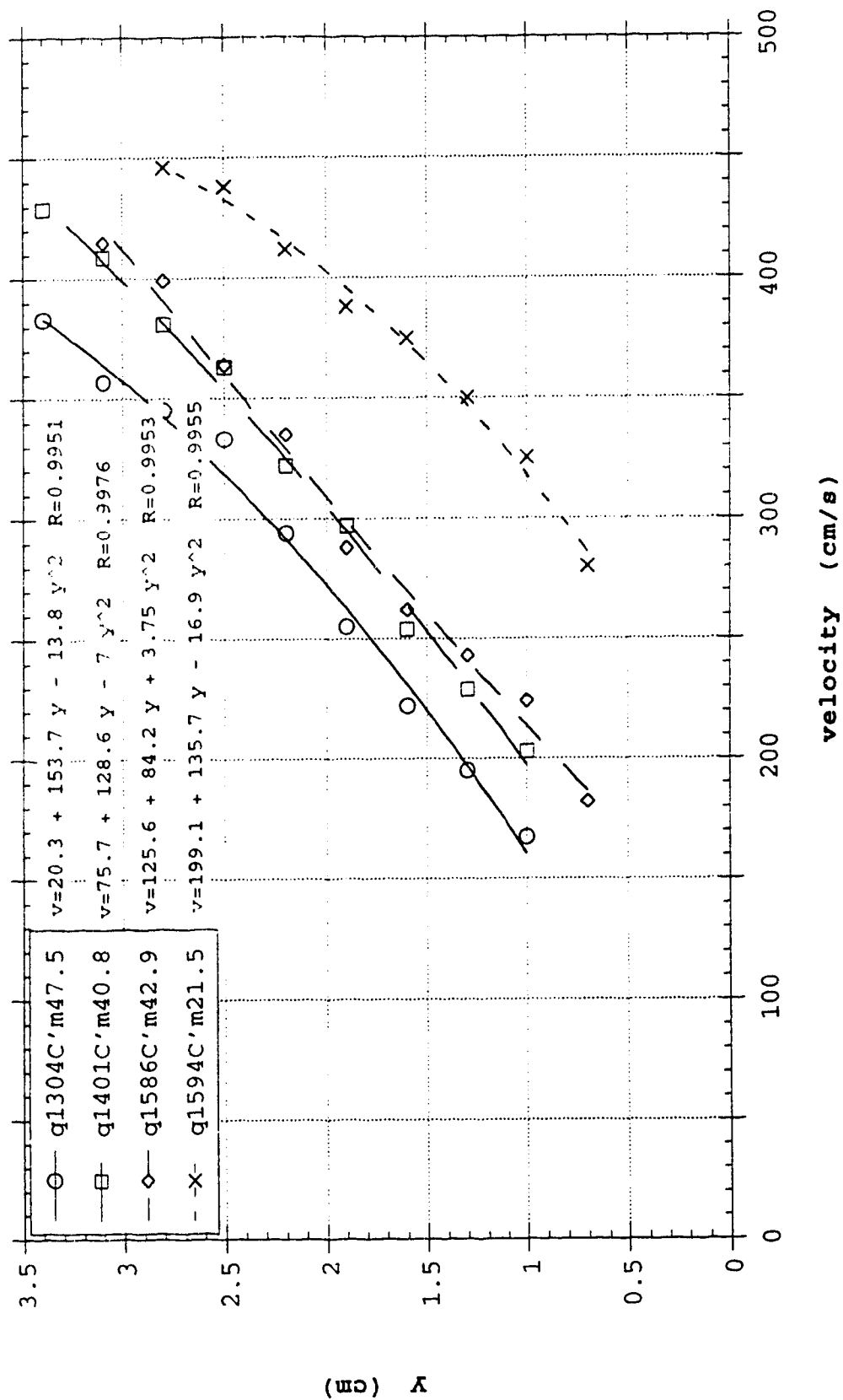


Figure E-5 Polynomial velocity fit for particle D3, group 6.45, channel centre

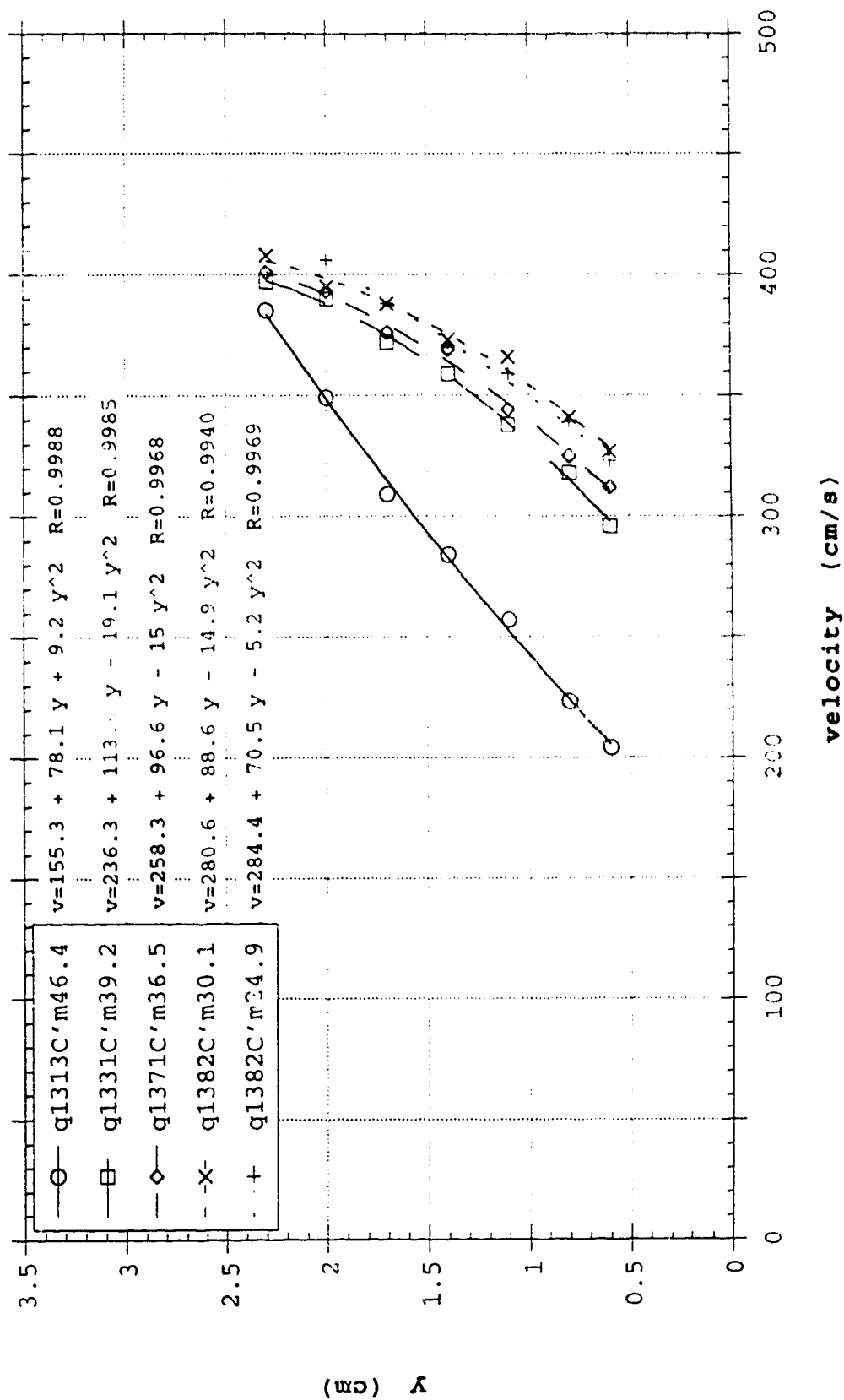


Figure E-6 Polynomial velocity fit for particle D3, group 7.90, channel centre

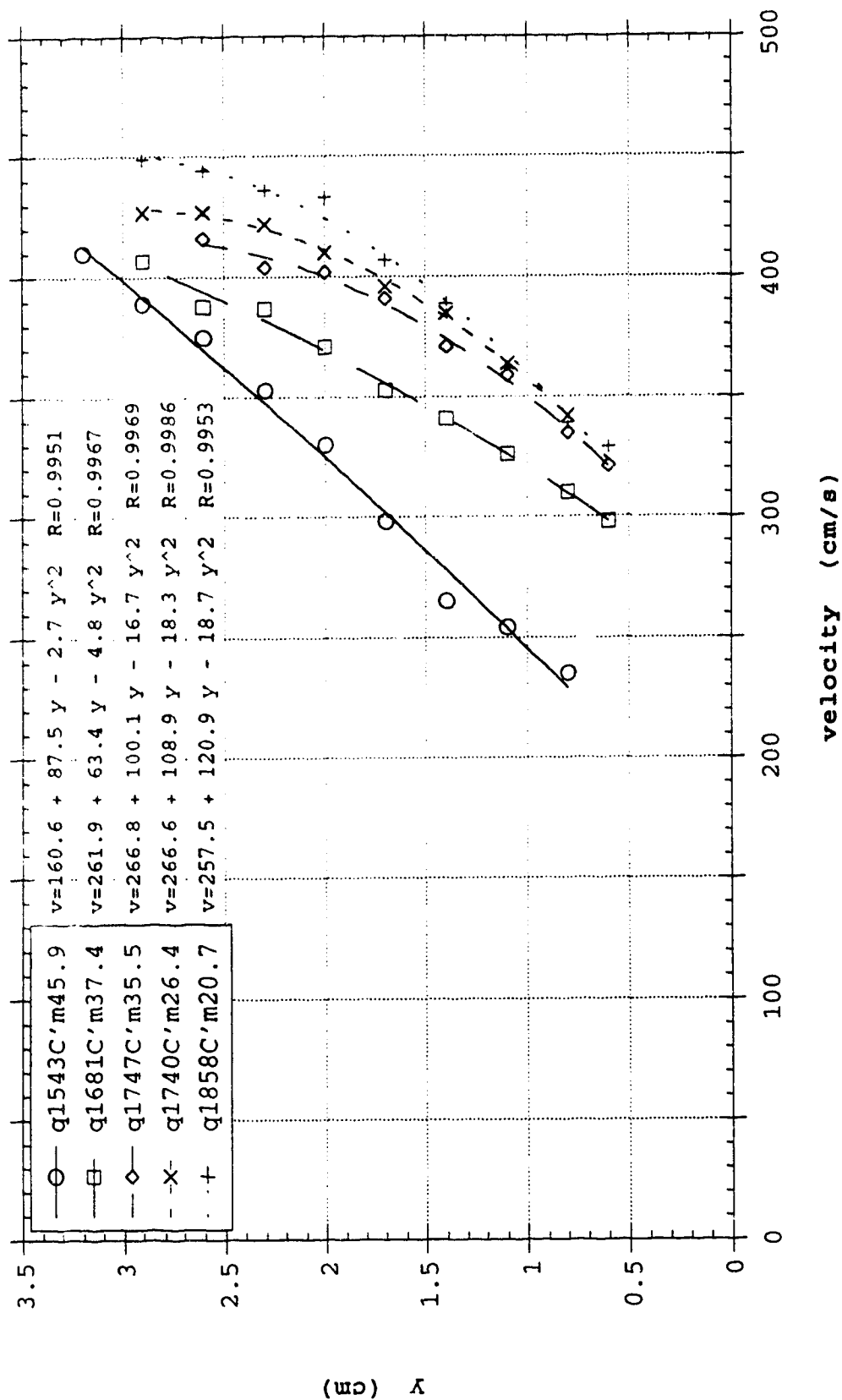


Figure E-7 Polynomial velocity fit for particle D4, group 6.45, channel centre

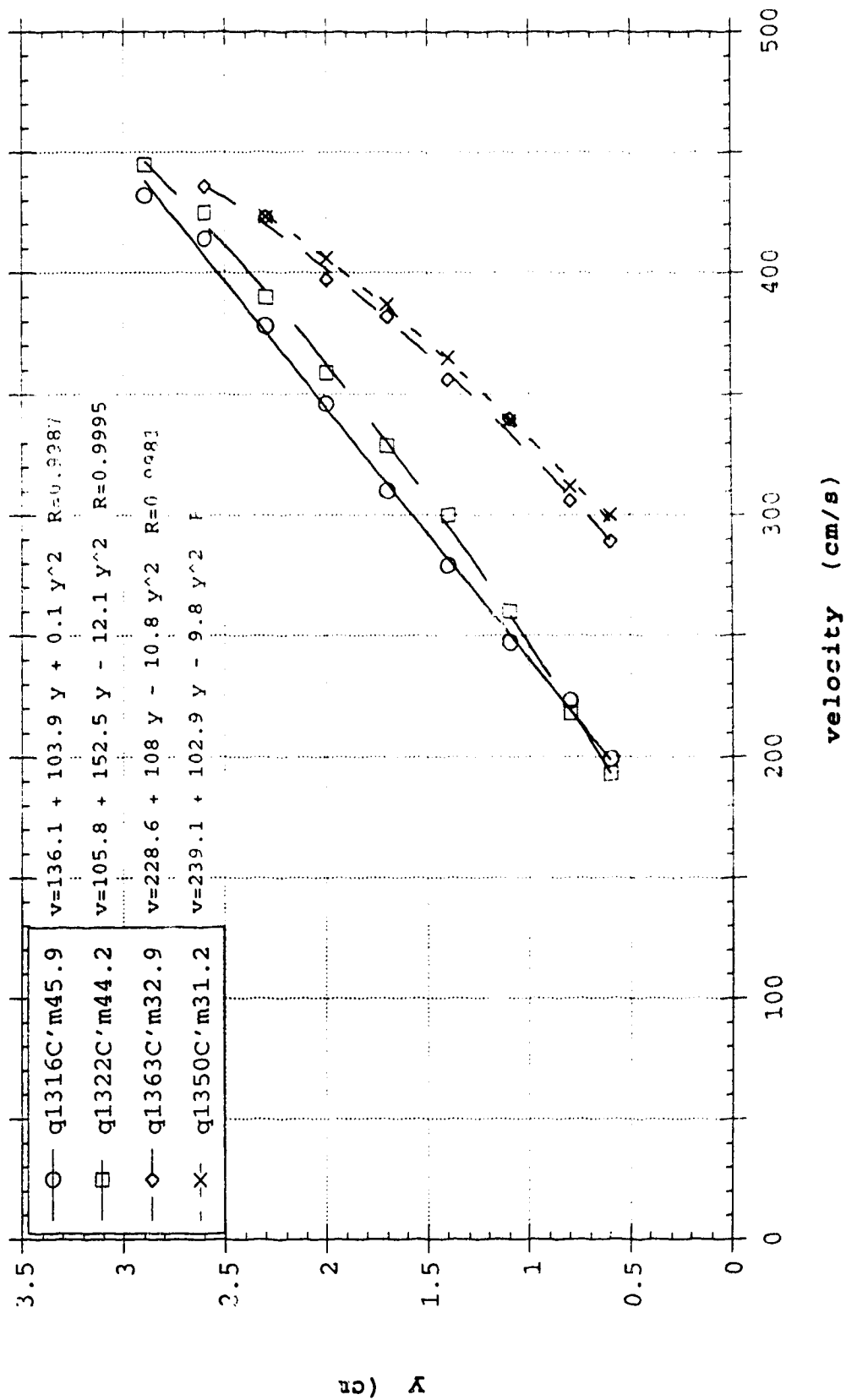


Figure E-8 Polynomial velocity fit for particle D4, group 7.90, channel centre

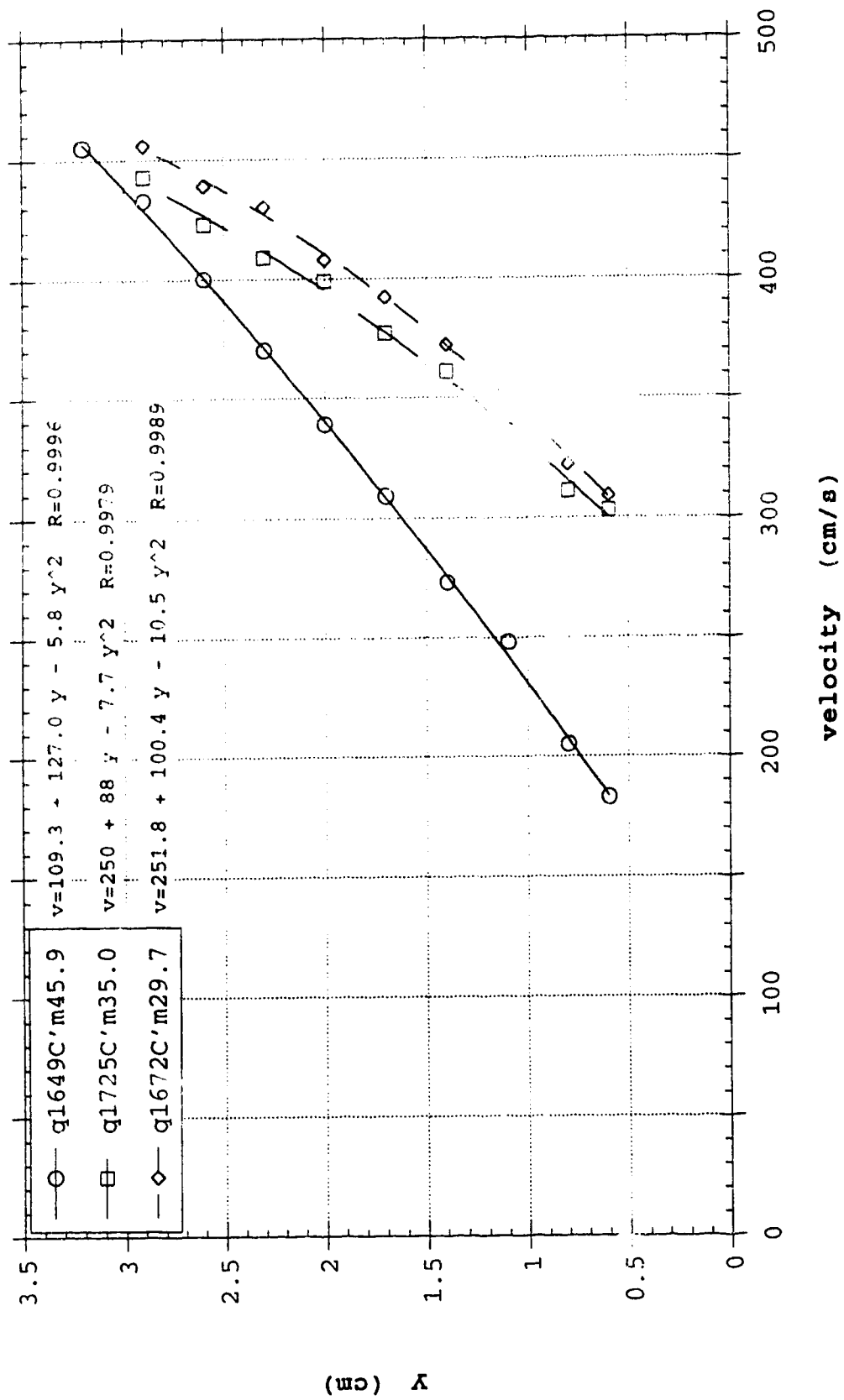


Table E1 Polynomial velocity and velocity gradient for
particle D1, channel centre

q (cm ² /s)	u = b ₁ + b ₂ y + b ₃ y ²					$\partial u/\partial y = b_2 + b_4 y$	
	Particle D1						
	C'm	b ₁	b ₂	b ₃	R	b ₂	b ₄
1087	38.7	84.3	80.4	20.3	0.9942	80.4	40.6
1060	36.5	90.7	126.4	9.3	0.9992	126.4	18.6
1095	19.2	191.9	143.3	-22.1	0.9999	143.3	-44.2
1423	4.8	196.4	164.7	-33.4	0.9978	164.7	-66.8
1225	37.8	89.5	82.4	15.7	0.9986	82.4	31.4
1183	36.9	79.2	116.9	4.6	0.9988	116.9	9.2
1355	32.5	134.5	109.3	5.8	0.9996	109.3	11.6
1417	26.5	176.5	117.1	-4.6	0.9948	117.1	-9.2
1533	15.3	212.1	117.4	-11.3	0.9988	117.4	-22.6
1638	7.5	200.6	156.8	-24.9	0.9909	156.8	-49.8

Table E2 Polynomial velocity and velocity gradient for
particle D2, channel centre

q (cm ² /s)	u = b ₁ + b ₂ y + b ₃ y ²					$\partial u/\partial y = b_2 + b_4 y$	
	Particle D2						
	C'm	b ₁	b ₂	b ₃	R	b ₂	b ₄
1131	48.7	104.2	142.5	-20.5	0.9985	142.5	-41
1112	47.9	115.7	119.5	-7.3	0.9969	119.5	-14.6
1366	29.9	218.5	89.1	3.8	0.9956	89.1	7.6
1329	19.7	237.1	144.6	-33.9	0.9995	144.6	-67.8
1304	47.5	20.3	153.7	-13.8	0.9951	153.7	-27.6
1401	40.8	75.7	128.6	-7	0.9976	128.6	-14
1586	42.9	125.6	84.2	3.75	0.9953	84.2	7.5
1594	21.5	199.1	135.7	-16.9	0.9955	135.7	-33.8

Table E3 Polynomial velocity and velocity gradient for
particle D3, channel centre

q (cm ² /s)	u = b ₁ + b ₂ y + b ₃ y ²					$\partial u/\partial y = b_2 + b_4 y$	
	Particle D3						
	C'm	b ₁	b ₂	b ₃	R	b ₂	b ₄
1313	46.4	155.3	78.1	9.2	0.9988	78.1	18.4
1331	39.2	236.3	113.9	-19.1	0.9985	113.9	-38.2
1371	36.5	258.3	96.6	-15	0.9968	96.6	-30
1382	30.1	280.6	88.6	-14.9	0.994	88.6	-29.8
1382	24.9	284.4	70.5	-5.2	0.9969	70.5	-10.4
1543	45.9	160.6	87.5	-2.7	0.9951	87.5	-5.4
1681	37.4	261.9	63.4	-4.8	0.9967	63.4	-9.6
1747	35.5	266.8	100.1	-16.7	0.9969	100.1	-33.4
1740	26.4	266.6	108.9	-18.3	0.9986	108.9	-36.6
1858	20.7	257.5	120.9	-18.7	0.9953	120.9	-37.4

Table E4 Polynomial velocity and velocity gradient for
particle D4, channel centre

q (cm ² /s)	u = b ₁ + b ₂ y + b ₃ y ²					$\partial u/\partial y = b_2 + b_4 y$	
	Particle D4						
	C'm	b ₁	b ₂	b ₃	R	b ₂	b ₄
1316	45.9	136.1	103.9	0.1	0.9987	103.9	0.2
1322	44.2	105.8	152.5	-12.1	0.9995	152.5	-24.2
1363	32.9	228.6	108	-10.8	0.9981	108	-21.6
1350	31.2	239.1	102.9	-9.8	0.9991	102.9	-19.6
1649	45.9	109.3	127	-5.8	0.9996	127	-11.6
1725	35.0	250	88	-7.7	0.9997	88	-15.4
1672	29.7	251.8	100.4	-10.5	0.9989	100.4	-21

Figure E-9a Concentration vs velocity coefficients for
Particle D1, Slope=28.6%, channel centre

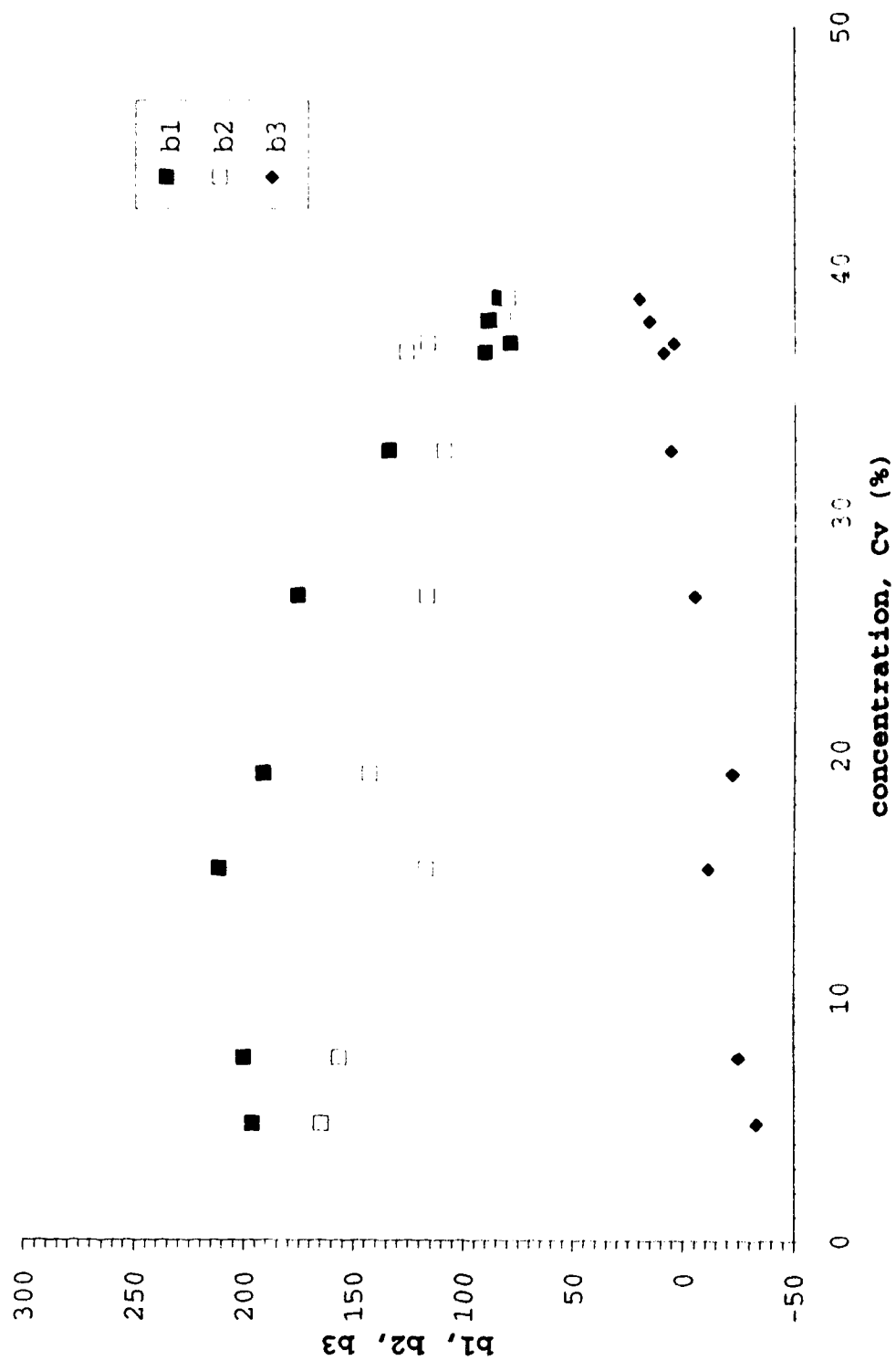


Figure E-9b Concentration vs velocity coefficients for
Particle D2, Slope=28.6%, channel centre

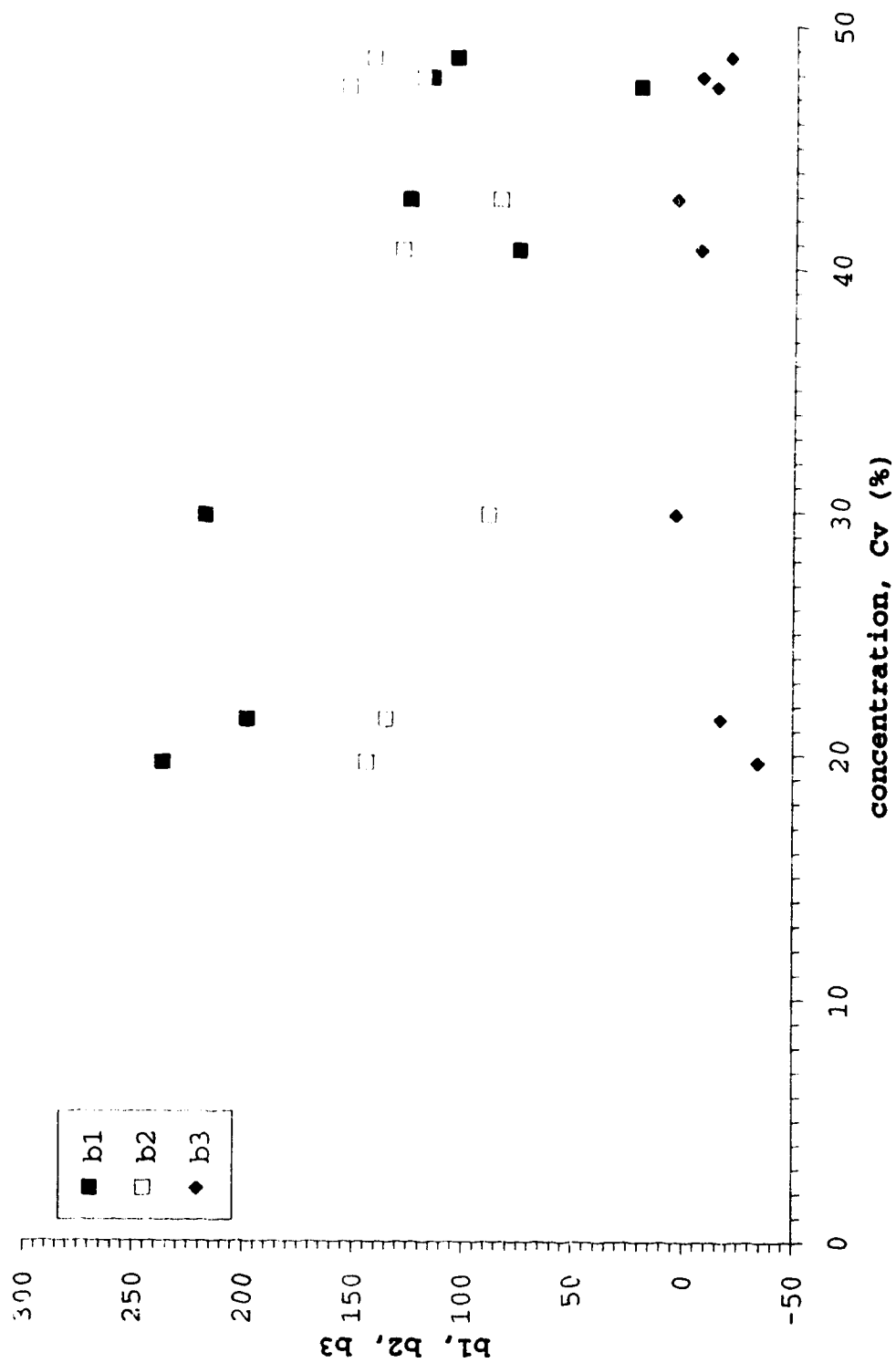


Figure E-9c Concentration vs velocity coefficients for
Particle D3, Slope=28.6%, channel centre

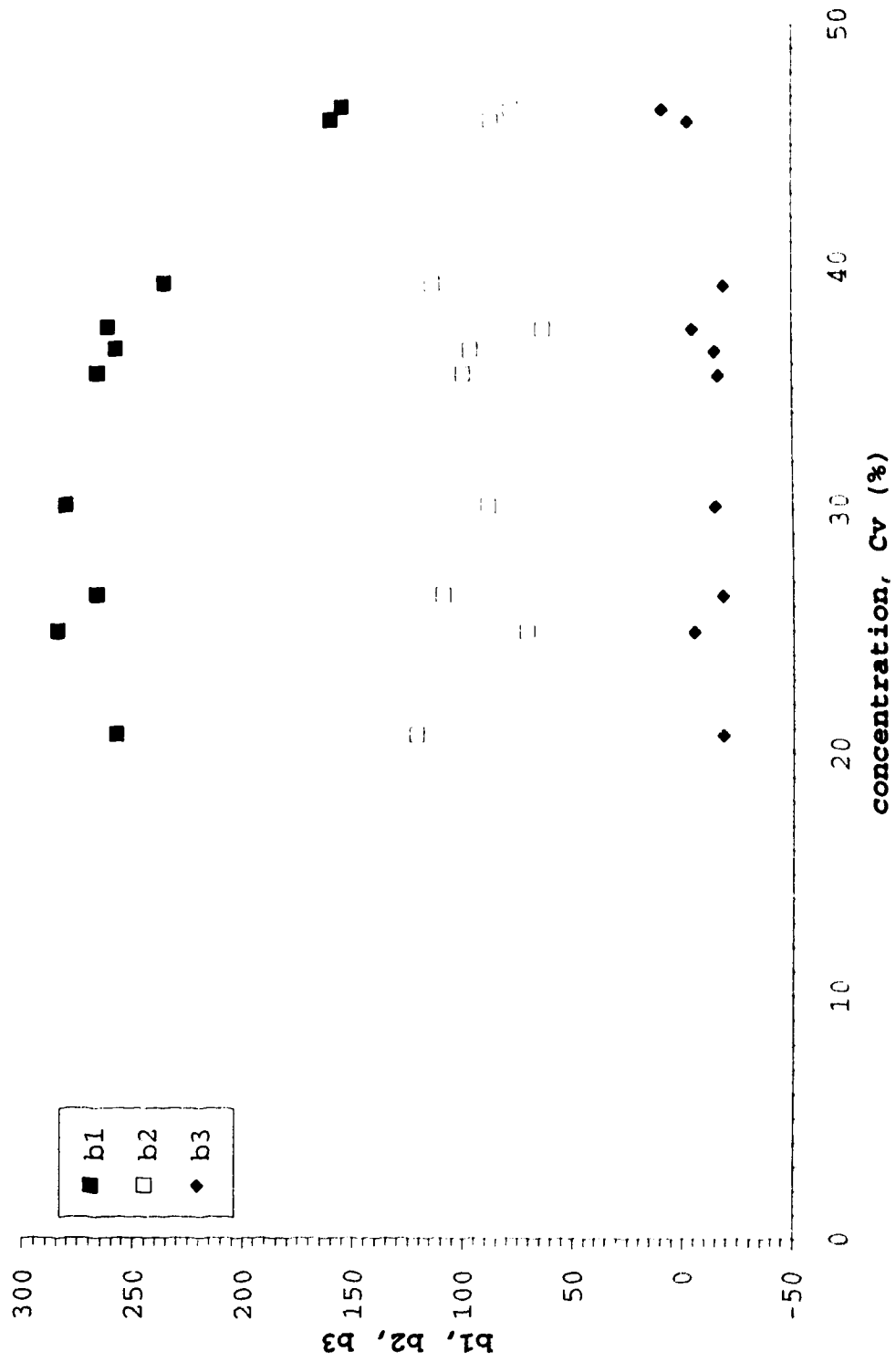
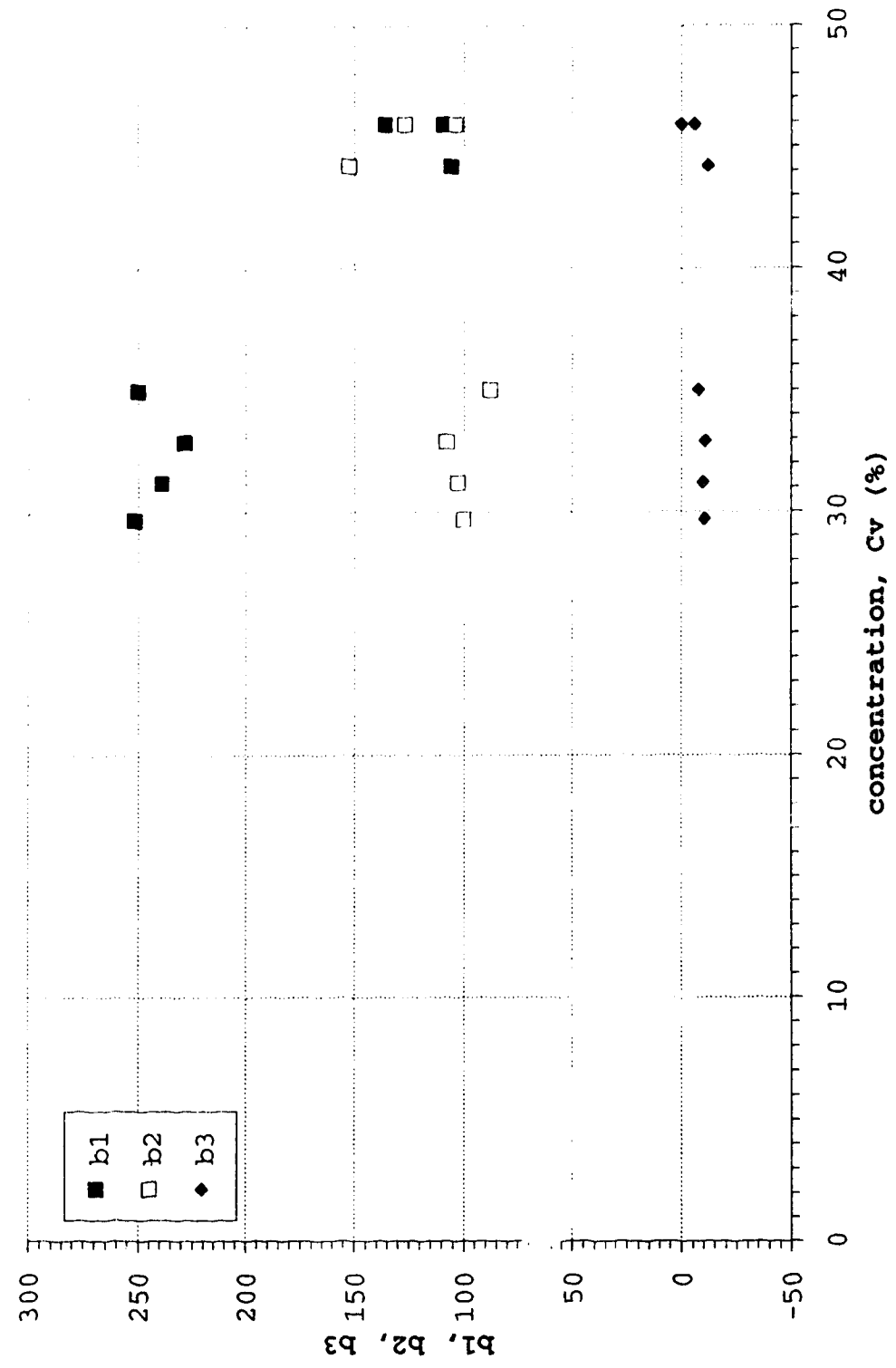


Figure E-9d Concentration vs velocity coefficients for
Particle D4, Slope=28.6%, channel centre



E.2 Viscosity

In Chapter 5 it was concluded that for the cases where the velocity profiles were nearly linear, the increase in shear with depth was the result of a change in viscosity with depth. Figure E-10 to E-13 shows the viscosity varying with concentration for each profile and particle size. The viscosity was calculated by dividing the shear at a point with the velocity gradient at that point obtained from the polynomial velocity fit. When plotted against the measured point concentration, the exponential nature of the curve is apparent. It can be seen that at a given concentration, the viscosity is different for each profile. Furthermore, there are two distinct trends shown by the negative and positive exponential curves. These trends are probably an indication of different mechanisms for viscosity. At lower concentration or smaller particle size the turbulent component of the viscosity may be dominating. But at higher concentration or larger particle sizes the positive exponential curves indicate viscosity trends similar to those displayed by Equations 2-5.4 to 2-5.6.

The negative exponential curves displayed in E-10 to E-13 is mainly for lower concentrations where the velocity profiles are approaching that of clear water where the flow is more turbulent. This suggests the possibility that the two regimes displayed by the positive and negative exponential curves could be for laminar and turbulent flows.

Figure E-10 Cv vs μ_r , particle D1

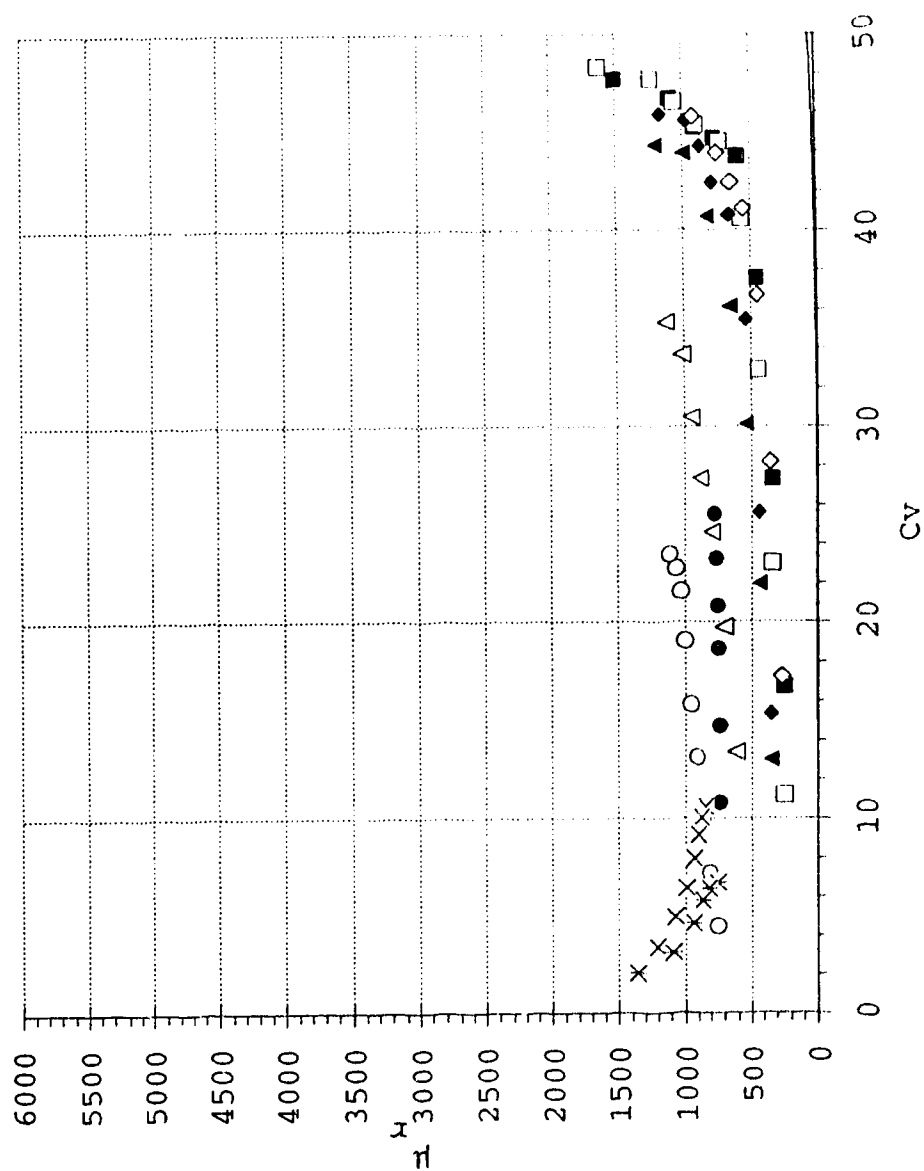


Figure E-11 Cv vs μ_r , particle D2

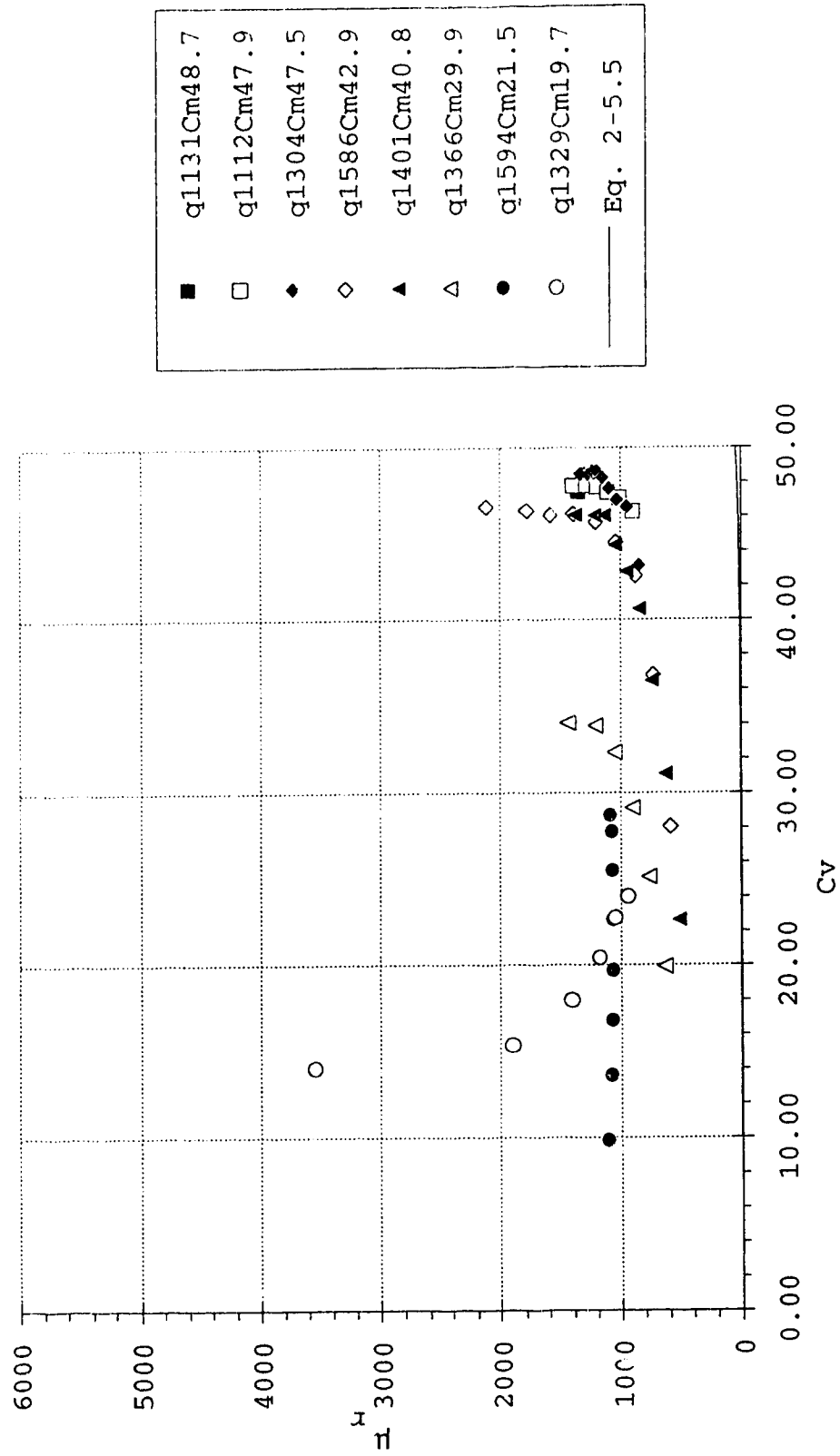


Figure E-12 Cv vs μ_r particle D3

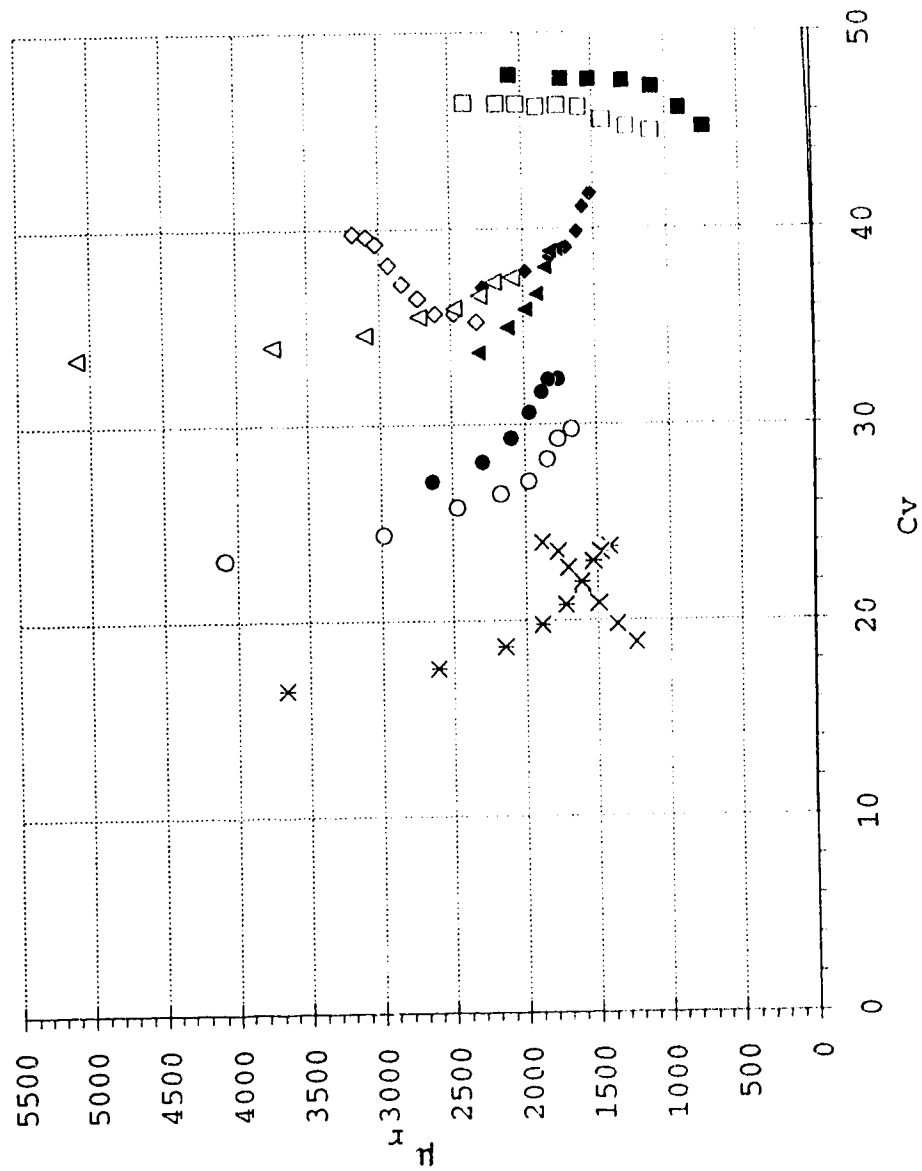


Figure E-13 Cv vs μ_r , particle D4

